

**A Formal Vinyl Sulfonyl Nazarov Cyclization Accesses 9-(tosylmethyl)-2,3,4,4a-tetrahydro-
1*H*-fluorenes**

by

Alexander Morton Berne

B.A. Chemistry, Boston University, 2012

Submitted to the Graduate Faculty of
The Kenneth P. Dietrich School of Arts and Sciences in partial fulfillment
of the requirements for the degree of
Master of Science

University of Pittsburgh

2015

UNIVERSITY OF PITTSBURGH
THE KENNETH P. DIETRICH SCHOOL OF ARTS & SCIENCES

This thesis was presented

by

Alexander Morton Berne

It was defended on

May 28th, 2015

and approved by

Paul E. Floreancig, Professor, Department of Chemistry

Dennis P. Curran, Distinguished Service Professor of Chemistry and Bayer Professor,
Department of Chemistry

Thesis Director: Kay M. Brummond, Professor and Department Chair, Department of
Chemistry

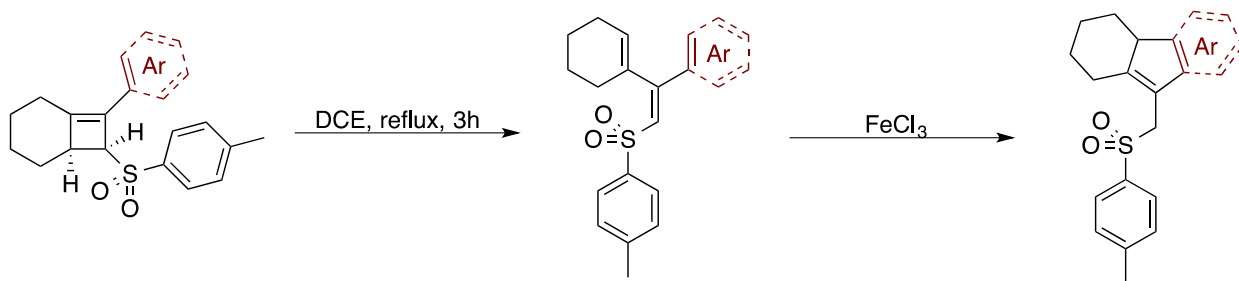
Copyright © by Alexander Morton Berne

2015

A Formal Vinyl Sulfonyl Nazarov Cyclization Accesses 9-(tosylmethyl)-2,3,4,4a-tetrahydro-1H-fluorenes

Alexander Morton Berne, M.S.

University of Pittsburgh, 2015



During the course of a proposed route to synthesize ladderane lipids, a novel one-pot 4π electrocyclic ring opening followed by a Nazarov-type 4π electrocyclization reaction was discovered. The reaction was studied further due to its potential as a method for accessing the privileged tetrahydrofluorene scaffold and the opportunities for further functionalization provided by the allyl sulfone moiety. Optimized conditions for the transformation involved refluxing model substrate 7-phenyl-8-tosylbicyclo[4.2.0]oct-6-ene in 1,2-dichloroethane for 3 h to generate intermediate (E)-1-((2-(cyclohex-1-en-1-yl)-2-phenylvinyl)sulfonyl)-4-methylbenzene. Upon cooling to room temperature, addition of 1.2 equiv iron(III) chloride promotes cyclization to furnish 9-(tosylmethyl)-2,3,4,4a-tetrahydro-1H-fluorene after 10 h in 78% yield. In order to determine the effect electronics may have on the transformation, functionality was introduced onto the phenyl ring. While no noticeable effect was observed on the electrocyclic ring opening step, the nature of the substituents significantly affected the quantity of promoter required for the cyclization step. Although a superstoichiometric amount of

iron(III) chloride and heat was required with an electron withdrawing substituent on the aryl ring, electron donating substituents lowered the activation barrier to cyclization – necessitating only catalytic amounts of iron(III) chloride at room temperature. This transformation represents the first report of a Nazarov cyclization with a vinyl sulfone on the central carbon.

TABLE OF CONTENTS

1.0 REACTION DISCOVERY	1
1.1 PROPOSED APPLICATION OF INTRAMOLECULAR [2+2] REACTION OF ALLENE-YNES TO LADDERANE LIPID SYNTHESIS	1
1.1.1 Background on Ladderane Lipids	1
1.1.2 Retrosynthesis.....	3
1.1.3 Forward Synthesis and Formation of Unexpected Tetrahydrofluorene.....	4
1.2 PROPOSED MECHANISM OF REACTION	10
2.0 POTENTIAL UTILITY AND PRECEDENCE OF SULFONYL FUNCTIONALIZED TETRAHYDROFLUORENES	14
2.1 THE SULFONE MOIETY	14
2.2 THE [6,5,6]-SYSTEM IN BIOLOGICALLY ACTIVE NATURAL PRODUCTS	16
2.3 THE NAZAROV CYCLIZATION.....	18
2.3.1 The Classical Reaction.....	18
2.3.2 Nazarov Cyclizations with Aromatic Rings.....	21
2.3.3 Nazarov Cyclizations to Directly Prepare Indenes	21
3.0 REACTION OPTIMIZATION	23
3.1 NMR SCREENING EXPERIMENTS	23

3.2	OPTIMIZATION OF REACTION ON A 50 MILLIGRAM SCALE	27
3.3	EVIDENCE FOR LEWIS ACID CATALYSIS	28
3.4	A NOTE ON THE DIENYL SULFONE MOIETY	30
4.0	EFFECT OF ELECTRONIC PERTURBATION OF PHENYL RING ON TRANSFORMATION.....	31
4.1	OPPORTUNITIES FOR STUDY AND EXTENSION OF TRANSFORMATION	35
5.0	CONCLUSIONS	37
	APPENDIX	38
	BIBLIOGRAPHY	200

LIST OF TABLES

Table 1.1. Determination of reagent that promotes cyclization.....	13
Table 3.1. Crude ¹ H NMR results of screening different acids	25
Table 3.2. Crude ¹ H NMR results of screening different solvents with select acids.....	26
Table 4.1. Exposure of cyclobutenes with variations on the aryl ring to optimized reaction conditions.....	32

LIST OF FIGURES

Figure 1.1. Select ladderane lipids.....	2
Figure 1.2. X-ray crystal structure of 1.8	8
Figure 1.3. Rationale for observed syn hydrogens in 1.8	8
Figure 1.4. ¹ H NMR and ¹³ C NMR evidence for 1.25	10
Figure 1.5. X-ray crystal structure of 1.25	10
Figure 1.6. X-ray crystal structure of 1.26	12
Figure 2.1. Select sulfone-containing prescription drugs.....	15
Figure 2.2. Select prescription drugs containing the aryl sulfone motif.....	16
Figure 2.3. Gibberellic acid (2.8).....	16
Figure 2.4. Select taiwaniaquinoids.....	17
Figure 2.5. Natural products formed by alcohol expulsion and subsequent Nazarov cyclization	22
Figure 3.1. Key ¹ H NMR resonances used to determine product ratio.....	24

LIST OF SCHEMES

Scheme 1.1. Retrosynthetic strategy to make model ladderane 1.4	3
Scheme 1.2. Synthesis of allene-yne 1.10	5
Scheme 1.3. Mukai's thermal [2+2] results with heteroatom and malonate tethers.....	6
Scheme 1.4. Our thermal [2+2] results an all carbon tether	6
Scheme 1.5. Proposed pathway from 1.9 to 1.7	7
Scheme 1.6. Optimized hydrogenation conditions	7
Scheme 1.7. Result of silylation	9
Scheme 1.8. Predicted outcome of proto-desilylation	9
Scheme 1.9. Initial reaction to form tetrahydrofluorene 1.25	10
Scheme 1.10. Proposed mechanism to account for the formation of tetrahydrofluorene 1.25	11
Scheme 1.11. Subjecting proposed intermediates to reaction conditions.....	12
Scheme 2.1. Some general transformations of aryl sulfones	15
Scheme 2.2. General mechanism of the Nazarov cyclization.....	19

Scheme 2.3. Key step in the Nazarov cyclization.....	19
Scheme 2.4. Pentadienyl cation favored for imino-Nazarov variant.....	20
Scheme 2.5. The vinylogous Nazarov reaction	20
Scheme 2.6. Nazarov variant to construct indene type core structures	21
Scheme 2.7. Nazarov variant to construct aryl substituted indenenes.....	22
Scheme 3.1. Different products observed during acid screen.....	24
Scheme 3.2. Consumption of FeCl ₃ by water.....	27
Scheme 3.3. Optimized conditions	28
Scheme 3.4. Diagnostic reactions to determine whether transformation is promoted by a Lewis or Brønsted acid	29
Scheme 4.1. Synthesis of cyclobutenes with variations on the aryl ring.....	31
Scheme 4.2. Yield of the electrocyclic ring opening step from cyclobutene 4.20a to diene 4.20b	34
Scheme 4.3. Current route to product	35
Scheme 4.4. Proposed improved route to product	36

LIST OF ABBREVIATIONS

DCE	1,2-dichloroethane
DCM	Dichloromethane
<i>o</i> DCB	1,2-Dichlorobenzene
PCC	Pyridinium chlorochromate
TEA	Triethylamine
TFA	Trifluoroacetic acid
TfOH	Trifluoromethanesulfonic acid
THF	Tetrahydrofuran
TMSOTf	Trimethylsilyl triflate
TsCl	<i>p</i> -Toluenesulfonyl chloride
TsOH	<i>p</i> -Toluenesulfonic acid

1.0 REACTION DISCOVERY

1.1 PROPOSED APPLICATION OF INTRAMOLECULAR [2+2] REACTION OF ALLENE-YNES TO LADDERANE LIPID SYNTHESIS

The first general intramolecular [2+2] reaction of allene-ynes was reported by Brummond and Chen in 2005 for the preparation of bicyclo[4.2.0]octa-1,6-dienes and bicyclo[5.2.0]nona-1,7-dienes.¹ Because of the unique ring system created in the former case, it was postulated that the reaction could be applied to the synthesis of certain ladderane lipid derivatives that share the same skeleton.

1.1.1 Background on Ladderane Lipids

The anaerobic oxidation of ammonium ions by nitrite to give nitrogen gas and water was discovered to occur in certain bacterial species isolated from a wastewater bioreactor.² These anaerobic ammonium oxidizing (anammox) bacteria contain a large intracellular organelle called the anammoxosome where the unique biochemical reaction takes place.³ Within the anammoxosome membrane are lipid structures containing linearly concatenated cyclobutane rings (ladderanes, select examples are shown in Figure 1.1).³ It is proposed that these ladderane structures allow for unusually dense packing within the membrane, which limits the diffusion of hydrazine and hydroxylamine – intermediates in the anammox process that are not only toxic,

but also require energetic investment to make.³

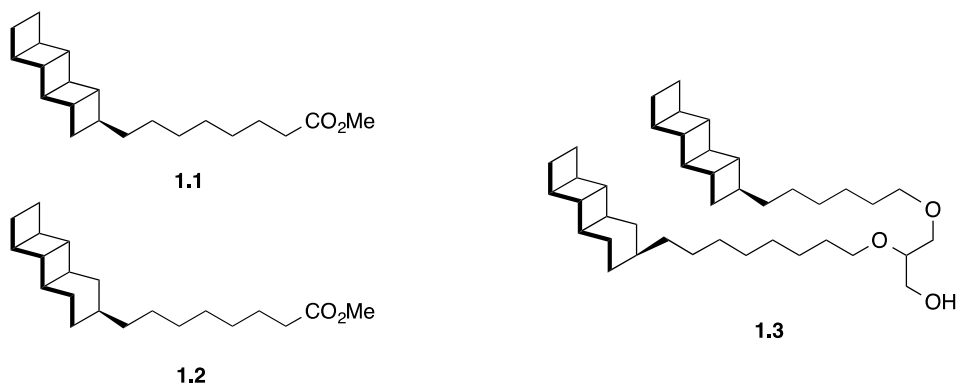
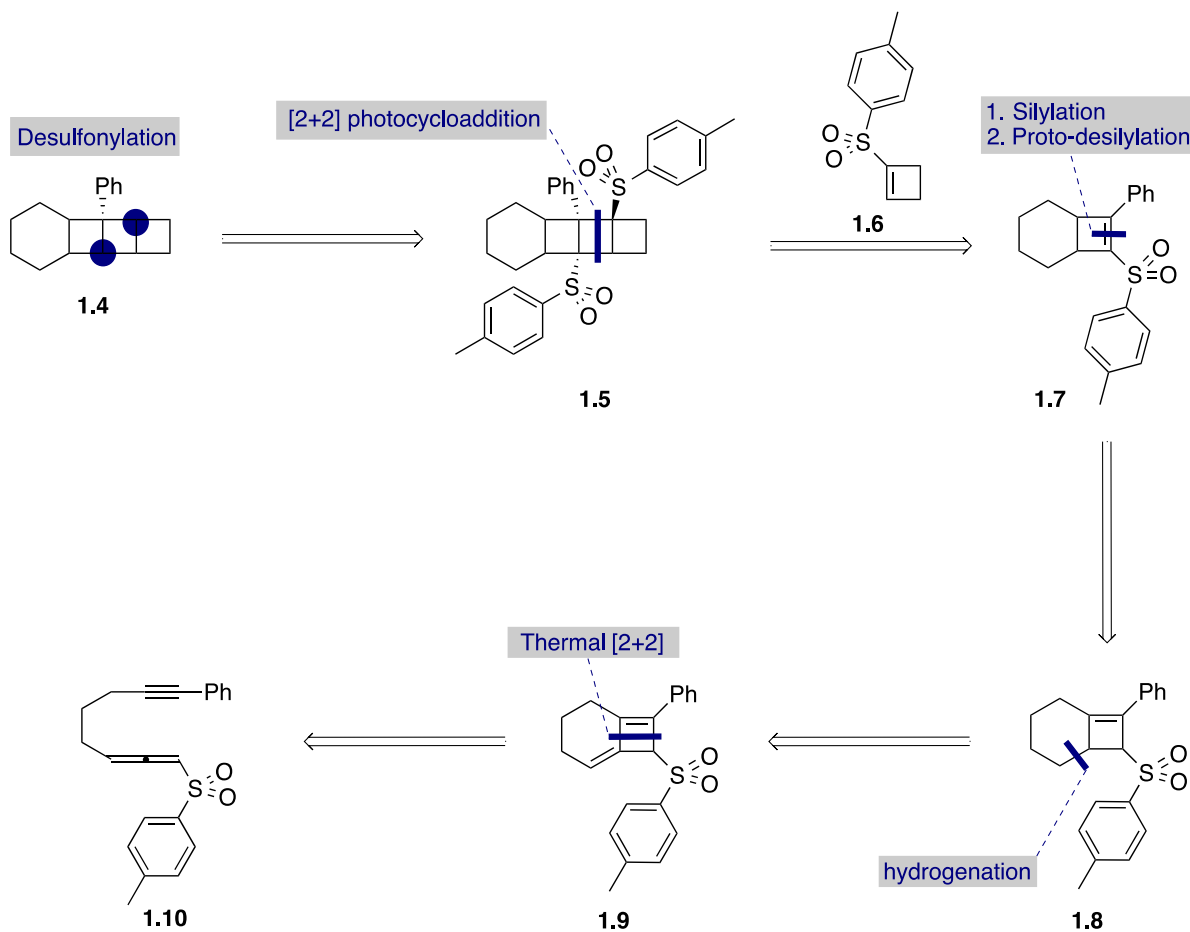


Figure 1.1. Select ladderane lipids

Elucidating the anammox biochemical mechanism may lead to an efficient method to clean wastewater contaminated with ammonia and nitrates. Unfortunately, anammox bacteria divide only once every 2-3 weeks under optimal laboratory conditions, limiting the ability of biochemists to study the mechanism.³ A synthetic method to provide meaningful amounts of ladderane lipid derivatives would greatly facilitate the study of the anammox process. Additionally, because of their unique structural features, a novel synthesis of ladderane lipid derivatives would be of interest to organic chemists. While several groups have reported syntheses of concatenated cyclobutane rings of varying length, only Corey has been able to synthesize one of the ladderane lipids. His asymmetric synthesis of pentacycloanammoxic acid methyl ester (**1.1**) gave a 1.9% yield over 17 steps.⁴ Although Corey's synthesis confirmed the molecular structure of **1.1**, it did not provide a convenient route to large quantities of material.

1.1.2 Retrosynthesis

Our objective was to provide an efficient route to meaningful quantities of ladderane lipid derivatives of the bicyclo[4.2.0]octyl variety such as **1.2** for biological study. We expected that model ladderane **1.4** (Scheme 1.1) could be furnished by intermolecular [2+2] photocycloaddition of cyclobutene **1.7** with **1.6** and subsequent desulfonylation. Cyclobutene **1.7** could result from a silylation, proto-desilylation strategy to migrate the alkene in cyclobutene **1.8**,⁵ which, in turn, would be fashioned from a selective hydrogenation of the tri-substituted alkene in alkyldiene cyclobutene **1.9**. A thermal [2+2] cyclization of allene-yne precursor **1.10** should access the desired bicyclo[4.2.0]octyl ring system in alkyldiene cyclobutene **1.9**.

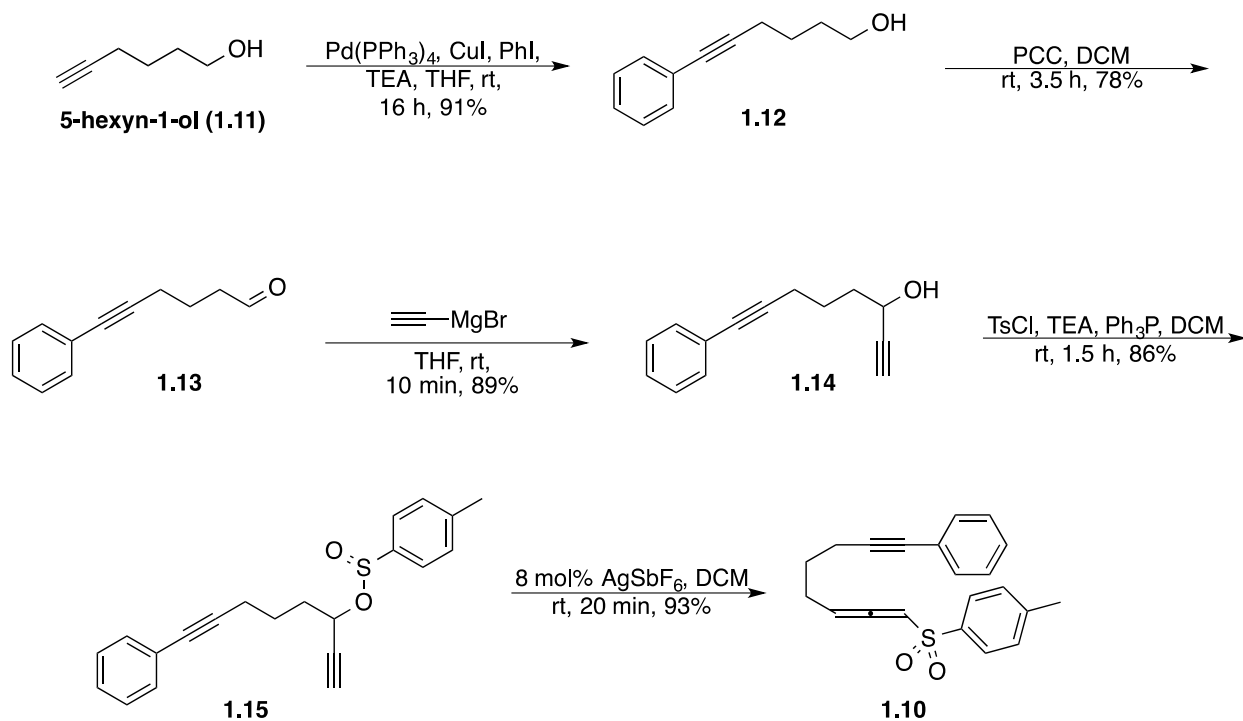


Scheme 1.1. Retrosynthetic strategy to make model ladderane **1.4**

The proposed route would be facilitated by the sulfone moiety, which would presumably activate the allene for cycloaddition, acidify the proton on its alpha carbon for the silylation step, activate the olefin in **1.7** for photocycloaddition,⁶ and be easily removed in the final step.⁷ As an additional benefit, the tendency of compounds bearing the sulfone moiety to crystallize would ease purification and provide the option of confirming intermediate structures by X-ray crystallography. In order to test our proposed route, precursor **1.10** needed to be synthesized.

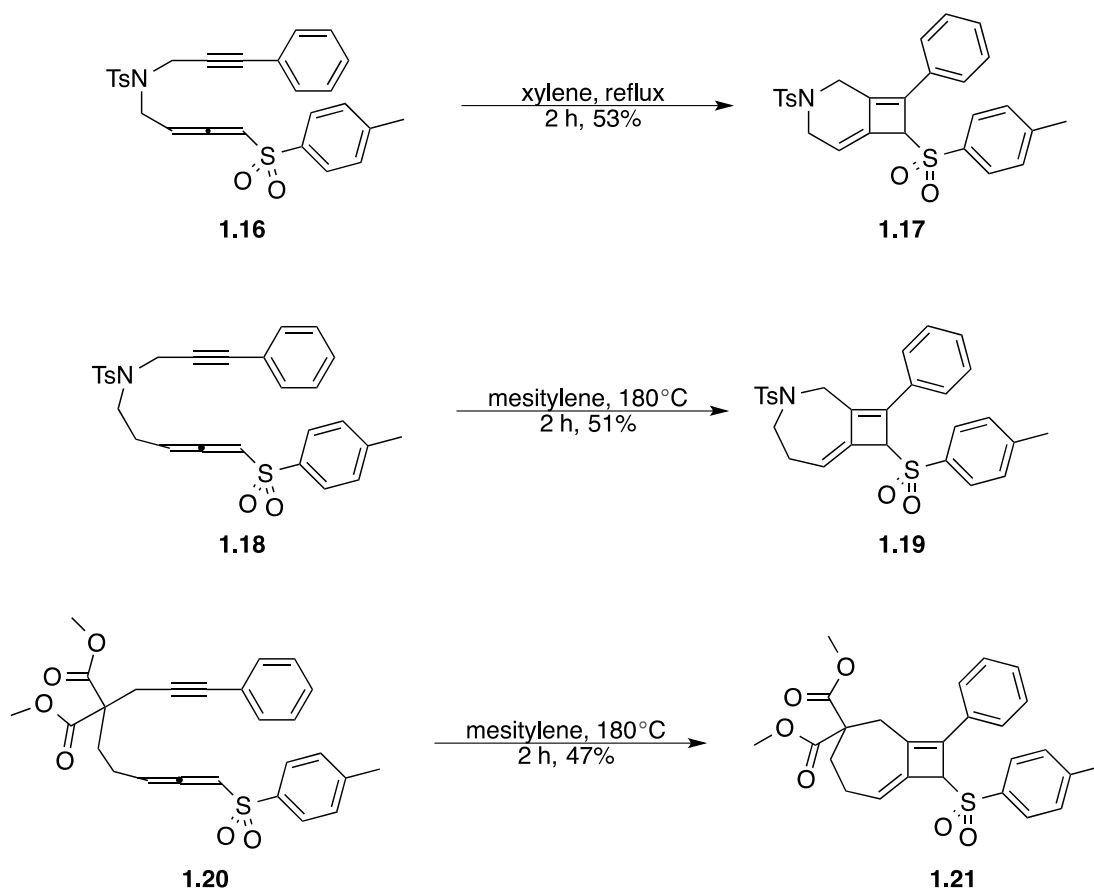
1.1.3 Forward Synthesis and Formation of Unexpected Tetrahydrofluorene

Allene-yne **1.10** was synthesized in five steps from commercially available 5-hexyn-1-ol (**1.11**). Subjecting **1.11** to Sonagashira conditions⁸ afforded coupled product **1.12** in 91% yield. Subsequent oxidation with PCC gave aldehyde **1.12** in 78% yield, which was followed by Grignard addition of ethynylmagnesium bromide to afford alcohol **1.14** in 89% yield. Reacting alcohol **1.14** with tosyl chloride, triphenylphosphine, and triethylamine⁹ furnished sulfinate **1.15** in 86% yield, which upon exposure to 8 mol% silver hexafluoroantimonate underwent a 2,3 sigmatropic rearrangement⁹ to give the desired allene-yne precursor **1.10** in 93% yield. Overall, the allene-yne was formed over five steps in 51% yield (Scheme 1.2).

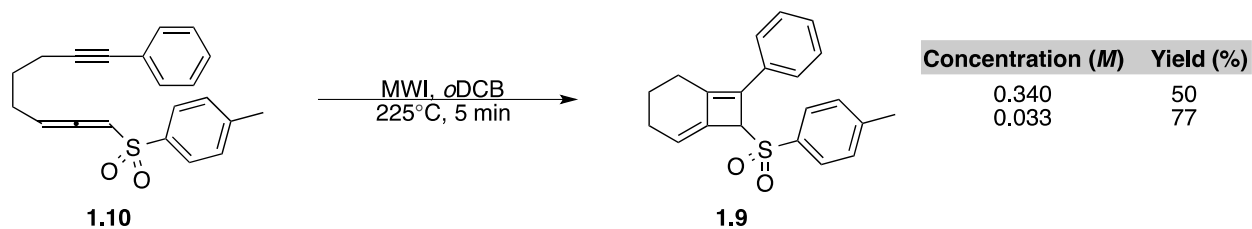


Scheme 1.2. Synthesis of allene-yne **1.10**

As a precedent for the subsequent thermal [2+2] reaction, Mukai reported heating heteroatom substituted allene-yne **1.16** in xylene at reflux for 2 h to obtain alkylidene cyclobutene **1.17** in 53% yield (Scheme 1.3).¹⁰ Additionally, when allene-ynes **1.18** and **1.20** were heated in mesitylene at 180 °C for 2 h, alkylidene cyclobutenes **1.19** and **1.20** were obtained in 51% and 47% yields respectively.¹⁰ We were pleased to find that when subjecting allene-yne **1.10** – with an all carbon tether – to microwave irradiation at 225 °C for 5 min in 1,2-dichlorobenzene at a concentration of 0.3 M, a 50% yield of alkylidene cyclobutene **1.9** was obtained, roughly matching Mukai’s yield (Scheme 1.4). It was postulated that decreasing the concentration would limit intermolecular reactions and increase the yield of the intramolecular transformation. Indeed, upon dilution to 0.03 M, a 77% yield of alkylidene cyclobutene **1.9** was achieved.

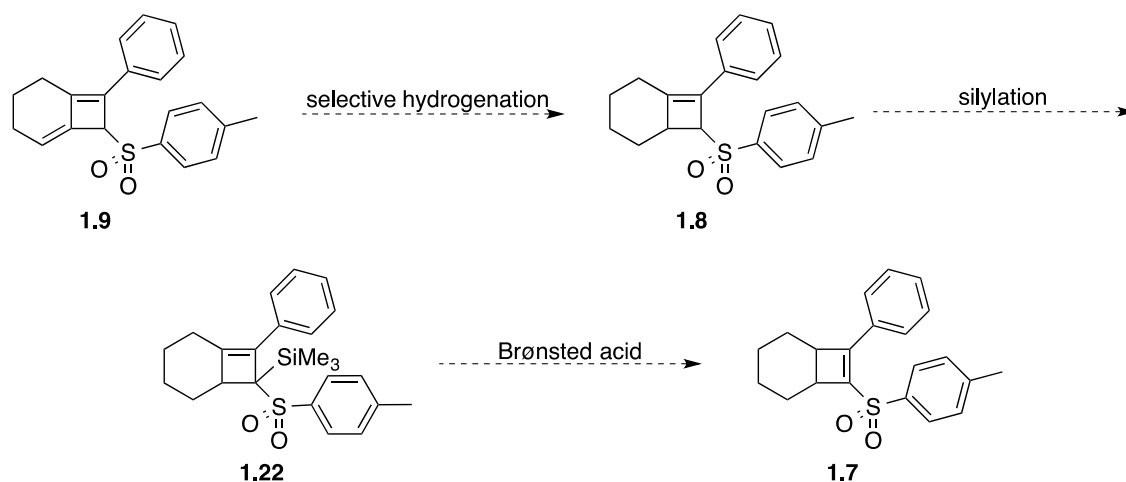


Scheme 1.3. Mukai's thermal [2+2] results with heteroatom and malonate tethers



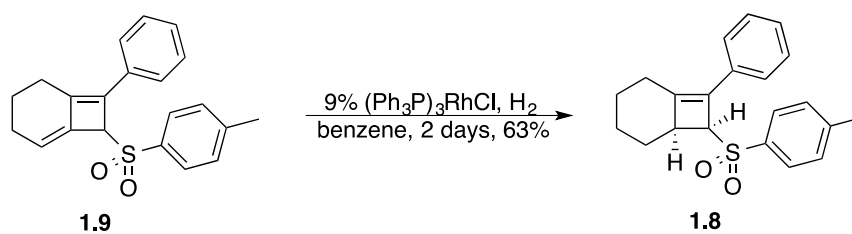
Scheme 1.4. Our thermal [2+2] results with an all carbon tether

With alkylidene cyclobutene **1.9** in hand, we envisioned a selective hydrogenation on the trisubstituted olefin in **1.9** to generate cyclobutene **1.8**. Subsequently, we expected that a silylation to give **1.22** followed by a proto-desilylation would furnish **1.7** (Scheme 1.5).



Scheme 1.5. Proposed pathway from **1.9** to **1.7**

Attempted selective reduction of the tri-substituted olefin in alkylidene cyclobutene **1.9** with palladium on carbon under H₂ atmosphere yielded complex mixtures. However, we found that (Ph₃P)₃RhCl (Wilkinson's catalyst) in benzene under H₂ atmosphere was able to selectively reduce the tri-substituted double bond cleanly. We were able to reduce the catalyst loading to 9 mol%, which provided cyclobutene **1.8** after stirring for 2 days in 63% yield (Scheme 1.6).



Scheme 1.6. Optimized hydrogenation conditions

Wilkinson's catalyst is unreactive towards tetra-substituted double bonds and displays limited reactivity towards tri-substituted double bonds.¹¹ However, the relief of ring strain in **1.9** provides an extra driving force for the hydrogenation to take place. Although Wilkinson's catalyst can be directed by pendent polar groups,¹² a crystal structure of **1.8** showed syn

hydrogens on the cyclobutene ring (Figure 1.2), revealing that hydrogenation had occurred on the more sterically accessible face (Figure 1.3).

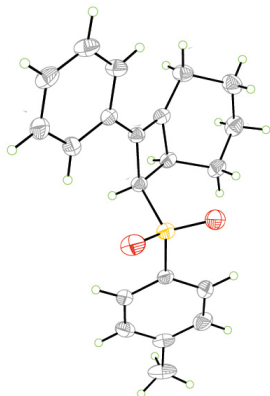


Figure 1.2. X-ray crystal structure of **1.8**

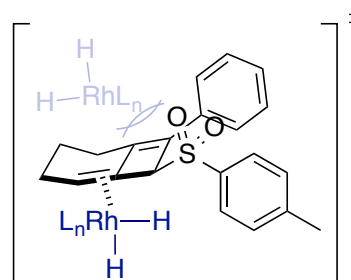
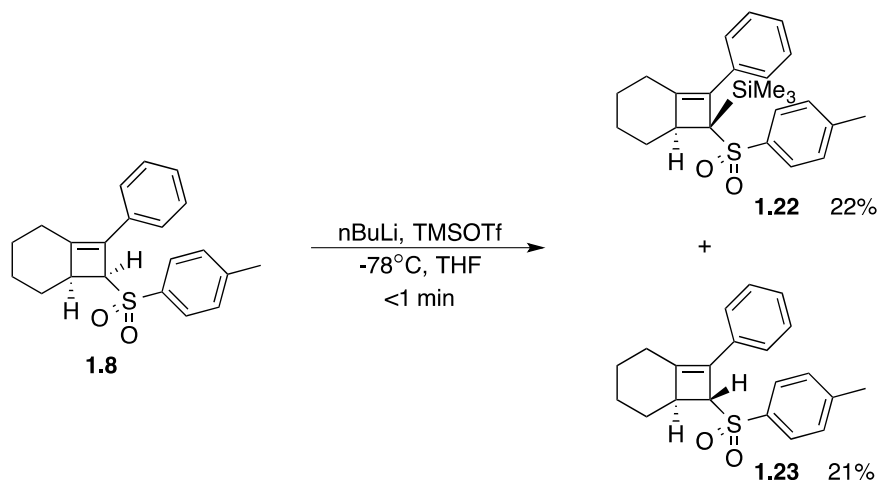


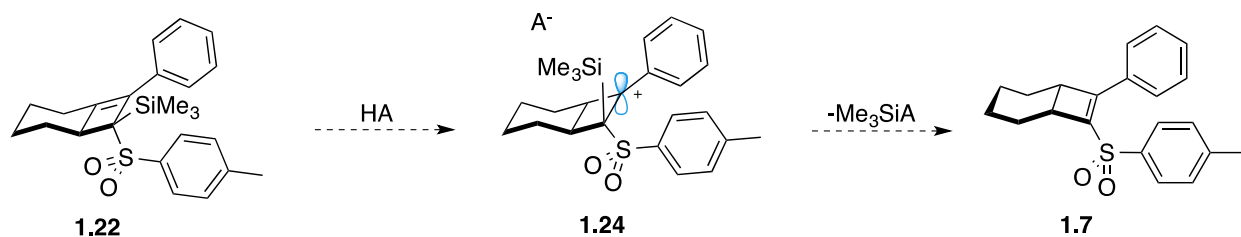
Figure 1.3. Rationale for observed syn hydrogens in **1.8**

With cyclobutene **1.8** in hand, we planned to migrate the cyclobutene alkene to the desired position in **1.7** via a silylation and proto-desilylation strategy.⁵ Silylation of **1.8** with butyllithium and trimethylsilyl triflate afforded both the desired silylated cyclobutene product **1.22** in low yield (22%) with a significant amount of stereoinverted starting material (21%) **1.23** – evidently a result of anion inversion (Scheme 1.7). The identity of **1.23** was confirmed after subjecting it to the silylation conditions and obtaining the same mixture of **1.22** and **1.23**. The relative configuration of **1.22** was extrapolated after inducing a thermal electrocyclic ring opening and obtaining an X-ray crystal structure of the resulting diene (Figure 1.6).



Scheme 1.7. Result of silylation

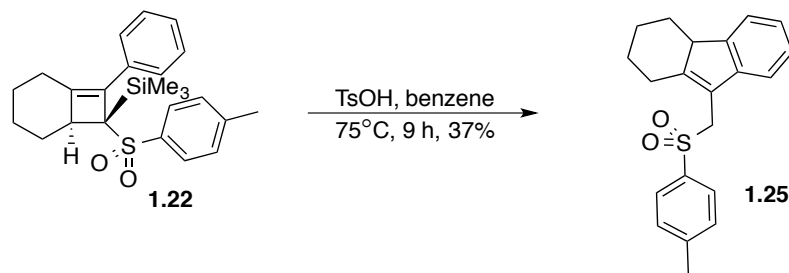
We predicted that exposure of silylated cyclobutene **1.22** to a Brønsted acid would result in protonation of the olefin at the ring fusion, generating benzylic cation **1.24**. Subsequent hyperconjugative stabilization by the C – Si sigma bond and eventual loss of the trimethylsilyl group would provide vinyl sulfone **1.7** (Scheme 1.8).



Scheme 1.8. Predicted outcome of proto-desilylation

Initial conditions for the proto-desilylation of **1.22** were taken from Funk.⁵ A 0.08 M solution of silylated cyclobutene **1.22** in benzene was stirred with 1 equiv of TsOH. After gradual heating, the reaction mixture was stirred at 75 °C for 9 h, at which point starting material had disappeared by TLC. Purification of the crude material resulted in isolation of only one clean product – tetrahydrofluorene **1.25** in 37% yield (Scheme 1.9). Evidence for the structure of tetrahydrofluorene **1.25** includes ¹H NMR chemical shifts of the benzylic proton at 3 ppm (dd, *J* = 12.4, 6.0 Hz) and the protons on the sulfone's alpha carbon at 4.32 ppm (ABq, 2H, Δδ_{AB} =

0.12, $J_{AB} = 14.2$ Hz) (Figure 1.4). The identity of tetrahydrofluorene **1.25** was confirmed by an X-ray crystal structure (Figure 1.5).



Scheme 1.9. Initial reaction to form tetrahydrofluorene **1.25**

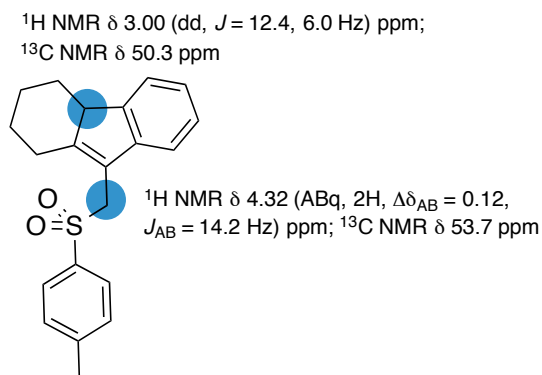


Figure 1.4. $^1\text{H NMR}$ and $^{13}\text{C NMR}$ evidence for **1.25**

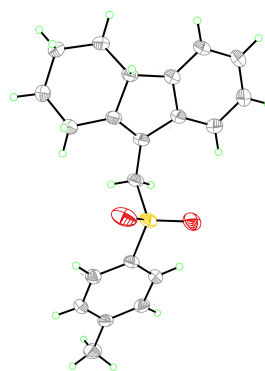
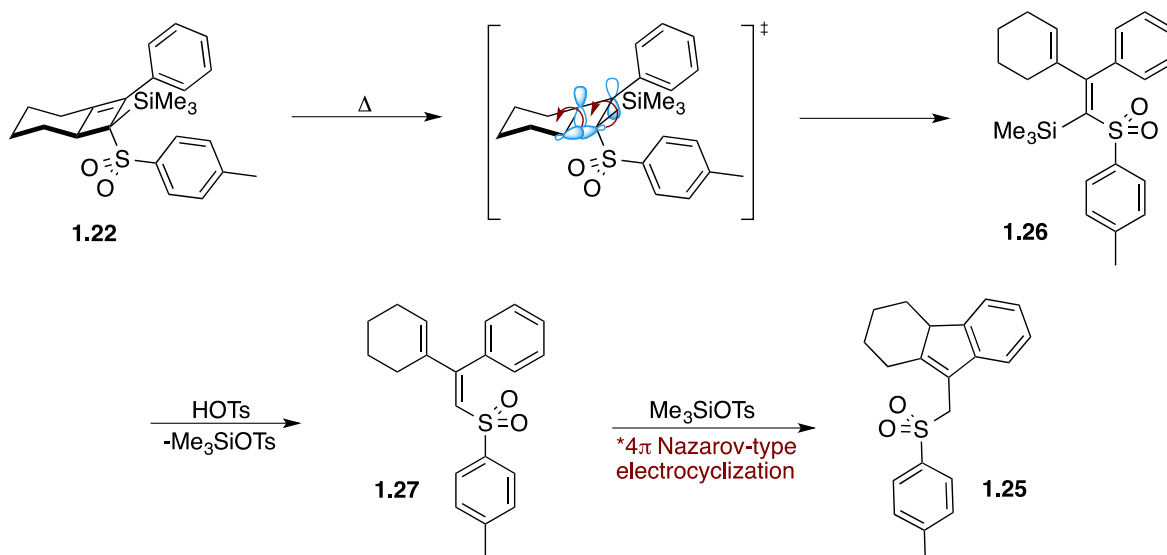


Figure 1.5. X-ray crystal structure of **1.25**

1.2 PROPOSED MECHANISM OF REACTION

Scheme 1.10 shows a proposed mechanism to account for the formation of this unexpected product. Thermally induced 4π electrocyclic ring opening of cyclobutene **1.22** generates silylated diene **1.26** (Scheme 1.10). Proto-desilylation of vinyl silane **1.26** with TsOH furnishes diene **1.27**. It is proposed that upon exposure to the trimethylsilyl group – acting as a Lewis acid¹³ – diene **1.27** undergoes a Nazarov-type¹⁴ 4π electrocyclization (Section 2.3) to give

tetrahydrofluorene **1.25**.



Scheme 1.10. Proposed mechanism to account for the formation of tetrahydrofluorene **1.25**

To test the mechanism, proposed intermediates were subjected to the reaction conditions on a sub 10 mg scale. Silylated diene **1.26** was obtained as the sole product from the thermally induced conrotatory 4π electrocyclic ring opening of silylated cyclobutene **1.22** and its identity was confirmed by an X-ray crystal structure (Figure 1.6). The exclusive torquoselectivity of the electrocyclic ring opening is the result of the formation of a highly strained trans double bond in a cyclohexene ring in the alternative product. When silylated diene **1.26** was exposed to TsOH acid in benzene at 68 °C, tetrahydrofluorene **1.25** was obtained, supporting the mechanistic proposal (Scheme 1.11). Additionally, since the proto-desilylation of the vinyl silane occurs in the subsequent step, subjecting diene **1.28** – obtained from the thermally induced 4π electrocyclic ring opening of cyclobutene **1.8** – to the reaction conditions should also yield tetrahydrofluorene **1.25**. However, at that point in the proposed mechanism, there is also a trimethylsilyl group in solution. As a result, trimethylsilyl triflate was added in order to recreate the conditions in the flask at the time the intermediate formed. Although diene **1.28** is the

opposite geometrical isomer of proposed intermediate diene **1.27**, this difference should not affect the outcome of the reaction. When diene **1.28** was subjected to TsOH and trimethylsilyl triflate in benzene at 80 °C overnight, tetrahydrofluorene **1.25** was obtained, also supporting the mechanism (Scheme 1.11).

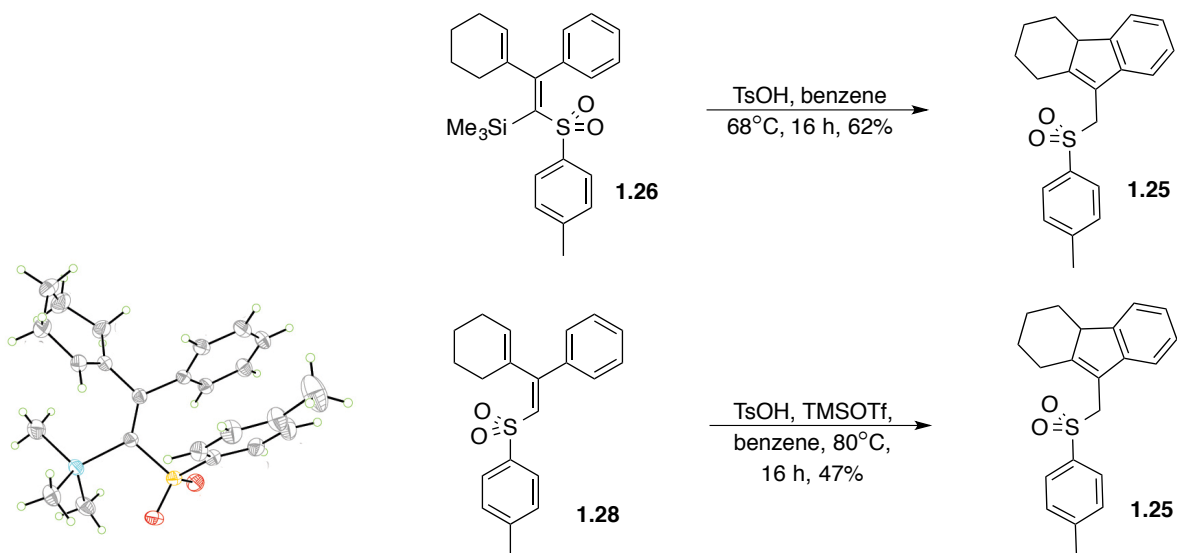
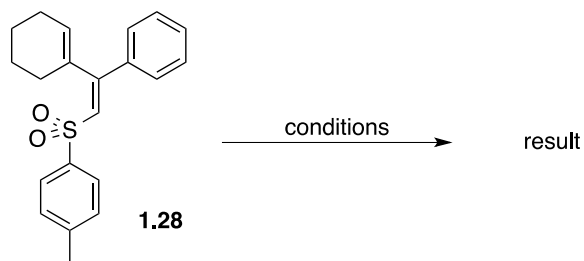


Figure 1.6. X-ray crystal structure of **1.26** **Scheme 1.11.** Subjecting proposed intermediates to reaction conditions

To determine what – the trimethylsilyl group, TsOH, or heat – was promoting the cyclization, diene **1.28** was subjected to 3 reactions. First, diene **1.28** was heated in benzene at 75 °C for 16 h, yielding only recovered starting material (Table 1.1, entry 1). When diene **1.28** was subjected to TsOH at room temperature for 3 h, no change occurred by TLC (entry 2). As a result, the reaction was heated to 75 °C for an additional 20 h, giving a complex mixture with only a trace amount of tetrahydrofluorene **1.25** (entry 3). When diene **1.28** was subjected to an equivalent of trimethylsilyl triflate at room temperature for 23 h, 70% conversion to tetrahydrofluorene **1.25** was observed by ¹H NMR (entry 4), revealing that the trimethylsilyl group acted as the promoter for the cyclization.

Table 1.1. Determination of reagent that promotes cyclization



entry	conditions	result
1	benzene, 75 °C, 16 h	recovered s.m.
2	HOTs, benzene, rt, 3 h	recovered s.m.
3	HOTs, benzene, 75 °C, 20 h	complex mixture
4	TMSOTf, benzene, rt, 23 h	70% ¹ H NMR conversion to 1.25

These preliminary studies supported the proposed mechanism and revealed that the cyclization could proceed directly from diene **1.28** with a Lewis acid. As a result, the low yielding silylation step could be avoided.

Due to this vinyl sulfonyl Nazarov cyclization's potential as a powerful method to prepare the privileged tetrahydrofluorene scaffold and the diverse array of further functionalization made possible by the allyl sulfone, the transformation warranted further study.

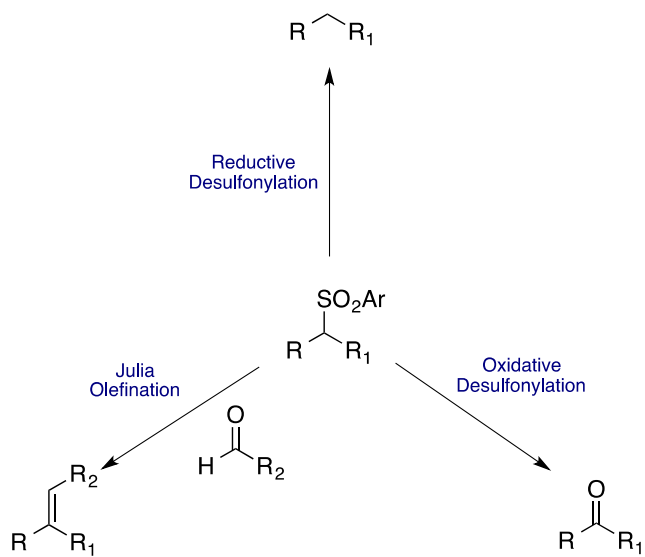
2.0 POTENTIAL UTILITY AND PRECEDENCE OF SULFONYL FUNCTIONALIZED TETRAHYDROFLUORENES

2.1 THE SULFONE MOIETY

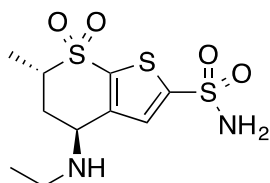
Often referred to as a chemical chameleon, the sulfone moiety is a versatile organic functional group.¹⁵ Traditionally, sulfones are introduced within a synthetic sequence – their reactivity exploited for a desired transformation – and removed prior to the final product.¹⁶ Aryl sulfonyl synthons in particular are widely used because of their facile introduction and removal, affordability, and tendency to give crystalline intermediates for easy purification.¹⁵

While aryl sulfones are commonly exploited to acidify protons on their alpha carbons, they can also be readily transformed into other valuable functional groups. For example, saturated aryl sulfones can be reacted with an oxidant to give aldehydes or ketones (Scheme 2.1). Additionally, sulfones and aldehydes can be coupled together to give E-alkenes with the Julia olefination.

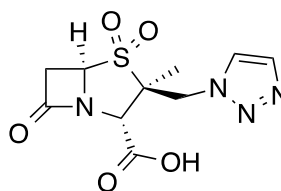
Recently, however, the sulfone has been gaining prominence as a component of final compounds with medicinal or functional utility.¹⁶ Some sulfone bearing prescription drugs include Dorzolamide (**2.1**) and Tazobactam (**2.2**).¹⁷ Prescription drugs containing the aryl sulfone motif include the former drug Vioxx (**2.3**), Eletriptan (**2.4**), Dapsone (**2.5**), Erivedge (**2.6**), and Bicalutamide (**2.7**).¹⁸



Scheme 2.1. Some general transformations of aryl sulfones¹⁶



Dorzolamide (2.1)
Anti-glaucoma agent



Tazobactam (2.2)
Antibiotic

Figure 2.1. Select sulfone-containing prescription drugs¹⁷

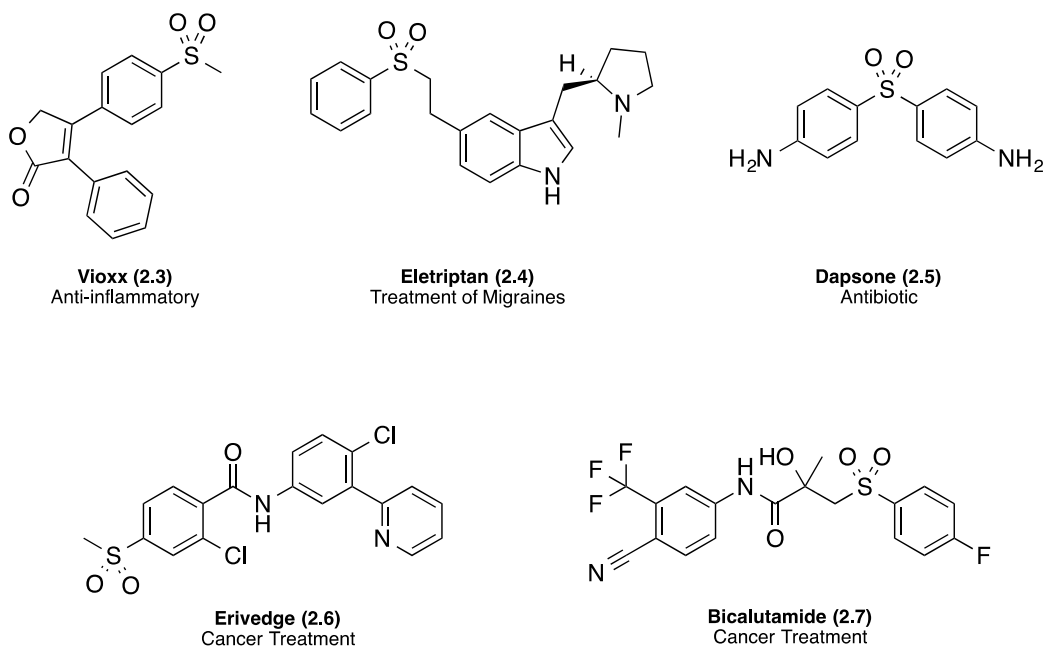


Figure 2.2. Select prescription drugs containing the aryl sulfone motif¹⁸

2.2 THE [6,5,6]-SYSTEM IN BIOLOGICALLY ACTIVE NATURAL PRODUCTS

Beyond the opportunities for accessing new chemical space provided by the sulfone, the prevalence of the carbon skeleton in **1.25** provides opportunities for applications of the transformation to existing spheres of interest. The [6,5,6]-ring system is most notably present in the gibberellins and taiwaniaquinoids. The gibberellins are a set of over a hundred highly functionalized diterpenoids – a few are sold commercially in agriculture as plant hormones that regulate growth and influence a variety of developmental processes.¹⁹

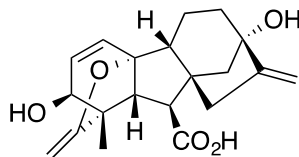


Figure 2.3. Gibberellic acid (**2.8**)¹⁹

The gibberellins are typified by gibberellic acid (**2.8**), which is produced in the ton quantities by the fermentation of the fungus *Gibberella fujikuroi*. A method to access novel derivatives of these structures could lead to new agricultural products with unique biological effects.¹⁹

The taiwaniaquinoids include 12 diterpenes that were isolated from *Taiwania cryptomerioides*, a threatened tree species indigenous to Taiwan. The activities of these compounds were tested against human oral epidermoid carcinoma KB cells using the clinically used chemotherapeutic drug etoposide as a positive control. Taiwaniaquinol D (**2.9**) and taiwaniaquinone F (**2.10**) showed the most activity – around a third and a quarter of etoposide respectively. Four other taiwaniaquinoids showed weak activity, and the rest were inactive. All of the active compounds contained a formyl substituent at C9 of the tetrahydrofluorene skeleton, while all but one of the inactive compounds contained no carbon substituent at that position. This observation led the author of the study to conclude that the formyl substituent plays an important role in antitumoral cytotoxic activity.²⁰

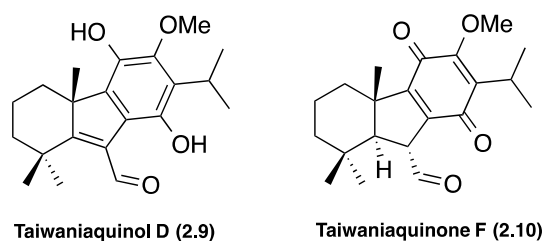


Figure 2.4. Select taiwaniaquinoids

Given the promising anticancer activity of these compounds, several syntheses of the taiwaniaquinoids have been reported. As for the synthesis of the compound bearing the most activity – **2.9** – four syntheses have been reported. Installation of the formyl group has invariably

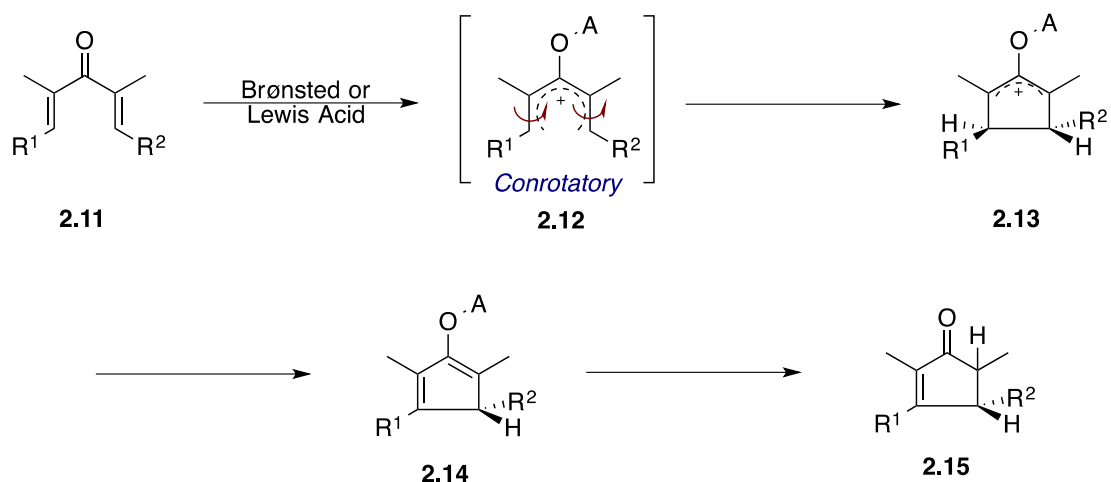
been the last step. Trauner²¹ and Majetich²² utilized a Nazarov cyclization followed by a multistep elaboration of the resulting ketone to a formyl group. Li²³ reported a ring contraction by a Wolff rearrangement followed by a multistep reduction of the resulting ester to an aldehyde, while Alvarez-Manzaneda²⁴ reported a Heck cyclization, oxidation and ketone elaboration procedure.

Beyond allowing for new substitution patterns, using the vinyl sulfonyl Nazarov cyclization followed by a one-step oxidative desulfonylation procedure could allow for a more efficient synthesis of compounds of this type.

2.3 THE NAZAROV CYCLIZATION

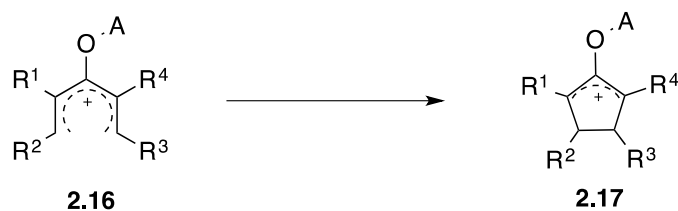
2.3.1 The Classical Reaction

Nazarov cyclization terminology was originally limited to a Lewis acid or Brønsted acid promoted transformation of divinyl ketones into substituted cyclopentenones. The reaction commences with acid coordination to dienone **2.11** to form pentadienyl cation **2.12**. Conrotatory 4π electrocyclization affords oxallyl cation **2.13**. Deprotonation to **2.14** followed by protonation of the enolate furnishes cyclopentenone **2.15**.¹⁴



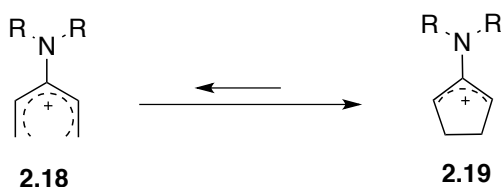
Scheme 2.2. General mechanism of the Nazarov cyclization¹⁴

While the Nazarov cyclization has excellent potential as a stereospecific method to give 5-membered carbocycles, it has historically been underutilized due to significant limitations in its application to synthesis. These limitations include the need for super-stoichiometric quantities of either a strong Brønsted or Lewis acid on unactivated substrates, the lack of regioselectivity in the deprotonation step, the loss of a stereocenter due to deprotonation, and the lack of stereoselectivity in the protonation of the enolate.¹⁴ Recently, however, general rules governing the favorability of the cyclization has made possible the use of catalytic and mild acids to achieve cyclization for activated substrates.¹⁴ As a general rule, substituents that stabilize oxallyl cation **2.17** over pentadienyl cation **2.16** – termed activated substrates – favor cyclization. On the other hand, substituents that stabilize pentadienyl cation **2.16** over oxallyl cation **2.17** – termed deactivated substrates – disfavor cyclization.¹⁴



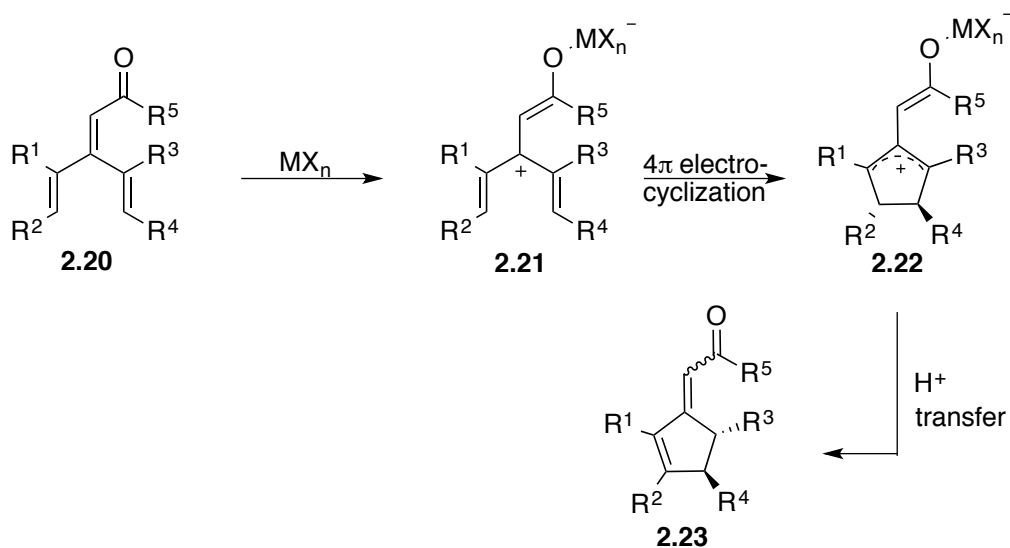
Scheme 2.3. Key step in the Nazarov cyclization

Recently, a few reports²⁵ of divinyl imine cyclizations have appeared in the literature. Because the nitrogen lone pair stabilizes pentadienyl cation **2.18** over allylic cation **2.19**,²⁶ more activated substrates are required to push the cyclization forward. Due to this inherent challenge, the imino-Nazarov variant has so far been less useful than its keto congener.



Scheme 2.4. Pentadienyl cation favored for imino-Nazarov variant

As an extension of the Nazarov cyclization, West²⁷ has reported a vinylogous Nazarov cyclization, which intercepts the pentadienyl cation through the use of an enone in the 3-position (Scheme 2.5). Presumably due to the thermodynamic stability afforded by conjugation to the carbonyl, all but one of the products gave the exocyclic double bond – providing a mixture of geometrical isomers.



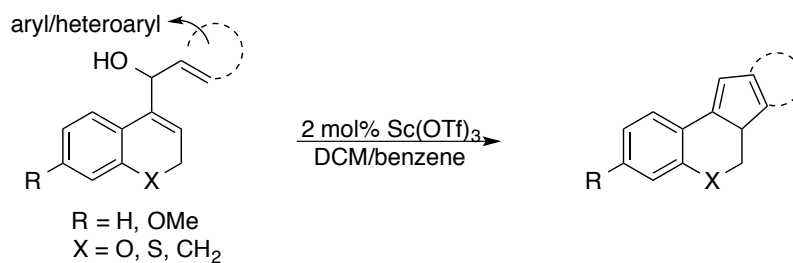
Scheme 2.5. The vinylogous Nazarov reaction²⁷

2.3.2 Nazarov Cyclizations with Aromatic Rings

Nazarov cyclizations with aromatic rings to form indanone derivatives avoid two of the major problems associated with the classical Nazarov cyclization, including regioselective deprotonation and re-protonation due to the thermodynamic favorability of regenerating and maintaining aromaticity. Indeed, Trauner utilized Nazarov cyclizations with aromatic rings to form indanones as the key steps in his synthesis of the taiwaniaquinoids.²¹ However, super-stoichiometric quantities of strong acid are still required to favor cyclization with unactivated systems.²⁸ Recently, however, Frontier has shown that polarized systems involving aromatic rings and hetero-aromatic rings can favor cyclization under catalytic conditions.²⁹

2.3.3 Nazarov Cyclizations to Directly Prepare Indenes

A recent derivation of the aromatic Nazarov cyclization involves the $\text{Sc}(\text{OTf})_3$ catalyzed reaction of aryl and heteroaryl vinyl alcohols to achieve indene core structures (Scheme 2.6).³⁰ For substrates that did not cyclize with $\text{Sc}(\text{OTf})_3$, 1 equiv TfOH in dry benzene was used.



Scheme 2.6. Nazarov variant to construct indene type core structures

Mechanistically, Lewis acid catalyzed expulsion of the alcohol generates the benzylic cation, which subsequently undergoes a Nazarov cyclization to the indene product. The same strategy –

although using 1.5 equiv of SnCl₄ as the Lewis acid – was applied in short syntheses of dichroanone and taiwaniaquinone H.³¹

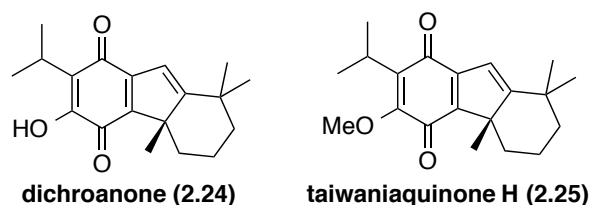
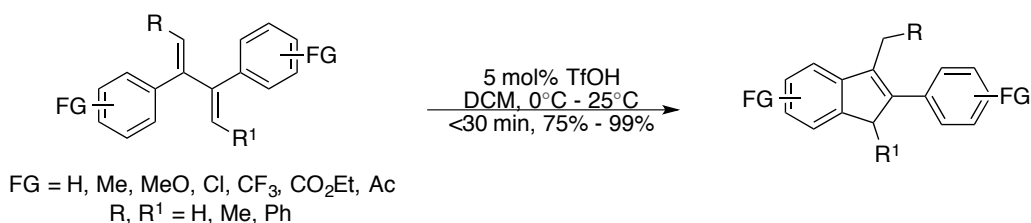


Figure 2.5. Natural products formed by alcohol expulsion and subsequent Nazarov cyclization

A triflic acid catalyzed cyclization of 2,3 aryl substituted 1,3-dienes was reported as a preparative method for aryl substituted indenenes (Scheme 2.7).³² Although the authors propose a Friedel-Crafts cyclization, a 4 π cyclization is more likely based on computational evidence.^{33, 34}



Scheme 2.7. Nazarov variant to construct aryl substituted indenenes³²

Presumably, the triflic acid protonates the olefin adjacent to the more electron rich aromatic ring. Subsequent Nazarov cyclization generates the indene. The other aromatic ring stabilizes the allylic cation intermediate – lowering the activation energy of the cyclization.³³

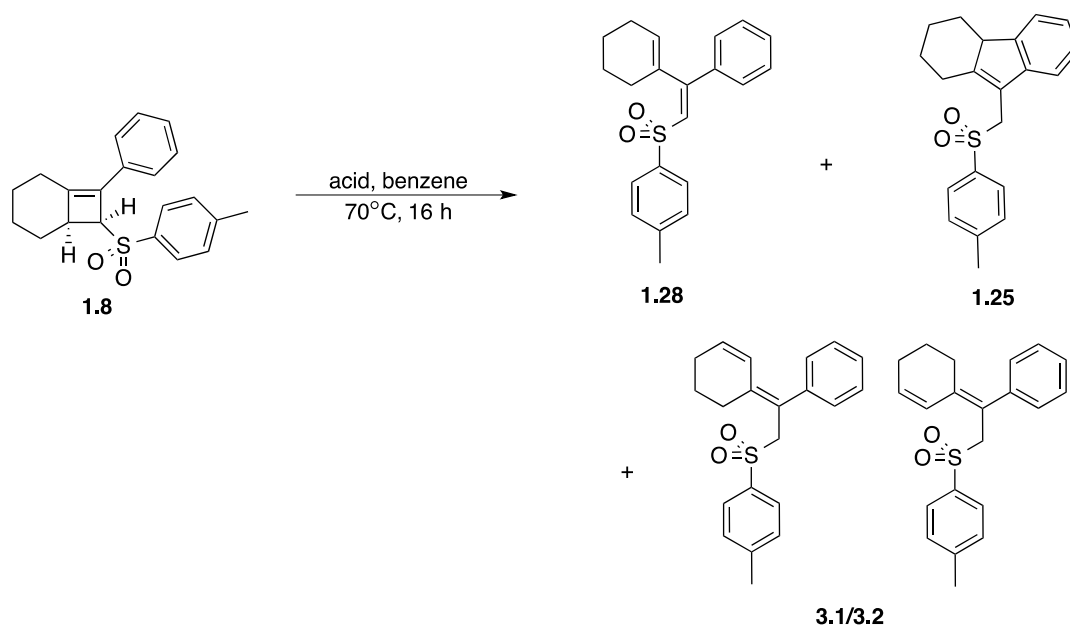
A vinyl sulfonyl Nazarov cyclization would complement these existing cyclization processes by providing new opportunities for both product derivation and further functionalization.

3.0 REACTION OPTIMIZATION

3.1 NMR SCREENING EXPERIMENTS

In order to maximize the utility of the transformation, optimal conditions needed to be found. The first point of variation from the original conditions was the acid. In a typical experiment, 7 mg (0.02 mmol) of cyclobutene **1.8** was stirred with acid (0.5 equiv) in benzene (0.7 mL) at 70 °C. A ¹H NMR of the resulting crude product mixture was taken and the percentage of each species was determined. During the optimization process, three major products were observed. Diene **1.28** (the result of heating the starting material), the desired tetrahydrofluorene **1.25**, and a mixture proposed to be the diene isomerized products **3.1/3.2** (Scheme 3.1).

Figure 3.1 shows the key resonances that were used in determining the ratio of the compounds. The cyclohexene proton at 5.75 – 5.66 ppm (m) in diene **1.28** and the benzylic proton at the ring fusion of tetrahydrofluorene **1.25** at 3.00 ppm (dd, $J = 12.4, 6.0$ Hz) provided isolated peaks for ratio determination. Compounds **3.1/3.2** could not be separated, so evidence for their structures comes from the alkenyl protons – protons H₁ and H₃ resonate at 5.96 and 5.81 (dt, $J = 10.1, 4.0$ Hz) ppm while protons H₂ and H₄ resonate at 6.42 and 6.04 (dt, $J = 10.0, 1.8$ Hz) ppm (Figure 3.1). The triplet coupling values differentiate these two sets of protons.



Scheme 3.1. Different products observed during acid screen

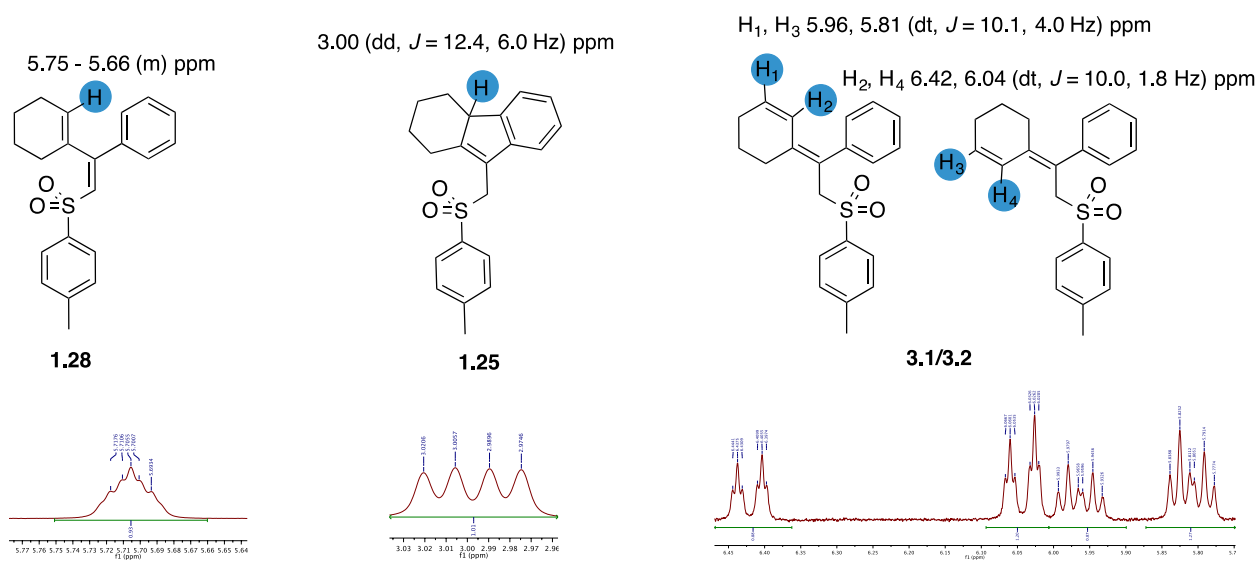


Figure 3.1. Key ^1H NMR resonances used to determine product ratio

Of the 8 acids screened, 4 gave either a complex mixture or exclusively diene **1.28** (Table 3.1, entries 5-8, ^1H NMRs for each entry are included in the Appendix). Trifluoroacetic acid (entry 1) and tin(IV) chloride (entry 3) gave only minimal conversion to diene isomerized

mixture **3.1/3.2** and the desired tetrahydrofluorene **1.25** respectively.

Table 3.1. Crude ¹H NMR results of screening different acids^{a, b}

entry	acid	1.28 (%)	1.25 (%)	3.1/3.2 (%)
1	TFA ^c	83	0	17
2	FeCl ₃	26	74	0
3	SnCl ₄	73	27	0
4	Cu(OTf) ₂	0	38	62
5	Sc(OTf) ₃ ^d	0	39	61
6	BF ₃ •OEt ₂		<i>Recovered 1.28</i>	
7	AlCl ₃		<i>Complex mixture^e</i>	
8	TiCl ₄		<i>Complex mixture^e</i>	

^aConditions: 7 mg **1.8** was heated to 70°C with acid (0.5 equiv) in 0.7 mL of benzene for 16 h. ^bUnless otherwise noted, ratios were determined from the integration of the cyclohexene proton in diene **1.28**, the integration of the benzylic proton in tetrahydrofluorene **1.25**, and half of the total integration of the alkenyl protons in the diene isomerized mixture **3.1/3.2**. The ratio of **3.1/3.2** was determined from half the integration of the alpha sulfonyl protons. ^dOther products were also present. ^eDiene **1.28** and tetrahydrofluorene **1.25** were components in the mixture.

By far the cleanest result was obtained with iron(III) chloride (entry 2), with 74% exclusive conversion to tetrahydrofluorene **1.25**, while copper(II) triflate afforded a 38:62 mixture of tetrahydrofluorene **1.25** and diene isomerized mixture **3.1/3.2** (entry 4).

As a result, iron(III) chloride, copper(II) triflate, and the original promoter trimethylsilyl triflate were each screened against 3 different solvents – DCE, 1,4-dioxane, and toluene. These solvents were chosen due to their capability of heating the cyclobutene to the point of electrocyclic ring opening while still providing a facile product isolation.

Table 3.2. Crude ¹H NMR results of screening different solvents with select acids^{a,b}

entry	acid	solvent	1.28 (%)	1.25 (%)	3.1/3.2 (%)
1		DCE	0	100	0
2	FeCl ₃	1,4-dioxane	100	0	0
3		Toluene ^c	0	100	0
4		DCE	0	100	0
5	Cu(OTf) ₂	1,4-dioxane ^c	100	0	0
6		Toluene	0	0	100
7		DCE ^c	0	100	0
8	TMSOTf	1,4-dioxane ^c	41	0	59
9		Toluene ^c	0	100	0

^aConditions: 7 mg **1.8** was heated to 70°C with acid (0.5 equiv) in 0.7 mL of solvent for 16 h. ^bRatios were determined from the integration of the vinyl sulfone proton in diene **1.28**, the integration of the benzylic proton in tetrahydrofluorene **1.25**, and half of the total integration of the alkenyl protons in the diene isomerized mixture **3.1/3.2**. ^cOther products were also present.

With DCE, copper(II) triflate and iron(III) chloride gave exclusively and cleanly tetrahydrofluorene **1.25** (Table 3.2, entries 1 and 4, ¹H NMRs for each entry are included in the Appendix). In toluene, however, copper(II) triflate gave exclusively the diene isomerized mixture **3.1/3.2** (entry 6), while iron(III) chloride gave relatively clean conversion to the tetrahydrofluorene **1.25** (entry 3), but not as clean as with dichloroethane. Hardly any reaction was observed in 1,4-dioxane with copper(II) triflate or iron(III) chloride (entries 2 and 5). As for trimethylsilyl triflate, full conversion to tetrahydrofluorene **1.25** was observed – with some baseline impurities – in DCE and toluene (entries 7 and 9), and some conversion to the diene isomerized mixture **3.1/3.2** occurred in 1,4-dioxane (entry 8). We do not have an explanation for these unusual solvent effects.

3.2 OPTIMIZATION OF REACTION ON A 50 MILLIGRAM SCALE

Based on the crude ^1H NMR screenings, the most promising acid solvent combinations were copper(II) triflate with DCE and iron(III) chloride with DCE. As a result, both sets of conditions were scaled up from 0.02 mmol (7 mg) to 0.15 mmol (50 mg) cyclobutene **1.8**. Unfortunately, on the larger scale, the reaction with copper(II) triflate gave a 30:70 mixture of tetrahydrofluorene **1.25** and the diene isomerized mixture of **3.1/3.2** respectively by crude ^1H NMR. As a result, a scale up of the iron(III) chloride reaction in dichloroethane was performed. Although iron(III) chloride gave exclusive conversion to tetrahydrofluorene **1.25**, there were problems with the reaction stalling after one night of stirring. This could be due to the consumption of iron(III) chloride by trace amounts of water to give $\text{Fe}(\text{OH})_3$, HCl , and heat.³⁵ The equilibrium is driven to the right with heat (Scheme 3.2).



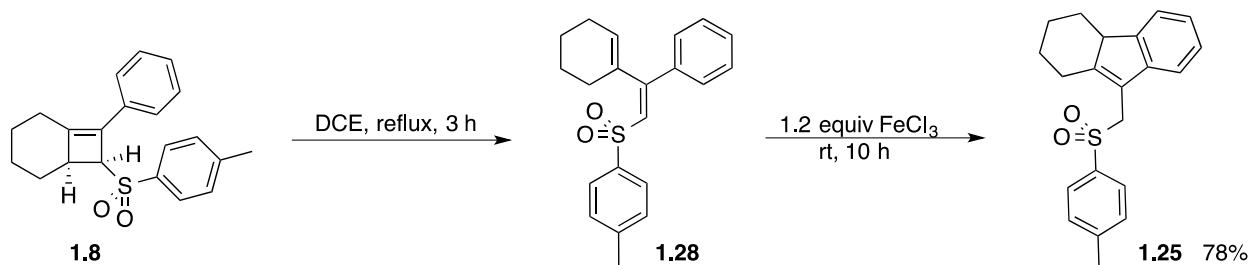
Scheme 3.2. Consumption of FeCl_3 by water

In order to minimize this process, it was decided to make the reaction two steps – albeit still in one pot. In the first step, the electrocyclic ring opening of cyclobutene **1.8** would take place by refluxing the cyclobutene in 1,2-dichloroethane. Once this step was complete, the reaction would be cooled to room temperature and iron(III) chloride would be added in order to furnish tetrahydrofluorene **1.25**.

This new procedure was attempted with 0.50 equiv of iron(III) chloride, which resulted in the reaction stalling after a day. As a result, another 0.50 equiv of iron(III) chloride was added resulting in the reaction completing after a second day in 68% yield. To be sure that the amount

of catalyst spread over the two days could not be reduced, another reaction was attempted where the first dose was 0.25 equiv of iron(III) chloride. Unfortunately, this resulted in almost no conversion overnight. As a result, the reaction was attempted with 1 equiv of iron(III) chloride, which resulted in nearly full conversion to tetrahydrofluorene **1.25** overnight in 72% yield. In order to remove all trace of starting material from the crude product, the loading of iron(III) chloride had to be increased slightly.

The transformation of model cyclobutene **1.8** to tetrahydrofluorene **1.25** was optimized to the following conditions: a solution of cyclobutene **1.8** in DCE (0.03 M) was refluxed for 3 h to generate diene **1.28**. Upon cooling to room temperature, 1.2 equiv FeCl₃ was added. The reaction was stirred for an additional 10 h to furnish tetrahydrofluorene **1.25** in 78% yield (Scheme 3.3).

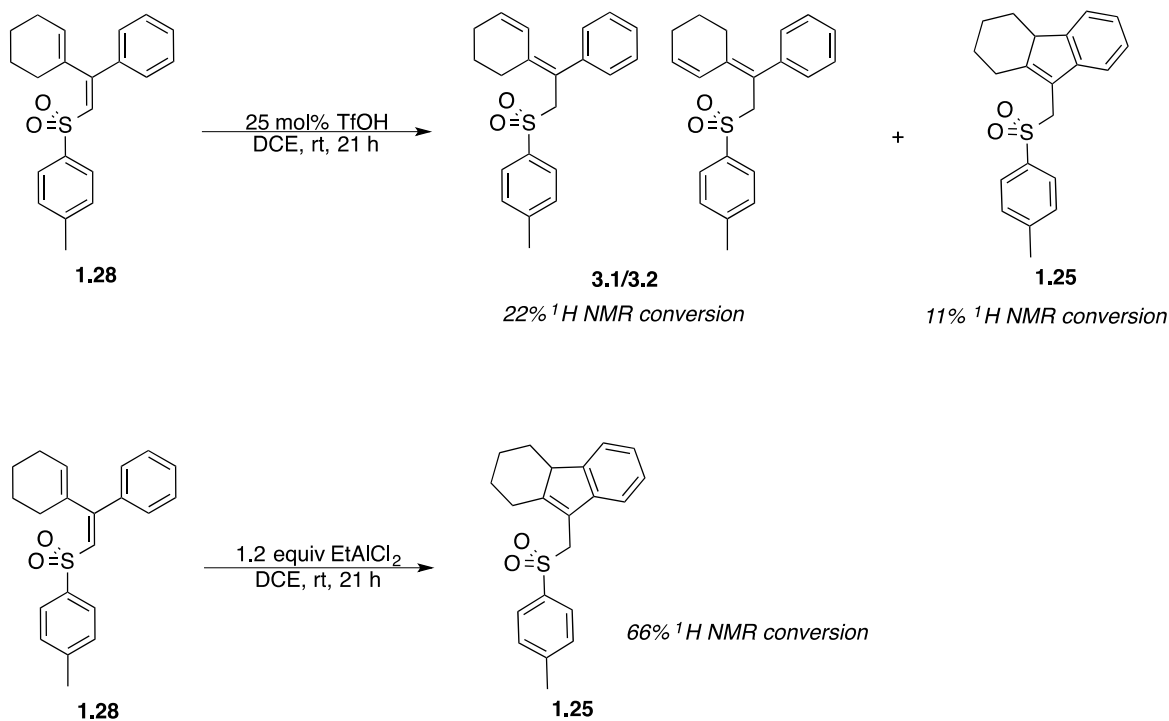


Scheme 3.3. Optimized conditions

3.3 EVIDENCE FOR LEWIS ACID CATALYSIS

In order to confirm that iron(III) chloride acts as a Lewis acid to promote cyclization of diene **1.28** to tetrahydrofluorene **1.25** rather than trace amounts of Brønsted acid in the reagent, two additional reactions were performed. To determine if a strong Brønsted acid may afford tetrahydrofluorene **1.25**, diene **1.28** was subjected to 25 mol% TfOH in DCE at room

temperature. After 21 h, a ^1H NMR spectrum of the worked up reaction product revealed a 6:2:1 ratio of starting material **1.28**, the diene isomerized mixture of **3.1/3.2**, and tetrahydrofluorene **1.25** (Scheme 3.4). Because of the low conversion of starting material and only trace amount of tetrahydrofluorene **1.25** formed, it was concluded that a trace amount of TfOH could not be predominantly responsible for the reaction in cases where it would be a contaminant in the Lewis acid. In order to prove that a Lewis acid could effect the transformation, diene **1.28** was subjected to 1.2 equiv of ethylaluminum dichloride – a reagent that is both a Lewis acid and a Brønsted base³⁶ – at room temperature in dichloroethane. Stirring for 21 h resulted in a 2:1 mixture of tetrahydrofluorene **1.25** to starting diene **1.28** plus minor baseline impurities. Because ethylaluminum dichloride was able to transform most of diene **1.28** to tetrahydrofluorene **1.25**, it was concluded that a Lewis acid is responsible for the transformation.



Scheme 3.4. Diagnostic reactions to determine whether transformation is promoted by a Lewis or Brønsted acid

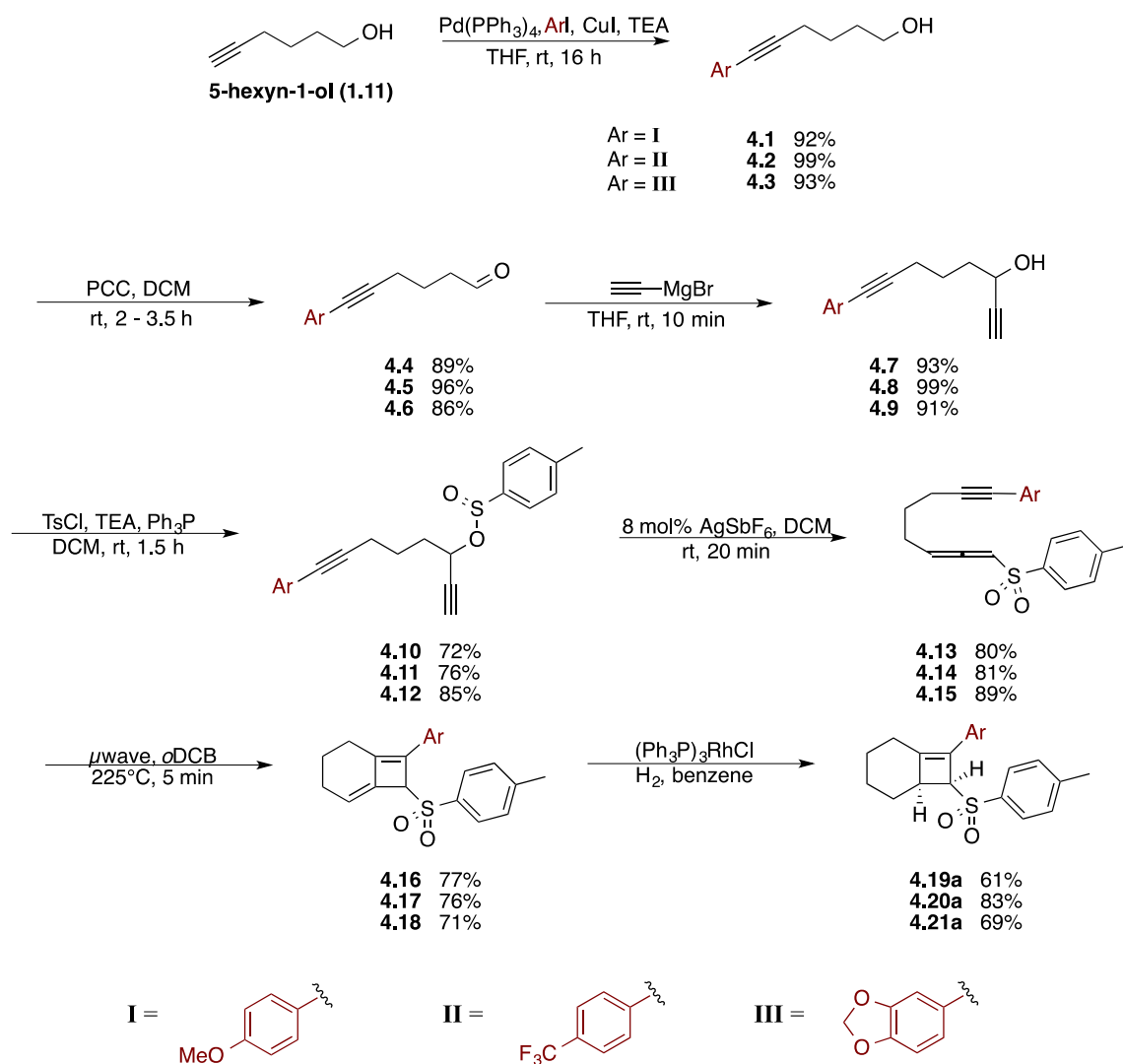
Because the sulfone is the only polarized group on diene **1.28**, and due to scattered reports of the sulfone moiety being sensitive to Lewis acid,¹³ it is proposed that the Lewis acid coordinates to the sulfone to afford the cyclization.

3.4 A NOTE ON THE DIENYL SULFONE MOIETY

In light of the mild conditions to effect transformation of diene **1.28** to indene **1.25** on an unactivated system, an extra driving force related to the dienyl sulfone moiety – a uniquely reactive functionality – is proposed. Many dienyl sulfones polymerize on standing,³⁷ are prone to self-dimerization through Diels-Alder reactions,^{37, 39} and are the only general class of 1,3 dienes that react with both electron rich and electron deficient dienophiles.³⁷ Because of their reactivity, isolating and characterizing dienyl sulfones can be a challenge.^{38, 39} Although diene **1.28** is not as prone to polymerization as less substituted 1-sulfonyl 1,3 dienes,^{38, 39} an advantage of our method is that cyclobutene **1.8** is a stable source of diene **1.28**. As a result, the reactive diene **1.28** is formed in situ. Although the source of the reactivity of some dienyl sulfones has yet to be described in the literature, it may be related to the thermodynamic stability of olefins in the allylic position of sulfones over ones in the vinylic position in most systems.⁵

4.0 EFFECT OF ELECTRONIC PERTURBATION OF PHENYL RING ON TRANSFORMATION

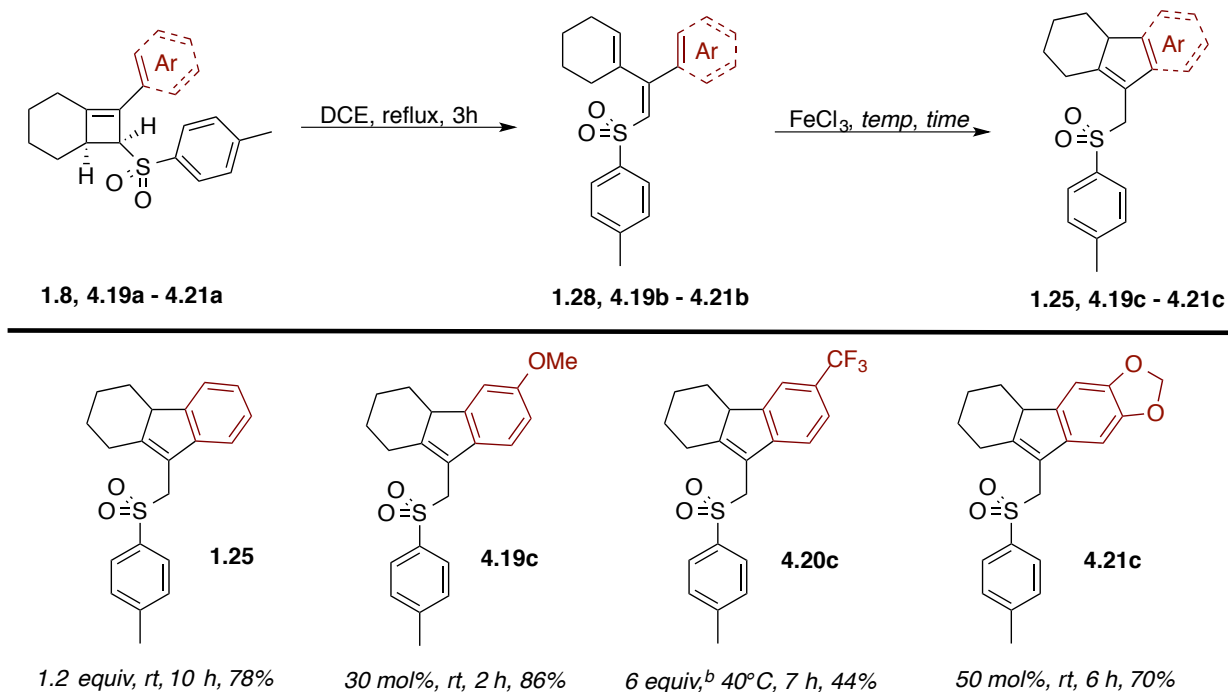
Cyclobutenes with functionality introduced onto the aryl ring were prepared in the same manner as cyclobutene **1.8** (Scheme 4.1) with no major differences in yield.



Scheme 4.1. Synthesis of cyclobutenes with variations on the aryl ring

These cyclobutenes were subsequently exposed to the optimized reaction conditions to determine the effect electronics might play in the cyclization process (Table 4.1).

Table 4.1. Exposure of cyclobutenes with variations on the aryl ring to optimized reaction conditions^a



^aYields refer to isolated yields after purification. ^bOver 2 additions.

With a resonance donating *p*-methoxy substituent on the aryl ring (cyclobutene **4.19a**), no effect was observed on the rate of the electrocyclic ring opening. However, exposure of diene **4.19b** to the optimized conditions found for diene **1.28** resulted in nearly immediate transformation to tetrahydrofluorene **4.19c** – having gone to completion by the time the reaction progress was first monitored after 5 min – in 60% yield. Because of the opportunity to reduce the quantity of promoter to catalytic amounts, and due to concern about adding another variable because of the effect of temperature in the hydrolysis of FeCl₃ (Scheme 3.2), the quantity of FeCl₃ was varied as a first measure rather than temperature.

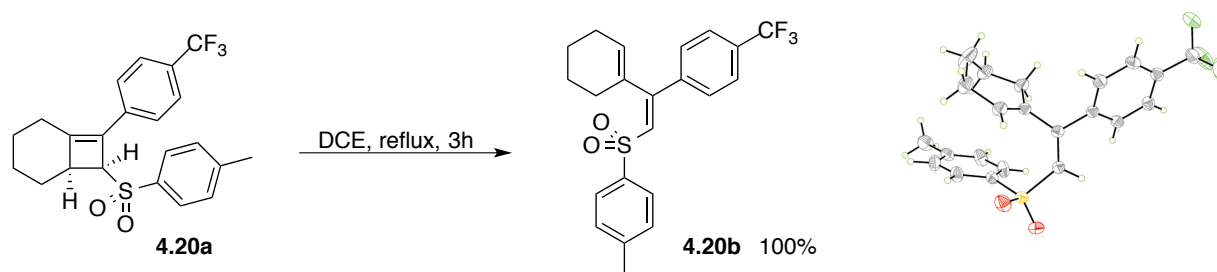
The rate of cyclization proved to be quite sensitive to the quantity of promoter. Only a trace amount of tetrahydrofluorene **4.19c** was detected when diene **4.19b** was exposed to 10

mol% FeCl₃ for 21 h. As a result, the cyclization was attempted with 25 mol% FeCl₃, giving tetrahydrofluorene **4.19c** in 69% yield after 6 h. Optimal conditions for the cyclization were found to be 30 mol% FeCl₃, resulting in full conversion to tetrahydrofluorene **4.19c** after 2 h in 86% yield. These relatively mild conditions can be rationalized due to the resonance stabilizing ability of the *p*-methoxy substituent on the intermediate benzylic cation.

Conversely, when diene **4.20b** – with the inductively destabilizing *p*-trifluoromethyl group on the benzene ring – was exposed to 1.2 equiv FeCl₃ at room temperature, no conversion was observed after 4 h. To see if any quantity of FeCl₃ would promote the cyclization at room temperature, diene **4.20b** was stirred with 12 equiv FeCl₃, which resulted in a complex mixture after 20 h with none of the desired tetrahydrofluorene **4.20c** and a significant amount of unreacted diene **4.20b** remaining in the reaction mixture. Because of these poor results at room temperature, the cyclization was attempted with heat.

Diene **4.20b** was stirred with 1 equiv FeCl₃ at 40°C, giving only a trace amount of conversion to tetrahydrofluorene **4.20c**. When diene **4.20b** was exposed to 3 equiv FeCl₃ at 40°C, the reaction stalled overnight. Although the reaction had not gone to completion, it was worked up after 23 h, resulting in a 50% yield of tetrahydrofluorene **4.20c** along with 18% of recovered diene **4.20b** after column chromatography. To see if an even greater amount of promoter would cause the reaction to go to completion, diene **4.20b** was exposed to 4 equiv FeCl₃ at 40°C. Again, the reaction stalled overnight with little improvement in conversion compared with 3 equiv FeCl₃. As a result, another 2 equiv FeCl₃ was added, causing full conversion to tetrahydrofluorene **4.20c** after an additional 4 h. Optimal conditions for the cyclization involved exposing diene **4.20b** to 4 equiv FeCl₃ for 4 h followed by another addition of 2 equiv FeCl₃ to give tetrahydrofluorene **4.20c** after an additional 3 h in 44% yield.

To investigate whether the electrocyclic ring opening or the electrocyclization was the source of this low yield, cyclobutene **4.20a** was subjected to refluxing DCE for 3 h and diene **4.20b** was isolated and purified (Scheme 4.2). Because diene **4.20b** was obtained in quantitative yield, the cyclization to tetrahydrofluorene **4.20c** is the low yielding step. The identity of diene **4.20b** was confirmed by an X-ray crystal structure (Scheme 4.2), which also confirmed the geometry of dienes **1.28**, **4.19b**, and **4.21b** by analogy.



Scheme 4.2. Yield of the electrocyclic ring opening step from cyclobutene **4.20a** to diene **4.20b**

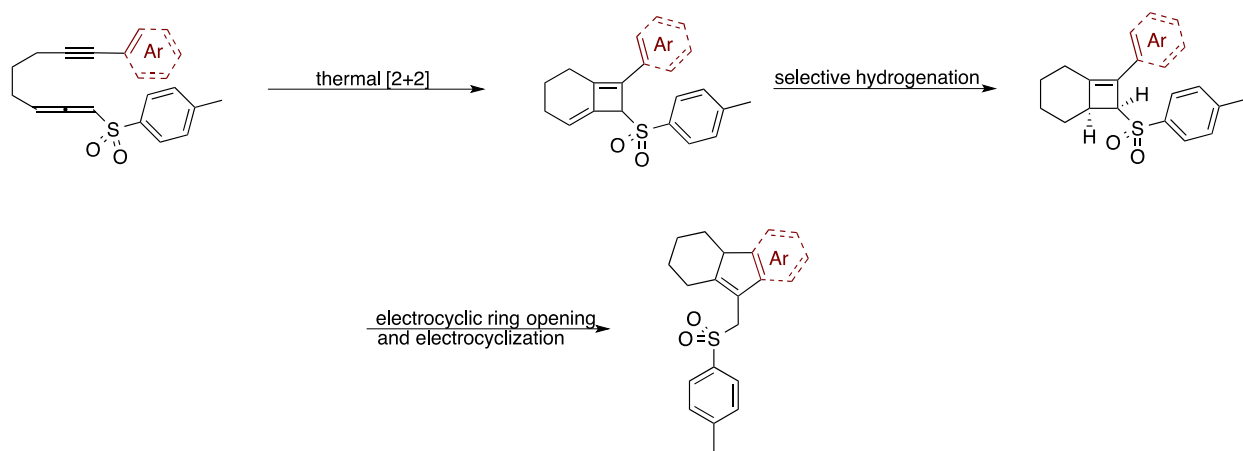
To test the regioselectivity of the cyclization, [1,3]dioxole substituted cyclobutene **4.21a** was subjected to the reaction conditions. When diene **4.21b** was exposed to 30 mol% FeCl_3 at room temperature – the same conditions as diene **4.19b** – the cyclization stalled overnight. The requirement of more promoter for the cyclization of diene **4.21b** compared to diene **4.19b** is likely due to the presence of both a resonance stabilizing oxygen and an inductively destabilizing oxygen, which provides less net stabilization on the intermediate benzylic cation than the resonance stabilizing methoxy group in diene **4.19b**.

Optimized conditions for the cyclization included exposure of diene **4.21b** to 50 mol% FeCl_3 at room temperature for 6 h to give tetrahydrofluorene **4.21c** as a single product in 70% yield, revealing that the cyclization is highly regioselective. The reason that only one product was observed rather than a mixture could be due to steric hinderance of the [1,3]dioxole group inhibiting cyclization at the alternative position.

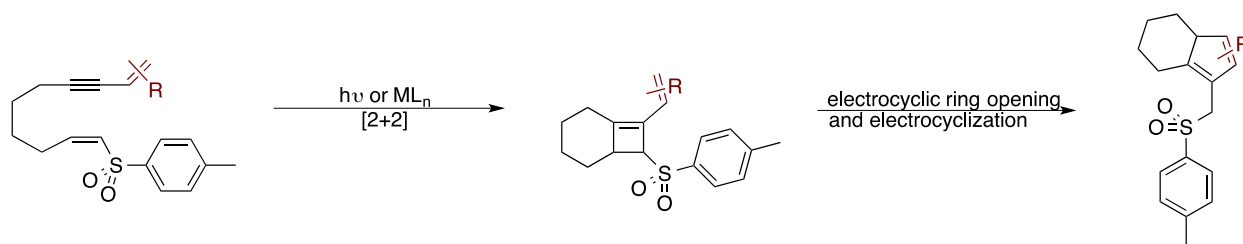
4.1 OPPORTUNITIES FOR STUDY AND EXTENSION OF TRANSFORMATION

While the electronic effects on the cyclization have been studied somewhat, the effect of sterics on both the electrocyclic ring opening and the cyclization process present another point of variation to expose the scope of the reaction. Additionally, mechanistic studies to elucidate the precise interaction of the Lewis acid with the diene to promote the cyclization would provide more clarity on the nature of the transformation.

Beyond requiring harsher conditions and giving lower yields for the cyclization of substrates bearing an electron withdrawing group on the aromatic ring, another limitation of the transformation is the currently long route to synthesize the starting cyclobutene. Rather than the current thermal [2+2] allene-yne cycloaddition and subsequent selective hydrogenation of the tri-substituted double bond (Scheme 4.3), a photocatalytic or transition metal catalyzed [2+2] cycloaddition of a vinyl sulfone with the alkyne to directly form the cyclobutene would eliminate a step (Scheme 4.4). As an additional benefit, because the required hydrogenation in the current route precludes alkenes lacking aromaticity, this new route would allow both aryl and alkenyl groups to be carried onto the cyclization step – extending opportunities for diversity.



Scheme 4.3. Current route to product



Scheme 4.4. Proposed improved route to product

A more general vinyl sulfonyl Nazarov cyclization would presumably yield methyl sulfone substituted cyclopentadienes rather than the alkyldiene cyclopentenes produced in the closely related vinylogous Nazarov cyclization (Scheme 2.5). In both cases the electron withdrawing groups destabilize adjacent alkenyl groups resulting in regioselectivity for the internal position. However, in the case of the vinylogous Nazarov cyclization, stability provided by conjugation with the carbonyl group favors the exocyclic position. On the other hand, the sulfone cannot be conjugated with an alkenyl group,⁴⁰ so the internal position is favored for the double bond.

5.0 CONCLUSIONS

During the course of a proposed route to synthesize ladderane lipids, a one-pot 4π electrocyclic ring opening followed by a Lewis acid promoted formal vinyl sulfonyl Nazarov cyclization reaction was discovered and optimized. The transformation can be used to construct substituted 9-(tosylmethyl)-2,3,4,4a-tetrahydro-1*H*-fluorenes from 7-phenyl-8-tosylbicyclo[4.2.0]oct-6-enes. Utilizing the resulting allyl sulfone, these products presumably lend themselves to easy further functionalization.

When electron donating groups are introduced onto the phenyl ring only a catalytic amount of promoter is required for the cyclization step. Conversely, an electron withdrawing group on the aryl ring requires a superstoichiometric amount of promoter and heat.

Opportunities for further study include determining the effect of sterics on the transformation and the precise interaction of the Lewis acid with the diene. Additionally, the reaction has the potential to be extended to substrates bearing alkenyl groups without aromaticity.

This vinyl sulfonyl Nazarov cyclization could complement existing cyclization processes by providing new opportunities for both product derivation and further functionalization.

APPENDIX

Supporting Info

A Formal Vinyl Sulfonyl Nazarov Cyclization Accesses 9-(tosylmethyl)-2,3,4,4a-tetrahydro-1*H*-fluorenes

Contents:

1. Compound Characterization Checklist	39
2. General Methods	40
3. Synthesis of Tetrahydrofluorene Compounds	41
4. Synthesis of Silylated Compounds	75
5. Crystal Structure Reports	79
6. ¹ H NMR Spectra of Entries in Optimization Tables 3.1 and 3.2	106
7. ¹ H NMR and ¹³ C NMR Spectra of Compounds	116

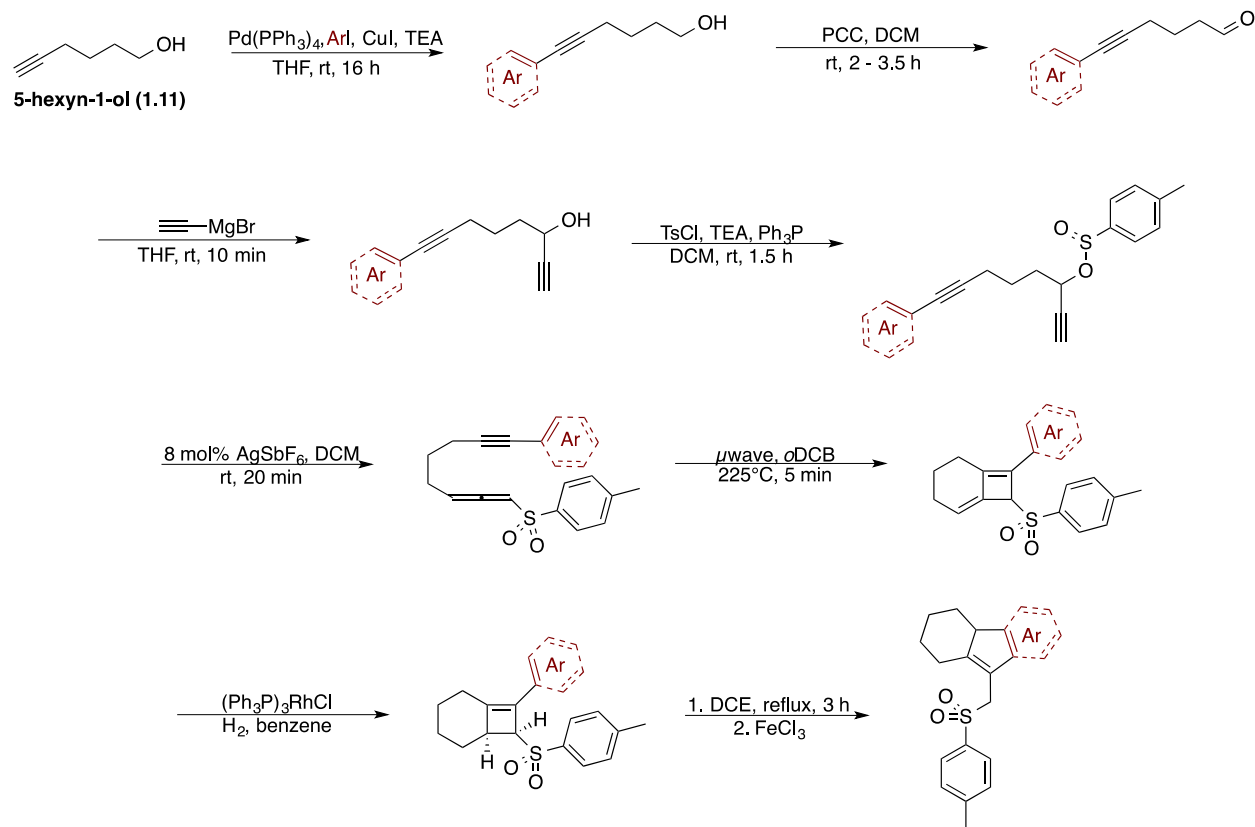
1. Compound Characterization Checklist

Compound or structure number (with substituent/isomer identifier if needed)	IDENTITY							PURITY	
	Known compound [citation given]	IR	Melting Point	¹ H NMR	¹³ C NMR	High resolution MS	X-ray [ORTEP and CIF in SI*]	Copy of ¹ H/ ¹³ C NMR in SI	
1.8	X	X	X	X	X	X	X	X	
1.9	X	X	X	X	X			X	
1.10	X		X	X	X			X	
1.12	X		X	X				X	
1.13	X		X	X	X			X	
1.14	X		X	X	X			X	
1.15	X		X	X	X			X	
1.22	X	X	X	X	X			X	
1.23	X		X	X	X			X	
1.25	X	X	X	X	X	X		X	
1.26	X	X	X	X	X	X		X	
1.28	X		X	X	X			X	
3.1/3.2			X	X				X	
4.1	X		X	X				X	
4.2	X		X	X				X	
4.3	X		X	X	X			X	
4.4	X		X	X	X			X	
4.5	X		X	X	X			X	
4.6	X		X	X	X			X	
4.7	X		X	X	X			X	
4.8	X		X	X	X			X	
4.9	X		X	X	X			X	
4.10	X		X	X	X			X	
4.11	X		X	X	X			X	
4.12	X		X	X	X			X	
4.13	X		X	X	X			X	
4.14	X		X	X	X			X	
4.15	X		X	X	X			X	
4.16	X		X	X	X			X	
4.17	X		X	X	X			X	
4.18	X		X	X	X			X	
4.19a	X		X	X	X			X	
4.19b	X		X	X	X			X	
4.19c	X	X	X	X	X			X	
4.20a	X	X	X	X	X			X	
4.20b	X	X	X	X	X	X		X	
4.20c	X	X	X	X	X			X	
4.21a	X		X	X	X			X	
4.21b	X		X	X	X			X	
4.21c	X	X	X	X	X			X	

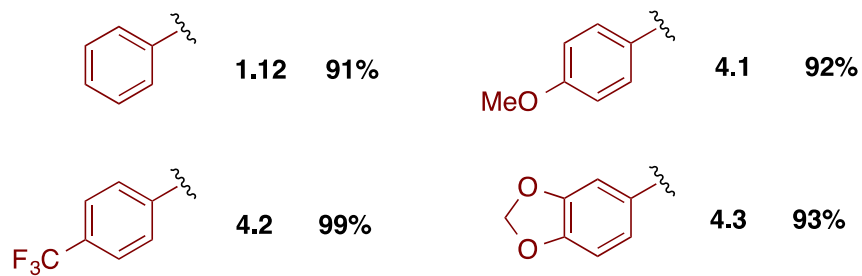
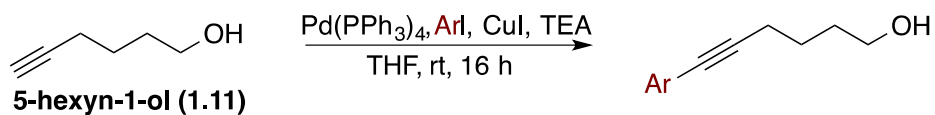
2. General Methods

All reactions were carried out in flame-dried glassware sealed with a rubber septa, under a nitrogen atmosphere, and stirred with teflon-coated magnetic stir bar unless otherwise noted. Commercially available chemicals were purchased from Aldrich Chemical Co., GFS Chemicals, Strem Chemicals, Acros Organics, Alfa Aesar, and Advanced Chemtech and used without further purification unless noted differently. 1,2 Dichloroethane (DCE) was purified by distillation over calcium sulfate. Purification of compounds by flash chromatography was performed using silica gel (40-63 μm particle size, 60 \AA pore size) purchased from Sorbent Technologies. TLC analyses were performed on Silicycle silica gel F₂₅₄ glass plates (250 μm thickness, 60 \AA pore size). ¹H and ¹³C NMR spectra were obtained on Bruker Avance 300 MHz, 400 MHz, 500 MHz, or 600 MHz spectrometers at room temperature unless otherwise noted. Spectra were referenced to residual chloroform (7.26 ppm, ¹H, 77.16 ppm, ¹³C), benzene (7.16 ppm, ¹H, 128.0 ppm, ¹³C), or TMS (0.00 ppm ¹H and ¹³C NMR). Chemical shifts (δ) are reported in ppm, multiplicities are indicated by s (singlet), d (doublet), t (triplet), q (quartet) and m (multiplet). Coupling constants (*J*) are reported in hertz (Hz). High resolution mass spectra were obtained on a Waters Q-TOF Ultima API, Micromass UK Limited high resolution mass spectrometer. IR spectra were recorded using a Nicolet IR 200 FT-IR. Melting points were uncorrected and determined on a Mel-Temp instrument.

3. Synthesis of Tetrahydrofluorene Compounds

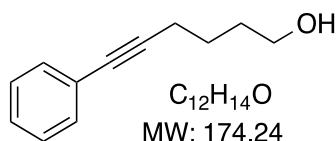


General Procedure I: *Songashira Coupling*



To a three neck round bottom flask equipped with a stirbar was added 5-hexyn-1-ol (1 equiv), triethylamine (21 equiv), and tetrahydrofuran followed by iodoarene (2.0 equiv), tetrakis(triphenylphosphine) palladium(0) (0.01 equiv), and copper(I) iodide (0.02 equiv) through the sidearm. The reaction was stirred for 16 h at room temperature under nitrogen, over which time it precipitated light yellow solids. The reaction mixture was gravity filtered, and the solids were washed with Et₂O. The filtrate was concentrated under reduced pressure and purified by silica gel column chromatography with 20% ethyl acetate in hexanes as the mobile phase to yield the coupled product.

6-phenylhex-5-yn-1-ol (**1.12**)



General Procedure I was followed with 5-hexyn-1-ol (2.81 mL, 25.5 mmol), iodobenzene (5.68 mL, 51 mmol), triethylamine (75 mL, 533 mmol), tetrahydrofuran (14 mL), tetrakis(triphenylphosphine) palladium (0) (0.295 g, 0.26 mmol, 0.01 equiv), and copper (I) iodide (0.102 g, 0.54 mmol, 0.02 equiv) to yield 4.05 g of coupled product **1.12** in 91% yield as a yellow oil. Compound **1.12** has been previously characterized.⁴¹

Data for **1.12** (AMB_E2_029)

¹H NMR (400 MHz, CDCl₃)

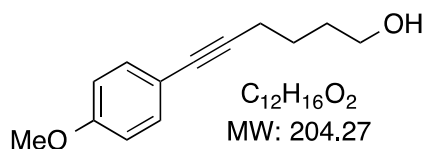
δ 7.44 – 7.37 (m, 2H), 7.32 – 7.24 (m, 3H), 3.70 (t, *J* = 6.1 Hz, 2H), 2.46 (t, *J* = 6.7 Hz, 2H), 1.83 – 1.61 (m, 5H) ppm;

¹³C NMR (101 MHz, CDCl₃)

δ 131.6 (2C), 128.3 (2C), 127.7, 124.0, 90.0, 81.1, 62.5, 32.0, 25.1, 19.3 ppm;

TLC R_f = 0.28 (30% ethyl acetate in hexanes, UV, silica gel)

6-(4-methoxyphenyl)hex-5-yn-1-ol (**4.1**).



General Procedure I was followed with 5-hexyn-1-ol (0.94 mL, 8.5 mmol), 4-iodoanisole (3.98 g, 17 mmol), triethylamine (25 mL, 178 mmol), tetrahydrofuran (4.7 mL), tetrakis(triphenylphosphine) palladium (0) (0.098 g, 0.09 mmol), and copper (I) iodide (0.034 g,

0.18 mmol) to yield 1.59 g of coupled product **4.1** in 92% yield as a brown oil. Compound **4.1** has been previously characterized.⁴¹

Data for 4.1 (AMB_E3_30)

¹H NMR (300 MHz, CDCl₃)

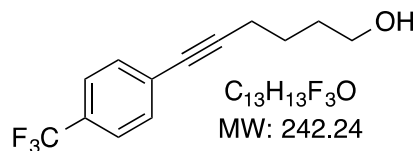
δ 7.37 – 7.26 (m, 2H), 6.88 – 6.74 (m, 2H), 3.78 (s, 3H), 3.69 (t, *J* = 6.1 Hz, 2H), 2.43 (t, *J* = 6.7 Hz, 2H), 1.82 – 1.64 (m, 4H), 1.62 (brs, 1H) ppm;

¹³C NMR (76 MHz, CDCl₃)

δ 159.2, 133.0 (2C), 116.2, 114.0 (2C), 88.4, 80.8, 62.6, 55.4, 32.0, 25.3, 19.3 ppm;

TLC R_f = 0.22 (30% ethyl acetate in hexanes, UV, silica gel)

6-(4-(trifluoromethyl)phenyl)hex-5-yn-1-ol (**4.2**).



General Procedure I was followed with 5-hexyn-1-ol (0.94 mL, 8.5 mmol), 1-iodo-4-(trifluoromethyl) benzene (2.50 mL, 17 mmol), triethylamine (25 mL, 178 mmol), tetrahydrofuran (4.7 mL), tetrakis(triphenylphosphine) palladium (0) (0.098 g, 0.09 mmol), and copper (I) iodide (0.034 g, 0.18 mmol) to yield 2.34 g of coupled product **4.2** in 113% yield with residual solvent as a yellow oil. Compound **4.2** has been previously characterized.⁴¹

Data for 4.2 (AMB_E3_13)

¹H NMR (300 MHz, CDCl₃)

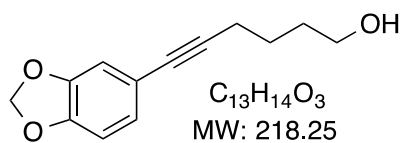
δ 7.53 (d, *J* = 8.3 Hz, 2H), 7.47 (d, *J* = 8.4 Hz, 2H), 3.71 (t, *J* = 6.1 Hz, 2H), 2.47 (t, *J* = 6.6 Hz, 2H), 1.83 – 1.62 (m, 4H), 1.51 (brs, 1H) ppm;

¹³C NMR (76 MHz, CDCl₃)

δ 131.9 (2C), 129.5 (q, *J*_{CF} = 33 Hz), 127.9 (q, *J*_{CF} = 1 Hz), 125.3 (q, *J*_{CF} = 4 Hz) (2C), 124.2 (q, *J*_{CF} = 274 Hz), 92.9, 80.0, 62.5, 32.0, 25.0, 19.4 ppm;

TLC R_f = 0.22 (30% ethyl acetate in hexanes, UV, silica gel)

6-(benzo[*d*][1,3]dioxol-5-yl)hex-5-yn-1-ol (**4.3**).



General Procedure I was followed with 5-hexyn-1-ol (0.94 mL, 8.5 mmol), 1-iodo-3,4-methylenedioxy benzene (2.21 mL, 17 mmol), triethylamine (25 mL, 178 mmol), tetrahydrofuran (4.7 mL), tetrakis(triphenylphosphine) palladium (0) (0.098 g, 0.09 mmol), and copper (I) iodide (0.034 g, 0.18 mmol) to yield 1.73 g of coupled product **4.3** in 93% yield as a brown oil.

Data for **4.3** (AMB_E3_54)

1H NMR (500 MHz, $CDCl_3$)

δ 6.90 (dd, $J = 8.0, 1.5$ Hz, 1H), 6.83 (d, $J = 1.5$ Hz, 1H), 6.71 (d, $J = 8.0$ Hz, 1H), 5.93 (s, 2H), 3.69 (t, $J = 6.3$ Hz, 2H), 2.41 (t, $J = 6.8$ Hz, 2H), 1.77 – 1.69 (m, 2H), 1.69 – 1.62 (m, 2H), 1.60 (brs, 1H) ppm;

^{13}C NMR (126 MHz, $CDCl_3$)

δ 147.4, 147.4, 125.9, 117.3, 111.7, 108.4, 101.2, 88.2, 80.8, 62.5, 32.0, 25.2, 19.2 ppm;

IR (thin film)

3349, 2939 cm^{-1} ;

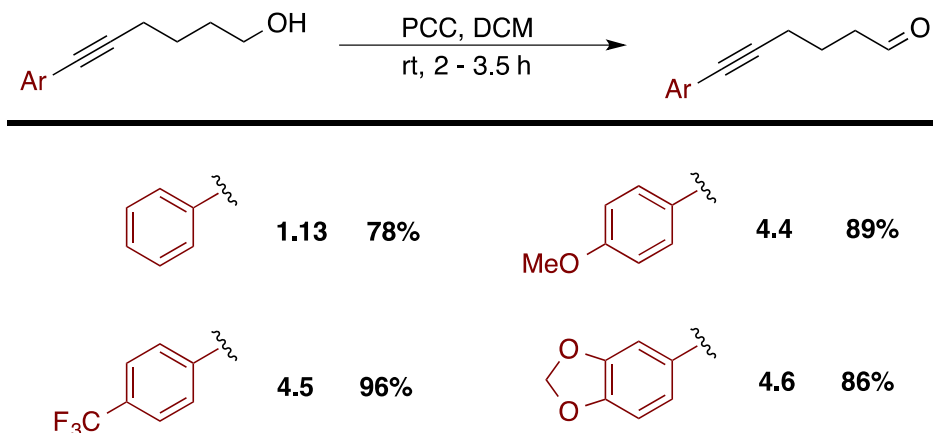
HRMS (TOF MS ES+)

$[M+H]^+$ calcd for $C_{13}H_{14}O_3$, 219.1021; found, 219.1027;

TLC

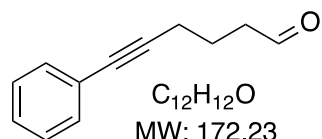
$R_f = 0.09$ (20% ethyl acetate in hexanes, UV, silica gel)

General Procedure II: PCC Oxidation



To a one-neck round-bottom flask equipped with a septum pierced with a needle and a stir bar was added pyridinium chlorochromate (2.0 equiv) and dichloromethane with stirring. **Alcohol** (1 equiv) was added all at once via syringe, and the reaction turned dark brown and thick. The reaction was run under air. After 2 h – 3.5 h, starting material was consumed by TLC, so diethyl ether and silica gel were added to the vessel. The suspension was stirred for 30 minutes, filtered through a pad of silica gel with diethyl ether washings, and concentrated under reduced pressure to afford the aldehyde, which was carried on to the next step without further purification.

6-phenylhex-5-ynal (**1.13**).



General Procedure II was followed with pyridinium chlorochromate (10.21 g, 47.5 mmol), dichloromethane (93 mL), and alcohol **1.12** (4.12 g, 23.8 mmol) for 3.5 h to yield 3.19 g of aldehyde **1.13** in 78%

yield as a brown oil.

Data for **1.13** (AMB_E2_067)

1H NMR (400 MHz, $CDCl_3$)

δ 9.84 (t, $J = 1.3$ Hz, 1H), 7.48 – 7.37 (m, 2H), 7.35 – 7.23 (m, 3H), 2.66 (td, $J = 7.2, 1.3$ Hz, 2H), 2.50 (t, $J = 6.9$ Hz, 2H), 1.95 (p, $J = 7.0$ Hz, 2H) ppm;

^{13}C NMR (101 MHz, $CDCl_3$)

δ 202.1, 131.6 (2C), 128.3 (2C), 127.8, 123.7, 88.8, 81.8, 42.8, 21.3, 18.9 ppm;

IR (thin film)

2944, 1707 cm^{-1} ;

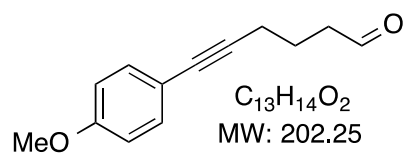
HRMS (TOF MS ES+)

$[M+H]^+$ calcd for $C_{12}H_{12}O$, 173.0961; found, 173.0970;

TLC

$R_f = 0.56$ (30% ethyl acetate in hexanes, UV, silica gel)

6-(4-methoxyphenyl)hex-5-ynal (**4.4**).



General Procedure II was followed with pyridinium chlorochromate (3.55 g, 16.5 mmol), dichloromethane (32 mL), and alcohol **4.1** (1.69 g, 8.3 mmol) for 3 h to yield 1.50 g of

aldehyde **4.4** in 89% yield as a dark brown oil.

Data for 4.4 (AMB_E3_05)

¹H NMR (300 MHz, CDCl₃)

δ 9.84 (t, *J* = 1.2 Hz, 1H), 7.32 (d, *J* = 8.8 Hz, 2H), 6.81 (d, *J* = 8.8 Hz, 2H), 3.80 (s, 3H), 2.65 (td, *J* = 7.2, 1.3 Hz, 2H), 2.48 (t, *J* = 6.8 Hz, 2H), 1.93 (p, *J* = 7.1 Hz, 2H) ppm;

¹³C NMR (76 MHz, CDCl₃)

δ 202.1, 159.4, 133.0 (2C), 115.9, 114.0 (2C), 87.2, 81.6, 55.4, 43.0, 21.5, 19.0 ppm;

IR (thin film)

2935, 1722, 1605, 1510, 1247 cm⁻¹;

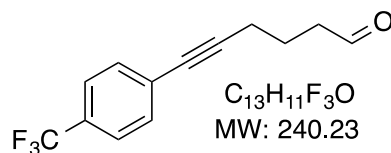
HRMS (TOF MS ES+)

[M+H]⁺ calcd for C₁₃H₁₄O₂, 203.1067; found, 203.1072;

TLC

R_f = 0.50 (30% ethyl acetate in hexanes, UV, silica gel)

6-(4-(trifluoromethyl)phenyl)hex-5-ynal (**4.5**).



General Procedure II was followed with pyridinium chlorochromate (3.55 g, 16.5 mmol), dichloromethane (32 mL), and alcohol **4.2** (2.01 g, 8.3 mmol) for 3 h to yield 1.91 g of aldehyde **4.5** in 96% yield as a brown oil.

Data for 4.5 (AMB_E3_15)

¹H NMR (400 MHz, CDCl₃)

δ 9.85 (t, *J* = 1.1 Hz, 1H), 7.54 (d, *J* = 8.3 Hz, 2H), 7.48 (d, *J* = 8.2 Hz, 2H), 2.66 (td, *J* = 7.2, 1.2 Hz, 2H), 2.52 (t, *J* = 6.9 Hz, 2H), 1.96 (p, *J* = 7.0 Hz, 2H) ppm;

¹³C NMR (101 MHz, CDCl₃)

δ 201.7, 131.9 (2C), 129.7 (q, *J*_{CF} = 33 Hz), 127.6 (q, *J*_{CF} = 1 Hz), 125.3 (q, *J*_{CF} = 4 Hz) (2C), 124.1 (q, *J*_{CF} = 273 Hz), 91.7, 80.7, 42.9, 21.2, 19.0 ppm;

IR (thin film)

2918, 1726, 1324, 1166, 1125, 1105, 1067 cm⁻¹;

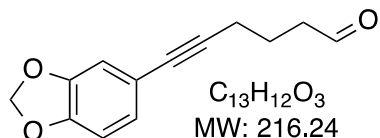
HRMS (TOF MS ES+)

$[M+H]^+$ calcd for $C_{13}H_{11}OF_3$, 241.0835; found, 241.0842;

TLC

$R_f = 0.49$ (30% ethyl acetate in hexanes, UV, silica gel)

6-(benzo[d][1,3]dioxol-5-yl)hex-5-ynal (4.6).



General Procedure II was followed with pyridinium chlorochromate (3.32 g, 15.4 mmol), dichloromethane (30 mL), and alcohol **4.3** (1.68 g, 7.7 mmol) for 2 h to yield 1.42 g of

aldehyde **4.6** in 86% yield as a dark brown oil.

Data for 4.6 (AMB_E3_58)

1H NMR (500 MHz, $CDCl_3$)

δ 9.82 (t, $J = 1.3$ Hz, 1H), 6.89 (dd, $J = 8.0, 1.5$ Hz, 1H), 6.83 (d, $J = 1.5$ Hz, 1H), 6.71 (d, $J = 8.0$ Hz, 1H), 5.94 (s, 2H), 2.62 (td, $J = 7.2, 1.3$ Hz, 2H), 2.45 (t, $J = 6.9$ Hz, 2H), 1.91 (p, $J = 7.0$ Hz, 2H) ppm;

^{13}C NMR (126 MHz, $CDCl_3$)

δ 202.0, 147.5, 147.4, 126.0, 117.0, 111.7, 108.4, 101.3, 87.1, 81.6, 42.9, 21.4, 18.9 ppm;

IR (thin film)

2899, 1722 cm^{-1} ;

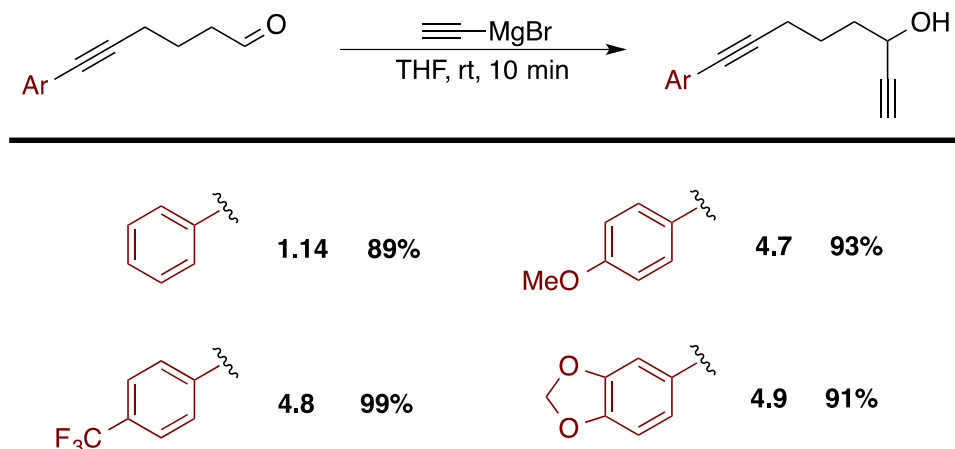
HRMS (TOF MS ES+)

$[M+H]^+$ calcd for $C_{13}H_{12}O_3$, 217.0865; found, 217.0872;

TLC

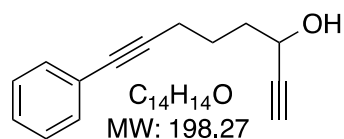
$R_f = 0.46$ (20% ethyl acetate in hexanes, UV, silica gel)

General Procedure III: Grignard Addition



A round bottom flask with a stirbar was charged with a solution of ethynylmagnesium bromide (0.5 M in tetrahydrofuran) (1.7 equiv). The solution was cooled to 0°C in an ice bath and **aldehyde** (1 equiv) in tetrahydrofuran was added slowly. After 10 min, TLC indicated the reaction was complete. Saturated ammonium chloride solution and water were added to the flask and the mixture was extracted with ethyl acetate. After extraction, the product was dried with magnesium sulfate, filtered, and concentrated to give the alcohol, which was carried on to the next step without further purification.

8-phenylocta-1,7-diyn-3-ol (**1.14**).



General Procedure III was followed with ethynylmagnesium bromide (0.5 M in tetrahydrofuran) (58.7 mL, 29.4 mmol), aldehyde **1.13** (2.93 g, 17.1 mmol), and tetrahydrofuran (23.5 mL) to yield

3.01 g of alcohol **1.14** in 89% yield as a brown oil.

Data for **1.14** (AMB_E2_059)

1H NMR (400 MHz, $CDCl_3$)

δ 7.42 – 7.36 (m, 2H), 7.32 – 7.26 (m, 3H), 4.46 (s, 1H), 2.54 – 2.42 (m, 3H), 1.96 – 1.87 (m, 2H), 1.85 (s, 1H), 1.84 – 1.77 (m, 2H) ppm;

^{13}C NMR (101 MHz, $CDCl_3$)

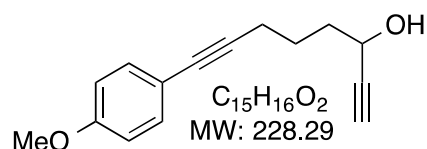
δ 131.7 (2C), 128.3 (2C), 127.7, 123.9, 89.6, 84.8, 81.3, 73.3, 62.0, 36.8, 24.4, 19.2 ppm;

IR (thin film)
3287, 2937, 2231, 2115 cm^{-1}

HRMS (TOF MS ES+)
[M+H]⁺ calcd for C₁₄H₁₄O, 199.1117; found, 199.1134;

TLC R_f = 0.47 (30% ethyl acetate in hexanes, UV, silica gel)

8-(4-methoxyphenyl)octa-1,7-diyn-3-ol (4.7).



General Procedure III was followed with ethynylmagnesium bromide (0.5 M in tetrahydrofuran) (10.6 mL, 5.29 mmol), aldehyde **4.4** (622 mg, 3.07 mmol), and tetrahydrofuran (4.2 mL) to yield 652 mg of alcohol **4.7** in 93% yield as a brown oil.

Data for 4.7 (AMB_E3_48)

¹H NMR (300 MHz, CDCl₃)

δ 7.41 – 7.27 (m, 2H), 6.86 – 6.76 (m, 2H), 4.45 (td, $J = 6.3, 1.8$ Hz, 1H), 3.79 (s, 3H), 2.54 – 2.40 (m, 3H), 2.02 (brs, 1H), 1.95 – 1.86 (m, 2H), 1.86 – 1.73 (m, 2H) ppm;

¹³C NMR (76 MHz, CDCl₃)

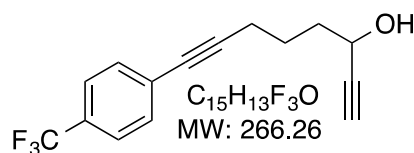
δ 159.2, 133.0 (2C), 116.1, 114.0 (2C), 88.0, 84.9, 81.0, 73.3, 62.1, 55.4, 36.9, 24.5, 19.2 ppm;

IR (thin film)
3288, 2953, 2536, 1606 cm^{-1}

HRMS (TOF MS ES+)
[M+H]⁺ calcd for C₁₅H₁₆O₂, 229.1223; found, 229.1235;

TLC R_f = 0.34 (30% ethyl acetate in hexanes, UV, silica gel)

8-(4-(trifluoromethyl)phenyl)octa-1,7-diyn-3-ol (4.8).



General Procedure III was followed with ethynylmagnesium bromide (0.5 M in tetrahydrofuran) (26.5 mL, 13.3 mmol), aldehyde **4.5** (1.84 g, 7.7 mmol), and tetrahydrofuran (10.6 mL) to yield 1.2 g of alcohol **4.8** in 63% yield as a brown oil.

mL) to yield 2.01 g of alcohol **4.8** in 99% yield as an orange oil.

Data for **4.8** (AMB_E3_17)

¹H NMR (300 MHz, CDCl₃)

δ 7.54 (d, *J* = 8.5 Hz, 2H), 7.48 (d, *J* = 8.4 Hz, 2H), 4.51 – 4.41 (m, 2H), 2.56 – 2.44 (m, 3H), 2.13 – 1.66 (m, 5H) ppm;

¹³C NMR (76 MHz, CDCl₃)

δ 131.9 (2C), 129.6 (q, *J*_{CF} = 33 Hz), 127.9 (q, *J*_{CF} = 1 Hz), 125.3 (q, *J*_{CF} = 4 Hz) (2C), 124.2 (q, *J*_{CF} = 274 Hz), 92.5, 84.7, 80.2, 73.4, 62.0, 36.8, 24.2, 19.3 ppm;

IR (thin film)

3305, 2939, 2232, 1616 cm⁻¹

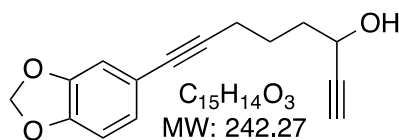
HRMS (TOF MS ES+)

[M+H]⁺ calcd for C₁₅H₁₃OF₃, 267.0991; found, 267.1006;

TLC

R_f = 0.36 (30% ethyl acetate in hexanes, UV, silica gel)

8-(benzo[*d*][1,3]dioxol-5-yl)octa-1,7-diyn-3-ol (4.9**).**



General Procedure III was followed with ethynylmagnesium bromide (0.5 M in tetrahydrofuran) (21.9 mL, 10.9 mmol), aldehyde **4.6** (1.37 g, 6.34 mmol), and tetrahydrofuran (8.7 mL)

to yield 1.40 g of alcohol **4.9** in 91% yield as a brown oil.

Data for **4.9** (AMB_E3_60)

¹H NMR (500 MHz, CDCl₃)

δ 6.90 (dd, *J* = 8.0, 1.5 Hz, 1H), 6.84 (d, *J* = 1.4 Hz, 1H), 6.71 (d, *J* = 8.0 Hz, 1H), 5.94 (s, 2H), 4.47 – 4.41 (m, 1H), 2.49 (d, *J* = 1.9 Hz, 1H), 2.44 (t, *J* = 6.9 Hz, 2H), 2.09 (brs, 1H), 1.92 – 1.83 (m, 2H), 1.81 – 1.73 (m, 2H) ppm;

¹³C NMR (126 MHz, CDCl₃)

δ 147.4, 147.4, 126.0, 117.2, 111.8, 108.4, 101.3, 87.8, 84.8, 81.0, 73.3, 62.0, 36.8, 24.4, 19.1 ppm;

IR (thin film)

3291, 2900 cm⁻¹

HRMS

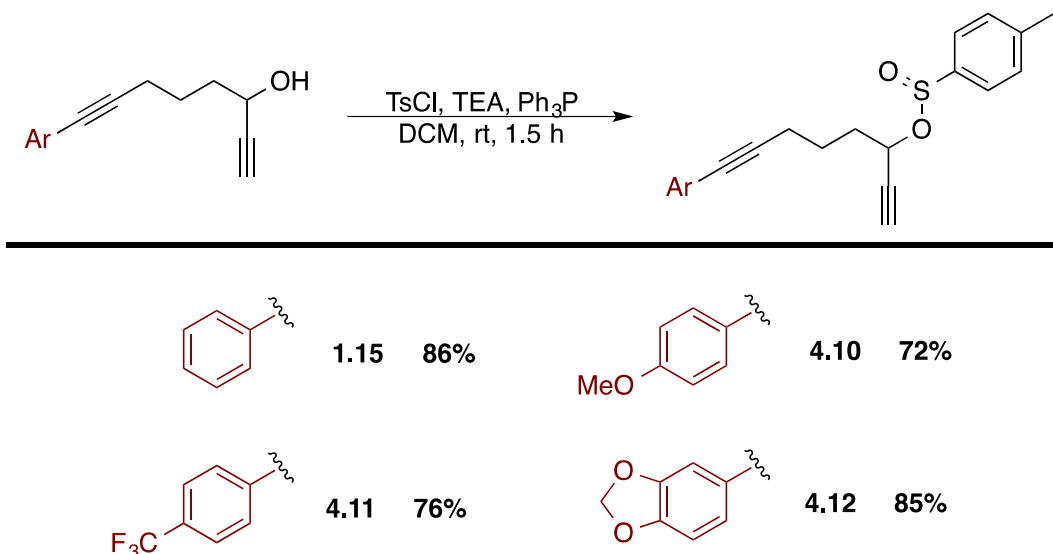
(TOF MS ES+)

$[M+H]^+$ calcd for $C_{15}H_{14}O_3$, 243.1021; found, 243.1028;

TLC

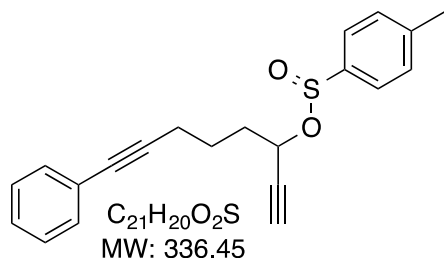
$R_f = 0.24$ (20% ethyl acetate in hexanes, UV, silica gel)

General Procedure IV: Sulfinylation



Sulfinylation was performed in a manner analogous to a literature procedure.⁹ A three-necked round-bottomed flask equipped with a stirbar was charged with tosyl chloride (1 equiv), dichloromethane, and triethylamine (1.1 equiv), resulting in a colorless solution. The solution was put in a cold water bath in order to cool the contents below 20°C (internal temperature). To this solution was added, dropwise over 90 minutes by means of an addition funnel, a well-mixed solution of **alcohol** (1 equiv) and triphenylphosphine (1 – 1.3 equiv) in dichloromethane. The rate of the addition was to keep the temperature of the reaction mixture constant. After the addition was complete, a TLC indicated that the reaction was complete. As a result, the solution was transferred to a one-neck round-bottomed flask and silica gel was added. The resulting mixture was concentrated on a rotary evaporator and the resulting dry silica gel was added to a pre-packed column for purification.

8-phenylocta-1,7-diyn-3-yl 4-methylbenzenesulfinate (**1.15**).



General Procedure IV was followed with tosyl chloride (3.80 g, 20.1 mmol), dichloromethane (50 mL), triethylamine (3.09 mL, 21.9 mmol), **1.14** (3.96 g, 20.1 mmol), triphenylphosphine (5.24 g, 20.1 mmol), and dichloromethane (50 mL). The sulfinate was purified by

column with 20% ethyl acetate in hexanes as the mobile phase to yield 5.78 g of sulfinate **1.15** as an inseparable 1:1 mixture of diastereomers in 86% yield as a yellow oil.

Data for 1.15 (AMB_E2_060)

1H NMR (400 MHz, $CDCl_3$)

δ 7.65 (d, $J = 8.1$ Hz, 2H), 7.42 – 7.27 (m, 7H), 5.02 – 4.91 (m, 1H), 2.67 (d, $J = 2.1$ Hz, 1H), 2.49 – 2.38 (m, 5H), 2.10 – 1.90 (m, 2H), 1.86 – 1.70 (m, 2H) ppm;

^{13}C NMR (101 MHz, $CDCl_3$)

δ 143.1,[†] 143.1,[‡] 142.3,[†] 141.6,[‡] 131.6 (2C),[†] 131.6 (2C),[‡] 129.8 (2C),[†] 129.7 (2C),[‡] 128.3 (2C),^{††} 127.7,^{††} 125.5 (2C),[†] 125.1 (2C),[‡] 123.9,[†] 123.8,[‡] 89.2,[†] 89.2,[‡] 81.4,[†] 81.4,[‡] 81.2,[†] 80.9,[‡] 76.1,[†] 75.4,[‡] 67.5,[†] 65.0,[‡] 35.9,[†] 35.3,[‡] 24.1,[†] 24.1,[‡] 21.7,[†] 21.6,[‡] 19.0,[†] 18.9[‡] ppm;

IR (thin film)

2926, 1145 cm^{-1} ;

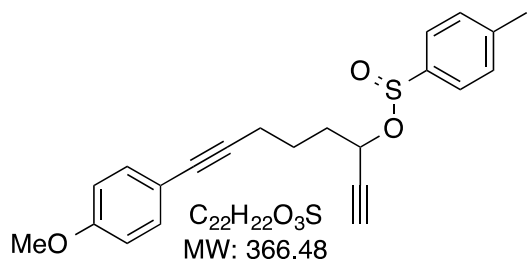
HRMS (TOF MS ES+)

$[M+H]^+$ calcd for $C_{21}H_{20}O_2S$, 337.1262; found, 337.1235;

TLC

$R_f = 0.60$ (30% ethyl acetate in hexanes, UV, silica gel)

8-(4-methoxyphenyl)octa-1,7-diyn-3-yl 4-methylbenzenesulfinate (**4.10**).



General Procedure IV was followed with tosyl chloride (1.27 g, 6.7 mmol), dichloromethane (17 mL), triethylamine (1.03 mL, 7.3 mmol), **4.7** (1.53 g, 6.7 mmol), triphenylphosphine (1.75 g, 6.7 mmol), and dichloromethane (16 mL). The sulfinate was

purified by column with 20% ethyl acetate in hexanes as the mobile phase to yield 1.76 g of sulfinate **4.10** as an inseparable 1:1 mixture of diastereomers in 72% yield as a yellow oil.

Data for 4.10 (AMB_E3_07)

¹H NMR (300 MHz, CDCl₃)
δ 7.65 (d, *J* = 8.2 Hz, 2H), 7.37 – 7.28 (m, 4H), 6.81 (d, *J* = 8.8 Hz, 2H), 5.03 – 4.90 (m, 1H), 3.80 (s, 3H), 2.67 (d, *J* = 2.1 Hz, 1H), 2.46 – 2.37 (m, 5H), 2.10 – 1.91 (m, 2H), 1.84 – 1.71 (m, 2H) ppm;

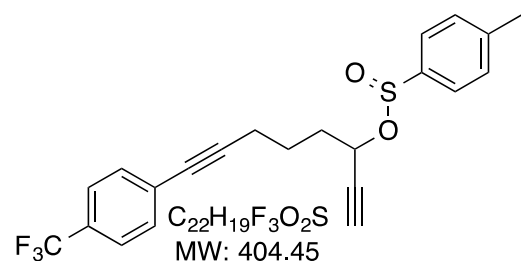
¹³C NMR (101 MHz, CDCl₃)
δ 159.2, †† 143.2, ‡ 143.1, † 142.5, ‡ 141.8, † 133.0 (2C), †† 129.9 (2C), † 129.7 (2C), ‡ 125.6 (2C), † 125.2 (2C), ‡ 116.1, † 116.1, ‡ 114.0 (2C), †† 87.7, † 87.6, ‡ 81.3, † 81.2, ‡ 81.1, † 81.0, ‡ 76.1, † 75.4, ‡ 67.6, † 65.2, ‡ 55.4, †† 36.0, † 35.4, ‡ 24.3, † 24.2, ‡ 21.7, † 21.7, ‡ 19.1, † 19.0[‡] ppm;

IR (thin film)
2954, 2932, 1606, 1510, 1246, 1135 cm⁻¹;

HRMS (TOF MS ES+)
[M+H]⁺ calcd for C₂₂H₂₂O₃S, 367.1362; found, 367.1371;

TLC R_f = 0.55 (30% ethyl acetate in hexanes, UV, silica gel)

8-(4-(trifluoromethyl)phenyl)octa-1,7-diyn-3-yl 4-methylbenzenesulfinate (**4.11**).



General Procedure IV was followed with tosyl chloride (1.40 g, 7.4 mmol), dichloromethane (18 mL), triethylamine (1.13 mL, 8.0 mmol), **4.8** (1.96 g, 7.4 mmol), triphenylphosphine (1.93 g, 7.4 mmol), and dichloromethane (18 mL). The sulfinate was purified

by column with 10% ethyl acetate in hexanes as the mobile phase to yield 2.27 g of sulfinate **4.11** as a separable 1:1 mixture of diastereomers in 76% yield as a yellow oil.

Data for 4.11 (AMB_E3_18)

Diastereomer 1:

¹H NMR (300 MHz, CDCl₃)

δ 7.65 (d, J = 8.2 Hz, 2H), 7.53 (d, J = 8.4 Hz, 2H), 7.47 (d, J = 8.4 Hz, 2H), 7.32 (d, J = 7.9 Hz, 2H), 4.95 (td, J = 6.4, 2.1 Hz, 1H), 2.49 (t, J = 7.0 Hz, 2H), 2.43 (s, 3H), 2.38 (d, J = 2.2 Hz, 1H), 2.10 – 1.96 (m, 2H), 1.89 – 1.75 (m, 2H) ppm;

^{13}C NMR (101 MHz, CDCl_3)

δ 143.2, 141.6, 132.0 (2C), 129.8 (2C), 127.8, 125.6 (2C), 125.3 (q, $J_{\text{CF}} = 4$ Hz) (2C), 92.2, 80.9, 80.4, 75.5, 64.7, 36.0, 24.0, 21.7, 19.1 ppm;

*signal/noise too small to observe quartets corresponding to CF_3 group and its bonded carbon.

IR (thin film)

2924, 1323, 1128, 1067 cm^{-1} ;

HRMS (TOF MS ES+)

$[\text{M}+\text{H}]^+$ calcd for $\text{C}_{22}\text{H}_{19}\text{O}_2\text{F}_3\text{S}$, 405.1131; found, 405.1140;

TLC

$R_f = 0.61$ (30% ethyl acetate in hexanes, UV, silica gel)

Diastereomer 2:

^1H NMR (300 MHz, CDCl_3)

δ 7.65 (d, J = 8.2 Hz, 2H), 7.53 (d, J = 8.3 Hz, 2H), 7.46 (d, J = 8.4 Hz, 2H), 7.33 (d, J = 7.9 Hz, 2H), 4.99 (td, J = 6.3, 2.1 Hz, 1H), 2.68 (d, J = 2.1 Hz, 1H), 2.50 – 2.35 (m, 5H), 2.08 – 1.92 (m, 2H), 1.87 – 1.72 (m, 2H) ppm;

^{13}C NMR (101 MHz, CDCl_3)

δ 143.2, 142.5, 132.0, 129.9, 127.8, 125.3 (q, $J_{\text{CF}} = 4$ Hz) (2C), 125.2 (2C), 92.1, 81.2, 80.3, 76.2, 67.6, 35.4, 24.0, 21.7, 19.1 ppm;

*signal/noise too small to observe quartets corresponding to CF_3 group and its bonded carbon.

IR (thin film)

2924, 1323, 1166, 1129, 1067 cm^{-1} ;

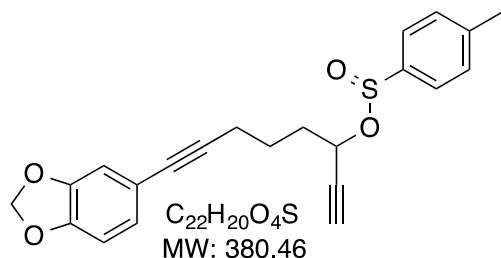
HRMS (TOF MS ES+)

$[\text{M}+\text{H}]^+$ calcd for $\text{C}_{22}\text{H}_{19}\text{O}_2\text{F}_3\text{S}$, 405.1131; found, 405.1142;

TLC

$R_f = 0.58$ (30% ethyl acetate in hexanes, UV, silica gel)

8-(benzo[*d*][1,3]dioxol-5-yl)octa-1,7-diyn-3-yl 4-methylbenzenesulfinate (4.12).



General Procedure IV was followed with tosyl chloride (1.05 g, 5.5 mmol), dichloromethane (14 mL), triethylamine (0.85 mL, 6.1 mmol), **4.9** (1.34 g, 5.5 mmol), triphenylphosphine (1.89 g, 7.2 mmol), and dichloromethane (13 mL). The sulfinate was purified

by column with 20% ethyl acetate in hexanes as the mobile phase to yield 1.79 g of sulfinate **4.12** as an inseparable 1:1 mixture of diastereomers in 85% yield as a light brown oil.

Data for 4.12 (AMB_E3_62)

1H NMR (500 MHz, $CDCl_3$)

δ 7.64 (d, $J = 8.1$ Hz, 2H), 7.32 (dd, $J = 7.8, 5.7$ Hz, 2H), 6.89 (ddd, $J = 7.1, 5.4, 1.5$ Hz, 1H), 6.83 (dd, $J = 5.6, 1.4$ Hz, 1H), 6.71 (d, $J = 8.0$ Hz, 1H), 5.94 (s, 2H), 4.96 (dtd, $J = 11.0, 6.4, 2.1$ Hz, 1H), 2.67 (d, $J = 2.1$ Hz, 1H), 2.45 – 2.36 (m, 5H), 2.06 – 1.93 (m, 2H), 1.85 – 1.70 (m, 2H) ppm;

^{13}C NMR (126 MHz, $CDCl_3$)

δ 147.4,^{†‡} 147.4,^{†‡} 143.1,[†] 143.1,[‡] 142.4,[†] 141.7,[‡] 129.8 (2C),[†] 129.7 (2C),[‡] 126.0,[†] 126.0,[‡] 125.5 (2C),[†] 125.2 (2C),[‡] 117.2,[†] 117.2,[‡] 111.8,[†] 111.8,[‡] 108.4,^{†‡} 101.3,^{†‡} 87.5,[†] 87.4,[‡] 81.3,[†] 81.2,[‡] 81.1,[†] 81.0,[‡] 76.1,[†] 75.4,[‡] 67.5,[†] 65.1,[‡] 36.0,[†] 35.3,[‡] 24.2,[†] 24.1,[‡] 21.7,[†] 21.7,[‡] 19.0,[†] 18.9[‡] ppm;

IR (thin film)

2955, 1600, 1488, 1247, 1135 cm^{-1} ;

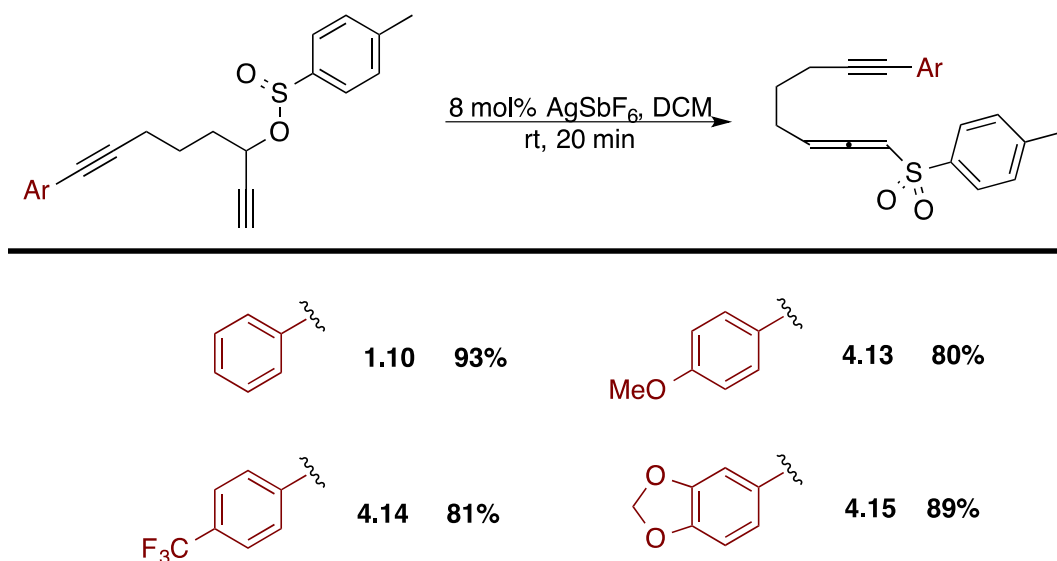
HRMS (TOF MS ES⁺)

$[M+H]^+$ calcd for $C_{22}H_{20}O_4S$, 381.1155; found, 381.1159;

TLC

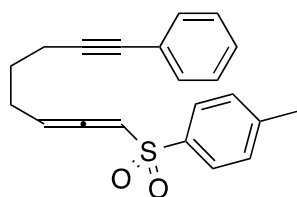
$R_f = 0.40$ (20% ethyl acetate in hexanes, UV, silica gel)

General Procedure V: [2,3] Sigmatropic Rearrangement



[2,3] sigmatropic rearrangement was performed in a manner analogous to a literature procedure.⁹ A round-bottomed flask equipped with a stirbar was charged with silver hexafluoroantimonate (0.08 equiv) and protected with a nitrogen atmosphere. **Sulfinate** (1 equiv) in dichloromethane was introduced to the flask over 3 minutes and the reaction was allowed to stir for 10 minutes to completion. The contents were passed through a short silica gel plug and the pad of silica was rinsed with diethyl ether. After concentration of filtrate on a rotovap, the crude product was purified by silica gel column chromatography with 20% ethyl acetate in hexanes as the mobile phase to provide the allene.

1-methyl-4-((8-phenylocta-1,2-dien-7-yn-1-yl)sulfonyl)benzene (**1.10**).



$\text{C}_{21}\text{H}_{20}\text{O}_2\text{S}$
MW: 336.45

General Procedure V was followed with silver hexafluoroantimonate (0.17 g, 0.49 mmol), **1.15** (2.01 g, 5.97 mmol), and dichloromethane (25 mL) to yield 1.97 g of allene **1.10** in 93% yield as a yellow oil.

Data for **1.10** (AMB_E2_033)

$^1\text{H NMR}$ (300 MHz, CDCl_3)

δ 7.79 (d, $J = 8.3$ Hz, 2H), 7.40 – 7.33 (m, 2H), 7.29 – 7.26 (m, 5H), 6.21 (dt, $J = 5.9, 2.9$ Hz, 1H), 5.87 (q, $J = 6.9$ Hz, 1H), 2.45 (t, $J = 6.9$ Hz, 2H), 2.38 (s, 3H), 2.31 (qd, $J = 7.2, 2.9$ Hz, 2H), 1.70 (p, $J = 7.5$ Hz, 2H) ppm;

^{13}C NMR (76 MHz, CDCl_3)

δ 205.5, 144.5, 138.5, 131.6 (2C), 129.9 (2C), 128.3 (2C), 127.8, 127.8 (2C), 123.8, 101.8, 100.4, 89.1, 81.5, 27.4, 26.9, 21.7, 18.8 ppm;

IR (thin film)

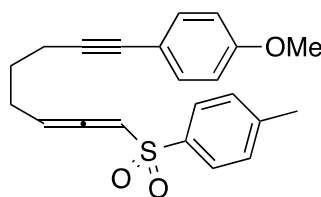
3021, 2934, 2228, 1954, 1597, 1318, 1145 cm^{-1} ;

HRMS (TOF MS ES+)

$[\text{M}+\text{H}]^+$ calcd for $\text{C}_{21}\text{H}_{20}\text{O}_2\text{S}$, 337.1257; found, 337.1274;

TLC $R_f = 0.60$ (30% ethyl acetate in hexanes, UV, silica gel)

1-methoxy-4-(8-tosylocta-6,7-dien-1-yn-1-yl)benzene (**4.13**).



$\text{C}_{22}\text{H}_{22}\text{O}_3\text{S}$
MW: 366.48

General Procedure V was followed with silver hexafluoroantimonate (60 mg, 0.17 mmol), **4.10** (798 mg, 2.18 mmol), and dichloromethane (7 mL) to yield 640 mg of allene **4.13** in 80% yield as a yellow oil.

Data for **4.13** (AMB_E3_34)

^1H NMR (300 MHz, CDCl_3)

δ 7.85 – 7.74 (m, 2H), 7.34 – 7.26 (m, 4H), 6.86 – 6.74 (m, 2H), 6.20 (dt, $J = 5.9, 2.9$ Hz, 1H), 5.86 (q, $J = 6.9$ Hz, 1H), 3.79 (s, 3H), 2.42 (t, $J = 6.9$ Hz, 2H), 2.39 (s, 3H), 2.30 (qd, $J = 7.2, 2.9$ Hz, 2H), 1.68 (p, $J = 7.0$ Hz, 2H) ppm;

^{13}C NMR (76 MHz, CDCl_3)

δ 205.5, 159.3, 144.5, 138.5, 133.0 (2C), 129.9 (2C), 127.8 (2C), 116.0, 114.0 (2C), 101.7, 100.4, 87.5, 81.2, 55.4, 27.6, 26.9, 21.7, 18.8 ppm;

IR (thin film)

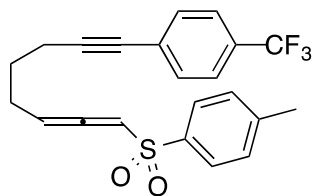
2936, 1954, 1318, 1145 cm^{-1} ;

HRMS (TOF MS ES+)

$[\text{M}+\text{H}]^+$ calcd for $\text{C}_{22}\text{H}_{22}\text{O}_3\text{S}$, 367.1362; found, 367.1378;

TLC $R_f = 0.18$ (20% ethyl acetate in hexanes, UV, silica gel)

1-methyl-4-((8-(4-(trifluoromethyl)phenyl)octa-1,2-dien-7-yn-1-yl)sulfonyl)benzene (4.14).



$C_{22}H_{19}F_3O_2S$
MW: 404.45

General Procedure V was followed with silver hexafluoroantimonate (0.150 g, 0.44 mmol), **4.11** (2.21 g, 5.47 mmol), and dichloromethane (17.6 mL) to yield 1.79 g of allene **4.14** in 81% yield as a yellow oil.

Data for 4.14 (AMB_E3_19)

1H NMR (300 MHz, $CDCl_3$)

δ 7.79 (d, $J = 8.3$ Hz, 2H), 7.54 (d, $J = 8.3$ Hz, 2H), 7.47 (d, $J = 8.3$ Hz, 2H), 7.29 (d, $J = 8.0$ Hz, 2H), 6.21 (dt, $J = 5.9, 2.9$ Hz, 1H), 5.88 (q, $J = 7.0, 6.1$ Hz, 1H), 2.49 (t, $J = 6.9$ Hz, 2H), 2.40 (s, 3H), 2.33 (qd, $J = 7.2, 2.9$ Hz, 2H), 1.82 – 1.68 (m, 2H) ppm;

^{13}C NMR (76 MHz, $CDCl_3$)

δ 205.6, 144.6, 138.6, 131.9 (2C), 129.9 (2C), 129.6 (q, $J_{CF} = 33$ Hz), 127.8 (3C), 125.2 (q, $J_{CF} = 4$ Hz) (2C), 124.1 (q, $J_{CF} = 274$ Hz), 101.8, 100.2, 92.1, 80.4, 27.2, 26.9, 21.7, 18.8 ppm;

IR (thin film)

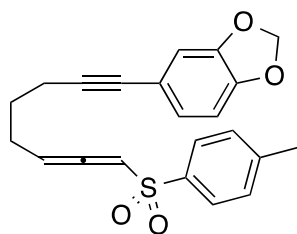
2934, 2230, 1956, 1322, 1145 cm^{-1} ;

HRMS (TOF MS ES+)

$[M+H]^+$ calcd for $C_{22}H_{19}O_2F_3S$, 405.1131; found, 405.1148;

TLC $R_f = 0.17$ (10% ethyl acetate in hexanes, UV, silica gel)

5-(8-tosylocta-6,7-dien-1-yn-1-yl)benzo[*d*][1,3]dioxole (4.15).



$C_{22}H_{20}O_4S$
MW: 380.46

General Procedure V was followed with silver hexafluoroantimonate (0.126 g, 0.37 mmol), **4.12** (1.74 g, 4.57 mmol), and dichloromethane (15 mL) to yield 1.56 g of allene **4.15** in 89% yield as an orange oil.

Data for **4.15** (AMB_E3_64)

¹H NMR (500 MHz, CDCl₃)

δ 7.78 (d, *J* = 8.3 Hz, 2H), 7.29 (d, *J* = 8.1 Hz, 2H), 6.88 (dd, *J* = 8.0, 1.5 Hz, 1H), 6.81 (d, *J* = 1.4 Hz, 1H), 6.71 (d, *J* = 8.0 Hz, 1H), 6.20 (dt, *J* = 5.9, 2.9 Hz, 1H), 5.94 (s, 2H), 5.86 (q, *J* = 6.8 Hz, 1H), 2.41 (d, *J* = 6.4 Hz, 5H), 2.29 (qd, *J* = 7.2, 2.9 Hz, 2H), 1.71 – 1.63 (m, 2H) ppm;

¹³C NMR (126 MHz, CDCl₃)

δ 205.5, 147.5, 147.4, 144.5, 138.5, 129.9 (2C), 127.8 (2C), 126.0, 117.1, 111.7, 108.4, 101.8, 101.3, 100.4, 87.3, 81.2, 27.5, 26.9, 21.7, 18.7 ppm;

IR (thin film)

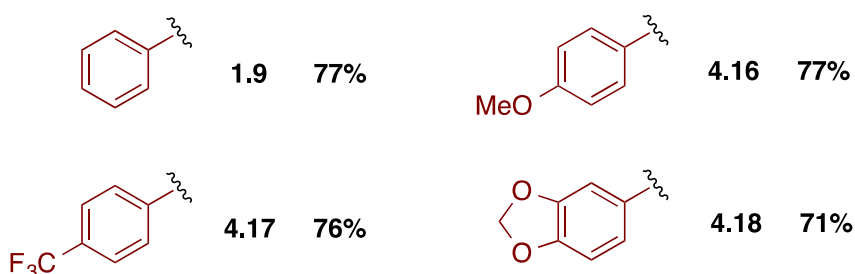
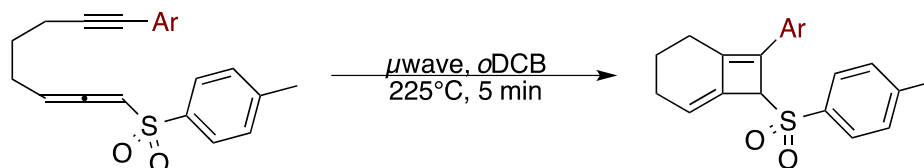
2902, 1954, 1597, 1319, 1146 cm⁻¹;

HRMS (TOF MS ES⁺)

[M+H]⁺ calcd for C₂₂H₂₀O₄S, 381.1161; found, 381.1147;

TLC R_f = 0.31 (20% ethyl acetate in hexanes, UV, silica gel)

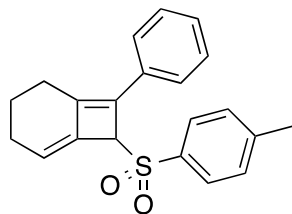
General Procedure VI: Thermal [2+2] Cycloaddition



Freshly purified **allene** was mixed well with 1,2-dichlorobenzene (0.04 *M*). The resulting solution was heated with stirring to 225°C in the microwave for five minutes resulting in full conversion to product. 1,2-dichlorobenzene was removed by filtering the product solution through a column and flushing with 100% hexanes until the liquid coming out was not UV

active. Then, 20% ethyl acetate in hexanes was added to the column to isolate the alkylidene cyclobutene.

7-phenyl-8-tosylbicyclo[4.2.0]octa-1,6-diene (1.9**).**



C₂₁H₂₀O₂S
MW: 336.45

General Procedure VI was followed with **1.10** (858 mg, 2.55 mmol) and 1,2-dichlorobenzene (60 mL) to yield 661 mg of alkylidene cyclobutene **1.9** in 77% yield as a brown solid.

Data for **1.9** (AMB_E2_073)

MP 105 – 110 °C

¹H NMR (300 MHz, CDCl₃)

δ 7.59 (d, *J* = 8.2 Hz, 2H), 7.50 (d, *J* = 7.3 Hz, 2H), 7.36 (t, *J* = 7.4 Hz, 2H), 7.27 (q, *J* = 7.4, 6.4 Hz, 1H), 7.16 (d, *J* = 8.1 Hz, 2H), 5.62 (t, *J* = 4.0 Hz, 1H), 5.13 (s, 1H), 2.49 – 2.40 (m, 1H), 2.39 (s, 3H), 2.25 (t, *J* = 6.3 Hz, 1H), 2.18 – 2.06 (m, 2H), 1.79 – 1.61 (m, 1H), 1.59 – 1.44 (m, 1H) ppm;

¹³C NMR (101 MHz, CDCl₃)

δ 148.8, 144.4, 134.6, 134.1, 133.3, 133.1, 129.7 (2C), 128.7 (2C), 128.7 (2C), 127.9, 126.8 (2C), 115.4, 70.5, 24.5, 23.2, 22.4, 21.8 ppm;

IR (thin film)

2925, 1597, 1311, 1144, 1084 cm⁻¹

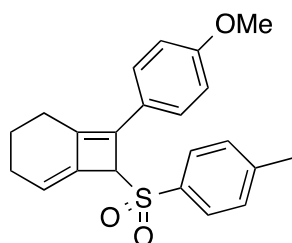
HRMS (TOF MS ES⁺)

[M+H]⁺ calcd for C₂₁H₂₀O₂S, 337.1257; found, 337.1275;

TLC

R_f = 0.39 (20% ethyl acetate in hexanes, UV, silica gel)

7-(4-methoxyphenyl)-8-tosylbicyclo[4.2.0]octa-1,6-diene (4.16).



C₂₂H₂₂O₃S
MW: 366.48

General Procedure VI was followed with **4.13** (640 mg, 1.55 mmol) and 1,2-dichlorobenzene (43 mL) to yield 495 mg of alkylidene cyclobutene **4.16** in 77% yield as a tan solid.

Data for 4.16 (AMB_E3_35)

¹H NMR (300 MHz, CDCl₃)

δ 7.56 (d, *J* = 8.2 Hz, 2H), 7.43 (d, *J* = 8.8 Hz, 2H), 7.15 (d, *J* = 8.1 Hz, 2H), 6.89 (d, *J* = 8.9 Hz, 2H), 5.54 (t, *J* = 4.1 Hz, 1H), 5.08 (s, 1H), 3.84 (s, 3H), 2.39 (s, 3H), 2.36 – 2.29 (m, 1H), 2.23 – 2.01 (m, 3H), 1.75 – 1.59 (m, 1H), 1.59 – 1.40 (m, 1H) ppm;

¹³C NMR (76 MHz, CDCl₃)

159.3, 146.2, 144.4, 134.2, 134.1, 133.2, 129.6 (2C), 128.6 (2C), 128.3 (2C), 126.1, 114.2 (2C), 113.8, 70.5, 55.4, 24.4, 23.0, 22.4, 21.7 ppm;

IR (thin film)

2923, 1300, 1177 cm⁻¹;

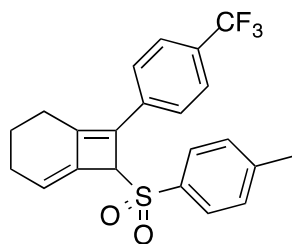
HRMS (TOF MS ES⁺)

[M+H]⁺ calcd for C₂₂H₂₂O₃S, 367.1362; found, 367.1383;

TLC

R_f = 0.34 (30% ethyl acetate in hexanes, UV, silica gel)

8-tosyl-7-(4-(trifluoromethyl)phenyl)bicyclo[4.2.0]octa-1,6-diene (4.17).



C₂₂H₁₉F₃O₂S
MW: 404.45

General Procedure VI was followed with **4.14** (985 mg, 2.44 mmol) and 1,2-dichlorobenzene (60 mL) to yield 750 mg of alkylidene cyclobutene **4.17** in 76% yield as a tan solid.

Data for 4.17 (AMB_E3_20)

¹H NMR (300 MHz, CDCl₃)

δ 7.63 – 7.51 (m, 6H), 7.17 (d, J = 8.0 Hz, 2H), 5.67 (t, J = 4.1 Hz, 1H), 5.13 (s, 1H), 2.52 – 2.36 (m, 4H), 2.34 – 2.20 (m, 1H), 2.20 – 2.04 (m, 2H), 1.81 – 1.63 (m, 1H), 1.63 – 1.48 (m, 1H) ppm;

^{13}C NMR (76 MHz, CDCl_3)

δ 151.4, 144.8, 136.3 (q, J_{CF} = 1 Hz), 133.9, 133.2, 133.2, 129.6 (2C), 129.3 (q, J_{CF} = 33 Hz), 128.9 (2C), 126.8 (2C), 125.6 (q, J_{CF} = 4 Hz) (2C), 124.2 (q, J_{CF} = 274 Hz), 117.3, 70.5, 24.5, 23.3, 22.3, 21.7 ppm;

IR (thin film)

2946, 1325, 1129, 1068 cm^{-1} ;

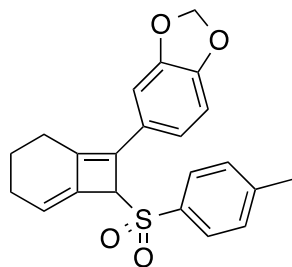
HRMS (TOF MS ES+)

$[\text{M}+\text{H}]^+$ calcd for $\text{C}_{22}\text{H}_{19}\text{O}_2\text{F}_3\text{S}$, 405.1131; found, 405.1152;

TLC

R_f = 0.41 (30% ethyl acetate in hexanes, UV, silica gel)

5-(8-tosylbicyclo[4.2.0]octa-1,6-dien-7-yl)benzo[d][1,3]dioxole (**4.18**)



$\text{C}_{22}\text{H}_{20}\text{O}_4\text{S}$
MW: 380.46

General Procedure VI was followed with **4.15** (337 mg, 0.89 mmol) and 1,2-dichlorobenzene (20 mL) to yield 240 mg of alkylidene cyclobutene **4.18** in 71% yield as a tan solid.

Data for **4.18** (AMB_E4_06)

^1H NMR (500 MHz, CDCl_3)

δ 7.58 (d, J = 8.2 Hz, 2H), 7.17 (d, J = 8.1 Hz, 2H), 7.06 (dd, J = 8.1, 1.4 Hz, 1H), 6.90 (d, J = 1.4 Hz, 1H), 6.81 (d, J = 8.1 Hz, 1H), 6.01 – 5.96 (m, 2H), 5.55 (t, J = 4.0 Hz, 1H), 5.04 (s, 1H), 2.47 – 2.29 (m, 4H), 2.20 – 2.02 (m, 3H), 1.72 – 1.60 (m, 1H), 1.56 – 1.45 (m, 1H) ppm;

^{13}C NMR (126 MHz, CDCl_3)

δ 147.9, 147.5, 146.8, 144.5, 134.3, 134.0, 133.3, 129.7 (2C), 128.7 (2C), 127.6, 121.5, 114.4, 108.8, 106.8, 101.3, 70.6, 24.5, 23.0, 22.4, 21.8 ppm;

IR (thin film)

2925, 1290, 1597, 1132, 1085 cm⁻¹;

HRMS

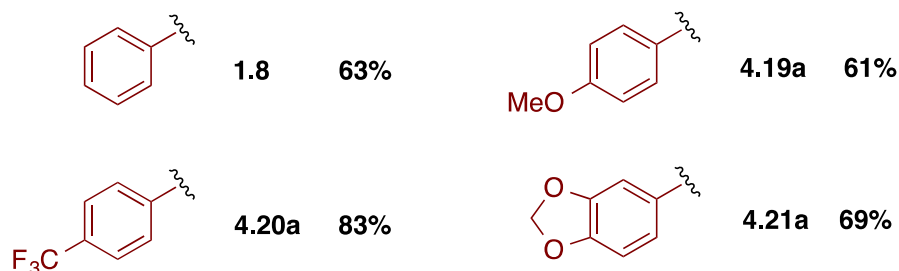
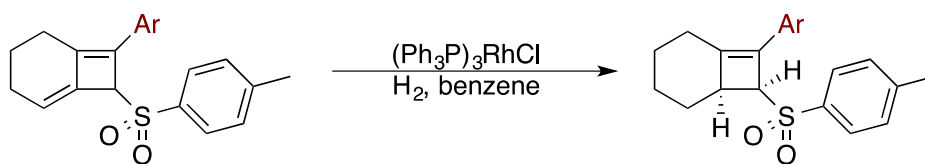
(TOF MS ES+)

[M+H]⁺ calcd for C₂₂H₂₀O₄S, 381.1155; found, 381.1164;

TLC

R_f = 0.29 (20% ethyl acetate in hexanes, UV, silica gel)

General Procedure VII: Hydrogenation

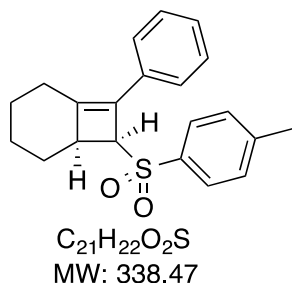


Method A: A solution of **alkylidene cyclobutene** (1 equiv) in benzene was added to a round-bottomed flask containing a stirbar and tris(triphenylphosphine)rhodium(I) chloride (Wilkinson's catalyst) (0.06 equiv). The reaction vessel was purged with a balloon containing hydrogen gas (Matheson Ultra High Purity) and the brown solution was stirred at room temperature overnight. The next day, if the reaction was not yet complete by NMR, another 0.03 equiv of Wilkinson's catalyst was added. This process was repeated everyday until the reaction had gone to completion. Once complete by NMR, the reaction vessel was diluted with ether and the contents of the reaction were filtered through a cotton plug. The resulting filtrate was concentrated to give the crude product. Cyclobutene was purified by column chromatography.

Method B: A solution of **alkylidene cyclobutene** (1 equiv) in benzene was added to a round-bottomed flask containing a stirbar and Wilkinson's catalyst (0.07 equiv). The reaction vessel was purged with a balloon containing hydrogen gas (Matheson Ultra High Purity) and the brown

solution was stirred at 40 °C overnight resulting in complete consumption of starting material by NMR. The reaction vessel was diluted with ether and the contents of the reaction were filtered through a cotton plug. The resulting filtrate was concentrated to give the crude product. Cyclobutene was purified by column chromatography.

7-phenyl-8-tosylbicyclo[4.2.0]oct-6-ene (**1.8**).



General Procedure VII, Method A was followed with **1.9** (583 mg, 1.75 mmol), benzene (7 mL), and Wilkinson's catalyst (150 mg, 0.16 mmol). Crude product was purified using a mobile phase of 20% ethyl acetate in hexanes to yield 367 mg of cyclobutene **1.8** in 63% yield as a white solid.

Data for **1.8** (AMB_E2_049)

MP 130 – 133 °C

1H NMR (601 MHz, $CDCl_3$)

δ 7.71 – 7.59 (m, 2H), 7.31 – 7.23 (m, 4H), 7.23 – 7.14 (m, 2H), 4.81 (dd, $J = 4.3, 3.6$ Hz, 1H), 2.84 (dd, $J = 14.4, 4.3$ Hz, 1H), 2.74 (dt, $J = 10.4, 4.5$ Hz, 1H), 2.43 (s, 3H), 2.13 – 2.04 (m, 1H), 1.97 – 1.89 (m, 1H), 1.87 – 1.80 (m, 1H), 1.76 – 1.69 (m, 1H), 1.62 – 1.51 (m, 2H), 1.32 – 1.20 (m, 1H) ppm;

^{13}C NMR (101 MHz, $CDCl_3$)

δ 152.2, 144.2, 138.2, 133.4, 129.6 (2C), 129.4, 128.3 (2C), 128.3 (2C), 127.3, 126.9 (2C), 66.4, 42.4, 27.9, 26.6, 26.3, 24.7, 21.7 ppm;

IR (thin film)

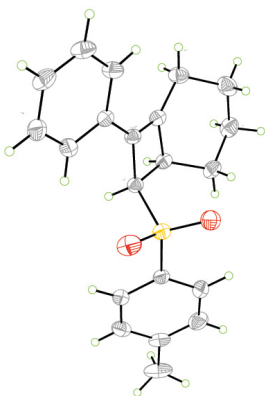
2935, 1597, 1302, 1143 cm^{-1}

HRMS (TOF MS ES+)

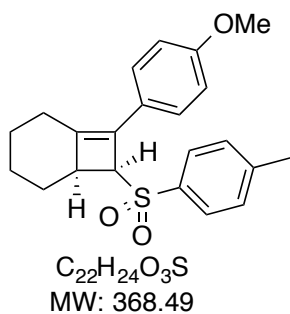
$[M+H]^+$ calcd for $C_{21}H_{22}O_2S$, 339.1413; found, 339.1428;

TLC $R_f = 0.39$ (30% ethyl acetate in hexanes, UV, silica gel)

Crystal Structure (See pg 79 for crystal structure report)



7-(4-methoxyphenyl)-8-tosylbicyclo[4.2.0]oct-6-ene (4.19a**).**



General Procedure VII, Method A was followed with **4.16** (302 mg, 0.82 mmol), benzene (6.5 mL), and Wilkinson's catalyst (115 mg, 0.12 mmol). Crude product was purified using a gradient mobile phase of 3%-10% ethyl acetate in hexanes to yield 185 mg of cyclobutene **4.19a** in 61% yield as a white solid.

Data for **4.19a** (AMB_E3_52)

1H NMR (300 MHz, $CDCl_3$)

δ 7.68 (d, $J = 8.3$ Hz, 2H), 7.31 – 7.27 (m, 2H), 7.26 – 7.22 (m, 2H), 6.82 – 6.71 (m, 2H), 4.77 (dd, $J = 4.8, 3.6$ Hz, 1H), 3.79 (s, 3H), 2.79 (dd, $J = 14.3, 4.0$ Hz, 1H), 2.70 (dt, $J = 10.8, 5.2$ Hz, 1H), 2.43 (s, 3H), 2.04 (qd, $J = 12.5, 3.2$ Hz, 2H), 1.96 – 1.86 (m, 1H), 1.81 (dt, $J = 13.9, 3.3$ Hz, 1H), 1.71 – 1.61 (m, 1H), 1.52 – 1.45 (m, 1H), 1.24 (qt, $J = 13.2, 3.0$ Hz, 1H) ppm;

^{13}C NMR (101 MHz, $CDCl_3$)

δ 158.8, 149.7, 144.2, 138.2, 129.6 (2C), 129.0, 128.4 (2C), 128.3 (2C), 126.4, 113.8 (2C), 66.5, 55.4, 42.2, 27.8, 26.5, 26.3, 24.7, 21.8 ppm;

IR (thin film)

2934, 1606, 1538, 1300, 1247, 1142 cm^{-1} ;

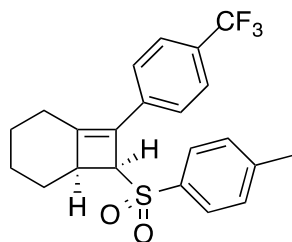
HRMS (TOF MS ES+)

$[M+H]^+$ calcd for $C_{22}H_{24}O_3S$, 369.1519; found, 369.1536;

TLC

$R_f = 0.34$ (30% ethyl acetate in hexanes, UV, silica gel)

8-tosyl-7-(4-(trifluoromethyl)phenyl)bicyclo[4.2.0]oct-6-ene (4.20a).



C₂₂H₂₁F₃O₂S
MW: 406.46

General Procedure VII, Method A was followed with **4.17** (690 mg, 1.71 mmol), benzene (7 mL), and Wilkinson's catalyst (144 mg, 0.16 mmol). Crude product was purified using a mobile phase of 20% ethyl acetate in hexanes to yield 576 mg of cyclobutene **4.20a** in 83% yield as a white solid.

Data for 4.20a (AMB_E3_21)

MP 137 – 140 °C

¹H NMR (300 MHz, CDCl₃)

δ 7.68 (d, *J* = 8.2 Hz, 2H), 7.47 (d, *J* = 8.6 Hz, 2H), 7.42 (d, *J* = 8.5 Hz, 2H), 7.31 – 7.26 (m, 2H), 4.87 – 4.78 (m, 1H), 2.84 (dd, *J* = 14.5, 4.0 Hz, 1H), 2.76 (dt, *J* = 10.3, 4.8 Hz, 1H), 2.44 (s, 3H), 2.21 – 2.04 (m, 2H), 2.03 – 1.91 (m, 1H), 1.90 – 1.77 (m, 1H), 1.73 – 1.63 (m, 1H), 1.63 – 1.50 (m, 1H), 1.27 (qt, *J* = 13.2, 2.7 Hz, 1H) ppm;

¹³C NMR (101 MHz, CDCl₃)

δ 155.3, 144.6, 137.9, 136.8 (q, *J*_{CF} = 1 Hz), 129.7 (2C), 129.0 (q, *J*_{CF} = 33 Hz), 128.3, 128.3 (2C), 127.1 (2C), 125.3 (q, *J*_{CF} = 4 Hz) (2C), 124.3 (q, *J*_{CF} = 273 Hz), 66.3, 42.6, 27.7, 26.8, 26.2, 24.5, 21.7 ppm;

IR (thin film)

2941, 1614, 1326, 1119 cm⁻¹;

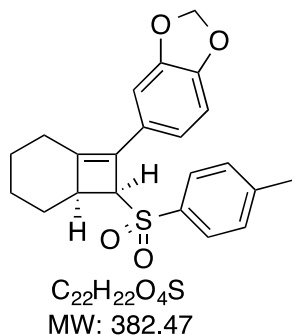
HRMS (TOF MS ES⁺)

[M+H]⁺ calcd for C₂₂H₂₁O₂F₃S, 407.1287; found, 407.1307;

TLC

R_f = 0.41 (30% ethyl acetate in hexanes, UV, silica gel)

5-(8-tosylbicyclo[4.2.0]oct-6-en-7-yl)benzo[d][1,3]dioxole (4.21a).



General Procedure VII, Method B was followed with **4.18** (228 mg, 0.60 mmol), benzene (2 mL), and Wilkinson's catalyst (40 mg, 0.12 mmol). Crude product was purified using a mobile phase of 20% ethyl acetate in hexanes to yield 158 mg of a 37:63 mixture of diene **4.21b** to cyclobutene **4.21a** respectively in 69% yield as a waxy solid.

Data for **4.21a** (AMB_E4_07)

1H NMR (400 MHz, $CDCl_3$)

δ 7.69 (d, $J = 8.2$ Hz, 2H), 7.34 – 7.27 (m, 2H), 6.82 – 6.75 (m, 2H), 6.66 (d, $J = 8.6$ Hz, 1H), 5.96 – 5.90 (m, 2H), 4.78 – 4.71 (m, 1H), 2.77 (dd, $J = 14.5, 3.9$ Hz, 1H), 2.70 (dt, $J = 10.0, 4.6$ Hz, 1H), 2.43 (s, 3H), 2.11 – 2.00 (m, 2H), 1.96 – 1.87 (m, 1H), 1.82 (dt, $J = 14.4, 2.9$ Hz, 1H), 1.70 – 1.64 (m, 1H), 1.53 – 1.46 (m, 1H), 1.23 – 1.17 (m, 1H) ppm;

^{13}C NMR (101 MHz, $CDCl_3$)

δ 150.4, 147.6, 146.8, 144.3, 138.1, 129.6, 129.0, 128.4, 127.7, 121.1, 108.3, 107.4, 101.1, 66.5, 42.2, 27.8, 26.4, 26.2, 24.7, 21.8 ppm;

IR (thin film)

2932, 1301, 1142 cm^{-1} ;

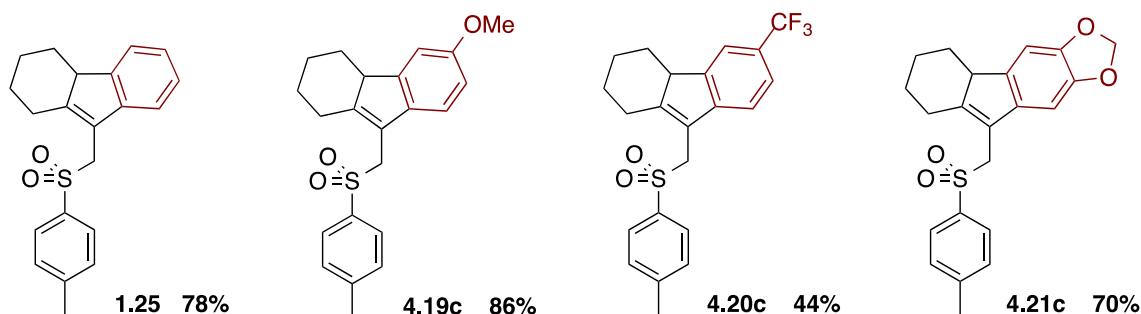
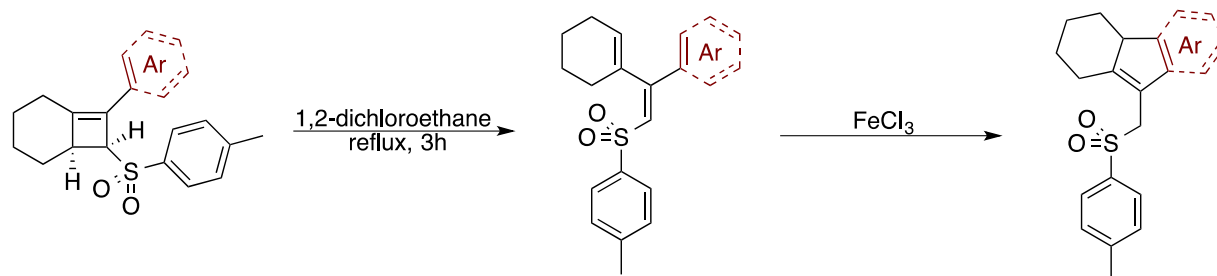
HRMS (TOF MS ES+)

$[M+H]^+$ calcd for $C_{22}H_{22}O_4S$, 383.1313; found, 383.1312;

TLC

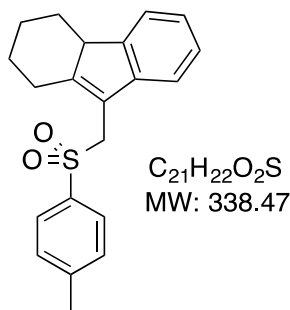
$R_f = 0.34$ (20% ethyl acetate in hexanes, UV, silica gel)

General Procedure VIII: *Electrocyclic Ring Opening and Electrocyclization*



A clear solution of **cyclobutene** in 1,2-dichloroethane (DCE) was heated to reflux for 3 h to generate **diene**. Upon cooling the yellow reaction mixture, iron(III) chloride was added, causing the solution to turn brown. Once starting material had been consumed, the reaction mixture was diluted with methylene chloride and transferred to a separatory funnel where it was washed with saturated sodium bicarbonate and water. The organic layer was dried over magnesium sulfate and concentrated to provide the crude product, which was purified to give the tetrahydrofluorene.

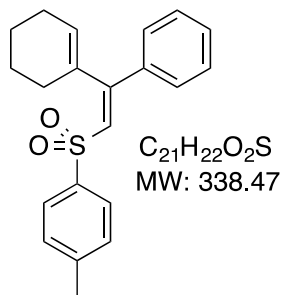
9-(tosylmethyl)-2,3,4,4a-tetrahydro-1H-fluorene (**1.25**).



General Procedure VIII was followed with **1.8** (50 mg, 0.15 mmol, 1 equiv) and 1,2 dichloroethane (5 mL) to give diene **1.28**. The reaction mixture was cooled to room temperature and iron(III) chloride (29 mg, 0.18 mmol, 1.20 equiv) was added causing the reaction to turn brown. The reaction was stirred at room temperature and monitored by TLC. 10 h after the addition of iron(III) chloride, the reaction had gone to

completion. The crude product was purified by silica gel column chromatography with 20% ethyl acetate in hexanes as the mobile phase to give 39 mg of tetrahydrofluorene **1.25** as a yellow solid in 78% yield.

Data for (*E*)-1-((2-(cyclohex-1-en-1-yl)-2-phenylvinyl)sulfonyl)-4-methylbenzene (1.28**)**



¹H NMR (300 MHz, CDCl₃)

δ 7.79 (d, *J* = 8.2 Hz, 2H), 7.42 – 7.27 (m, 7H), 6.68 (s, 1H), 5.75 – 5.66 (m, 1H), 2.43 (s, 3H), 2.18 – 2.09 (m, 2H), 1.70 – 1.62 (m, 2H), 1.62 – 1.52 (m, 2H), 1.52 – 1.42 (m, 2H) ppm;

¹³C NMR (76 MHz, CDCl₃)

δ 158.2, 143.8, 139.9, 137.2, 133.4, 131.0, 130.2, 129.5 (2C), 128.8 (2C), 128.0 (2C), 127.8, 127.6 (2C), 27.7, 25.4, 22.2, 21.7, 21.6 ppm;

IR (thin film)

2928, 1311, 1181, 1084 cm⁻¹;

HRMS (TOF MS ES⁺)

[M+H]⁺ calcd for C₂₁H₂₂O₂S, 339.1413; found, 339.1431;

TLC R_f = 0.55 (30% ethyl acetate in hexanes, UV, silica gel)

Data for **1.25** (AMB_E3_09)

MP 148 – 151 °C

¹H NMR (400 MHz, CDCl₃)

δ 7.62 (d, *J* = 8.2 Hz, 2H), 7.31 (d, *J* = 7.1 Hz, 1H), 7.23 – 7.16 (m, 4H), 7.16 – 7.07 (m, 1H), 4.32 (ABq, 2H, Δδ_{AB} = 0.12, *J*_{AB} = 14.2 Hz), 3.00 (dd, *J* = 12.4, 6.0 Hz, 1H), 2.51 – 2.43 (m, 2H), 2.38 (s, 3H), 1.93 – 1.74 (m, 3H), 1.49 (dtd, *J* = 13.3, 10.4, 3.0 Hz, 2H), 0.97 – 0.76 (m, 2H) ppm;

¹³C NMR (76 MHz, CDCl₃)

δ 155.0, 146.3, 144.7, 143.6, 135.8, 129.6 (2C), 128.9 (2C), 126.5, 124.3, 122.3, 120.9, 119.4, 53.7, 50.3, 32.3, 27.2, 26.6, 25.4, 21.7 ppm;

IR (thin film)

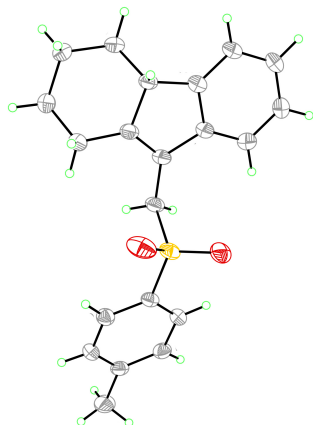
2930, 1597, 1463, 1301, 1133 cm⁻¹

HRMS (TOF MS ES⁺)

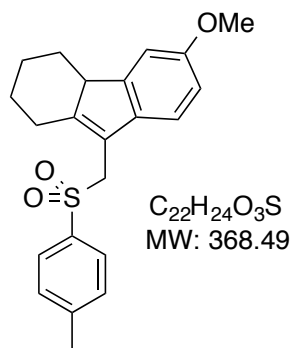
$[M+H]^+$ calcd for $C_{21}H_{22}O_2S$, 339.1413; found, 339.1429;

TLC $R_f = 0.39$ (30% ethyl acetate in hexanes, UV, silica gel)

Crystal Structure (See pg 85 for crystal structure report)



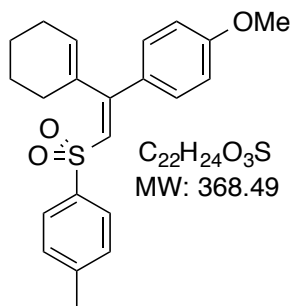
6-methoxy-9-(tosylmethyl)-2,3,4,4a-tetrahydro-1H-fluorene (**4.19c**).



General Procedure VIII was followed with **4.19a** (50 mg, 0.14 mmol, 1 equiv) and 1,2 dichloroethane (4.35 mL) to give diene **4.19b**. The reaction mixture was cooled to room temperature and 0.3 mL of a freshly prepared 0.14 M solution of iron(III) chloride in DCE (0.3 equiv) was added. The reaction was stirred at room temperature and monitored by NMR. 2 h after the addition of iron(III) chloride, the reaction had gone to completion. The crude product was purified by

silica gel column chromatography with 20% ethyl acetate in hexanes as the mobile phase to give 43 mg of tetrahydrofluorene **4.19c** as a yellow solid in 86% yield.

Data for (*E*)-1-((2-(cyclohex-1-en-1-yl)-2-(4-methoxyphenyl)vinyl)sulfonyl)-4-methyl



benzene (**4.19b**)

1H NMR (500 MHz, $CDCl_3$)

δ 7.78 (d, $J = 8.3$ Hz, 2H), 7.37 – 7.32 (m, 2H), 7.30 (d, $J = 8.0$ Hz, 2H), 6.89 – 6.84 (m, 2H), 6.63 (s, 1H), 5.64 – 5.58 (m, 1H), 3.82 (s, 3H), 2.43 (s, 3H), 2.14 – 2.09 (m, 2H), 1.73 – 1.67 (m, 2H), 1.62 – 1.57 (m, 2H), 1.52 – 1.46 (m, 2H) ppm;

^{13}C NMR (126 MHz, $CDCl_3$)

δ 161.5, 157.9, 143.7, 140.3, 133.6, 130.5, 129.5 (2C), 129.3, 129.2 (2C), 128.0 (2C), 125.7, 114.3 (2C), 55.5, 28.0, 25.4, 22.3, 21.7, 21.6 ppm;

IR (thin film)

2926, 1291, 1141, 1084 cm^{-1} ;

HRMS (TOF MS ES+)

$[\text{M}+\text{H}]^+$ calcd for $\text{C}_{22}\text{H}_{24}\text{O}_3\text{S}$, 369.1519; found, 369.1515;

TLC R_f = 0.34 (30% ethyl acetate in hexanes, UV, silica gel)

Data for 4.19c (AMB_E3_56)

MP 149 – 150 $^{\circ}\text{C}$

^1H NMR (500 MHz, CDCl_3)

δ 7.61 (d, J = 8.2 Hz, 2H), 7.21 (d, J = 8.1 Hz, 2H), 7.11 (d, J = 8.3 Hz, 1H), 6.90 (d, J = 2.0 Hz, 1H), 6.73 (dd, J = 8.4, 2.3 Hz, 1H), 4.28(ABq, 2H, $\Delta\delta_{\text{AB}}$ = 0.04, J_{AB} = 14.2 Hz), 3.81 (s, 3H), 2.95 (dd, J = 12.6, 5.4 Hz, 1H), 2.45 – 2.35 (m, 5H), 1.85 – 1.74 (m, 3H), 1.51 – 1.40 (m, 1H), 0.93 – 0.77 (m, 2H) ppm;

^{13}C NMR (101 MHz, CDCl_3)

δ 157.7, 152.7, 148.1, 144.6, 136.7, 135.7, 129.6 (2C), 128.9 (2C), 120.4, 119.8, 111.5, 109.5, 55.7, 53.9, 50.2, 32.3, 27.2, 26.5, 25.4, 21.7 ppm;

IR (thin film)

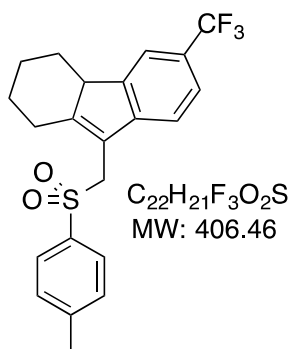
2929, 1582, 1478, 1315, 1134 cm^{-1}

HRMS (TOF MS ES+)

$[\text{M}+\text{H}]^+$ calcd for $\text{C}_{22}\text{H}_{24}\text{O}_3\text{S}$, 369.1524; found, 369.1530;

TLC R_f = 0.34 (30% ethyl acetate in hexanes, UV, silica gel)

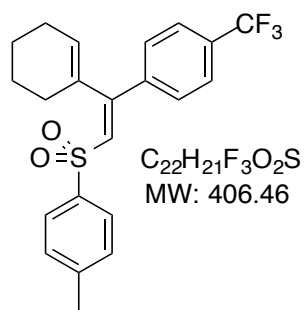
9-(tosylmethyl)-6-(trifluoromethyl)-2,3,4,4a-tetrahydro-1H-fluorene (4.20c).



General Procedure VIII was followed with **4.20a** (50 mg, 0.12 mmol, 1 equiv) and 1,2 dichloroethane (4.20 mL) to give diene **4.20b**. The reaction mixture was cooled to 40°C and iron(III) chloride (80 mg, 0.49 mmol, 4 equiv) was added. The reaction was stirred at 40°C and monitored by TLC. 4 h after the initial addition of iron(III) chloride, more iron(III) chloride (40 mg, 0.25 mmol, 2 equiv) was added to the

reaction mixture. 7 h after the first addition of iron(III) chloride, the reaction had gone to completion. The crude product was purified by silica gel column chromatography with 20% ethyl acetate in hexanes as the mobile phase to give 22 mg of tetrahydrofluorene **4.20c** as an orange solid in 44% yield.

Data for (*E*)-1-((2-(cyclohex-1-en-1-yl)-2-(4-(trifluoromethyl)phenyl)vinyl)sulfonyl)-



4-methylbenzene (4.20b)

MP 125 – 128 °C

¹H NMR (300 MHz, CDCl₃)

δ 7.79 (d, *J* = 8.3 Hz, 2H), 7.60 (d, *J* = 8.2 Hz, 2H), 7.48 (d, *J* = 8.2 Hz, 2H), 7.33 (d, *J* = 8.0 Hz, 2H), 6.71 (s, 1H), 5.83 – 5.73 (m, 1H), 2.44 (s, 3H), 2.20 – 2.09 (m, 2H), 1.67 – 1.61 (m, 2H), 1.61 – 1.52 (m, 2H), 1.52 – 1.40 (m, 2H) ppm;

¹³C NMR (76 MHz, CDCl₃)

δ 156.4, 144.2, 140.9 (q, *J*_{CF} = 1 Hz), 139.4, 132.9, 131.9 (q, *J*_{CF} = 33 Hz), 131.8, 129.8, 129.7 (2C), 128.1 (2C), 128.0 (2C), 125.8 (q, *J*_{CF} = 4 Hz) (2C), 123.9 (q, *J*_{CF} = 274 Hz), 27.5, 25.4, 22.1, 21.7, 21.4 ppm;

IR (thin film)

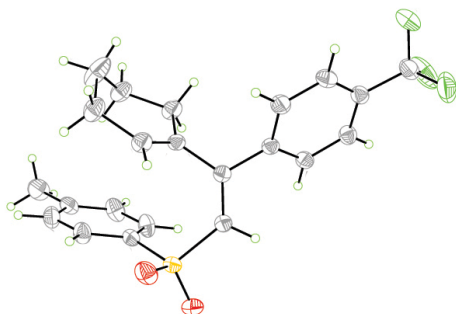
2932, 1324, 1142, 1067 cm⁻¹;

HRMS (TOF MS ES⁺)

[*M*+*H*]⁺ calcd for C₂₂H₂₁O₂F₃S, 407.1287; found, 407.1308;

TLC R_f = 0.47 (30% ethyl acetate in hexanes, UV, silica gel)

Crystal Structure (See pg 92 for crystal structure report)



Data for 4.20c (AMB_E4_17)

MP 147 – 150 °C

¹H NMR (500 MHz, CDCl₃)

δ 7.61 (d, *J* = 8.2 Hz, 2H), 7.53 (s, 1H), 7.44 (d, *J* = 8.0 Hz, 1H), 7.26 (d, *J* = 7.9 Hz, 1H), 7.21 (d, *J* = 8.0 Hz, 2H), 4.32 (ABq, 2H, Δδ_{AB} = 0.04, *J*_{AB} = 14.3 Hz), 3.05 (dd, *J* = 12.4, 6.0 Hz, 1H), 2.54 – 2.48 (m, 2H), 2.38 (s, 3H), 1.88 (tt, *J* = 29.5, 27.8, 9.1 Hz, 3H), 1.51 (dtd, *J* = 13.3, 10.3, 3.1 Hz, 1H), 0.98 – 0.78 (m, 2H) ppm;

¹³C NMR (126 MHz, CDCl₃)

δ 158.2, 147.0, 146.5, 145.0, 135.5, 129.7 (2C), 128.9 (2C), 126.4 (q, *J*_{CF} = 32 Hz), 125.0 (q, *J*_{CF} = 272 Hz), 124.0 (q, *J*_{CF} = 4 Hz), 120.7, 119.4, 119.1 (q, *J*_{CF} = 4 Hz), 53.5, 50.4, 32.0, 27.0, 26.8, 25.2, 21.7 ppm;

IR (thin film)

2933, 1619, 1597, 1437, 1328, 1136 cm⁻¹

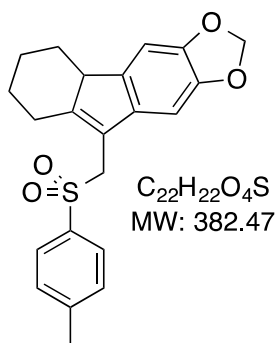
HRMS (TOF MS ES⁺)

[M+H]⁺ calcd for C₂₂H₂₁O₂F₃S, 407.1287; found, 407.1292;

TLC

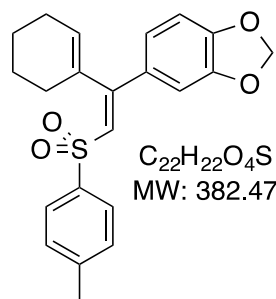
R_f = 0.24 (20% ethyl acetate in hexanes, UV, silica gel)

9-(tosylmethyl)-4b,6,7,8-tetrahydro-5H-fluoreno[2,3-*d*][1,3]dioxole (4.21c).



General Procedure VIII was followed with **4.21a** (50 mg, 0.13 mmol, 1 equiv) and 1,2 dichloroethane (3.90 mL) to give diene **4.21b**. The reaction mixture was cooled to room temperature and 0.5 mL of a freshly prepared 0.13 M solution of iron(III) chloride in DCE (0.5 equiv) was added. The reaction was stirred at room temperature and monitored by NMR. 6 h after the addition of iron(III) chloride, the reaction had gone to completion. The crude product was dissolved in a mixture of methylene chloride and methanol and slowly concentrated to a point where only 1 – 2 mL of the solvent system remained. The solid-liquid mixture was separated by vacuum filtration and the solid was washed with cold methanol to give 35 mg of tetrahydrofluorene **4.21c** as a tan solid in 70% yield.

Data for (*E*)-5-(1-(cyclohex-1-en-1-yl)-2-tosylvinyl)benzo[*d*][1,3]dioxole (4.21b)



1H NMR (500 MHz, $CDCl_3$)

δ 7.77 (d, $J = 8.2$ Hz, 2H), 7.30 (d, $J = 8.2$ Hz, 2H), 6.92 (dd, $J = 8.1, 1.7$ Hz, 1H), 6.85 (d, $J = 1.7$ Hz, 1H), 6.77 (d, $J = 8.1$ Hz, 1H), 6.59 (s, 1H), 5.98 (s, 2H), 5.65 – 5.60 (m, 1H), 2.43 (s, 3H), 2.14 – 2.08 (m, 2H), 1.73 – 1.65 (m, 2H), 1.60 – 1.53 (m, 2H), 1.52 – 1.44 (m, 2H) ppm;

^{13}C NMR (126 MHz, $CDCl_3$)

δ 157.8, 149.6, 148.3, 143.8, 140.1, 133.5, 131.2, 130.9, 129.5 (2C), 128.0 (2C), 126.4, 122.3, 108.5, 107.6, 101.7, 27.8, 25.3, 22.2, 21.7, 21.5 ppm;

IR (thin film)

2931, 1297, 1138, 1084 cm^{-1} ;

HRMS (TOF MS ES+)

$[M+H]^+$ calcd for $C_{22}H_{22}O_4S$, 383.1312; found, 383.1320;

TLC $R_f = 0.37$ (30% ethyl acetate in hexanes, UV, silica gel)

Data for 4.21c (AMB_E4_17)

MP 224 – 227 $^{\circ}C$

1H NMR (500 MHz, $CDCl_3$)

δ 7.62 (d, $J = 8.1$ Hz, 2H), 7.23 (d, $J = 8.0$ Hz, 2H), 6.82 (s, 1H), 6.72 (s, 1H), 5.91 (s, 2H), 4.24 (ABq, 2H, $\Delta\delta_{AB} = 0.04$, $J_{AB} = 14.3$ Hz), 2.88 (dd, $J = 12.4, 5.9$ Hz, 1H), 2.42 – 2.35 (m, 5H), 1.86 – 1.72 (m, 3H), 1.50 – 1.38 (m, 1H), 0.90 – 0.73 (m, 2H) ppm;

^{13}C NMR (126 MHz, $CDCl_3$)

δ 153.8, 146.7, 145.5, 144.8, 140.3, 137.5, 135.7, 129.6 (2C), 128.9 (2C), 120.5, 104.0, 101.0, 101.0, 53.9, 50.0, 32.5, 27.2, 26.6, 25.3, 21.7 ppm;

IR (thin film)

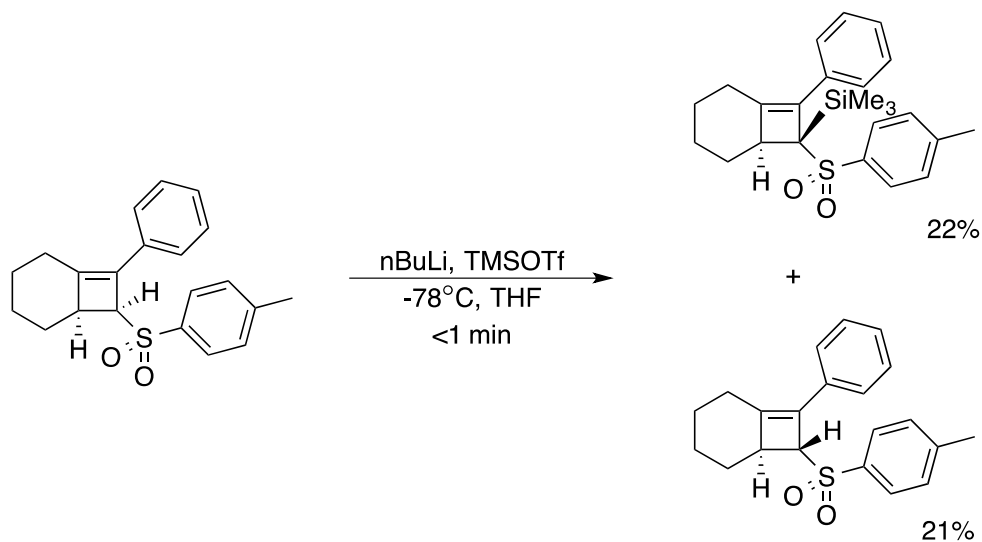
2919, 1596, 1470, 1300, 1130 cm^{-1}

HRMS (TOF MS ES+)

$[M+H]^+$ calcd for $C_{22}H_{22}O_4S$, 383.1317; found, 383.1328;

TLC $R_f = 0.34$ (20% ethyl acetate in hexanes, UV, silica gel)

4. Synthesis of Silylated Compounds



Trimethyl(8-phenyl-7-tosylbicyclo[4.2.0]oct-1(8)-en-7-yl)silane (1.22) and **7-phenyl-8-tosylbicyclo[4.2.0]oct-6-ene (1.23)**. A solution of n-BuLi in hexanes (1.6 M, 0.26 mL, 0.42 mmol, 1.2 equiv) was added dropwise to a brown stirred and cooled solution of **1.8** (122 mg, 0.36 mmol, 1 equiv) in tetrahydrofuran (0.70 mL) at 0°C under Argon. The mixture was stirred for 15 minutes turning dark brown before being cooled to -78°C. Trimethylsilyl triflate (0.04 mL, 0.22 mmol, 0.3 equiv) in dry tetrahydrofuran (0.22 mL) was added dropwise to the stirred and cooled mixture at -65 to -78°C, slowly turning the solution yellow. As soon as the reaction mixture turned yellow, it was immediately quenched with ammonium chloride. The reaction mixture was extracted with ethyl acetate. The extract was washed with water and brine, dried over magnesium sulfate, and concentrated. Purification of the crude product by silica gel column chromatography with 15% ethyl acetate in hexanes as the mobile phase afforded 33 mg of silylated product **1.22** in 22% yield as a white solid and 31 mg of isomerized starting material **1.23** in 21% yield as a clear oil.

Data for 1.22 (AMB_E1_052)

MP 115 – 119 °C

¹H NMR (400 MHz, CDCl₃)

δ 7.59 (d, *J* = 7.6 Hz, 2H), 7.49 (d, *J* = 8.2 Hz, 2H), 7.31 (t, *J* = 7.7 Hz, 2H), 7.24 – 7.16 (m, 1H), 7.09 (d, *J* = 8.1 Hz, 2H), 2.60 (dd, *J* = 14.4, 3.5 Hz, 1H), 2.38 – 2.27 (m, 4H), 2.09 – 1.95 (m, 1H), 1.76 – 1.63 (m, 2H), 1.63 – 1.50 (m, 2H), 1.19 – 0.98 (m, 2H), 0.36 (s, 9H) ppm;

¹³C NMR (151 MHz, CDCl₃)
δ 148.0, 143.5, 134.4, 134.3, 134.2, 129.7 (2C), 128.5 (3C), 127.4, 127.3 (2C),
69.9, 47.1, 29.6, 26.6, 25.8, 24.7, 21.7, 1.7 ppm;

IR (thin film)
2937, 1284, 1137 cm⁻¹;

HRMS (TOF MS ES+)
[M+H]⁺ calcd for C₂₄H₃₀O₂SSi, 411.1809; found, 411.1822;

TLC R_f = 0.65 (30% ethyl acetate in hexanes, UV, silica gel)

Data for 1.23 (AMB_E1_052)

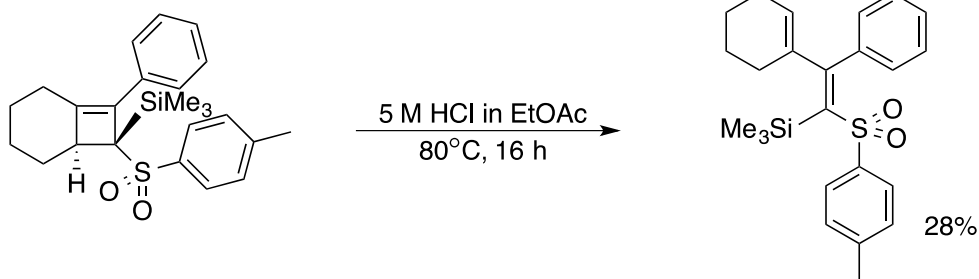
¹H NMR (400 MHz, CDCl₃)
δ 7.64 (d, *J* = 8.2 Hz, 2H), 7.33 (d, *J* = 7.1 Hz, 2H), 7.29 (d, *J* = 7.1 Hz, 2H), 7.22
(d, *J* = 7.8 Hz, 3H), 4.28 (s, 1H), 2.76 – 2.62 (m, 2H), 2.41 (s, 3H), 2.20 – 2.02
(m, 2H), 1.87 – 1.77 (m, 1H), 1.76 – 1.68 (m, 1H), 1.37 – 1.08 (m, 3H) ppm;

¹³C NMR (101 MHz, CDCl₃)
δ 151.1, 144.4, 135.4, 133.2, 130.3, 129.5 (2C), 128.9 (2C), 128.5 (2C), 127.5,
126.6 (2C), 68.5, 41.5, 31.2, 26.8, 26.0, 24.2, 21.8 ppm;

IR (thin film)
2932, 1597, 1290, 1320, 1086 cm⁻¹

HRMS (TOF MS ES+)
[M+H]⁺ calcd for C₂₁H₂₂O₂S, 339.1413; found, 339.1426;

TLC R_f = 0.50 (30% ethyl acetate in hexanes, UV, silica gel)



(Z)-2-(2-(cyclohex-1-en-1-yl)-2-phenyl-1-tosylvinyl)trimethylsilane (**1.26**). **1.22** (39 mg, 0.09 mmol), was dissolved in 4 mL of 5 M HCl in ethyl acetate solution. The solution was heated to 80°C overnight. After 16 h, the reaction mixture was washed with saturated sodium bicarbonate and water, dried over magnesium sulfate, and concentrated. Purification of the crude product by silica gel column chromatography with 15% ethyl acetate in hexanes as the mobile phase afforded 11 mg of diene product **1.26** in 28% yield as a white solid.

Data for 1.26 (AMB_E2_036)

MP 147 – 151 °C

¹H NMR (400 MHz, CDCl₃)

δ 7.46 (s, 1H), 7.23 (s, 1H), 7.11 (t, *J* = 7.4 Hz, 1H), 7.00 (d, *J* = 8.2 Hz, 2H), 6.82 (d, *J* = 8.0 Hz, 2H), 6.73 (s, 1H), 6.11 (s, 1H), 5.86 (t, *J* = 3.7 Hz, 1H), 2.25 (s, 3H), 2.21 – 2.07 (m, 2H), 1.76 – 1.66 (m, 1H), 1.63 – 1.38 (m, 5H), 0.47 (s, 9H) ppm;

¹³C NMR (101 MHz, CDCl₃)

δ 168.0, 145.4, 141.7, 141.7, 140.5, 138.3, 132.1, 130.2, 128.5 (2C), 128.4 (2C), 127.5 (2C), 127.1 (2C), 77.5, 77.2, 76.8, 27.6, 25.7, 22.1, 21.5, 21.5, 2.4 ppm;

IR (thin film)

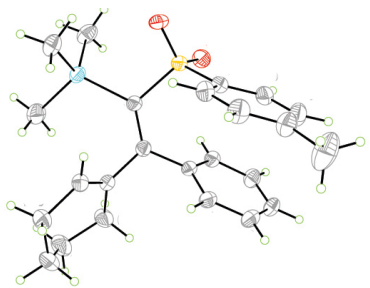
2929, 1283, 1131 cm⁻¹

HRMS (TOF MS ES⁺)

[*M*+*H*]⁺ calcd for C₂₄H₃₀O₂SSi, 411.1808; found, 411.1822;

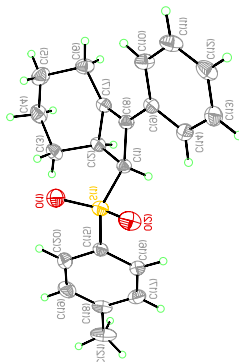
TLC R_f = 0.61 (30% ethyl acetate in hexanes, UV, silica gel)

Crystal Structure (See pg 99 for crystal structure report)



5. Crystal Structure Reports

Crystal Structure Report for cyclobutene 1.8



A specimen of $C_{21}H_{22}O_2S$, approximate dimensions 0.140 mm x 0.200 mm x 0.220 mm, was used for the X-ray crystallographic analysis. The X-ray intensity data were measured on a Bruker Apex II CCD system equipped with a Cu IMuS micro-focus source ($\lambda = 1.54178 \text{ \AA}$).

The frames were integrated with the Bruker SAINT software package using a narrow-frame algorithm. The integration of the data using a monoclinic unit cell yielded a total of 21003 reflections to a maximum θ angle of 68.22° (0.83 \AA resolution), of which 3179 were independent (average redundancy 6.607, completeness = 97.8%, $R_{\text{int}} = 2.97\%$, $R_{\text{sig}} = 2.11\%$) and 3086 (97.07%) were greater than $2\sigma(F^2)$. The final cell constants of $a = 10.9078(6) \text{ \AA}$, $b = 16.9822(9) \text{ \AA}$, $c = 10.9411(6) \text{ \AA}$, $\beta = 118.932(2)^\circ$, volume = $1773.77(17) \text{ \AA}^3$, are based upon the refinement of the XYZ-centroids of reflections above $20 \sigma(I)$. Data were corrected for absorption effects using the multi-scan method (SADABS). The calculated minimum and maximum transmission coefficients (based on crystal size) are 0.7080 and 0.7980.

The structure was solved and refined using the Bruker SHELXTL Software Package, using the space group $P 1 21/n 1$, with $Z = 4$ for the formula unit, $C_{21}H_{22}O_2S$. The final anisotropic full-matrix least-squares refinement on F^2 with 295 variables converged at $R1 = 3.43\%$, for the observed data and $wR2 = 12.85\%$ for all data. The goodness-of-fit was 1.740. The largest peak in the final difference electron density synthesis was $0.298 \text{ e}^-/\text{\AA}^3$ and the largest hole was $-0.316 \text{ e}^-/\text{\AA}^3$ with an RMS deviation of $0.039 \text{ e}^-/\text{\AA}^3$. On the basis of the final model, the calculated density was 1.267 g/cm^3 and $F(000)$, 720 e^- .

Table 1. Sample and crystal data for abe2_049.

Identification code	abe2_049	
Chemical formula	C ₂₁ H ₂₂ O ₂ S	
Formula weight	338.44 g/mol	
Temperature	230(2) K	
Wavelength	1.54178 Å	
Crystal size	0.140 x 0.200 x 0.220 mm	
Crystal system	monoclinic	
Space group	P 1 21/n 1	
Unit cell dimensions	a = 10.9078(6) Å b = 16.9822(9) Å c = 10.9411(6) Å	$\alpha = 90^\circ$ $\beta = 118.932(2)^\circ$ $\gamma = 90^\circ$
Volume	1773.77(17) Å ³	
Z	4	
Density (calculated)	1.267 g/cm ³	
Absorption coefficient	1.687 mm ⁻¹	
F(000)	720	

Table 2. Data collection and structure refinement for abe2_049.

Diffractometer	Bruker Apex II CCD	
Radiation source	IMuS micro-focus source, Cu	
Theta range for data collection	4.70 to 68.22°	
Index ranges	-12 ≤ h ≤ 13, -20 ≤ k ≤ 20, -13 ≤ l ≤ 12	
Reflections collected	21003	
Independent reflections	3179 [R(int) = 0.0297]	
Absorption correction	multi-scan	
Max. and min. transmission	0.7980 and 0.7080	
Structure solution technique	direct methods	
Structure solution program	SHELXS-97 (Sheldrick, 2008)	
Refinement method	Full-matrix least-squares on F ²	
Refinement program	SHELXL-97 (Sheldrick, 2008)	
Function minimized	Σ w(F _o ² - F _c ²) ²	
Data / restraints / parameters	3179 / 0 / 295	
Goodness-of-fit on F²	1.740	
Δ/σ_{max}	0.030	
Final R indices	3086 data; I > 2σ(I)	R1 = 0.0343, wR2 = 0.1274
	all data	R1 = 0.0349, wR2 = 0.1285

Weighting scheme	$w=1/[\sigma^2(F_o^2)+(0.0680P)^2]$ where $P=(F_o^2+2F_c^2)/3$
Extinction coefficient	0.0019(5)
Largest diff. peak and hole	0.298 and -0.316 eÅ ⁻³
R.M.S. deviation from mean	0.039 eÅ ⁻³

Table 3. Atomic coordinates and equivalent isotropic atomic displacement parameters (Å²) for abe2_049.

U(eq) is defined as one third of the trace of the orthogonalized U_{ij} tensor.

	x/a	y/b	z/c	U(eq)
S1	0.64420(3)	0.73446(2)	0.20769(3)	0.03478(18)
O1	0.75462(10)	0.73225(6)	0.35045(11)	0.0486(3)
O2	0.63887(11)	0.67197(6)	0.11589(12)	0.0520(3)
C1	0.47641(12)	0.73895(6)	0.20016(13)	0.0318(3)
C2	0.45722(11)	0.79376(6)	0.30650(12)	0.0339(3)
C3	0.57078(14)	0.84133(8)	0.42578(15)	0.0452(3)
C4	0.52733(16)	0.84984(9)	0.53928(17)	0.0514(4)
C5	0.5079(2)	0.77021(9)	0.59333(17)	0.0548(4)
C6	0.39526(16)	0.71874(8)	0.47717(16)	0.0440(3)
C7	0.42342(11)	0.71885(7)	0.35745(13)	0.0335(3)
C8	0.43991(11)	0.67091(7)	0.26860(12)	0.0318(3)
C9	0.41807(10)	0.58715(6)	0.23182(12)	0.0320(3)
C10	0.40523(14)	0.53185(7)	0.31950(14)	0.0408(3)
C11	0.38204(15)	0.45303(7)	0.28133(16)	0.0476(3)
C12	0.36973(14)	0.42800(8)	0.15612(17)	0.0475(3)
C13	0.37975(15)	0.48248(9)	0.06686(15)	0.0472(3)
C14	0.40538(13)	0.56114(8)	0.10585(13)	0.0409(3)
C15	0.65422(11)	0.82428(7)	0.13147(12)	0.0332(3)
C16	0.57334(13)	0.83377(7)	0.98889(13)	0.0377(3)
C17	0.57800(14)	0.90484(9)	0.92933(14)	0.0451(3)
C18	0.66232(14)	0.96624(8)	0.01001(16)	0.0453(3)
C19	0.74428(16)	0.95435(9)	0.15189(17)	0.0540(4)
C20	0.74065(14)	0.88387(9)	0.21365(14)	0.0471(3)
C21	0.6629(2)	0.04378(9)	0.9438(2)	0.0683(5)

Table 4. Bond lengths (Å) for

abe2_049.

S1-O1	1.4393(11)	S1-O2	1.4429(10)
S1-C15	1.7670(12)	S1-C1	1.7934(12)
C1-C8	1.5308(14)	C1-C2	1.5810(16)
C1-H1	0.890(18)	C2-C7	1.5046(15)
C2-C3	1.5252(17)	C2-H2	0.947(15)
C3-C4	1.535(2)	C3-H3A	0.991(17)
C3-H3B	1.00(2)	C4-C5	1.531(2)
C4-H4A	0.945(18)	C4-H4B	1.02(2)
C5-C6	1.542(2)	C5-H5A	1.00(3)
C5-H5B	0.96(2)	C6-C7	1.4831(19)
C6-H65A	1.03(2)	C6-H6B	0.939(19)
C7-C8	1.3451(17)	C8-C9	1.4660(16)
C9-C14	1.3890(17)	C9-C10	1.3970(16)
C10-C11	1.3885(18)	C10-H109	0.905(16)
C11-C12	1.377(2)	C11-H11	0.96(2)
C12-C13	1.388(2)	C12-H12	0.92(2)
C13-C14	1.3891(19)	C13-H13	0.95(2)
C14-H14	0.97(2)	C15-C16	1.3807(17)
C15-C20	1.3788(18)	C16-C17	1.3841(19)
C16-H16	0.97(2)	C17-C18	1.388(2)
C17-H17	0.94(2)	C18-C19	1.381(2)
C18-C21	1.5042(18)	C19-C20	1.384(2)
C19-H19	0.92(3)	C20-H20	0.969(19)
C21-H21D	0.97	C21-H21A	0.97
C21-H21B	0.97		

Table 5. Bond angles (°) for abe2_049.

O1-S1-O2	117.84(6)	O1-S1-C15	108.92(6)
O2-S1-C15	107.29(6)	O1-S1-C1	110.53(6)
O2-S1-C1	107.62(6)	C15-S1-C1	103.67(5)
C8-C1-C2	85.75(9)	C8-C1-S1	116.53(8)
C2-C1-S1	119.13(8)	C8-C1-H1	115.4(11)
C2-C1-H1	115.5(11)	S1-C1-H1	104.5(11)
C7-C2-C3	111.96(10)	C7-C2-C1	85.31(8)
C3-C2-C1	126.84(10)	C7-C2-H2	112.6(9)
C3-C2-H2	109.0(9)	C1-C2-H2	109.2(9)
C2-C3-C4	107.53(10)	C2-C3-H3A	110.6(10)
C4-C3-H3A	109.1(9)	C2-C3-H3B	112.4(11)
C4-C3-H3B	109.6(11)	H3A-C3-H3B	107.6(14)
C5-C4-C3	112.57(12)	C5-C4-H4A	111.6(11)
C3-C4-H4A	108.7(11)	C5-C4-H4B	106.6(12)
C3-C4-H4B	110.3(11)	H4A-C4-H4B	106.9(15)

C4-C5-C6	112.73(13)	C4-C5-H5A	108.8(15)
C6-C5-H5A	106.3(14)	C4-C5-H5B	108.5(14)
C6-C5-H5B	107.2(13)	H5A-C5-H5B	113.(2)
C7-C6-C5	107.72(11)	C7-C6-H65A	115.1(11)
C5-C6-H65A	109.7(11)	C7-C6-H6B	106.0(11)
C5-C6-H6B	110.9(11)	H65A-C6-H6B	107.5(15)
C8-C7-C6	142.64(11)	C8-C7-C2	95.83(10)
C6-C7-C2	121.39(11)	C7-C8-C9	136.46(10)
C7-C8-C1	93.10(10)	C9-C8-C1	130.12(10)
C14-C9-C10	118.21(11)	C14-C9-C8	120.38(10)
C10-C9-C8	121.38(10)	C11-C10-C9	120.38(12)
C11-C10-H109	117.3(11)	C9-C10-H109	122.4(11)
C12-C11-C10	120.84(12)	C12-C11-H11	118.7(12)
C10-C11-H11	120.5(12)	C11-C12-C13	119.42(12)
C11-C12-H12	120.4(13)	C13-C12-H12	120.2(13)
C14-C13-C12	119.86(13)	C14-C13-H13	120.9(12)
C12-C13-H13	119.2(12)	C13-C14-C9	121.27(12)
C13-C14-H14	119.2(12)	C9-C14-H14	119.5(12)
C16-C15-C20	120.84(11)	C16-C15-S1	118.84(9)
C20-C15-S1	120.31(10)	C15-C16-C17	119.00(12)
C15-C16-H16	120.2(11)	C17-C16-H16	120.7(11)
C16-C17-C18	121.30(13)	C16-C17-H17	120.6(13)
C18-C17-H17	118.0(13)	C19-C18-C17	118.32(12)
C19-C18-C21	121.20(14)	C17-C18-C21	120.47(15)
C20-C19-C18	121.29(13)	C20-C19-H19	120.7(15)
C18-C19-H19	118.0(15)	C15-C20-C19	119.22(13)
C15-C20-H20	116.8(11)	C19-C20-H20	123.8(11)
C18-C21-H21D	109.5	C18-C21-H21A	109.5
H21D-C21-H21A	109.5	C18-C21-H21B	109.5
H21D-C21-H21B	109.5	H21A-C21-H21B	109.5

Table 6. Anisotropic atomic displacement parameters (\AA^2) for *abe2_049*.

The anisotropic atomic displacement factor exponent takes the form: $-2\pi^2 [h^2 a^{*2} U_{11} + \dots + 2 h k a^* b^* U_{12}]$

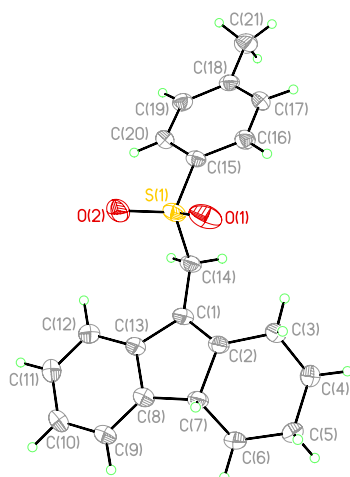
	U_{11}	U_{22}	U_{33}	U_{23}	U_{13}	U_{12}
S1	0.0334(2)	0.0339(2)	0.0393(3)	0.00388(9)	0.01935(18)	0.00183(9)
O1	0.0344(5)	0.0615(6)	0.0452(6)	0.0157(4)	0.0157(4)	0.0101(4)
O2	0.0620(6)	0.0367(5)	0.0714(7)	-0.0075(4)	0.0435(6)	-0.0023(4)
C1	0.0303(6)	0.0317(6)	0.0328(6)	0.0048(4)	0.0148(5)	0.0002(4)
C2	0.0317(5)	0.0292(6)	0.0411(6)	0.0028(4)	0.0180(5)	0.0010(4)
C3	0.0416(7)	0.0412(7)	0.0542(8)	-0.0089(5)	0.0242(6)	-0.0089(5)
C4	0.0507(7)	0.0480(7)	0.0576(8)	-0.0159(6)	0.0278(7)	-0.0066(6)

C5	0.0682(10)	0.0590(9)	0.0441(8)	-0.0087(6)	0.0327(8)	-0.0028(7)
C6	0.0541(8)	0.0389(6)	0.0509(8)	-0.0013(5)	0.0348(7)	-0.0001(6)
C7	0.0308(5)	0.0315(5)	0.0384(6)	0.0025(4)	0.0168(5)	-0.0001(4)
C8	0.0301(5)	0.0315(6)	0.0332(5)	0.0046(4)	0.0149(4)	-0.0002(4)
C9	0.0291(5)	0.0308(5)	0.0351(6)	0.0014(4)	0.0146(4)	-0.0012(4)
C10	0.0514(7)	0.0343(6)	0.0464(7)	0.0025(5)	0.0312(6)	-0.0009(5)
C11	0.0580(8)	0.0340(6)	0.0643(8)	0.0035(6)	0.0403(7)	-0.0039(5)
C12	0.0479(7)	0.0349(6)	0.0673(9)	-0.0102(6)	0.0337(7)	-0.0094(5)
C13	0.0517(7)	0.0462(7)	0.0457(7)	-0.0124(6)	0.0251(6)	-0.0105(5)
C14	0.0450(6)	0.0404(6)	0.0357(6)	-0.0011(5)	0.0184(5)	-0.0058(5)
C15	0.0311(5)	0.0369(6)	0.0364(6)	-0.0009(4)	0.0199(5)	-0.0022(4)
C16	0.0383(6)	0.0422(6)	0.0357(6)	-0.0021(5)	0.0203(5)	-0.0038(5)
C17	0.0463(7)	0.0529(7)	0.0426(7)	0.0106(5)	0.0268(6)	0.0063(5)
C18	0.0491(7)	0.0398(6)	0.0664(8)	0.0061(6)	0.0433(7)	0.0025(5)
C19	0.0577(8)	0.0459(8)	0.0632(9)	-0.0096(6)	0.0330(7)	-0.0202(6)
C20	0.0458(7)	0.0519(7)	0.0397(7)	-0.0047(6)	0.0175(6)	-0.0158(6)
C21	0.0869(11)	0.0467(8)	0.1103(14)	0.0219(8)	0.0785(12)	0.0120(7)

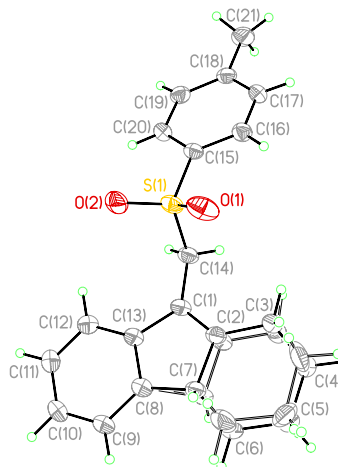
Table 7. Hydrogen atomic coordinates and isotropic atomic displacement parameters (\AA^2) for `abe2_049`.

	x/a	y/b	z/c	U(eq)
H1	0.4161(17)	0.7470(10)	0.1104(19)	0.040(4)
H2	0.3775(15)	0.8262(9)	0.2565(16)	0.035(3)
H3A	0.6620(18)	0.8136(10)	0.4655(17)	0.042(4)
H3B	0.5838(19)	0.8948(13)	0.395(2)	0.059(5)
H4A	0.4451(18)	0.8807(10)	0.5036(18)	0.046(4)
H4B	0.602(2)	0.8791(12)	0.623(2)	0.059(5)
H5A	0.597(3)	0.7402(15)	0.631(3)	0.078(7)
H5B	0.478(2)	0.7796(14)	0.661(2)	0.070(6)
H65A	0.394(2)	0.6641(12)	0.516(2)	0.058(5)
H6B	0.3059(19)	0.7409(10)	0.4437(18)	0.046(4)
H109	0.4114(15)	0.5453(10)	0.4024(17)	0.041(4)
H11	0.3775(18)	0.4147(12)	0.3432(19)	0.054(4)
H12	0.354(2)	0.3754(12)	0.131(2)	0.061(5)
H13	0.371(2)	0.4650(12)	-0.020(2)	0.059(5)
H14	0.4187(19)	0.5980(12)	0.0459(19)	0.058(5)
H16	0.5167(18)	0.7906(12)	-0.0686(18)	0.051(4)
H17	0.522(2)	0.9132(13)	-0.168(2)	0.064(5)
H19	0.803(3)	0.9945(15)	0.204(2)	0.076(6)
H20	0.8010(18)	0.8718(11)	0.311(2)	0.053(4)
H21D	0.7506	1.0708	0.0016	0.102
H21A	0.5856	1.0759	-0.0647	0.102
H21B	0.6528	1.0346	-0.1481	0.102

Crystal Structure Report for tetrahydrofluorene 1.25



Structure with only major conformer of cyclohexane ring shown



Structure showing 88:12 mixture of cyclohexane conformers

A specimen of $C_{21}H_{22}O_2S$, approximate dimensions 0.020 mm x 0.110 mm x 0.140 mm, was used for the X-ray crystallographic analysis. The X-ray intensity data were measured on a Bruker X8 Prospector Ultra system equipped with a Cu Imus microfocus ($\lambda = 1.54178 \text{ \AA}$).

The integration of the data using a **monoclinic** unit cell yielded a total of 16395 reflections to a maximum θ angle of 68.23° (0.83 \AA resolution), of which 3227 were independent (average redundancy 5.081, completeness = 99.6%, $R_{\text{int}} = 3.37\%$, $R_{\text{sig}} = 2.63\%$) and 2838 (87.95%) were greater than $2\sigma(F^2)$. The final cell constants of $a = 20.0380(4) \text{ \AA}$, $b = 5.46800(10) \text{ \AA}$, $c = 16.4410(3) \text{ \AA}$, $\beta = 101.1190(10)^\circ$, volume = $1767.59(6) \text{ \AA}^3$, are based upon the refinement of the XYZ-centroids of reflections above $20 \sigma(I)$. The calculated minimum and maximum transmission coefficients (based on crystal size) are 0.7980 and 0.9670.

The final anisotropic full-matrix least-squares refinement on F^2 with 309 variables converged at $R1 = 4.74\%$, for the observed data and $wR2 = 14.77\%$ for all data. The goodness-of-fit was 1.725. The largest peak in the final difference electron density synthesis was $0.556 \text{ e}^-/\text{\AA}^3$ and the largest hole was $-0.400 \text{ e}^-/\text{\AA}^3$ with an RMS deviation of $0.045 \text{ e}^-/\text{\AA}^3$. On the basis of the final model, the calculated density was 1.272 g/cm^3 and $F(000)$, 720 e^- .

Table 1. Sample and crystal data for berneE4_09.

Identification code	berneE4_09	
Chemical formula	C ₂₁ H ₂₂ O ₂ S	
Formula weight	338.44 g/mol	
Temperature	230(2) K	
Wavelength	1.54178 Å	
Crystal size	0.020 x 0.110 x 0.140 mm	
Crystal system	monoclinic	
Space group	P 1 21/c 1	
Unit cell dimensions	a = 20.0380(4) Å b = 5.46800(10) Å c = 16.4410(3) Å	$\alpha = 90^\circ$ $\beta = 101.1190(10)^\circ$ $\gamma = 90^\circ$
Volume	1767.59(6) Å ³	
Z	4	
Density (calculated)	1.272 g/cm ³	
Absorption coefficient	1.693 mm ⁻¹	
F(000)	720	

Table 2. Data collection and structure refinement for berneE4_09.

Diffractometer	Bruker X8 Prospector Ultra	
Radiation source	Imus microfocus, Cu	
Theta range for data collection	2.25 to 68.23°	
Index ranges	-23 ≤ h ≤ 24, -6 ≤ k ≤ 6, -19 ≤ l ≤ 19	
Reflections collected	16395	
Independent reflections	3227 [R(int) = 0.0337]	
Absorption correction	multi-scan	
Max. and min. transmission	0.9670 and 0.7980	
Refinement method	Full-matrix least-squares on F ²	
Refinement program	SHELXL-2014/7 (Sheldrick, 2014)	
Function minimized	Σ w(F _o ² - F _c ²) ²	
Data / restraints / parameters	3227 / 89 / 309	
Goodness-of-fit on F²	1.725	
Δ/σ_{max}	0.759	
Final R indices	2838 data; I > 2σ(I)	R1 = 0.0474, wR2 = 0.1438
	all data	R1 = 0.0537, wR2 = 0.1477
Weighting scheme	w = 1/[σ ² (F _o ²) + (0.0640P) ²] where P = (F _o ² + 2F _c ²)/3	

Largest diff. peak and hole	0.556 and -0.400 eÅ ⁻³
R.M.S. deviation from mean	0.045 eÅ ⁻³

Table 3. Atomic coordinates and equivalent isotropic atomic displacement parameters (Å²) for berneE4_09.

U(eq) is defined as one third of the trace of the orthogonalized U_{ij} tensor.

	x/a	y/b	z/c	U(eq)
S1	0.16749(3)	0.29973(10)	0.62415(3)	0.0406(2)
O1	0.18324(11)	0.0439(3)	0.62853(12)	0.0656(5)
C1	0.29112(11)	0.4025(5)	0.58610(13)	0.0464(5)
O2	0.12640(9)	0.3930(4)	0.54955(9)	0.0590(5)
C2	0.33738(13)	0.2189(6)	0.59619(17)	0.0382(7)
C3	0.35912(15)	0.0480(7)	0.66718(18)	0.0471(8)
C4	0.43576(17)	0.0773(9)	0.7008(2)	0.0532(9)
C5	0.4768(3)	0.0601(11)	0.6317(3)	0.0497(11)
C6	0.45378(14)	0.2504(6)	0.56479(19)	0.0434(7)
C7	0.37715(14)	0.2187(6)	0.52711(16)	0.0380(7)
C2'	0.3591(7)	0.346(3)	0.6226(8)	0.043(3)
C3'	0.3836(8)	0.190(3)	0.6943(9)	0.054(4)
C4'	0.4096(15)	0.972(5)	0.6762(12)	0.079(6)
C5'	0.4586(12)	0.991(6)	0.618(2)	0.066(7)
C6'	0.4244(13)	0.121(5)	0.5365(11)	0.078(6)
C7'	0.4032(6)	0.358(3)	0.5569(8)	0.043(4)
C8	0.34576(11)	0.4281(5)	0.47375(14)	0.0516(6)
C9	0.35972(13)	0.5198(6)	0.40126(14)	0.0559(7)
C10	0.31969(13)	0.7057(6)	0.36022(14)	0.0557(7)
C11	0.26554(13)	0.7977(5)	0.39217(15)	0.0560(6)
C12	0.25141(12)	0.7132(5)	0.46645(15)	0.0490(5)
C13	0.29198(10)	0.5285(5)	0.50772(12)	0.0430(5)
C14	0.24502(11)	0.4702(5)	0.64475(13)	0.0423(5)
C15	0.13016(9)	0.3767(4)	0.70949(11)	0.0340(4)
C16	0.14178(11)	0.2307(4)	0.77948(13)	0.0405(5)
C17	0.11461(11)	0.2985(4)	0.84755(13)	0.0425(5)
C18	0.07646(9)	0.5105(4)	0.84598(12)	0.0397(5)
C19	0.06557(11)	0.6529(4)	0.77485(14)	0.0421(5)
C20	0.09209(10)	0.5888(4)	0.70636(13)	0.0403(5)
C21	0.04651(12)	0.5842(6)	0.91967(14)	0.0591(7)

Table 4. Bond lengths (Å) for berneE4_09.

S1-O2	1.4327(18)	S1-O1	1.433(2)
S1-C15	1.7637(18)	S1-C14	1.787(2)
C1-C2	1.355(4)	C1-C2'	1.413(14)
C1-C13	1.464(3)	C1-C14	1.504(3)
C2-C3	1.493(4)	C2-C7	1.508(3)
C3-C4	1.537(5)	C3-H3A	0.98
C3-H3B	0.98	C4-C5	1.529(7)
C4-H4A	0.98	C4-H4B	0.98
C5-C6	1.520(7)	C5-H5A	0.98
C5-H5B	0.98	C6-C7	1.551(4)
C6-H6A	0.98	C6-H6B	0.98
C7-C8	1.505(4)	C7-H7	0.99
C2'-C3'	1.461(19)	C2'-C7'	1.523(15)
C3'-C4'	1.36(3)	C3'-H3'1	0.98
C3'-H3'2	0.98	C4'-C5'	1.51(4)
C4'-H4'1	0.98	C4'-H4'2	0.98
C5'-C6'	1.55(4)	C5'-H5'1	0.98
C5'-H5'2	0.98	C6'-C7'	1.42(3)
C6'-H6'1	0.98	C6'-H6'2	0.98
C7'-C8	1.654(12)	C7'-H7'	0.99
C8-C9	1.371(3)	C8-C13	1.417(3)
C9-C10	1.387(4)	C9-H9	0.93(3)
C10-C11	1.388(4)	C10-H10	0.96(3)
C11-C12	1.385(3)	C11-H11	0.94
C12-C13	1.389(3)	C12-H12	0.97(3)
C14-H14A	0.88(3)	C14-H14B	0.98(3)
C15-C16	1.383(3)	C15-C20	1.384(3)
C16-C17	1.386(3)	C16-H16	0.94(3)
C17-C18	1.386(3)	C17-H17	0.91(3)
C18-C19	1.387(3)	C18-C21	1.507(3)
C19-C20	1.380(3)	C19-H19	0.89(3)
C20-H20	0.90(3)	C21-H21A	0.97
C21-H21B	0.97	C21-H21C	0.97

Table 5. Bond angles (°) for berneE4_09.

O2-S1-O1	118.38(12)	O2-S1-C15	109.52(10)
O1-S1-C15	108.42(10)	O2-S1-C14	108.16(11)
O1-S1-C14	108.96(13)	C15-S1-C14	102.20(9)
C2-C1-C13	109.42(19)	C2'-C1-C13	107.6(5)
C2-C1-C14	126.4(2)	C2'-C1-C14	116.2(5)

C13-C1-C14	124.1(2)	C1-C2-C3	130.5(2)
C1-C2-C7	110.9(2)	C3-C2-C7	118.1(2)
C2-C3-C4	109.7(3)	C2-C3-H3A	109.7
C4-C3-H3A	109.7	C2-C3-H3B	109.7
C4-C3-H3B	109.7	H3A-C3-H3B	108.2
C5-C4-C3	111.7(3)	C5-C4-H4A	109.3
C3-C4-H4A	109.3	C5-C4-H4B	109.3
C3-C4-H4B	109.3	H4A-C4-H4B	107.9
C6-C5-C4	111.3(4)	C6-C5-H5A	109.4
C4-C5-H5A	109.4	C6-C5-H5B	109.4
C4-C5-H5B	109.4	H5A-C5-H5B	108.0
C5-C6-C7	110.6(3)	C5-C6-H6A	109.5
C7-C6-H6A	109.5	C5-C6-H6B	109.5
C7-C6-H6B	109.5	H6A-C6-H6B	108.1
C8-C7-C2	102.5(2)	C8-C7-C6	114.7(2)
C2-C7-C6	109.0(2)	C8-C7-H7	110.1
C2-C7-H7	110.1	C6-C7-H7	110.1
C1-C2'-C3'	128.1(11)	C1-C2'-C7'	109.4(9)
C3'-C2'-C7'	116.4(11)	C4'-C3'-C2'	114.9(14)
C4'-C3'-H3'1	108.6	C2'-C3'-H3'1	108.6
C4'-C3'-H3'2	108.6	C2'-C3'-H3'2	108.5
H3'1-C3'-H3'2	107.5	C3'-C4'-C5'	114.(2)
C3'-C4'-H4'1	108.8	C5'-C4'-H4'1	108.8
C3'-C4'-H4'2	108.8	C5'-C4'-H4'2	108.8
H4'1-C4'-H4'2	107.7	C4'-C5'-C6'	110.(2)
C4'-C5'-H5'1	109.6	C6'-C5'-H5'1	109.6
C4'-C5'-H5'2	109.6	C6'-C5'-H5'2	109.5
H5'1-C5'-H5'2	108.1	C7'-C6'-C5'	108.6(19)
C7'-C6'-H6'1	110.0	C5'-C6'-H6'1	110.0
C7'-C6'-H6'2	109.9	C5'-C6'-H6'2	109.9
H6'1-C6'-H6'2	108.4	C6'-C7'-C2'	111.7(13)
C6'-C7'-C8	102.0(14)	C2'-C7'-C8	100.9(8)
C6'-C7'-H7'	113.6	C2'-C7'-H7'	113.7
C8-C7'-H7'	113.7	C9-C8-C13	120.0(2)
C9-C8-C7	130.8(2)	C13-C8-C7	109.23(19)
C9-C8-C7'	125.3(4)	C13-C8-C7'	103.0(4)
C8-C9-C10	119.7(2)	C8-C9-H9	119.6(18)
C10-C9-H9	120.7(18)	C11-C10-C9	120.2(2)
C11-C10-H10	122.(2)	C9-C10-H10	118.(2)
C12-C11-C10	121.4(2)	C12-C11-H11	119.3
C10-C11-H11	119.3	C11-C12-C13	118.3(2)
C11-C12-H12	120.8(16)	C13-C12-H12	120.9(16)
C12-C13-C8	120.5(2)	C12-C13-C1	131.8(2)
C8-C13-C1	107.7(2)	C1-C14-S1	111.65(16)
C1-C14-H14A	112.0(17)	S1-C14-H14A	105.5(17)

C1-C14-H14B	115.0(15)	S1-C14-H14B	106.1(15)
H14A-C14-H14B	106.(2)	C16-C15-C20	121.20(18)
C16-C15-S1	119.68(16)	C20-C15-S1	119.06(16)
C15-C16-C17	119.2(2)	C15-C16-H16	119.1(16)
C17-C16-H16	121.7(16)	C16-C17-C18	120.7(2)
C16-C17-H17	118.4(17)	C18-C17-H17	120.9(17)
C17-C18-C19	118.80(18)	C17-C18-C21	120.8(2)
C19-C18-C21	120.4(2)	C20-C19-C18	121.5(2)
C20-C19-H19	115.9(17)	C18-C19-H19	122.5(17)
C19-C20-C15	118.6(2)	C19-C20-H20	123.5(18)
C15-C20-H20	117.9(18)	C18-C21-H21A	109.5
C18-C21-H21B	109.5	H21A-C21-H21B	109.5
C18-C21-H21C	109.5	H21A-C21-H21C	109.5
H21B-C21-H21C	109.5		

Table 6. Anisotropic atomic displacement parameters (\AA^2) for berneE4_09.

The anisotropic atomic displacement factor exponent takes the form: $-2\pi^2 [h^2 a^{*2} U_{11} + \dots + 2 h k a^* b^* U_{12}]$

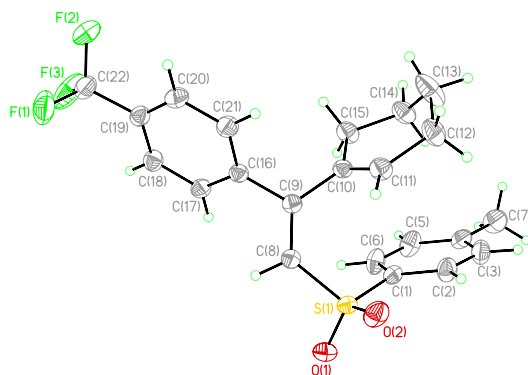
	U_{11}	U_{22}	U_{33}	U_{23}	U_{13}	U_{12}
S1	0.0463(3)	0.0465(3)	0.0330(3)	-0.0081(2)	0.0175(2)	-0.0063(2)
O1	0.0905(13)	0.0450(10)	0.0745(12)	-0.0135(9)	0.0491(10)	-0.0024(9)
C1	0.0368(10)	0.0677(15)	0.0383(10)	0.0053(11)	0.0163(8)	0.0008(10)
O2	0.0561(9)	0.0913(14)	0.0293(7)	-0.0076(8)	0.0077(6)	-0.0118(9)
C2	0.0332(13)	0.0499(17)	0.0331(13)	-0.0021(12)	0.0103(10)	-0.0063(12)
C3	0.0399(16)	0.063(2)	0.0404(14)	0.0093(15)	0.0117(11)	-0.0010(15)
C4	0.0417(18)	0.075(3)	0.0418(17)	0.0111(17)	0.0048(13)	0.0048(16)
C5	0.035(2)	0.064(3)	0.0508(19)	0.0091(19)	0.0098(17)	0.0056(18)
C6	0.0370(15)	0.0510(17)	0.0459(15)	0.0031(13)	0.0176(12)	-0.0011(12)
C7	0.0351(14)	0.0477(16)	0.0336(12)	-0.0026(12)	0.0126(10)	-0.0020(13)
C2'	0.042(6)	0.058(9)	0.033(5)	0.000(6)	0.016(4)	0.003(6)
C3'	0.049(8)	0.073(10)	0.041(7)	0.013(6)	0.005(5)	-0.005(7)
C4'	0.107(18)	0.085(13)	0.046(10)	0.034(9)	0.019(10)	0.021(13)
C5'	0.034(12)	0.072(16)	0.090(14)	0.015(12)	0.008(9)	0.012(10)
C6'	0.094(14)	0.098(13)	0.052(9)	0.016(9)	0.043(9)	0.037(12)
C7'	0.028(5)	0.065(9)	0.037(5)	0.008(6)	0.011(4)	0.004(6)
C8	0.0468(12)	0.0708(16)	0.0405(11)	0.0087(11)	0.0170(9)	0.0092(11)
C9	0.0538(13)	0.0785(18)	0.0410(11)	0.0086(12)	0.0230(10)	0.0125(13)
C10	0.0603(15)	0.0756(18)	0.0330(10)	0.0095(11)	0.0138(10)	0.0053(12)
C11	0.0534(13)	0.0698(17)	0.0431(12)	0.0116(12)	0.0055(10)	0.0105(12)
C12	0.0417(12)	0.0610(15)	0.0463(12)	0.0018(11)	0.0134(9)	0.0049(10)
C13	0.0392(10)	0.0564(13)	0.0355(10)	0.0022(10)	0.0127(8)	0.0017(9)
C14	0.0381(10)	0.0580(15)	0.0337(10)	-0.0033(10)	0.0145(8)	-0.0058(10)

C15	0.0332(9)	0.0397(10)	0.0313(9)	-0.0044(8)	0.0117(7)	-0.0055(8)
C16	0.0418(11)	0.0408(11)	0.0412(11)	0.0010(9)	0.0135(8)	0.0039(9)
C17	0.0424(11)	0.0546(13)	0.0323(10)	0.0072(10)	0.0115(8)	0.0011(9)
C18	0.0308(9)	0.0553(13)	0.0346(9)	-0.0060(9)	0.0104(7)	-0.0046(8)
C19	0.0361(10)	0.0472(12)	0.0452(11)	-0.0020(10)	0.0132(8)	0.0048(9)
C20	0.0407(10)	0.0448(12)	0.0364(10)	0.0062(9)	0.0104(8)	-0.0008(9)
C21	0.0512(13)	0.089(2)	0.0424(12)	-0.0066(12)	0.0214(10)	0.0076(13)

Table 7. Hydrogen atomic coordinates and isotropic atomic displacement parameters (\AA^2) for berneE4_09.

	x/a	y/b	z/c	U(eq)
H3A	0.3492	-0.1209	0.6488	0.056
H3B	0.3338	0.0837	0.7112	0.056
H4A	0.4442	0.2361	0.7285	0.064
H4B	0.4510	-0.0505	0.7420	0.064
H5A	0.5252	0.0844	0.6552	0.06
H5B	0.4715	-0.1036	0.6070	0.06
H6A	0.4804	0.2336	0.5210	0.052
H6B	0.4617	0.4145	0.5886	0.052
H7	0.3696	0.0635	0.4957	0.046
H3'1	0.4188	0.2790	0.7327	0.065
H3'2	0.3459	0.1592	0.7230	0.065
H4'1	0.3721	-0.1361	0.6516	0.095
H4'2	0.4331	-0.1041	0.7278	0.095
H5'1	0.4732	-0.1733	0.6046	0.079
H5'2	0.4989	0.0829	0.6440	0.079
H6'1	0.4567	0.1348	0.4990	0.094
H6'2	0.3851	0.0262	0.5087	0.094
H7'	0.4408	0.4776	0.5696	0.051
H9	0.3963(15)	0.457(6)	0.3803(17)	0.066(8)
H10	0.3297(17)	0.762(6)	0.309(2)	0.077(9)
H11	0.2379	0.9199	0.3628	0.067
H12	0.2141(15)	0.782(5)	0.4892(17)	0.055(7)
H14A	0.2635(13)	0.438(5)	0.6964(17)	0.048(7)
H14B	0.2318(13)	0.642(5)	0.6437(15)	0.043(6)
H16	0.1675(14)	0.087(5)	0.7795(15)	0.053(7)
H17	0.1239(14)	0.204(5)	0.8938(18)	0.056(8)
H19	0.0424(13)	0.793(5)	0.7710(16)	0.045(7)
H20	0.0852(14)	0.676(5)	0.6590(19)	0.058(8)
H21A	0.0026	0.6605	0.9007	0.071
H21B	0.0767	0.6991	0.9535	0.071
H21C	0.0410	0.4404	0.9523	0.071

Crystal Structure Report for diene **4.20b**



A specimen of $C_{22}H_{21}F_3O_2S$, approximate dimensions **0.080 mm** x **0.180 mm** x **0.190 mm**, was used for the X-ray crystallographic analysis. The X-ray intensity data were measured on a Bruker Apex II CCD system equipped with a Cu IMuS micro-focus ($\lambda = 1.54178 \text{ \AA}$).

The frames were integrated with the Bruker SAINT software package using a narrow-frame algorithm. The integration of the data using a **triclinic** unit cell yielded a total of **8000** reflections to a maximum θ angle of **68.17°** (**0.83 Å** resolution), of which **3499** were independent (average redundancy **2.286**, completeness = **96.2%**, $R_{\text{int}} = 2.32\%$, $R_{\text{sig}} = 2.63\%$) and **3119** (**89.14%**) were greater than $2\sigma(F^2)$. The final cell constants of $a = 6.3216(4) \text{ \AA}$, $b = 11.2486(8) \text{ \AA}$, $c = 14.3621(10) \text{ \AA}$, $\alpha = 75.807(4)^\circ$, $\beta = 87.904(4)^\circ$, $\gamma = 88.651(5)^\circ$, volume = **989.33(12) Å³**, are based upon the refinement of the XYZ-centroids of reflections above $20 \sigma(I)$. The calculated minimum and maximum transmission coefficients (based on crystal size) are **0.7220** and **0.8670**.

The final anisotropic full-matrix least-squares refinement on F^2 with **259** variables converged at $R1 = 4.48\%$, for the observed data and $wR2 = 14.37\%$ for all data. The goodness-of-fit was **1.643**. The largest peak in the final difference electron density synthesis was **0.494 e⁻/Å³** and the largest hole was **-0.368 e⁻/Å³** with an RMS deviation of **0.055 e⁻/Å³**. On the basis of the final model, the calculated density was **1.364 g/cm³** and $F(000)$, **424 e⁻**.

Table 1. Sample and crystal data for alex_e322.

Identification code	alex_e322	
Chemical formula	C ₂₂ H ₂₁ F ₃ O ₂ S	
Formula weight	406.45 g/mol	
Temperature	230(2) K	
Wavelength	1.54178 Å	
Crystal size	0.080 x 0.180 x 0.190 mm	
Crystal system	triclinic	
Space group	P -1	
Unit cell dimensions	a = 6.3216(4) Å b = 11.2486(8) Å c = 14.3621(10) Å	$\alpha = 75.807(4)^\circ$ $\beta = 87.904(4)^\circ$ $\gamma = 88.651(5)^\circ$
Volume	989.33(12) Å ³	
Z	2	
Density (calculated)	1.364 g/cm ³	
Absorption coefficient	1.832 mm ⁻¹	
F(000)	424	

Table 2. Data collection and structure refinement for alex_e322.

Diffractometer	Bruker Apex II CCD	
Radiation source	IMuS micro-focus, Cu	
Theta range for data collection	3.17 to 68.17°	
Index ranges	-6 ≤ h ≤ 7, -13 ≤ k ≤ 13, -16 ≤ l ≤ 17	
Reflections collected	8000	
Independent reflections	3499 [R(int) = 0.0232]	
Absorption correction	multi-scan	
Max. and min. transmission	0.8670 and 0.7220	
Refinement method	Full-matrix least-squares on F ²	
Refinement program	SHELXL-2014/6 (Sheldrick, 2014)	
Function minimized	Σ w(F _o ² - F _c ²) ²	
Data / restraints / parameters	3499 / 0 / 259	
Goodness-of-fit on F²	1.643	
Δ/σ_{max}	0.248	
Final R indices	3119 data; I > 2σ(I)	R1 = 0.0448, wR2 = 0.1399
	all data	R1 = 0.0494, wR2 = 0.1437
Weighting scheme	w = 1/[σ ² (F _o ²) + (0.0680P) ²] where P = (F _o ² + 2F _c ²)/3	

Largest diff. peak and hole	0.494 and -0.368 eÅ ⁻³
R.M.S. deviation from mean	0.055 eÅ ⁻³

Table 3. Atomic coordinates and equivalent isotropic atomic displacement parameters (Å²) for alex_e322.

U(eq) is defined as one third of the trace of the orthogonalized U_{ij} tensor.

	x/a	y/b	z/c	U(eq)
S1	0.46265(7)	0.84944(4)	0.43886(3)	0.03798(18)
O1	0.3881(3)	0.83965(14)	0.53623(11)	0.0563(4)
O2	0.6856(2)	0.86443(14)	0.41826(12)	0.0516(4)
F1	0.8073(3)	0.51031(13)	0.14704(15)	0.0890(6)
F2	0.7486(3)	0.44795(13)	0.02377(11)	0.0719(5)
F3	0.5369(3)	0.40268(17)	0.14501(15)	0.0936(7)
C1	0.3853(3)	0.71555(16)	0.40640(13)	0.0350(4)
C2	0.5398(3)	0.64005(18)	0.37972(16)	0.0453(5)
C3	0.4841(3)	0.52945(19)	0.36269(17)	0.0495(5)
C5	0.1233(3)	0.5726(2)	0.39436(19)	0.0535(6)
C6	0.1757(3)	0.68240(19)	0.41414(17)	0.0492(5)
C7	0.2122(5)	0.3742(2)	0.3493(2)	0.0622(6)
C8	0.3161(3)	0.97327(16)	0.37039(13)	0.0368(4)
C9	0.2661(3)	0.99308(15)	0.27866(12)	0.0316(4)
C10	0.3371(3)	0.91688(15)	0.21193(12)	0.0318(4)
C11	0.5390(3)	0.90126(18)	0.18961(14)	0.0405(4)
C12	0.6150(3)	0.8266(2)	0.12152(17)	0.0514(5)
C13	0.4358(4)	0.7899(3)	0.0671(2)	0.0775(9)
C14	0.2399(4)	0.7578(3)	0.1256(2)	0.0479(10)
C15	0.1602(3)	0.8620(2)	0.16819(15)	0.0437(5)
C16	0.1232(3)	0.09942(15)	0.23769(12)	0.0324(4)
C17	0.9381(3)	0.12267(16)	0.28591(13)	0.0365(4)
C18	0.8101(3)	0.22257(17)	0.24660(14)	0.0396(4)
C19	0.8681(3)	0.30091(16)	0.15916(13)	0.0369(4)
C20	0.0520(3)	0.27820(18)	0.11033(14)	0.0443(5)
C21	0.1770(3)	0.17717(18)	0.14898(14)	0.0419(4)
C22	0.7386(4)	0.41378(18)	0.11977(16)	0.0485(5)
C4	0.2750(3)	0.49408(17)	0.36899(15)	0.0437(5)
C14'	0.2504(15)	0.8265(9)	0.0718(7)	0.047(3)

Table 4. Bond lengths (Å) for alex_e322.

S1-O2	1.4348(16)	S1-O1	1.4383(16)
S1-C8	1.7606(18)	S1-C1	1.7664(18)
F1-C22	1.328(3)	F2-C22	1.337(3)
F3-C22	1.313(3)	C1-C6	1.378(3)
C1-C2	1.384(3)	C2-C3	1.381(3)
C2-H2A	0.94	C3-C4	1.383(3)
C3-H3A	0.94	C5-C6	1.384(3)
C5-C4	1.387(3)	C5-H5A	0.94
C6-H6A	0.94	C7-C4	1.509(3)
C7-H7A	0.97	C7-H7B	0.97
C7-H7C	0.97	C8-C9	1.330(3)
C8-H8A	0.94	C9-C10	1.486(2)
C9-C16	1.495(2)	C10-C11	1.323(3)
C10-C15	1.516(2)	C11-C12	1.497(3)
C11-H11A	0.94	C12-C13	1.519(3)
C12-H12A	0.98	C12-H12B	0.98
C13-C14	1.472(4)	C13-H13A	0.98
C13-H13B	0.98	C14-C15	1.517(3)
C14-H14A	0.98	C14-H14B	0.98
C15-H15A	0.98	C15-H15B	0.98
C16-C17	1.390(3)	C16-C21	1.393(3)
C17-C18	1.384(3)	C17-H17A	0.94
C18-C19	1.388(3)	C18-H18A	0.94
C19-C20	1.387(3)	C19-C22	1.495(3)
C20-C21	1.380(3)	C20-H20A	0.94
C21-H21A	0.94		

Table 5. Bond angles (°) for alex_e322.

O2-S1-O1	117.70(10)	O2-S1-C8	111.35(9)
O1-S1-C8	104.43(9)	O2-S1-C1	108.07(9)
O1-S1-C1	107.36(9)	C8-S1-C1	107.45(8)
C6-C1-C2	120.48(18)	C6-C1-S1	120.39(15)
C2-C1-S1	118.97(15)	C3-C2-C1	119.76(19)
C3-C2-H2A	120.1	C1-C2-H2A	120.1
C4-C3-C2	121.14(19)	C4-C3-H3A	119.4
C2-C3-H3A	119.4	C6-C5-C4	122.2(2)
C6-C5-H5A	118.9	C4-C5-H5A	118.9
C1-C6-C5	118.65(19)	C1-C6-H6A	120.7
C5-C6-H6A	120.7	C4-C7-H7A	109.5
C4-C7-H7B	109.5	H7A-C7-H7B	109.5

C4-C7-H7C	109.5	H7A-C7-H7C	109.5
H7B-C7-H7C	109.5	C9-C8-S1	127.82(14)
C9-C8-H8A	116.1	S1-C8-H8A	116.1
C8-C9-C10	125.69(16)	C8-C9-C16	118.39(15)
C10-C9-C16	115.92(15)	C11-C10-C9	122.68(16)
C11-C10-C15	122.30(16)	C9-C10-C15	114.98(15)
C10-C11-C12	123.86(17)	C10-C11-H11A	118.1
C12-C11-H11A	118.1	C11-C12-C13	112.50(19)
C11-C12-H12A	109.1	C13-C12-H12A	109.1
C11-C12-H12B	109.1	C13-C12-H12B	109.1
H12A-C12-H12B	107.8	C14-C13-C12	113.8(2)
C14-C13-H13A	108.8	C12-C13-H13A	108.8
C14-C13-H13B	108.8	C12-C13-H13B	108.8
H13A-C13-H13B	107.7	C13-C14-C15	111.7(2)
C13-C14-H14A	109.3	C15-C14-H14A	109.3
C13-C14-H14B	109.3	C15-C14-H14B	109.3
H14A-C14-H14B	107.9	C14-C15-C10	111.81(18)
C14-C15-H15A	109.3	C10-C15-H15A	109.3
C14-C15-H15B	109.3	C10-C15-H15B	109.3
H15A-C15-H15B	107.9	C17-C16-C21	119.17(17)
C17-C16-C9	121.68(16)	C21-C16-C9	119.15(16)
C18-C17-C16	120.34(17)	C18-C17-H17A	119.8
C16-C17-H17A	119.8	C17-C18-C19	119.90(18)
C17-C18-H18A	120.1	C19-C18-H18A	120.1
C18-C19-C20	120.17(17)	C18-C19-C22	120.10(18)
C20-C19-C22	119.65(18)	C21-C20-C19	119.70(17)
C21-C20-H20A	120.2	C19-C20-H20A	120.2
C20-C21-C16	120.69(18)	C20-C21-H21A	119.7
C16-C21-H21A	119.7	F3-C22-F1	107.0(2)
F3-C22-F2	106.49(19)	F1-C22-F2	104.37(18)
F3-C22-C19	113.73(17)	F1-C22-C19	112.03(17)
F2-C22-C19	112.61(18)	C3-C4-C5	117.77(18)
C3-C4-C7	121.5(2)	C5-C4-C7	120.7(2)

Table 6. Anisotropic atomic displacement parameters (\AA^2) for alex_e322.

The anisotropic atomic displacement factor exponent takes the form: $-2\pi^2 [h^2 a^{*2} U_{11} + \dots + 2 h k a^* b^* U_{12}]$

	U_{11}	U_{22}	U_{33}	U_{23}	U_{13}	U_{12}
S1	0.0414(3)	0.0397(3)	0.0342(3)	-0.01065(18)	-0.01166(19)	0.00472(19)
O1	0.0788(12)	0.0583(9)	0.0327(8)	-0.0124(6)	-0.0122(7)	0.0125(8)
O2	0.0409(8)	0.0496(8)	0.0661(10)	-0.0151(7)	-0.0172(7)	-0.0013(6)

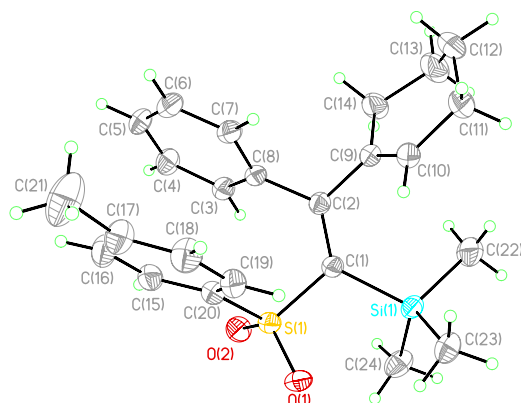
F1	0.1163(15)	0.0451(7)	0.1140(14)	-0.0314(8)	-0.0451(12)	0.0232(8)
F2	0.0913(12)	0.0615(8)	0.0536(8)	0.0042(6)	-0.0201(7)	0.0189(8)
F3	0.0495(9)	0.0842(11)	0.1173(15)	0.0296(10)	0.0025(9)	0.0220(8)
C1	0.0324(9)	0.0363(8)	0.0351(9)	-0.0059(7)	-0.0047(7)	0.0025(7)
C2	0.0309(9)	0.0479(10)	0.0602(13)	-0.0192(9)	-0.0060(8)	0.0037(8)
C3	0.0434(11)	0.0468(11)	0.0627(13)	-0.0220(10)	-0.0060(9)	0.0101(9)
C5	0.0340(11)	0.0452(10)	0.0784(16)	-0.0086(10)	-0.0064(10)	-0.0035(9)
C6	0.0346(11)	0.0437(10)	0.0671(14)	-0.0106(9)	0.0030(9)	0.0057(9)
C7	0.0711(17)	0.0465(11)	0.0712(16)	-0.0154(10)	-0.0196(13)	-0.0053(11)
C8	0.0415(10)	0.0345(8)	0.0360(9)	-0.0114(7)	-0.0079(7)	0.0034(7)
C9	0.0303(9)	0.0320(8)	0.0329(9)	-0.0084(6)	-0.0026(7)	-0.0036(7)
C10	0.0306(9)	0.0351(8)	0.0307(8)	-0.0092(6)	-0.0041(7)	-0.0006(7)
C11	0.0341(10)	0.0475(10)	0.0436(10)	-0.0170(8)	-0.0053(8)	-0.0034(8)
C12	0.0371(11)	0.0646(13)	0.0595(13)	-0.0294(11)	0.0066(9)	-0.0022(10)
C13	0.0544(14)	0.116(2)	0.088(2)	-0.0745(19)	0.0114(14)	-0.0153(15)
C14	0.0444(16)	0.0571(18)	0.0501(18)	-0.0275(15)	-0.0017(12)	-0.0099(13)
C15	0.0322(9)	0.0580(11)	0.0480(11)	-0.0257(9)	-0.0064(8)	-0.0026(9)
C16	0.0355(9)	0.0321(8)	0.0306(8)	-0.0088(6)	-0.0049(7)	-0.0020(7)
C17	0.0405(10)	0.0342(8)	0.0325(9)	-0.0037(7)	0.0001(7)	-0.0017(7)
C18	0.0362(10)	0.0397(9)	0.0425(10)	-0.0095(8)	0.0004(8)	0.0022(8)
C19	0.0383(10)	0.0337(8)	0.0388(10)	-0.0081(7)	-0.0079(8)	-0.0003(7)
C20	0.0523(12)	0.0424(9)	0.0331(9)	0.0002(7)	0.0011(8)	-0.0012(9)
C21	0.0416(10)	0.0458(9)	0.0353(10)	-0.0056(8)	0.0050(8)	0.0041(8)
C22	0.0522(13)	0.0401(10)	0.0495(12)	-0.0032(8)	-0.0090(9)	0.0050(9)
C4	0.0468(11)	0.0379(9)	0.0445(11)	-0.0049(8)	-0.0135(9)	0.0009(8)

Table 7. Hydrogen atomic coordinates and isotropic atomic displacement parameters (\AA^2) for alex_e322.

	x/a	y/b	z/c	U(eq)
H2A	0.6821	0.6639	0.3732	0.054
H3A	0.5901	0.4773	0.3466	0.059
H5A	-0.0198	0.5504	0.3982	0.064
H6A	0.0705	0.7333	0.4325	0.059
H7A	0.0735	0.3513	0.3785	0.093
H7B	0.3150	0.3109	0.3762	0.093
H7C	0.2076	0.3832	0.2804	0.093
H8A	0.2673	1.0325	0.4026	0.044
H11A	0.6408	0.9393	0.2182	0.049
H12A	0.6871	0.7524	0.1577	0.062
H12B	0.7181	0.8740	0.0753	0.062

H13A	0.4049	0.8579	0.0118	0.093
H13B	0.4827	0.7195	0.0424	0.093
H14A	0.2663	0.6850	0.1777	0.057
H14B	0.1305	0.7376	0.0856	0.057
H15A	0.0507	0.8315	0.2178	0.052
H15B	0.0959	0.9260	0.1178	0.052
H17A	-0.1003	1.0703	0.3455	0.044
H18A	-0.3158	1.2373	0.2791	0.048
H20A	0.0913	1.3314	0.0512	0.053
H21A	0.2998	1.1607	0.1151	0.05

Crystal Structure Report for silylated diene **1.26**



A clear colourless needle-like specimen of $C_{24}H_{30}O_2SSi$, approximate dimensions 0.020 mm x 0.020 mm x 0.160 mm, was used for the X-ray crystallographic analysis. The X-ray intensity data were measured on a Bruker Apex II CCD system equipped with a Cu IMuS micro-focus ($\lambda = 1.54178 \text{ \AA}$).

The frames were integrated with the Bruker SAINT software package using a narrow-frame algorithm. The integration of the data using a trigonal unit cell yielded a total of 31294 reflections to a maximum θ angle of 68.28° (0.83 \AA resolution), of which 4422 were independent (average redundancy 7.077, completeness = 99.4%, $R_{\text{int}} = 9.04\%$, $R_{\text{sig}} = 5.24\%$) and 3232 (73.09%) were greater than $2\sigma(F^2)$. The final cell constants of $a = 43.3309(15) \text{ \AA}$, $b = 43.3309(15) \text{ \AA}$, $c = 6.7259(3) \text{ \AA}$, volume = $10936.5(9) \text{ \AA}^3$, are based upon the refinement of the XYZ-centroids of reflections above $20 \sigma(I)$. The calculated minimum and maximum transmission coefficients (based on crystal size) are 0.5250 and 0.7230.

The structure was solved and refined using the Bruker SHELXTL Software Package, using the space group $R\bar{3}$, with $Z = 18$ for the formula unit, $C_{24}H_{30}O_2SSi$. The final anisotropic full-matrix least-squares refinement on F^2 with 261 variables converged at $R1 = 4.16\%$, for the observed data and $wR2 = 12.01\%$ for all data. The goodness-of-fit was 1.000. The largest peak in the final difference electron density synthesis was $0.198 \text{ e}^-/\text{\AA}^3$ and the largest hole was $-0.365 \text{ e}^-/\text{\AA}^3$ with an RMS deviation of $0.042 \text{ e}^-/\text{\AA}^3$. On the basis of the final model, the calculated density was 1.122 g/cm^3 and $F(000)$, 3960 e^- .

Table 1. Sample and crystal data for berne2.

Identification code	berne2	
Chemical formula	C ₂₄ H ₃₀ O ₂ SSi	
Formula weight	410.63 g/mol	
Temperature	220(2) K	
Wavelength	1.54178 Å	
Crystal size	0.020 x 0.020 x 0.160 mm	
Crystal habit	clear colourless needle	
Crystal system	trigonal	
Space group	R -3	
Unit cell dimensions	a = 43.3309(15) Å b = 43.3309(15) Å c = 6.7259(3) Å	α = 90° β = 90° γ = 120°
Volume	10936.5(9) Å ³	
Z	18	
Density (calculated)	1.122 g/cm ³	
Absorption coefficient	1.765 mm ⁻¹	
F(000)	3960	

Table 2. Data collection and structure refinement for berne2.

Diffractometer	Bruker Apex II CCD
Radiation source	IMuS micro-focus, Cu
Theta range for data collection	2.04 to 68.28°
Index ranges	-51 ≤ h ≤ 52, -52 ≤ k ≤ 51, -7 ≤ l ≤ 7
Reflections collected	31294
Independent reflections	4422 [R(int) = 0.0904]
Absorption correction	multi-scan
Max. and min. transmission	0.7230 and 0.5250
Structure solution technique	direct methods
Structure solution program	SHELXT-2014(Sheldrick, 2014)
Refinement method	Full-matrix least-squares on F ²
Refinement program	SHELXL-2014 (Sheldrick, 2014)
Function minimized	Σ w(F _o ² - F _c ²) ²
Data / restraints / parameters	4422 / 0 / 261
Goodness-of-fit on F²	1.000
Δ/σ_{max}	0.111
Final R indices	[3232 data; I > 2σ(I)] R1 = 0.0416, wR2 = 0.1046

	all data	R1 = 0.0673, wR2 = 0.1201
Weighting scheme	$w=1/[\sigma^2(F_o^2)+(0.0680P)^2]$	
	where $P=(F_o^2+2F_c^2)/3$	
Largest diff. peak and hole	0.198 and -0.365 eÅ ⁻³	
R.M.S. deviation from mean	0.042 eÅ ⁻³	

Table 3. Atomic coordinates and equivalent isotropic atomic displacement parameters (Å²) for berne2.

U(eq) is defined as one third of the trace of the orthogonalized U_{ij} tensor.

	x/a	y/b	z/c	U(eq)
S1	0.47428(2)	0.31916(2)	0.51012(8)	0.03709(16)
Si1	0.41138(2)	0.32883(2)	0.62538(9)	0.03743(17)
O1	0.48879(4)	0.35670(4)	0.5515(2)	0.0464(4)
O2	0.47367(4)	0.30913(4)	0.3052(2)	0.0470(4)
C1	0.43103(6)	0.29809(5)	0.6196(3)	0.0334(5)
C2	0.41593(6)	0.26375(5)	0.6836(3)	0.0330(5)
C3	0.43048(6)	0.22960(6)	0.4325(3)	0.0390(5)
C4	0.44160(7)	0.20534(6)	0.3880(4)	0.0470(6)
C5	0.45130(7)	0.19038(6)	0.5390(4)	0.0503(6)
C6	0.44936(7)	0.19881(6)	0.7344(4)	0.0491(6)
C7	0.43760(6)	0.22219(6)	0.7801(3)	0.0418(5)
C8	0.42869(6)	0.23848(5)	0.6294(3)	0.0350(5)
C9	0.38542(6)	0.24858(6)	0.8218(3)	0.0361(5)
C10	0.38820(6)	0.26433(7)	0.9962(3)	0.0398(5)
C11	0.35973(7)	0.24993(7)	0.1522(3)	0.0520(6)
C12	0.33236(9)	0.21149(8)	0.1155(5)	0.0735(9)
C13	0.32143(8)	0.20468(8)	0.8994(5)	0.0707(9)
C14	0.35298(7)	0.21377(6)	0.7647(4)	0.0533(7)
C15	0.51425(6)	0.28660(6)	0.5642(4)	0.0460(6)
C16	0.53326(7)	0.27571(7)	0.6802(4)	0.0565(7)
C17	0.53780(8)	0.28290(8)	0.8828(4)	0.0595(7)
C18	0.52381(8)	0.30269(8)	0.9641(4)	0.0567(7)
C19	0.50492(7)	0.31394(7)	0.8512(3)	0.0460(6)
C20	0.49988(6)	0.30551(6)	0.6511(3)	0.0387(5)
C21	0.55643(13)	0.26878(13)	0.0123(6)	0.1048(14)
C22	0.36232(7)	0.30356(8)	0.6673(4)	0.0600(7)
C23	0.43269(8)	0.36452(7)	0.8150(4)	0.0534(6)
C24	0.41731(8)	0.34814(7)	0.3709(3)	0.0555(7)

Table 4. Bond lengths (Å) for berne2.

S1-O2	1.4415(16)	S1-O1	1.4476(16)
S1-C20	1.771(2)	S1-C1	1.782(2)
Si1-C23	1.856(2)	Si1-C22	1.863(3)
Si1-C24	1.866(2)	Si1-C1	1.907(2)
C1-C2	1.361(3)	C2-C9	1.475(3)
C2-C8	1.498(3)	C3-C8	1.392(3)
C3-C4	1.390(3)	C3-H3A	0.94
C4-C5	1.378(3)	C4-H4A	0.94
C5-C6	1.378(3)	C5-H5A	0.94
C6-C7	1.377(3)	C6-H6A	0.94
C7-C8	1.396(3)	C7-H7A	0.94
C9-C10	1.331(3)	C9-C14	1.510(3)
C10-C11	1.497(3)	C10-H10	0.99(3)
C11-C12	1.506(4)	C11-H11A	0.98
C11-H11B	0.98	C12-C13	1.511(4)
C12-H12A	0.98	C12-H12B	0.98
C13-C14	1.519(3)	C13-H13A	0.98
C13-H13B	0.98	C14-H14A	0.98
C14-H14B	0.98	C15-C16	1.378(4)
C15-C20	1.382(3)	C15-H15A	0.94
C16-C17	1.389(4)	C16-H16A	0.94
C17-C18	1.386(4)	C17-C21	1.510(4)
C18-C19	1.372(3)	C18-H18A	0.94
C19-C20	1.383(3)	C19-H19A	0.94
C21-H21A	0.97	C21-H21B	0.97
C21-H21C	0.97	C22-H22A	0.97
C22-H22B	0.97	C22-H22C	0.97
C23-H23A	0.97	C23-H23B	0.97
C23-H23C	0.97	C24-H24A	0.97
C24-H24B	0.97	C24-H24C	0.97

Table 5. Bond angles (°) for berne2.

O2-S1-O1	117.07(10)	O2-S1-C20	109.34(10)
O1-S1-C20	106.24(10)	O2-S1-C1	112.62(10)
O1-S1-C1	104.52(10)	C20-S1-C1	106.34(10)
C23-Si1-C22	109.38(13)	C23-Si1-C24	110.94(12)
C22-Si1-C24	105.28(13)	C23-Si1-C1	112.72(11)
C22-Si1-C1	111.68(11)	C24-Si1-C1	106.56(10)

C2-C1-S1	119.89(16)	C2-C1-S11	128.21(16)
S1-C1-Si1	111.90(11)	C1-C2-C9	121.35(19)
C1-C2-C8	124.79(19)	C9-C2-C8	113.83(17)
C8-C3-C4	120.1(2)	C8-C3-H3A	119.9
C4-C3-H3A	119.9	C5-C4-C3	120.0(2)
C5-C4-H4A	120.0	C3-C4-H4A	120.0
C6-C5-C4	120.3(2)	C6-C5-H5A	119.9
C4-C5-H5A	119.9	C5-C6-C7	120.1(2)
C5-C6-H6A	119.9	C7-C6-H6A	119.9
C6-C7-C8	120.5(2)	C6-C7-H7A	119.7
C8-C7-H7A	119.7	C3-C8-C7	118.9(2)
C3-C8-C2	121.73(19)	C7-C8-C2	119.33(19)
C10-C9-C2	119.7(2)	C10-C9-C14	122.5(2)
C2-C9-C14	117.66(19)	C9-C10-C11	124.0(2)
C9-C10-H10	119.6(14)	C11-C10-H10	116.4(13)
C10-C11-C12	112.1(2)	C10-C11-H11A	109.2
C12-C11-H11A	109.2	C10-C11-H11B	109.2
C12-C11-H11B	109.2	H11A-C11-H11B	107.9
C11-C12-C13	111.7(2)	C11-C12-H12A	109.3
C13-C12-H12A	109.3	C11-C12-H12B	109.3
C13-C12-H12B	109.3	H12A-C12-H12B	107.9
C12-C13-C14	111.7(3)	C12-C13-H13A	109.3
C14-C13-H13A	109.3	C12-C13-H13B	109.3
C14-C13-H13B	109.3	H13A-C13-H13B	107.9
C9-C14-C13	112.0(2)	C9-C14-H14A	109.2
C13-C14-H14A	109.2	C9-C14-H14B	109.2
C13-C14-H14B	109.2	H14A-C14-H14B	107.9
C16-C15-C20	119.2(2)	C16-C15-H15A	120.4
C20-C15-H15A	120.4	C15-C16-C17	121.3(2)
C15-C16-H16A	119.3	C17-C16-H16A	119.3
C18-C17-C16	118.0(2)	C18-C17-C21	120.7(3)
C16-C17-C21	121.3(3)	C19-C18-C17	121.6(2)
C19-C18-H18A	119.2	C17-C18-H18A	119.2
C18-C19-C20	119.2(2)	C18-C19-H19A	120.4
C20-C19-H19A	120.4	C19-C20-C15	120.6(2)
C19-C20-S1	118.38(17)	C15-C20-S1	120.99(18)
C17-C21-H21A	109.5	C17-C21-H21B	109.5
H21A-C21-H21B	109.5	C17-C21-H21C	109.5
H21A-C21-H21C	109.5	H21B-C21-H21C	109.5
Si1-C22-H22A	109.5	Si1-C22-H22B	109.5
H22A-C22-H22B	109.5	Si1-C22-H22C	109.5
H22A-C22-H22C	109.5	H22B-C22-H22C	109.5
Si1-C23-H23A	109.5	Si1-C23-H23B	109.5
H23A-C23-H23B	109.5	Si1-C23-H23C	109.5
H23A-C23-H23C	109.5	H23B-C23-H23C	109.5

Si1-C24-H24A	109.5	Si1-C24-H24B	109.5
H24A-C24-H24B	109.5	Si1-C24-H24C	109.5
H24A-C24-H24C	109.5	H24B-C24-H24C	109.5

Table 6. Anisotropic atomic displacement parameters (\AA^2) for berne2.

The anisotropic atomic displacement factor exponent takes the form: $-2\pi^2[h^2 a^{*2} U_{11} + \dots + 2 h k a^* b^* U_{12}]$

	U_{11}	U_{22}	U_{33}	U_{23}	U_{13}	U_{12}
S1	0.0403(3)	0.0316(3)	0.0390(3)	0.0055(2)	0.0092(2)	0.0177(2)
Si1	0.0433(4)	0.0341(3)	0.0403(4)	0.0006(2)	0.0008(2)	0.0234(3)
O1	0.0505(10)	0.0274(8)	0.0560(10)	0.0056(7)	0.0096(7)	0.0156(8)
O2	0.0588(11)	0.0517(10)	0.0344(9)	0.0063(7)	0.0126(7)	0.0305(9)
C1	0.0367(12)	0.0306(11)	0.0332(11)	0.0007(8)	0.0038(9)	0.0170(9)
C2	0.0354(11)	0.0327(11)	0.0327(11)	-0.0009(8)	0.0003(8)	0.0184(10)
C3	0.0420(13)	0.0359(12)	0.0405(13)	-0.0007(9)	0.0017(9)	0.0206(11)
C4	0.0549(15)	0.0415(14)	0.0490(14)	-0.0112(11)	0.0019(11)	0.0274(12)
C5	0.0573(16)	0.0375(13)	0.0660(17)	-0.0020(11)	0.0075(12)	0.0312(13)
C6	0.0594(16)	0.0426(14)	0.0540(15)	0.0089(11)	0.0055(12)	0.0320(13)
C7	0.0498(14)	0.0369(12)	0.0419(13)	0.0062(9)	0.0077(10)	0.0240(11)
C8	0.0371(12)	0.0271(11)	0.0403(12)	0.0010(8)	0.0058(9)	0.0156(9)
C9	0.0362(12)	0.0312(11)	0.0439(13)	0.0020(9)	0.0049(9)	0.0191(10)
C10	0.0415(13)	0.0411(13)	0.0409(13)	0.0029(10)	0.0047(10)	0.0237(12)
C11	0.0588(16)	0.0588(16)	0.0438(15)	0.0069(11)	0.0148(11)	0.0336(14)
C12	0.075(2)	0.0557(18)	0.085(2)	0.0187(15)	0.0473(18)	0.0296(16)
C13	0.0439(16)	0.0479(16)	0.098(2)	-0.0074(15)	0.0221(15)	0.0062(13)
C14	0.0419(14)	0.0366(13)	0.0664(17)	-0.0090(11)	0.0098(12)	0.0084(11)
C15	0.0435(14)	0.0425(13)	0.0515(15)	-0.0007(10)	0.0086(10)	0.0212(11)
C16	0.0547(16)	0.0575(17)	0.0698(18)	-0.0048(13)	0.0035(13)	0.0373(14)
C17	0.0599(17)	0.0653(18)	0.0658(19)	0.0022(14)	-0.0048(13)	0.0407(15)
C18	0.0646(18)	0.0667(18)	0.0471(15)	0.0001(12)	-0.0023(12)	0.0391(15)
C19	0.0467(14)	0.0475(14)	0.0478(14)	0.0010(11)	0.0062(10)	0.0266(12)
C20	0.0355(12)	0.0345(12)	0.0444(13)	0.0025(9)	0.0062(9)	0.0163(10)
C21	0.137(4)	0.137(4)	0.094(3)	-0.010(2)	-0.031(2)	0.108(3)
C22	0.0477(16)	0.0576(17)	0.083(2)	0.0051(14)	0.0006(13)	0.0324(14)
C23	0.0640(17)	0.0493(15)	0.0555(16)	-0.0105(12)	0.0004(12)	0.0348(14)
C24	0.0776(19)	0.0519(16)	0.0483(15)	0.0031(11)	-0.0052(13)	0.0409(15)

Table 7. Hydrogen atomic coordinates and isotropic atomic

displacement parameters (\AA^2) for berne2.

	x/a	y/b	z/c	U(eq)
H3A	0.4242	0.2400	0.3294	0.047
H4A	0.4425	0.1991	0.2551	0.056
H5A	0.4593	0.1744	0.5084	0.06
H6A	0.4561	0.1886	0.8367	0.059
H7A	0.4356	0.2272	0.9138	0.05
H10	0.4102(7)	0.2871(7)	1.028(3)	0.047(7)
H11A	0.3479	0.2642	1.1543	0.062
H11B	0.3707	0.2521	1.2827	0.062
H12A	0.3113	0.2050	1.1976	0.088
H12B	0.3422	0.1964	1.1552	0.088
H13A	0.3107	0.2191	0.8612	0.085
H13B	0.3034	0.1795	0.8819	0.085
H14A	0.3588	0.1946	0.7719	0.064
H14B	0.3465	0.2153	0.6270	0.064
H15A	0.5111	0.2812	0.4277	0.055
H16A	0.5434	0.2632	0.6211	0.068
H18A	0.5273	0.3086	1.0999	0.068
H19A	0.4955	0.3272	0.9092	0.055
H21A	0.5675	0.2847	1.1242	0.157
H21B	0.5746	0.2673	0.9353	0.157
H21C	0.5392	0.2453	1.0609	0.157
H22A	0.3520	0.3176	0.6219	0.09
H22B	0.3575	0.2986	0.8081	0.09
H22C	0.3519	0.2813	0.5940	0.09
H23A	0.4199	0.3775	0.8233	0.08
H23B	0.4573	0.3807	0.7777	0.08
H23C	0.4321	0.3540	0.9433	0.08
H24A	0.4035	0.3601	0.3586	0.083
H24B	0.4092	0.3292	0.2730	0.083
H24C	0.4423	0.3652	0.3487	0.083

6. ¹H NMR Spectra of Entries in Optimization Tables 3.1 and 3.2

¹H NMR Spectra of Table 3.1 Entries in Numerical Order^a 106

¹H NMR Spectra of Table 3.2 Entries in Numerical Order^b 111

^aNMRs also may contain ethyl acetate. ^bNMRs also may contain ethyl acetate and/or methylene chloride and the solvent being screened.

Table 3.1, entry 1

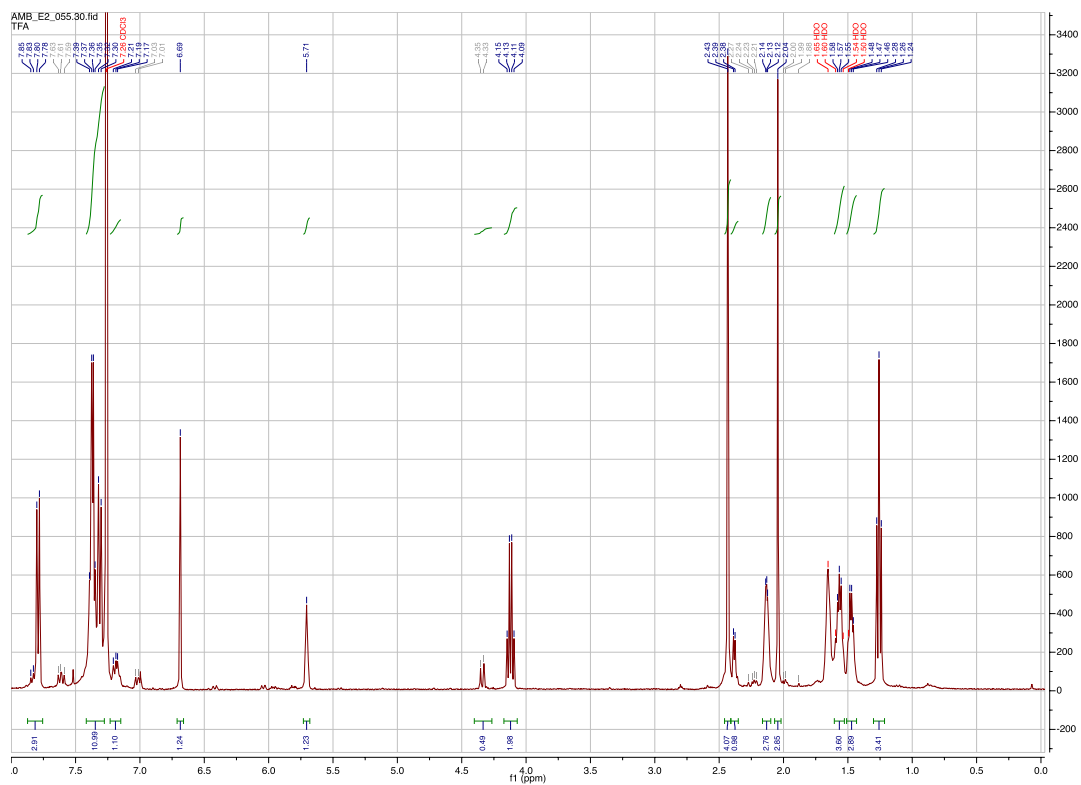


Table 3.1, entry 4

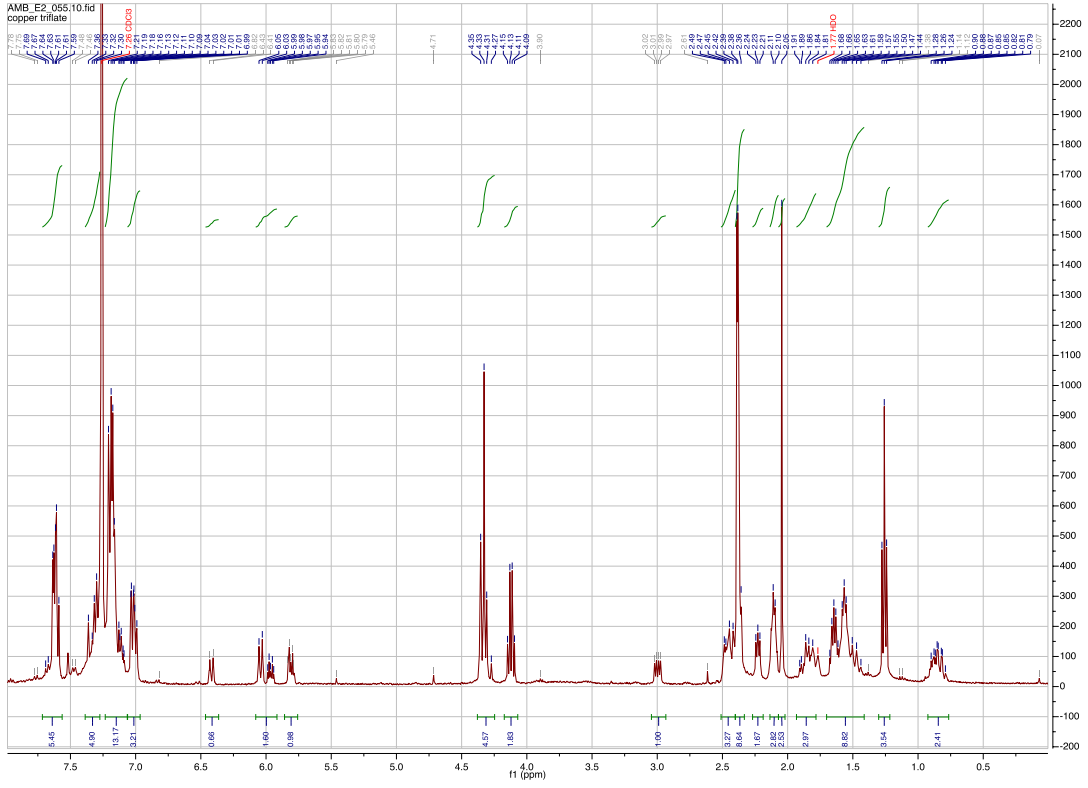


Table 3.1, entry 5

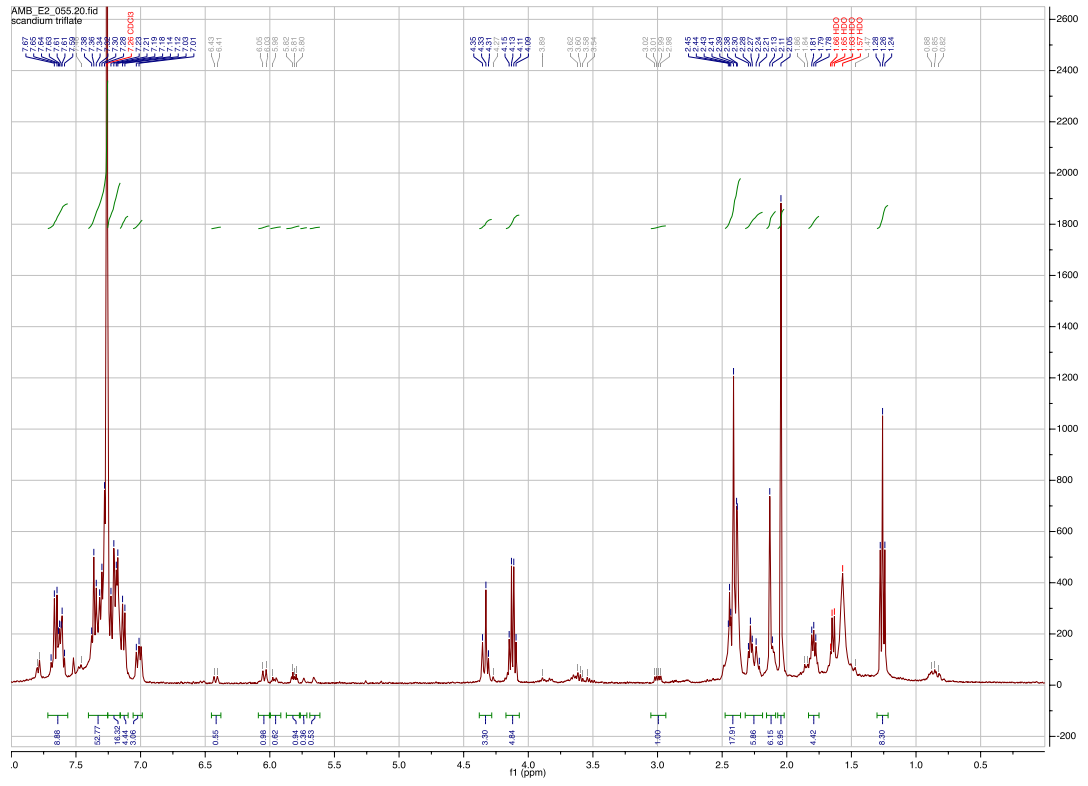


Table 3.2, entry 1

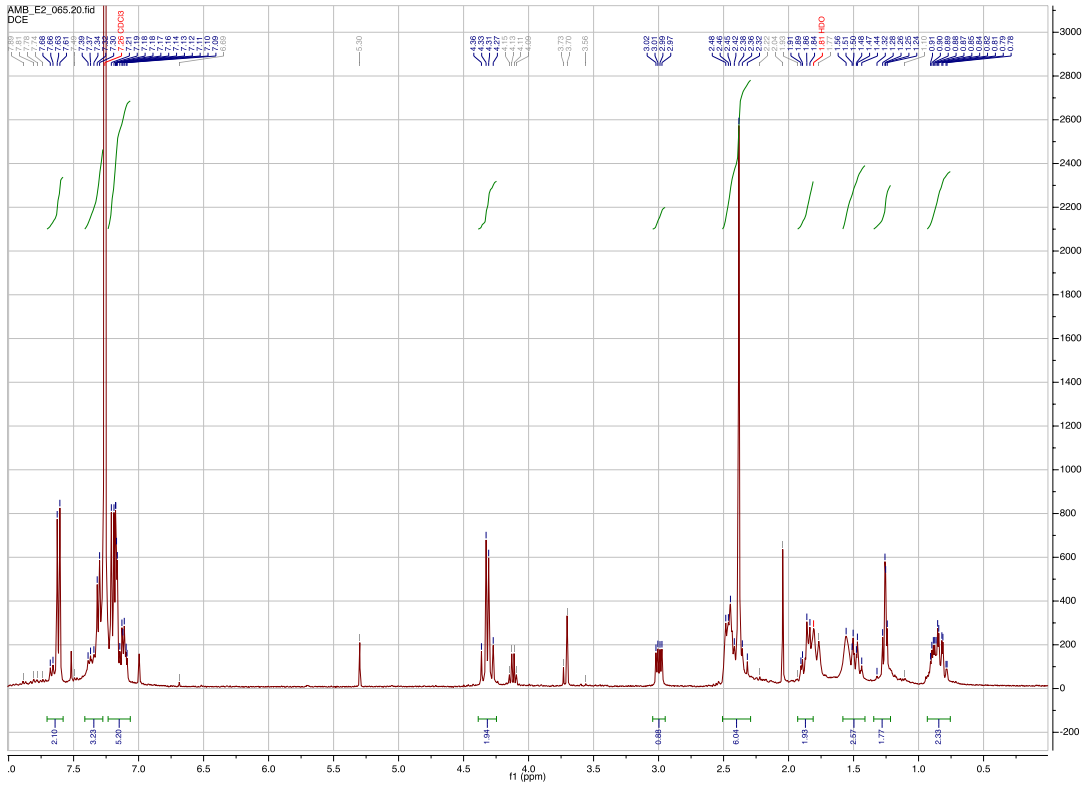


Table 3.2, entry 2

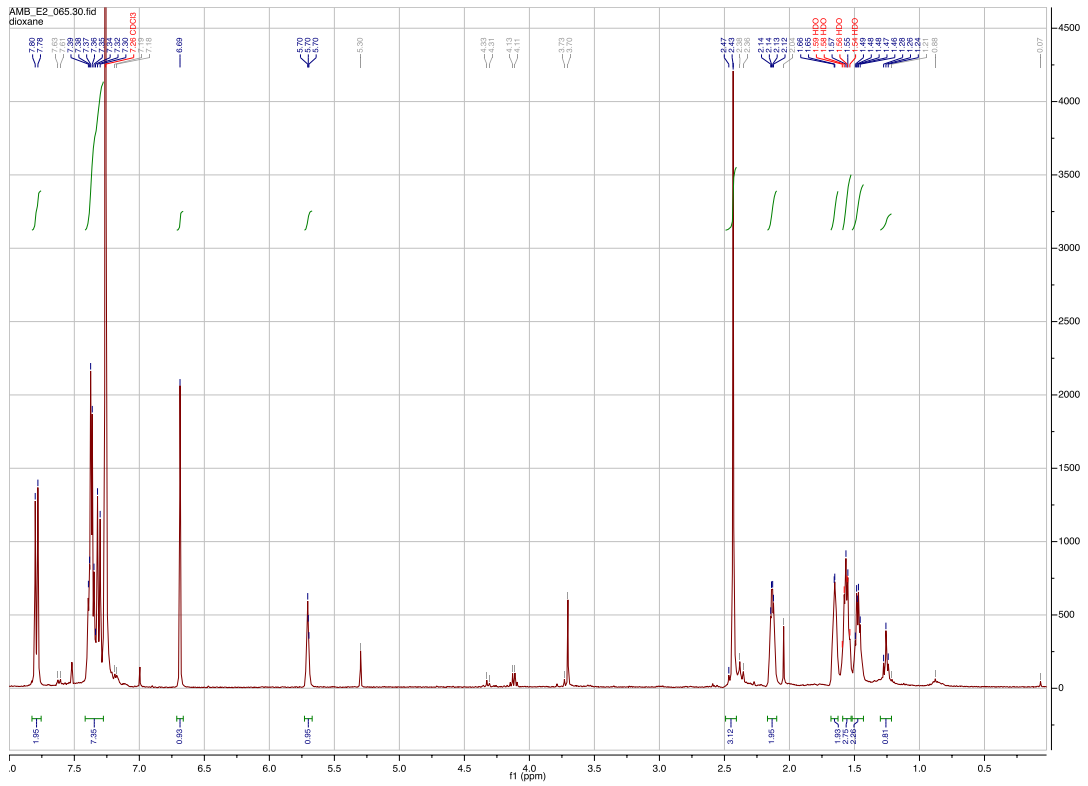


Table 3.2, entry 3

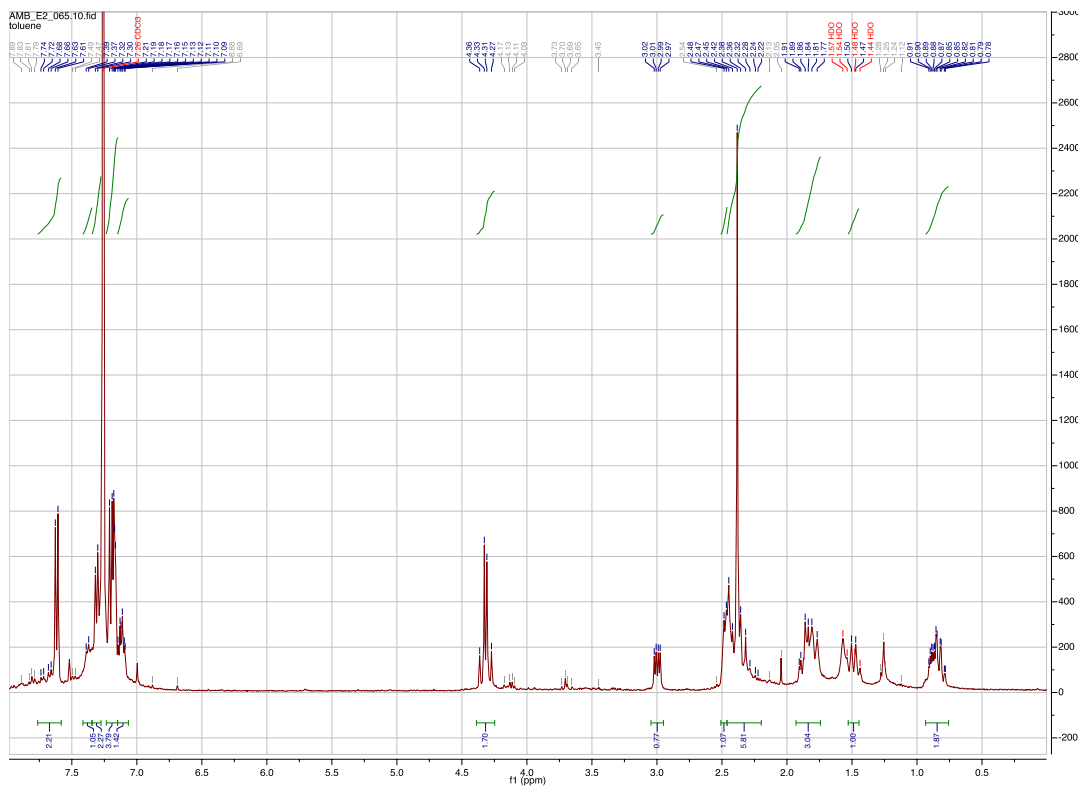


Table 3.2, entry 4

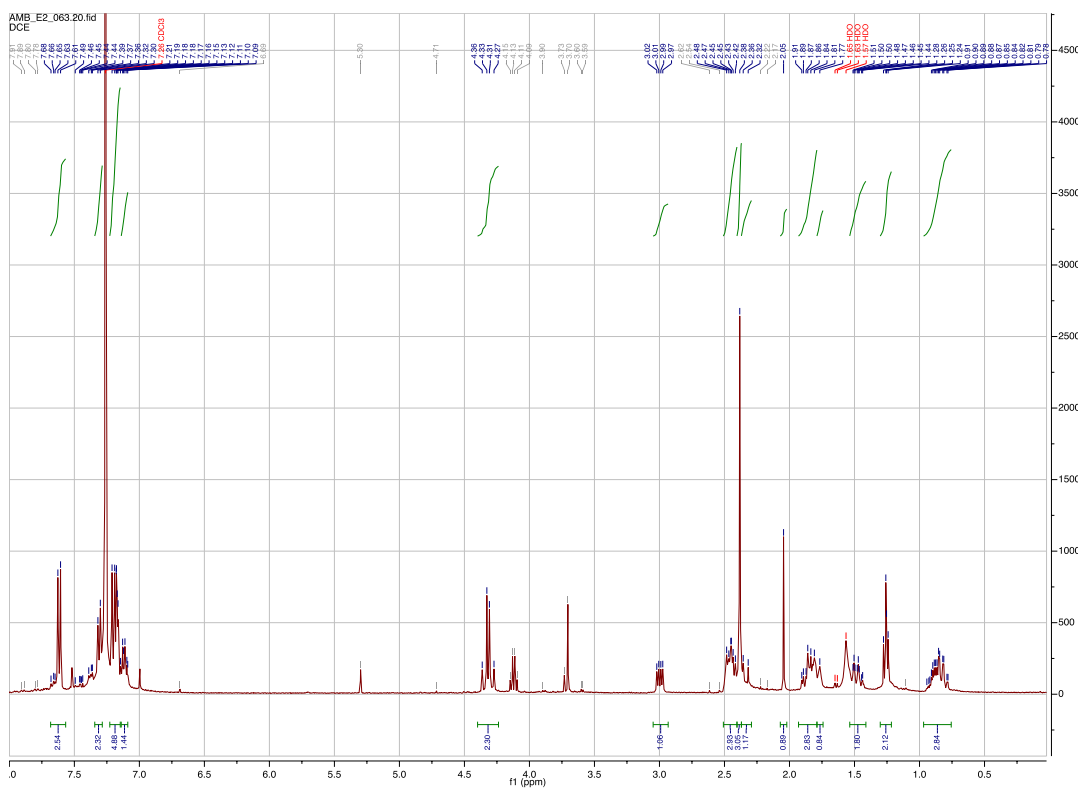


Table 3.2, entry 5

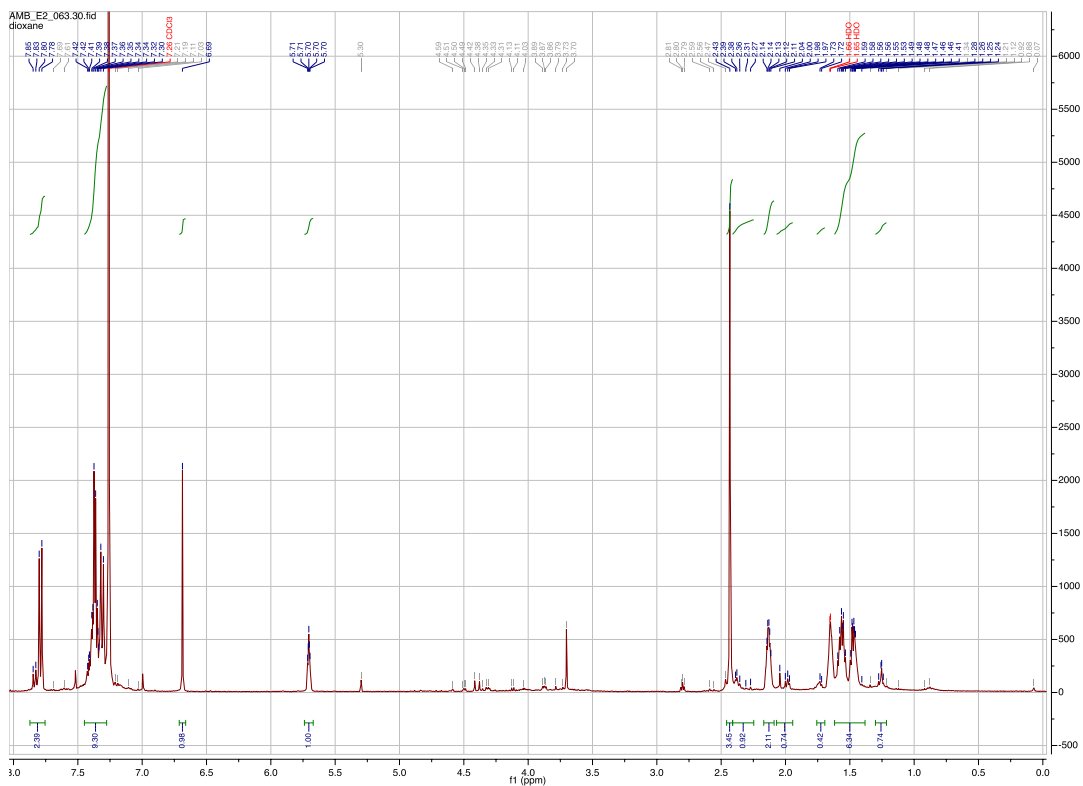


Table 3.2, entry 6

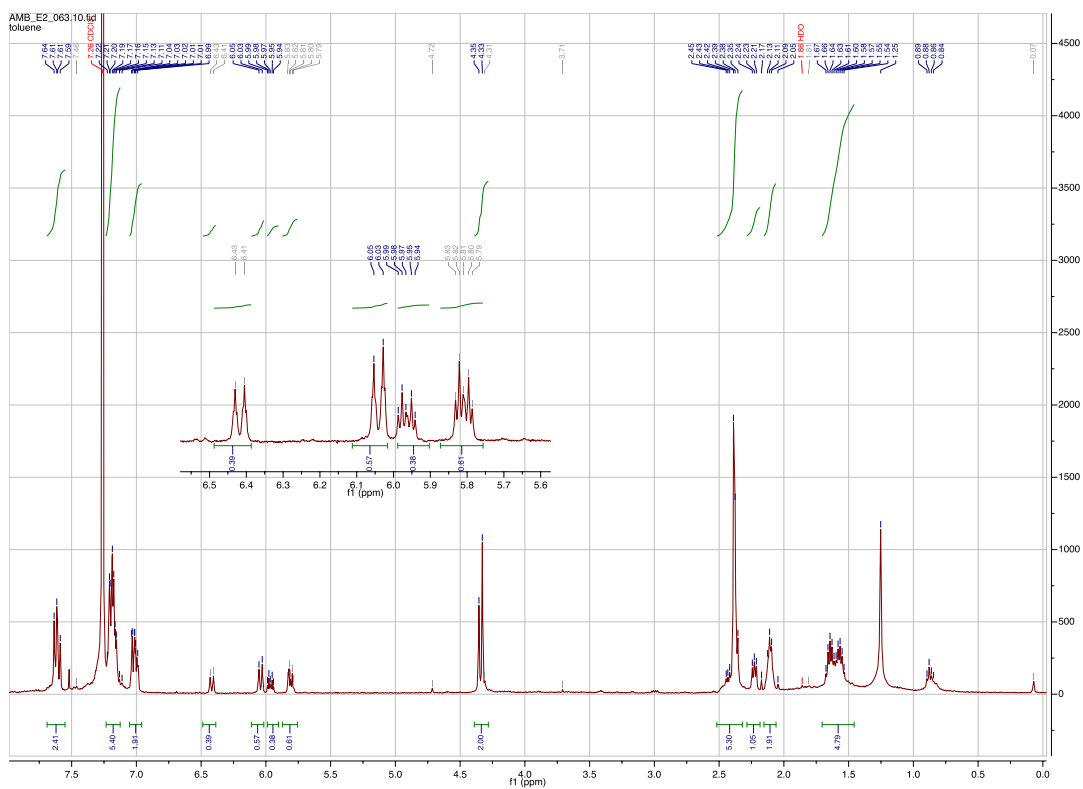


Table 3.2, entry 7

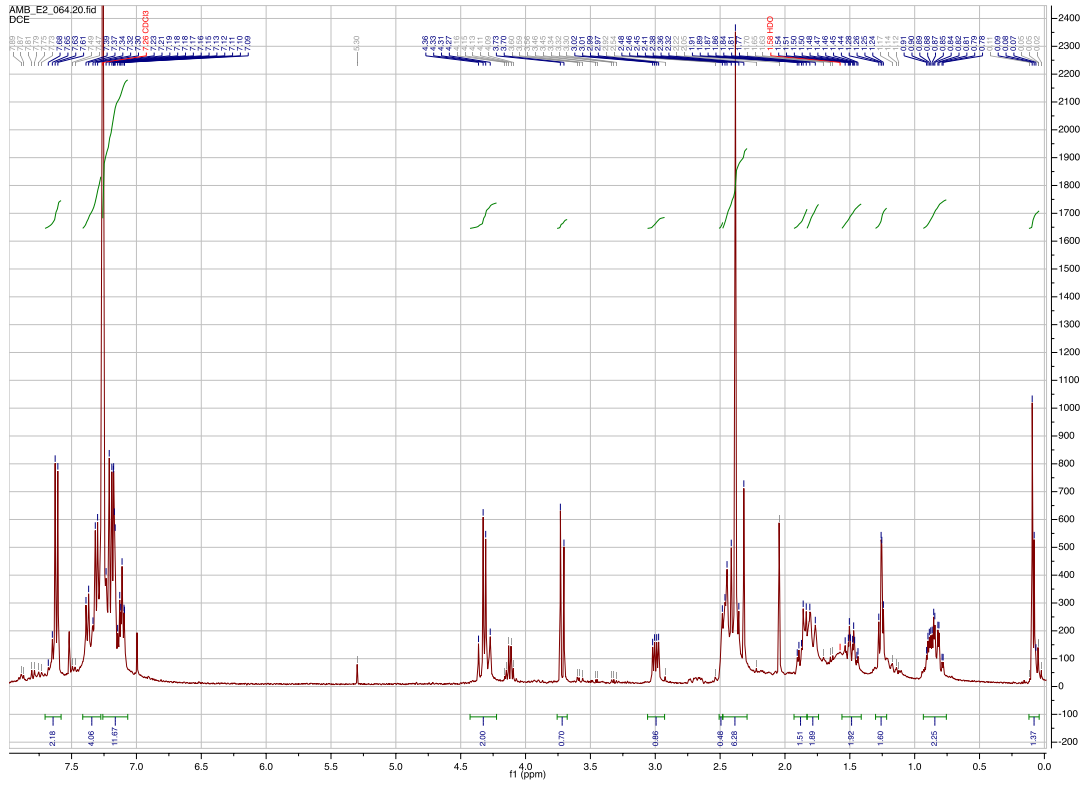
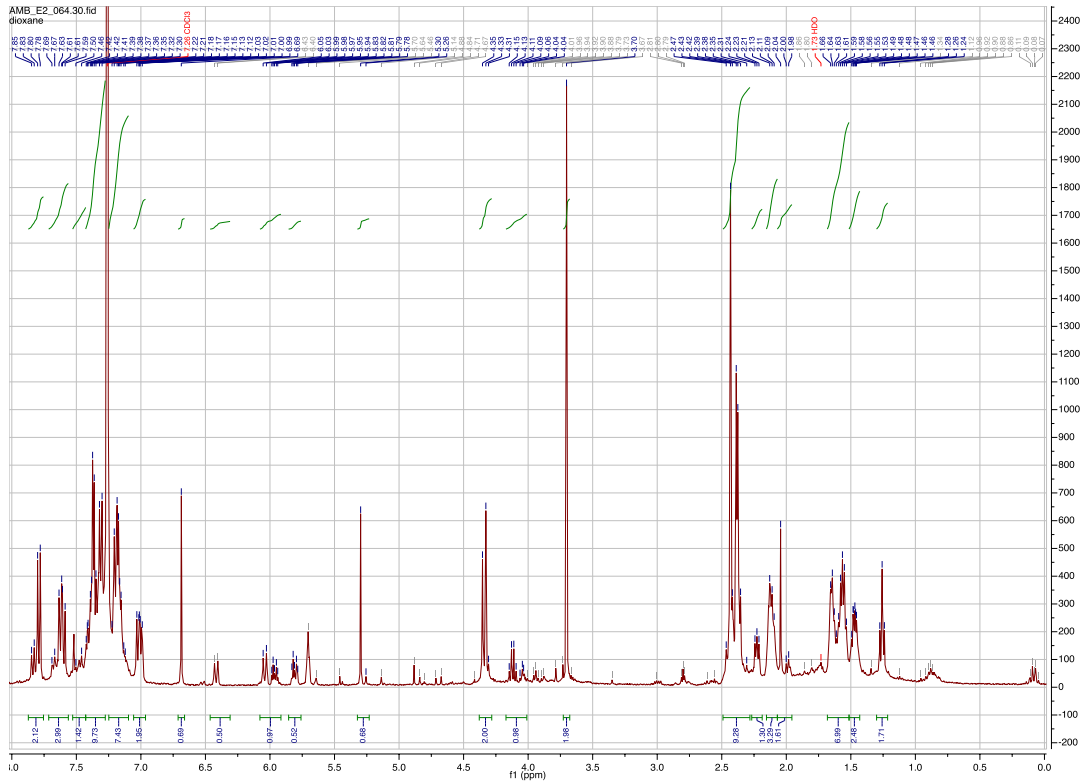
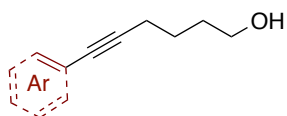


Table 3.2, entry 8

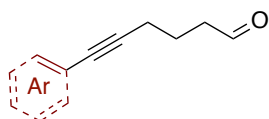


7. ^1H NMR and ^{13}C NMR Spectra of Compounds

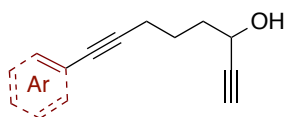
Coupled products **1.12, 4.1, 4.2, 4.3** 118



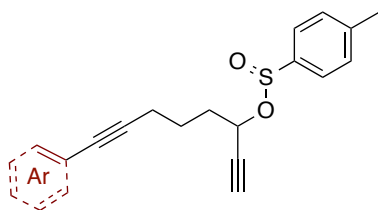
Aldehydes **1.13, 4.4, 4.5, 4.6** 126



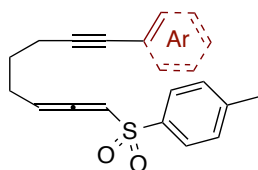
Alcohols **1.14, 4.7, 4.8, 4.9** 134



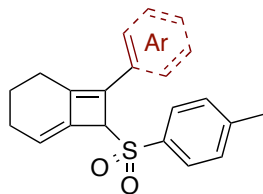
Sulfinates **1.15, 4.10, 4.11, 4.12** 142



Allene-ynes **1.10, 4.13, 4.14, 4.15** 152



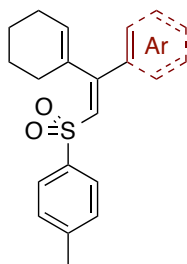
Alkylidene Cyclobutenes **1.9, 4.16, 4.17, 4.18**..... 160



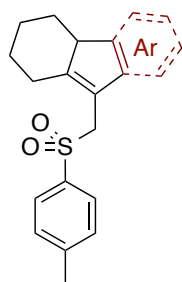
Cyclobutenes **1.8, 4.19a, 4.20a, 4.21a** 168



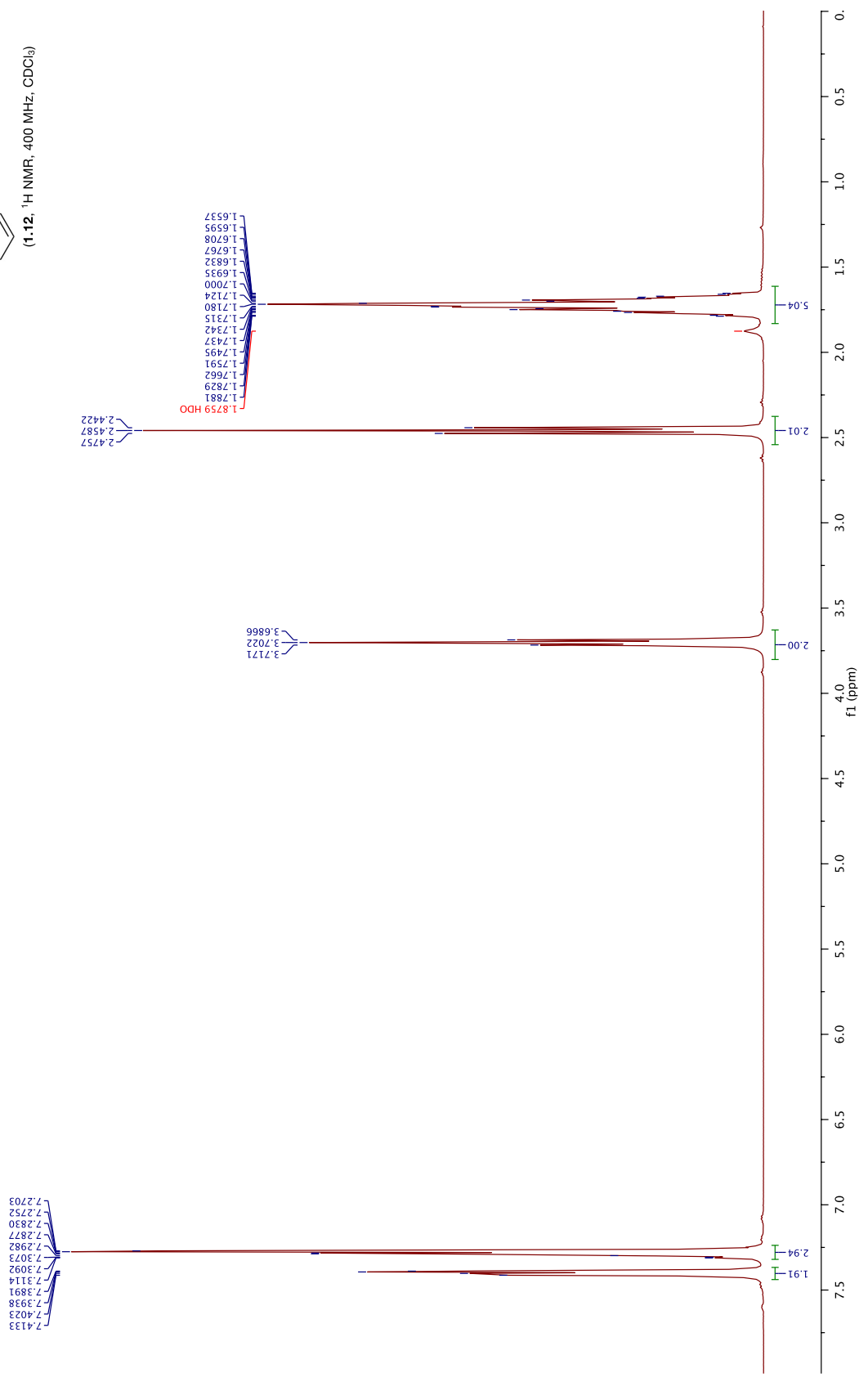
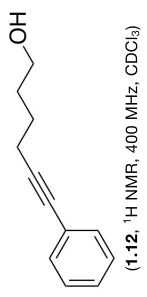
Dienes **1.28, 4.19b, 4.20b, 4.21b** 176

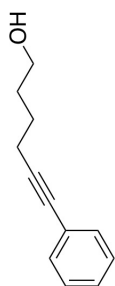


Tetrahydrofluorenes **1.25, 4.19c, 4.20c, 4.21c** 184

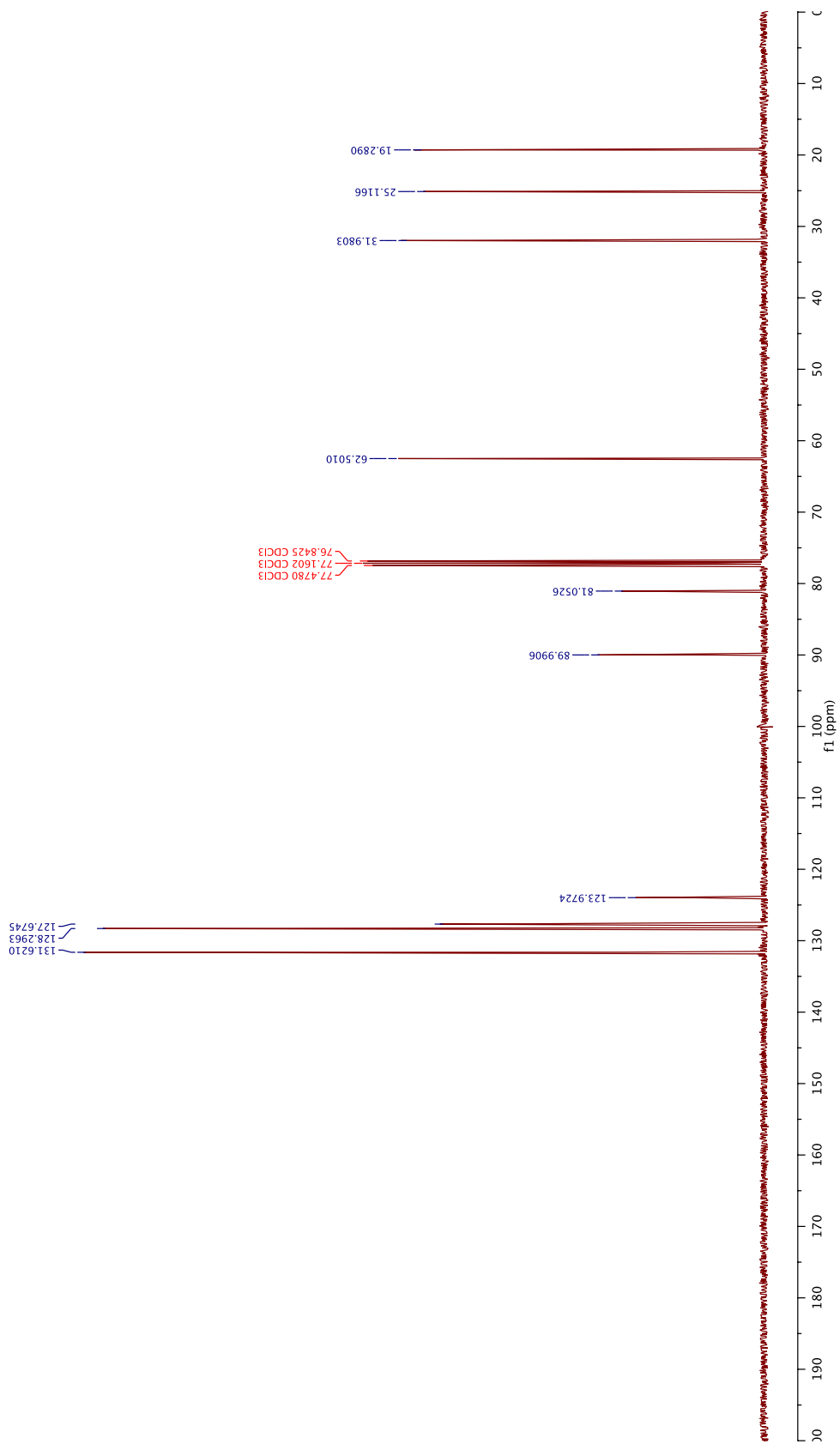


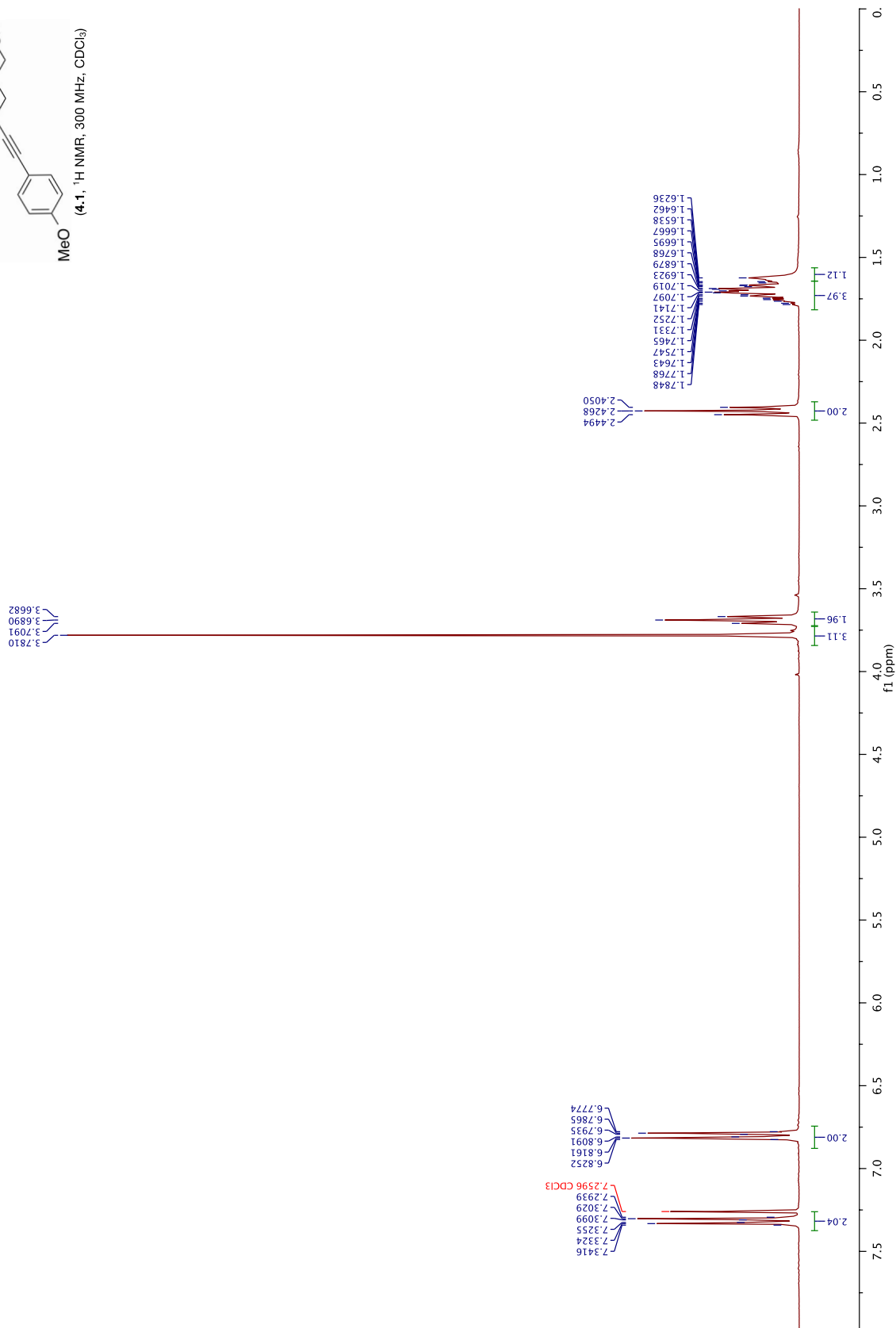
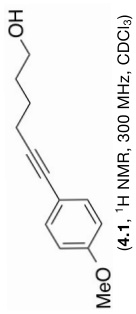
Compounds **1.22, 1.23, 1.26, 3.1/3.2**..... 192

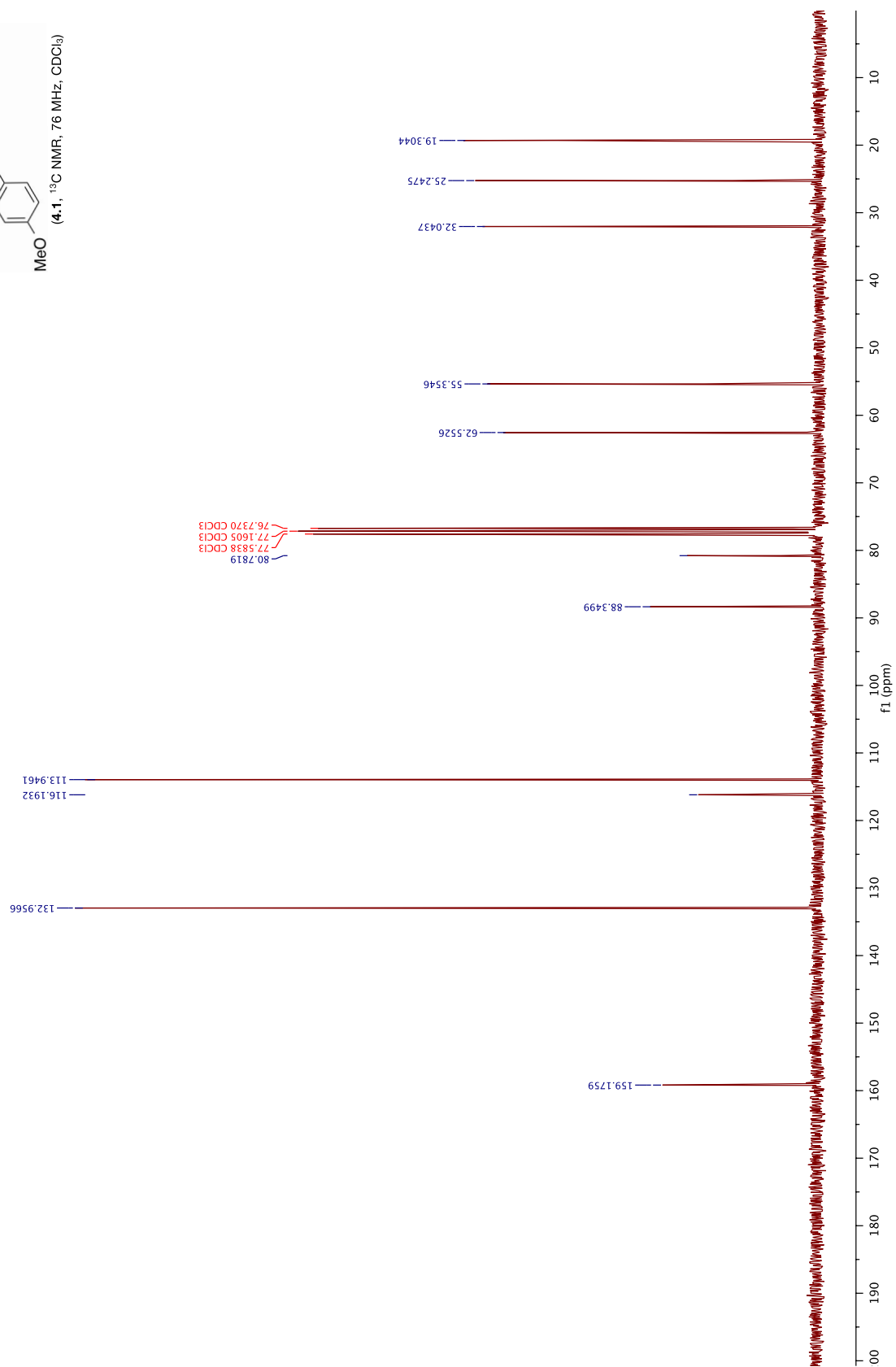
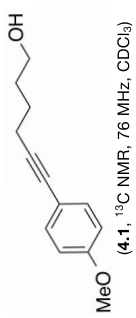


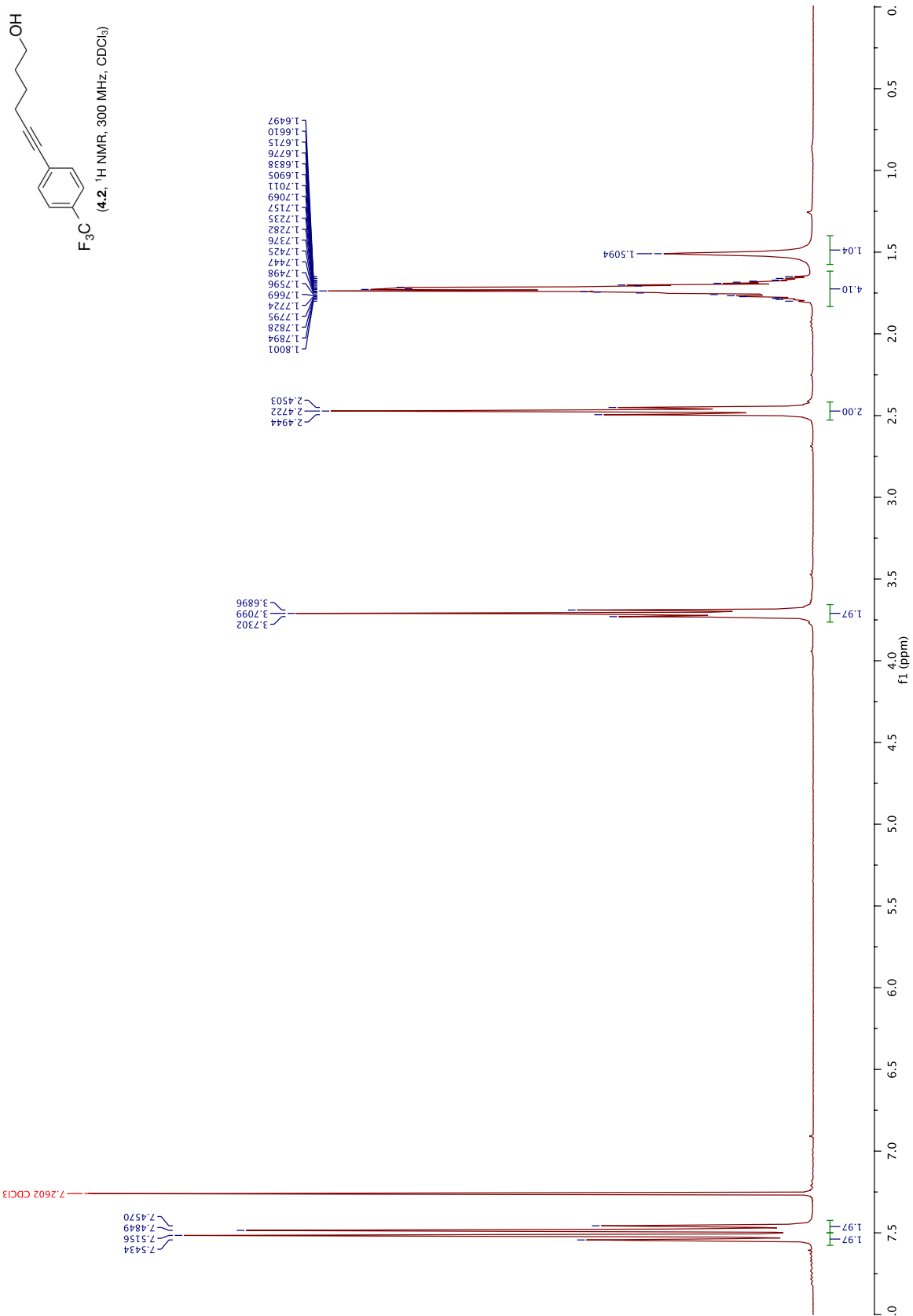


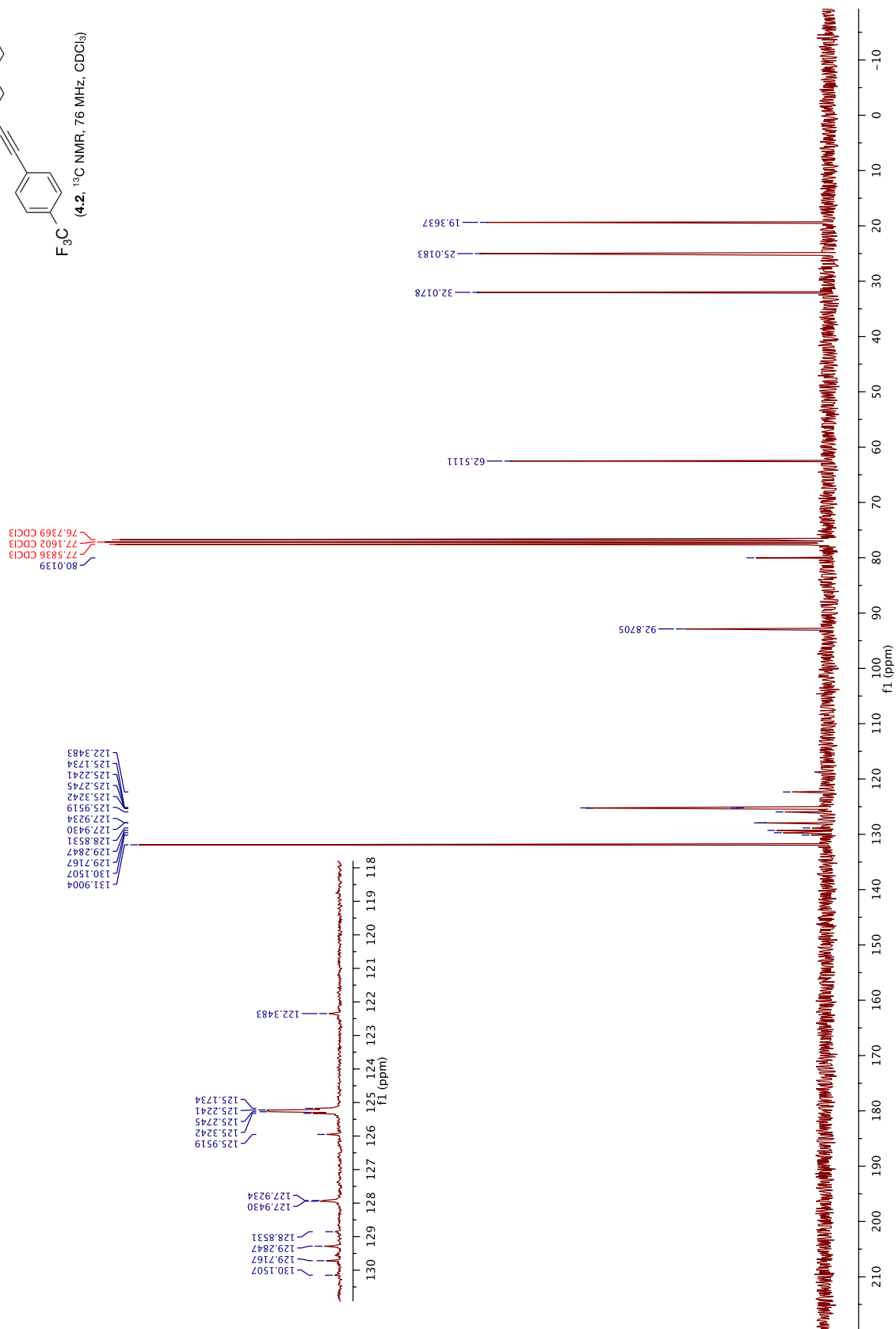
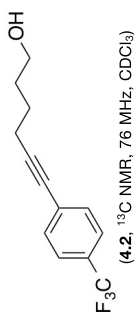
(1.12, ¹³C NMR, 101 MHz, CDCl₃)





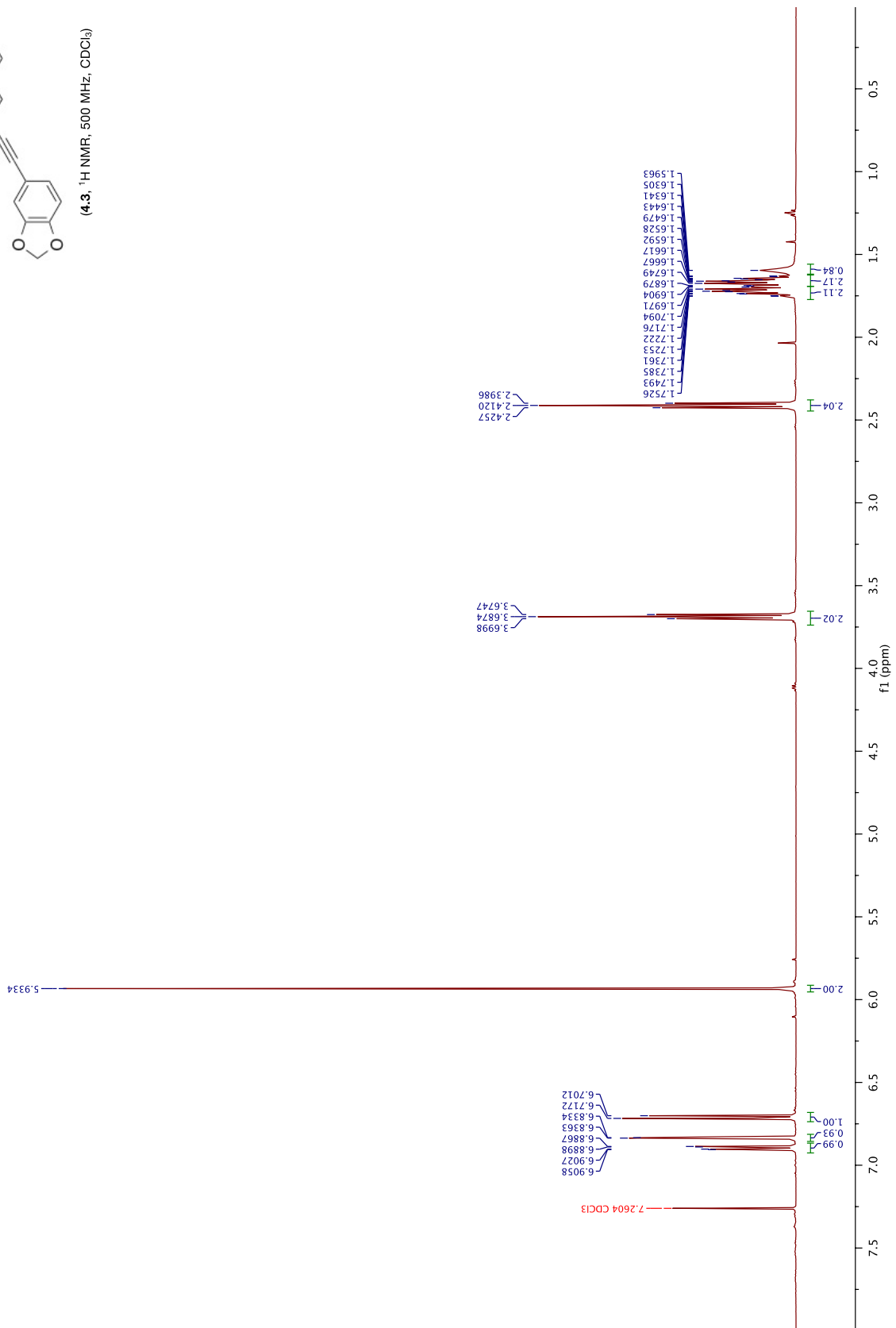






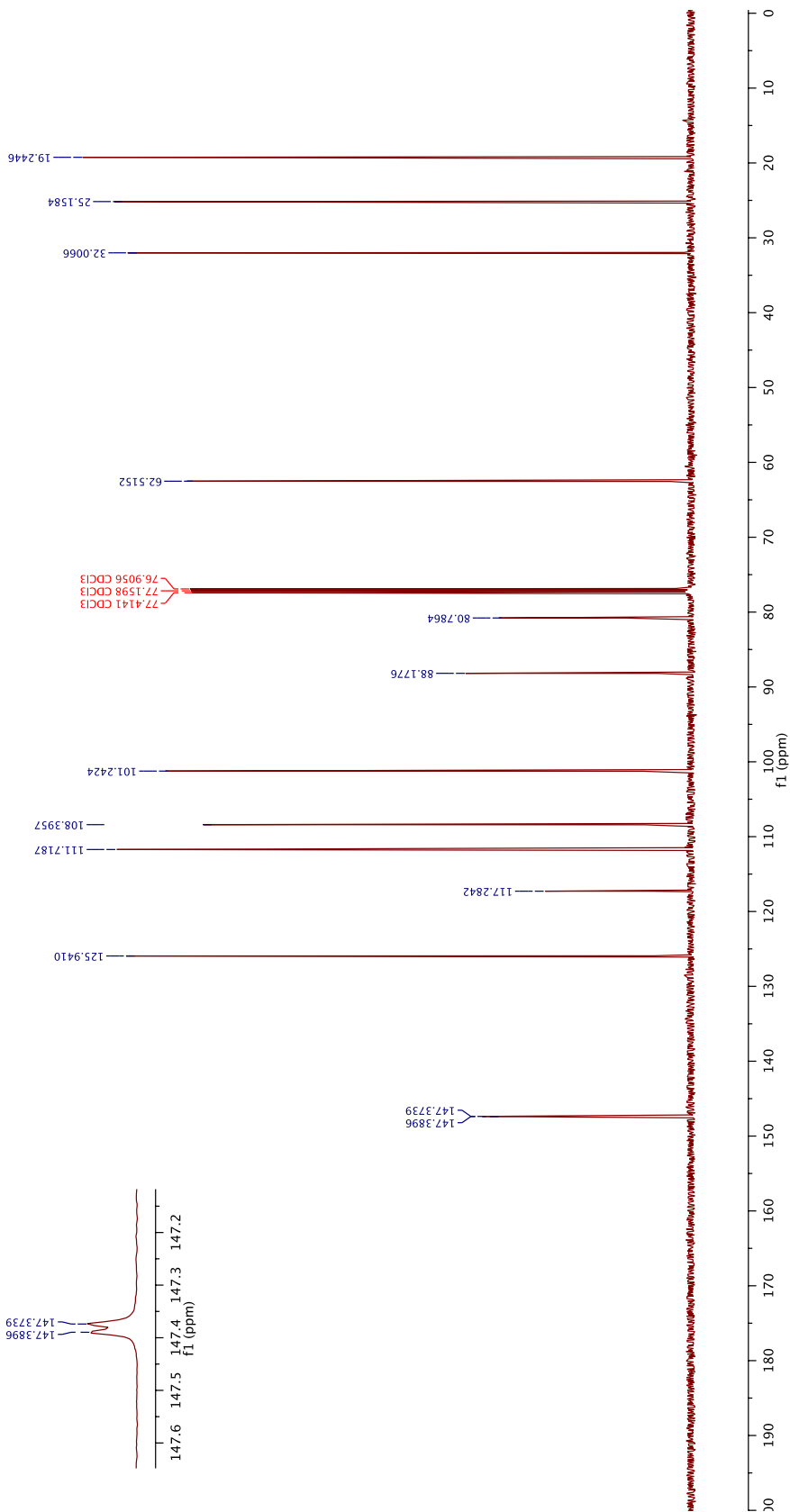


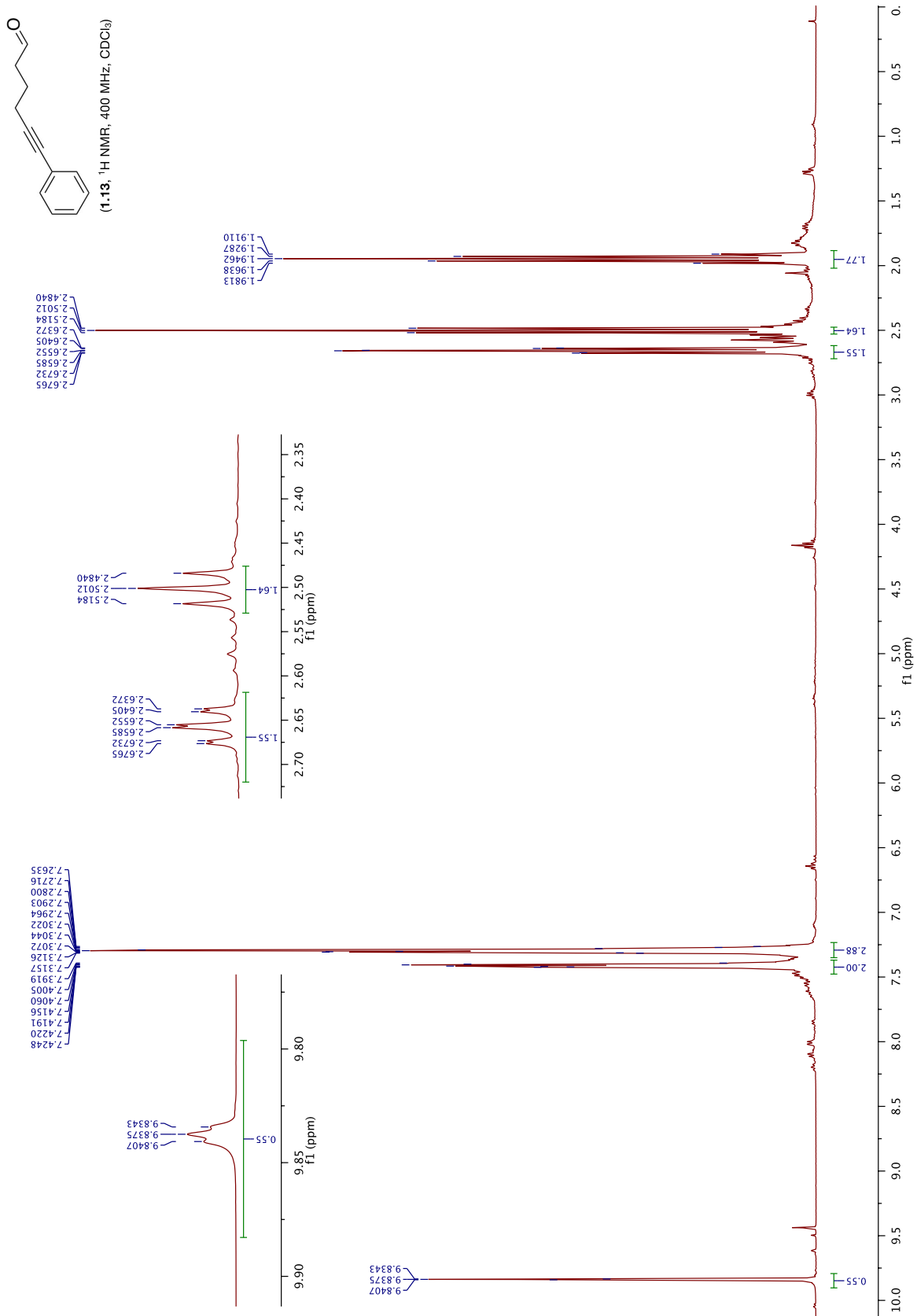
(4.3. ¹H NMR, 500 MHz, CDCl₃)

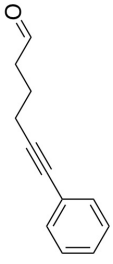




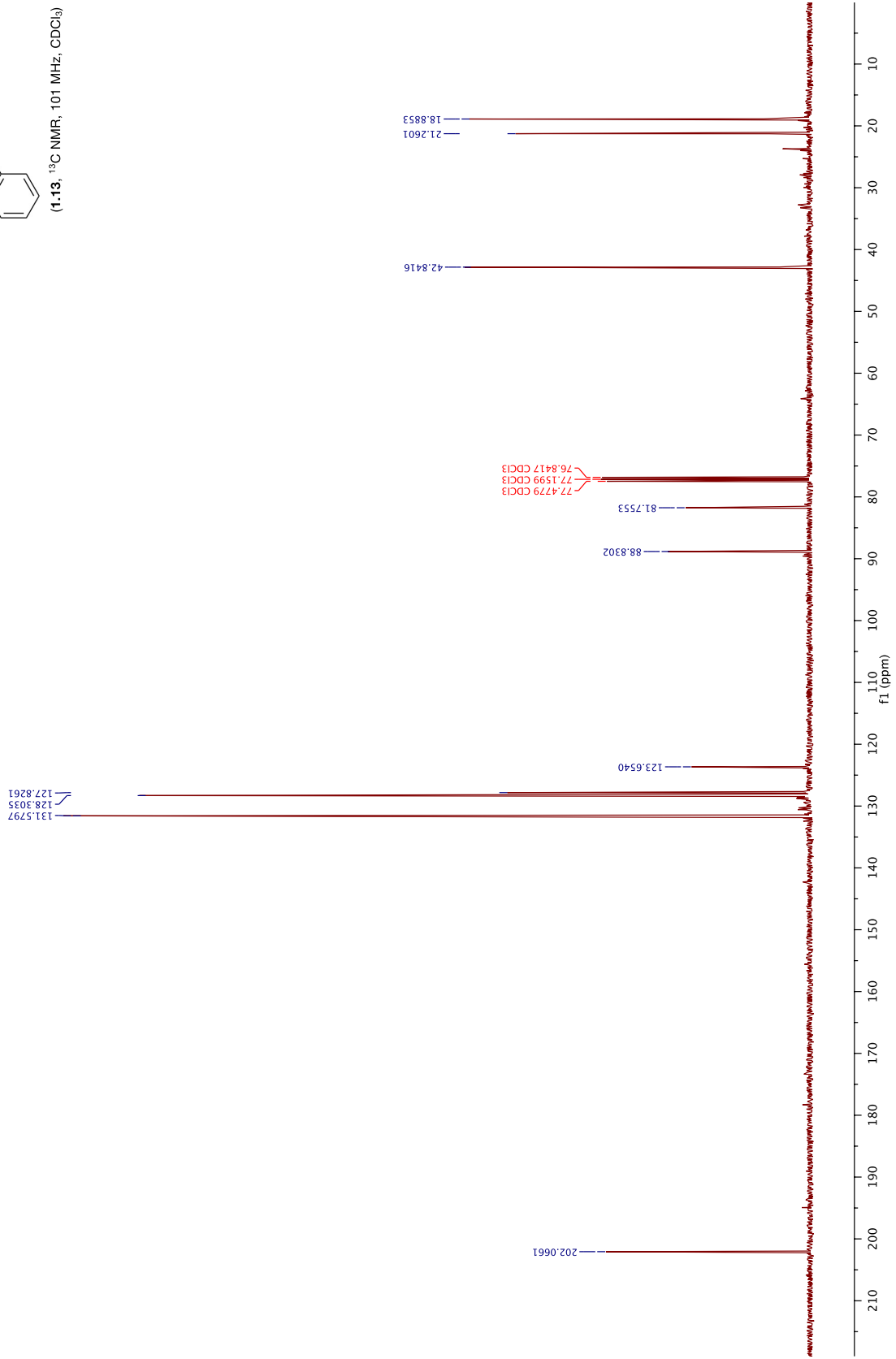
(4.3, ^{13}C NMR, 126 MHz, CDCl_3)

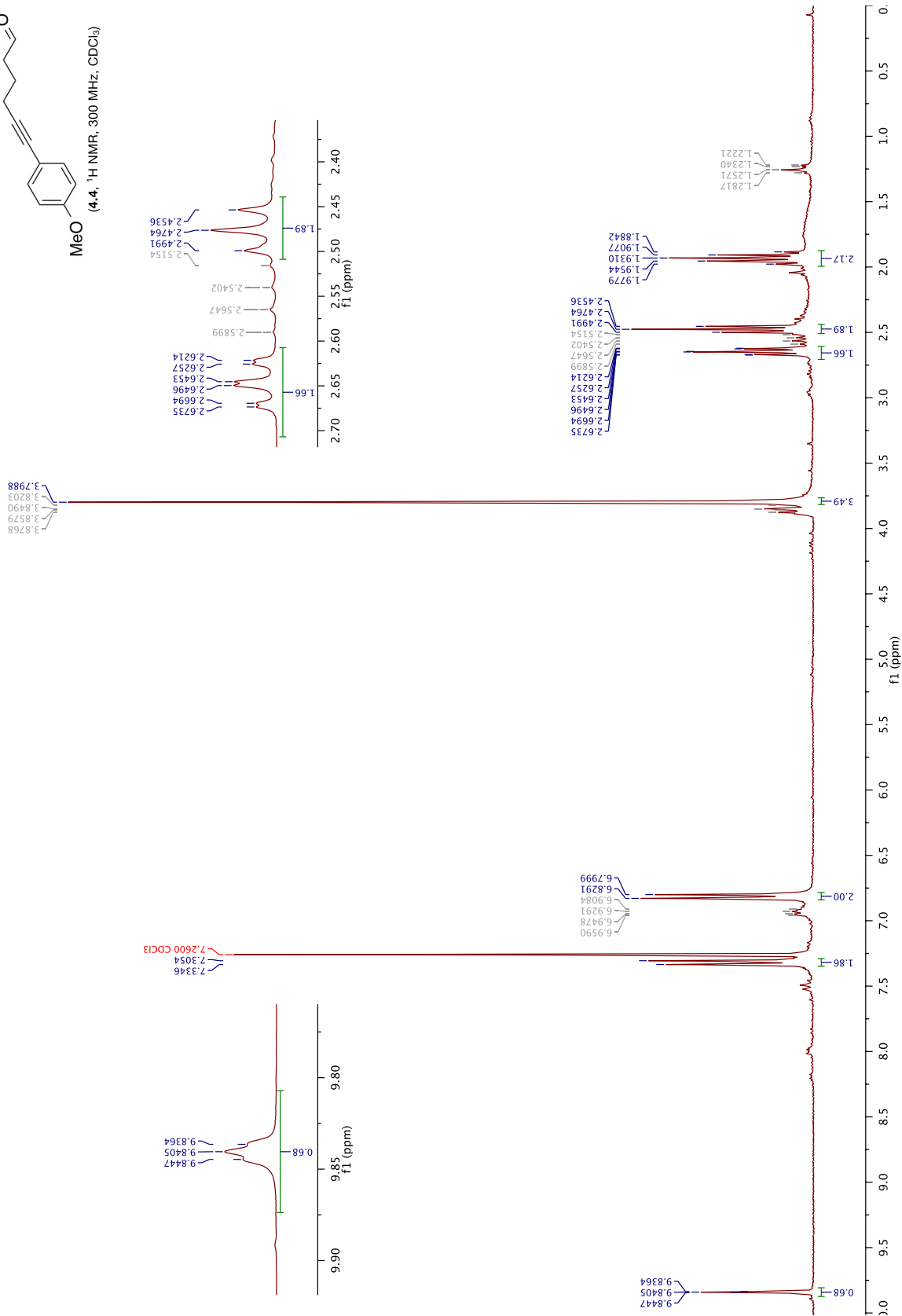
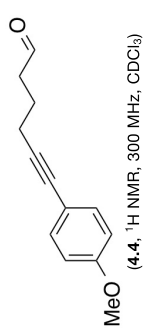


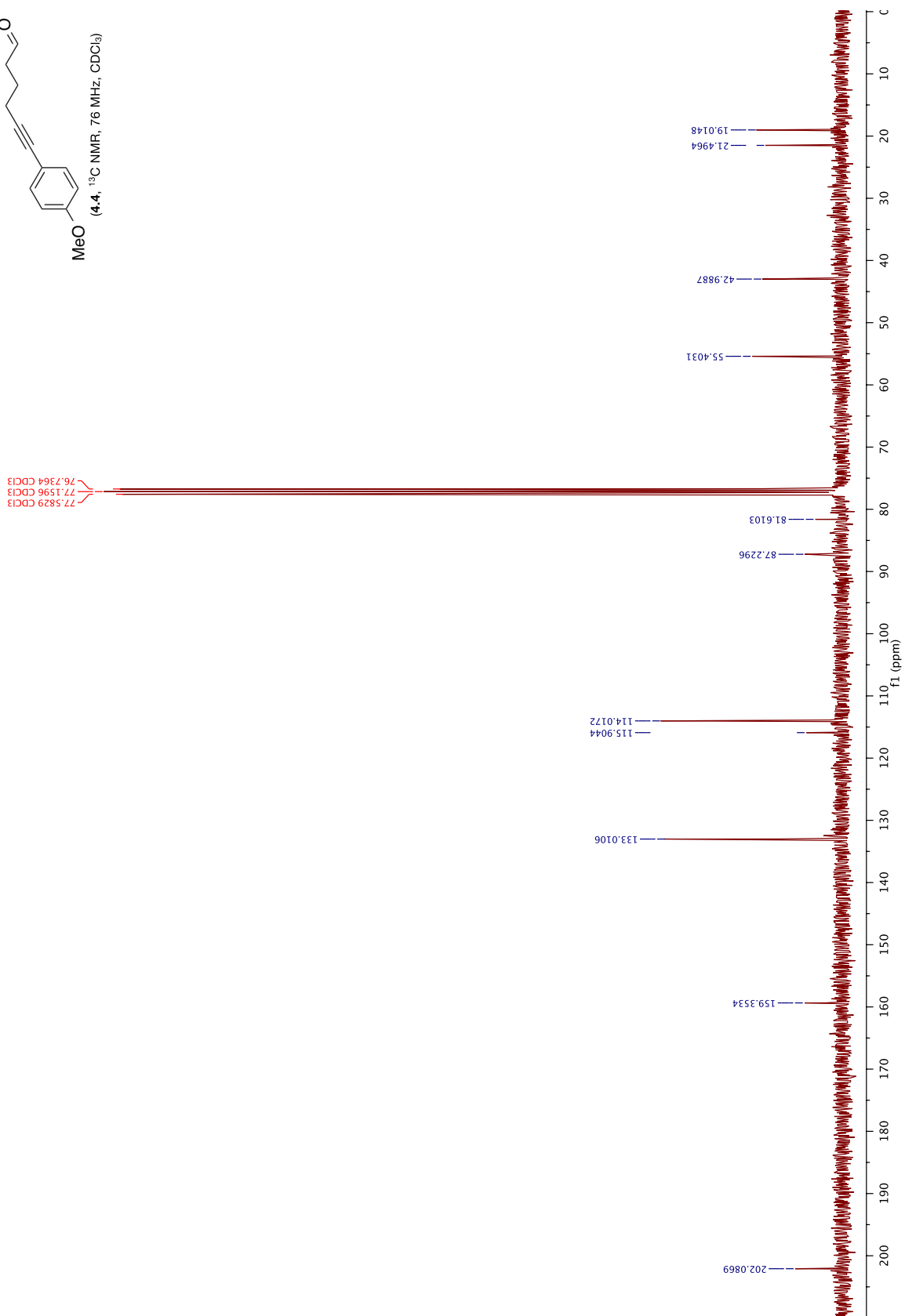
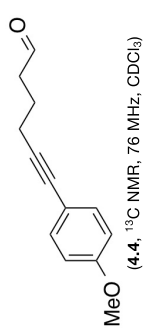


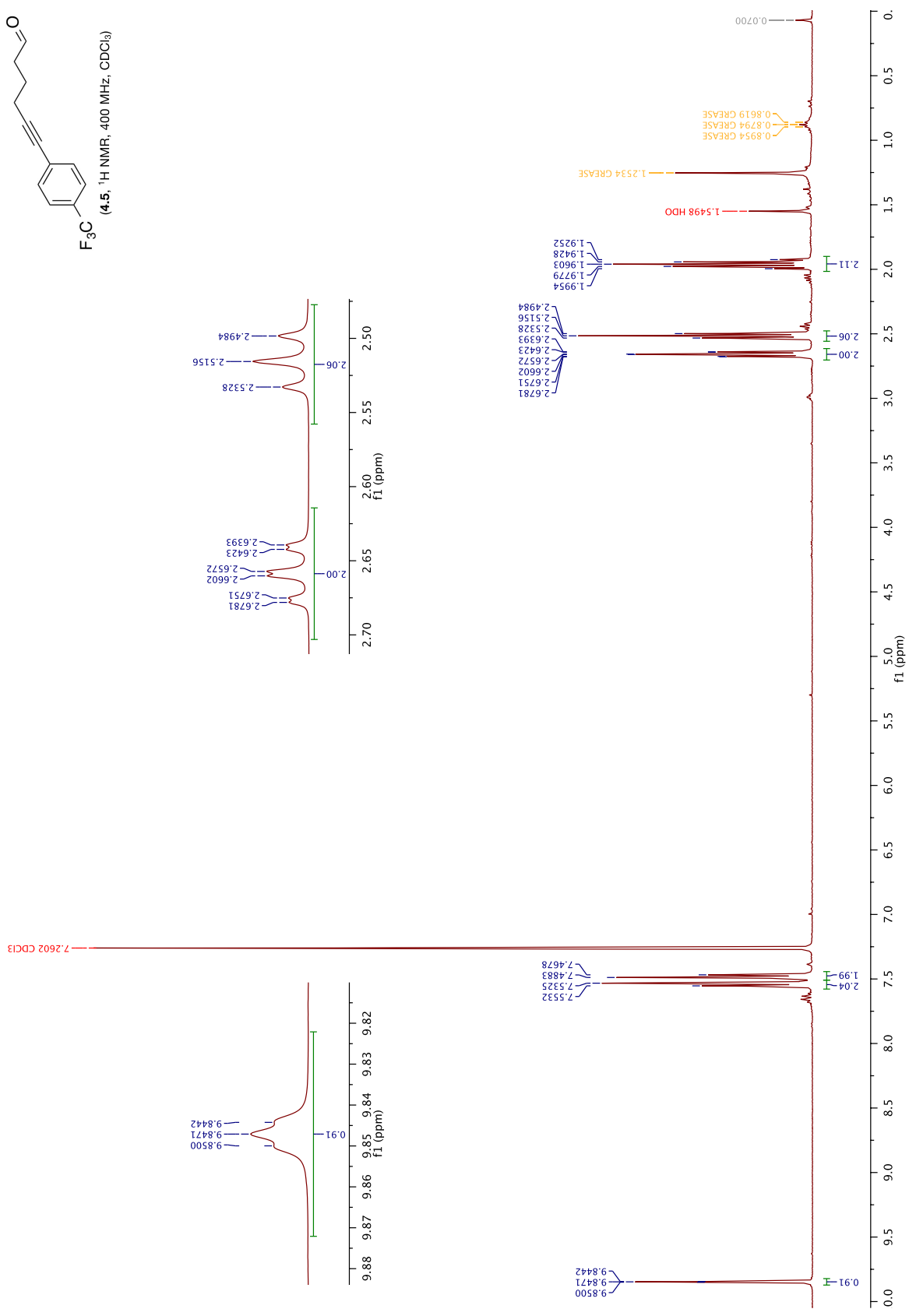
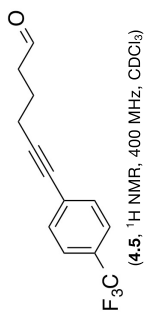


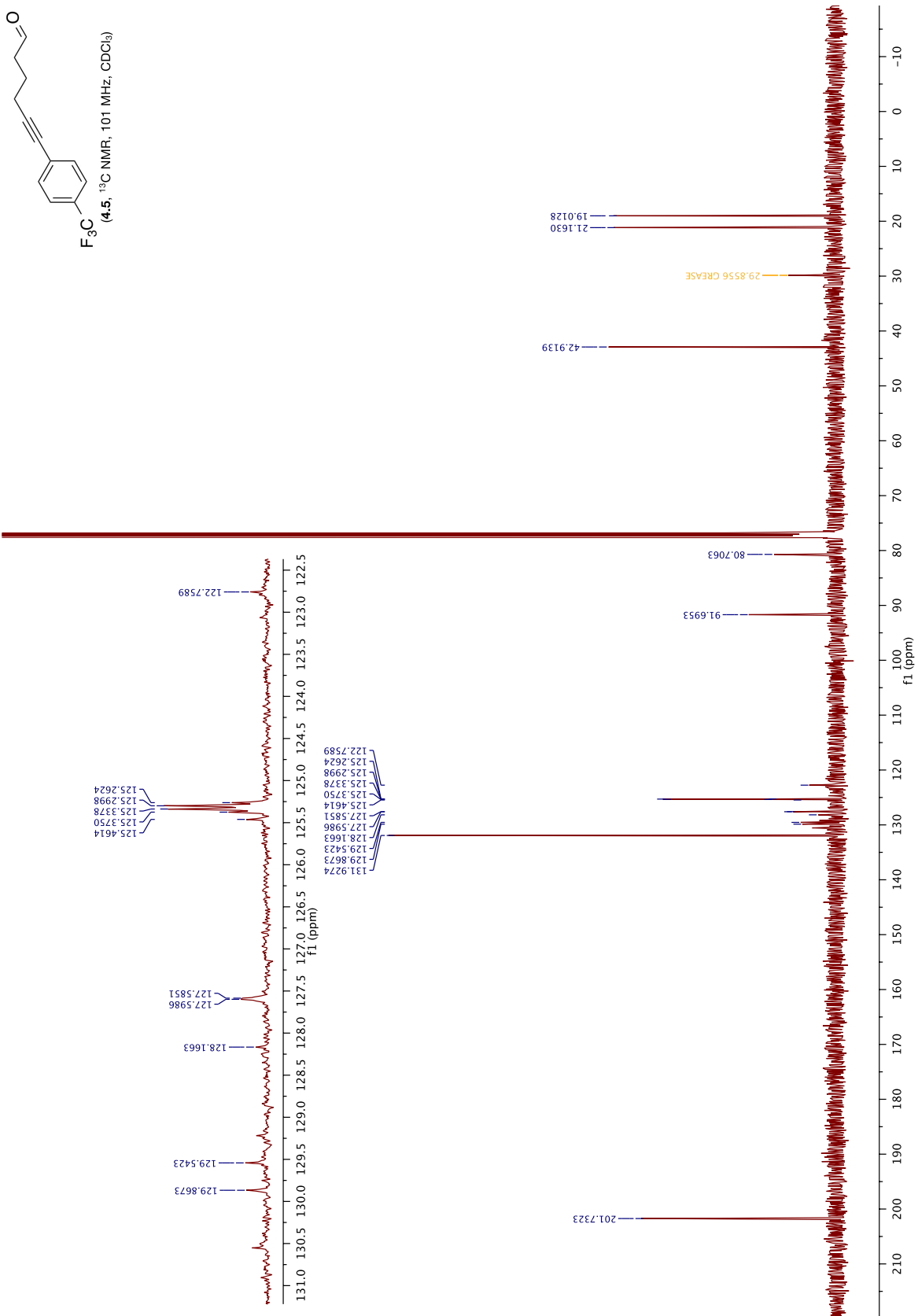
(1-13, ^{13}C NMR, 101 MHz, CDCl_3)

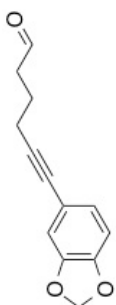




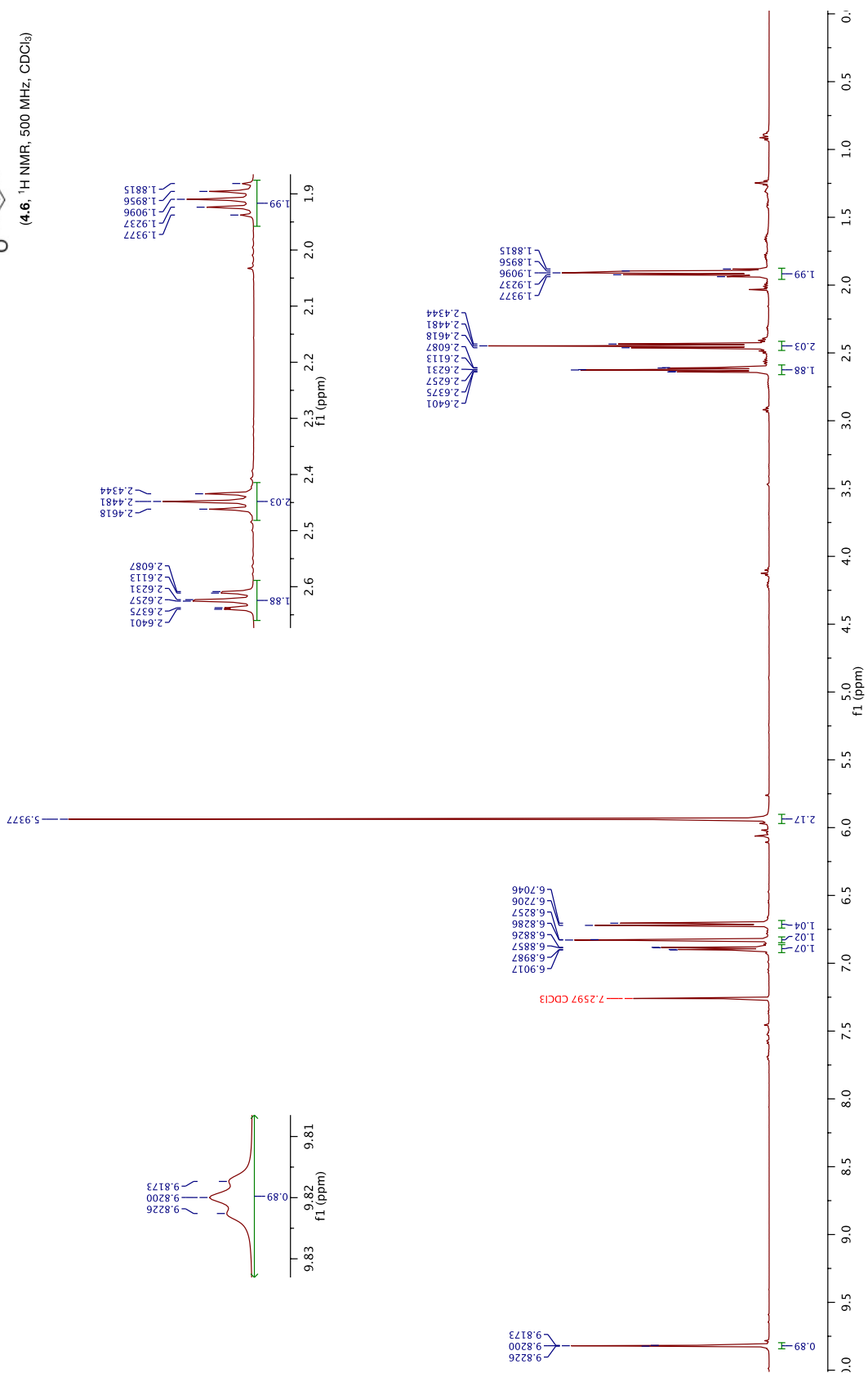


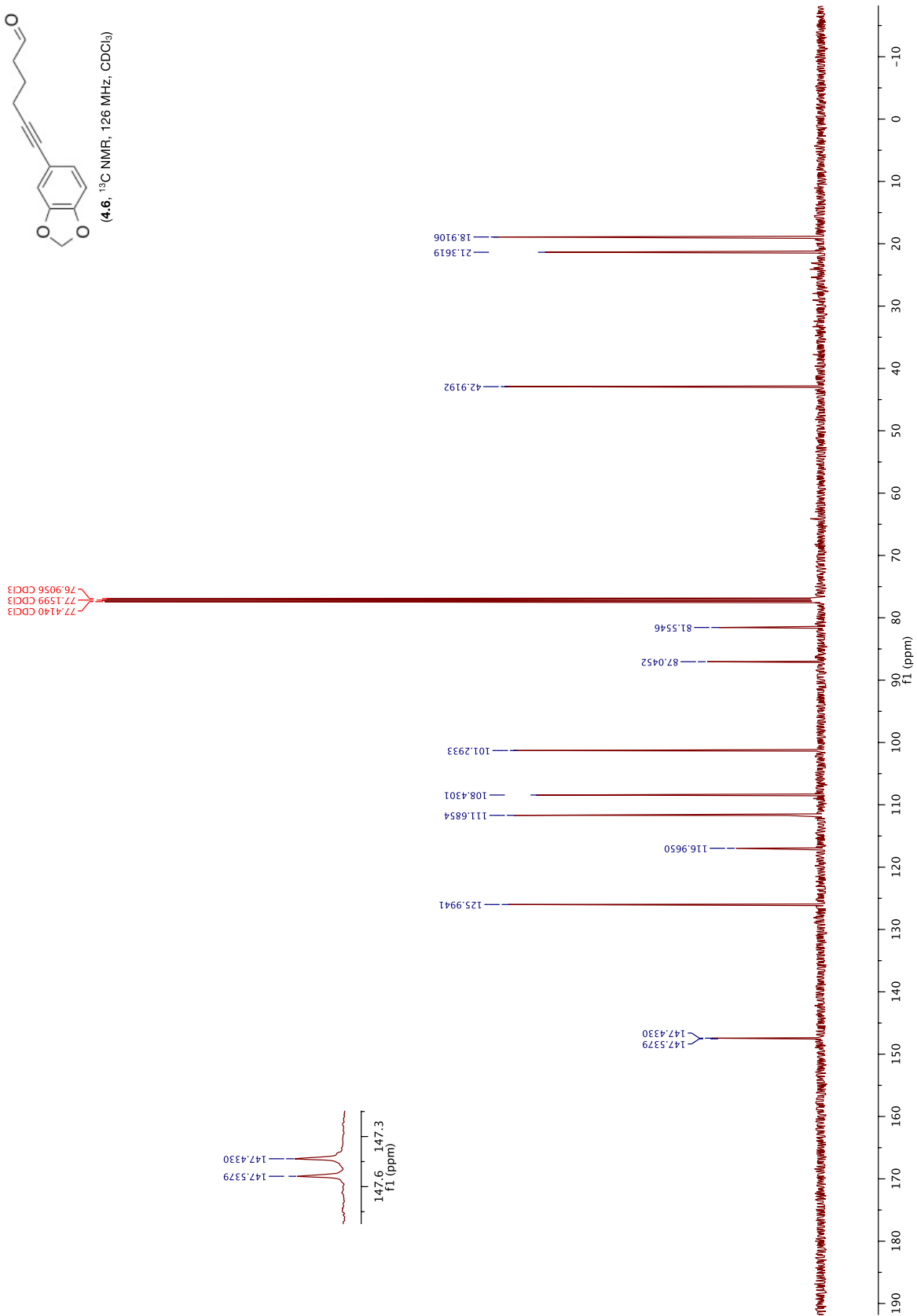
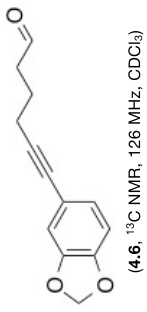






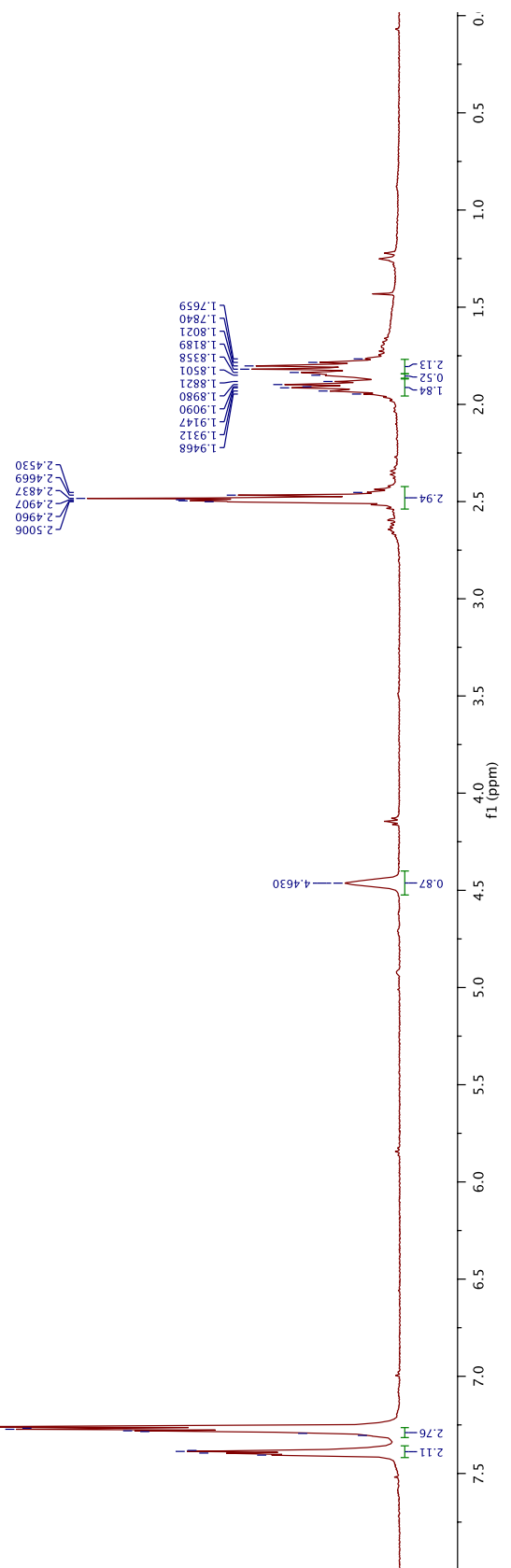
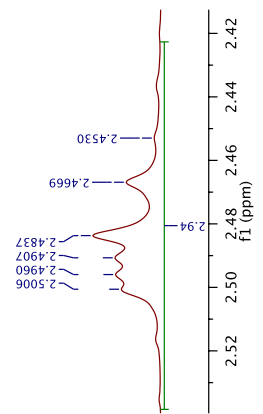
(4.6) ¹H NMR, 500 MHz, CDCl₃

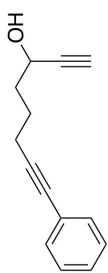




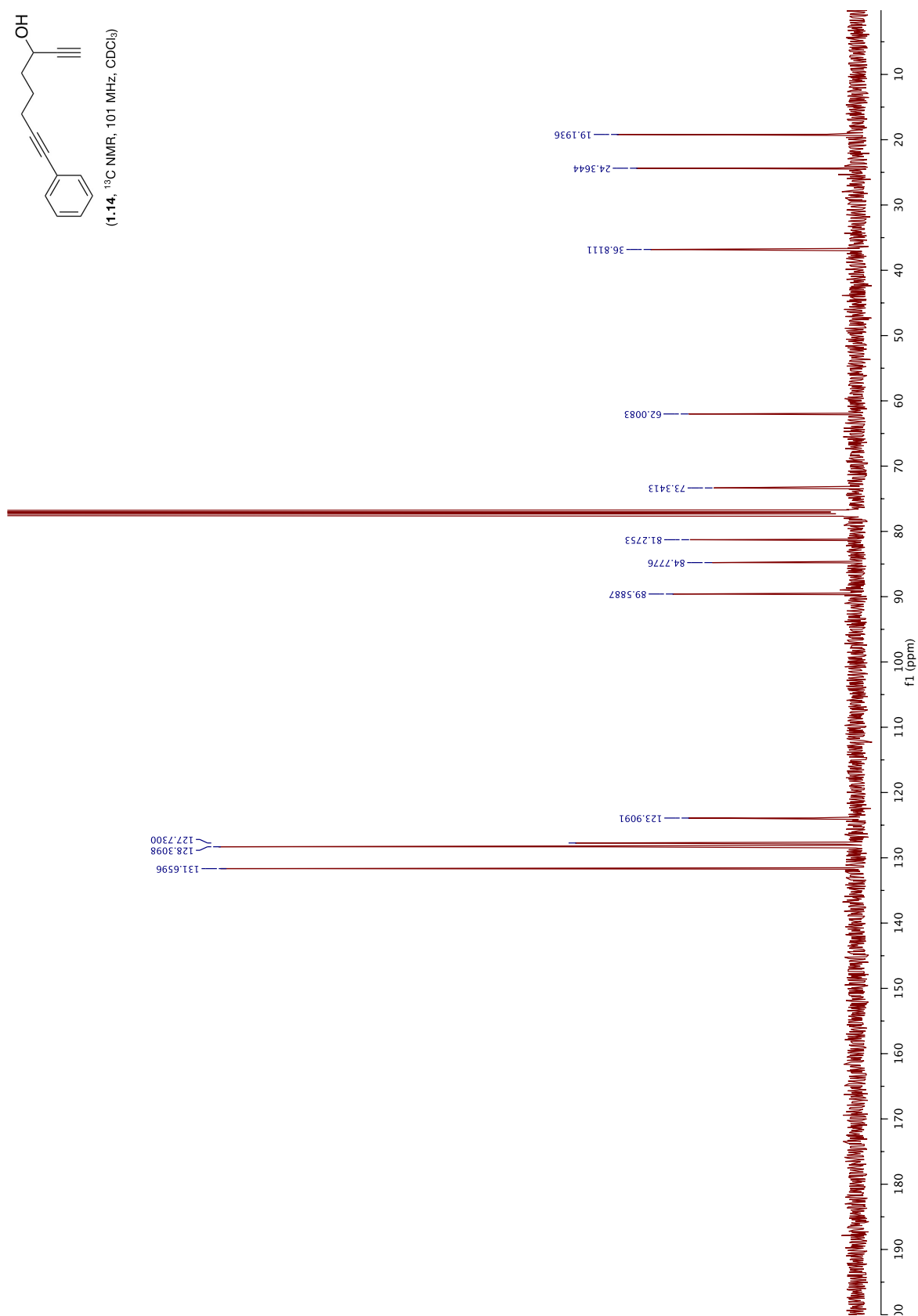


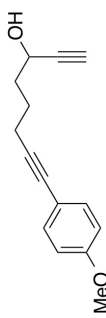
7.4054
 7.3949
 7.3865
 7.3814
 7.3042
 7.2937
 7.2843
 7.2803
 7.2726
 7.2672
 7.2596 CDCl₃



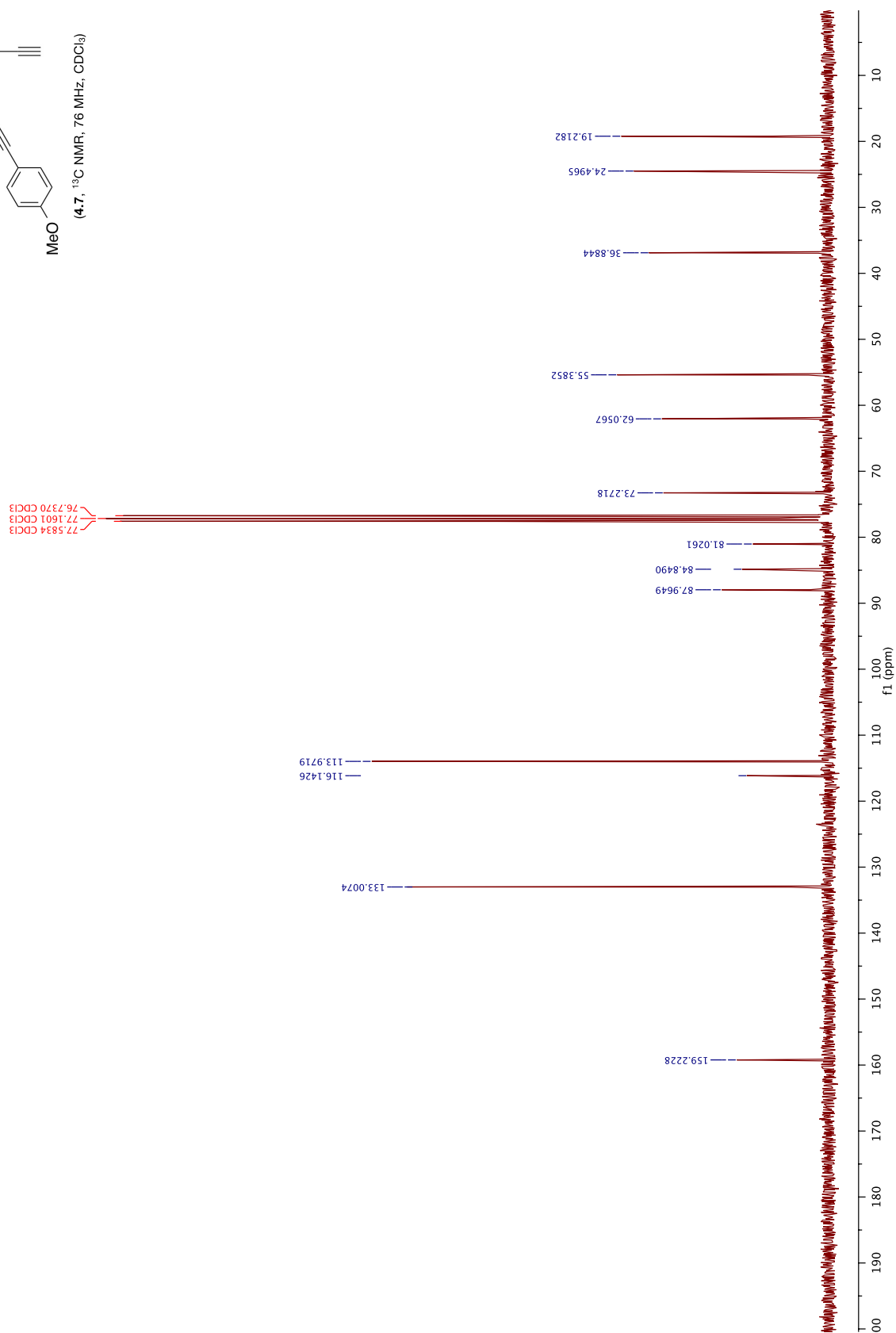


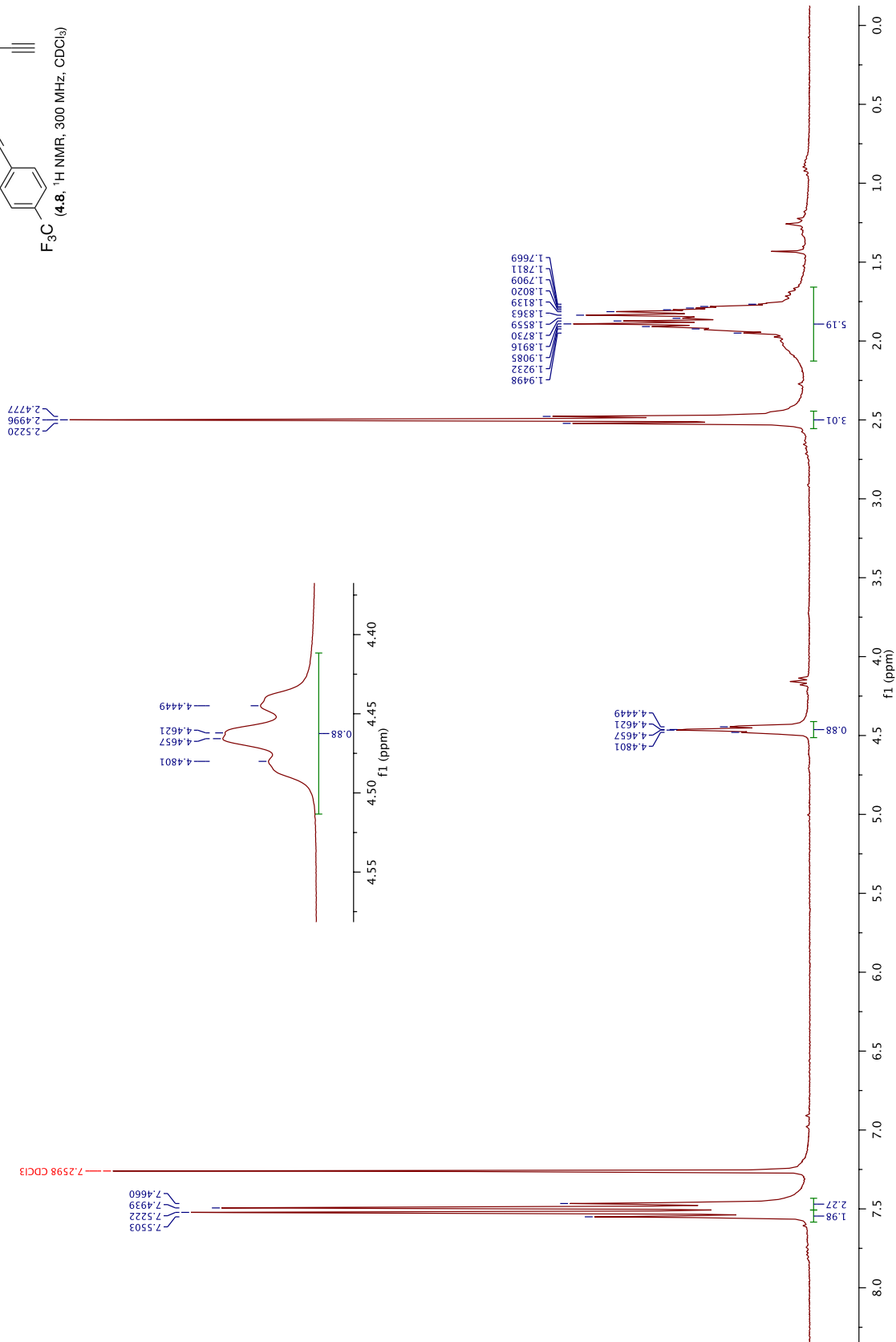
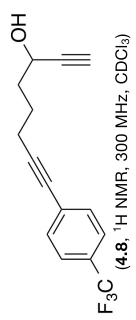
(1.14, ^{13}C NMR, 101 MHz, CDCl_3)

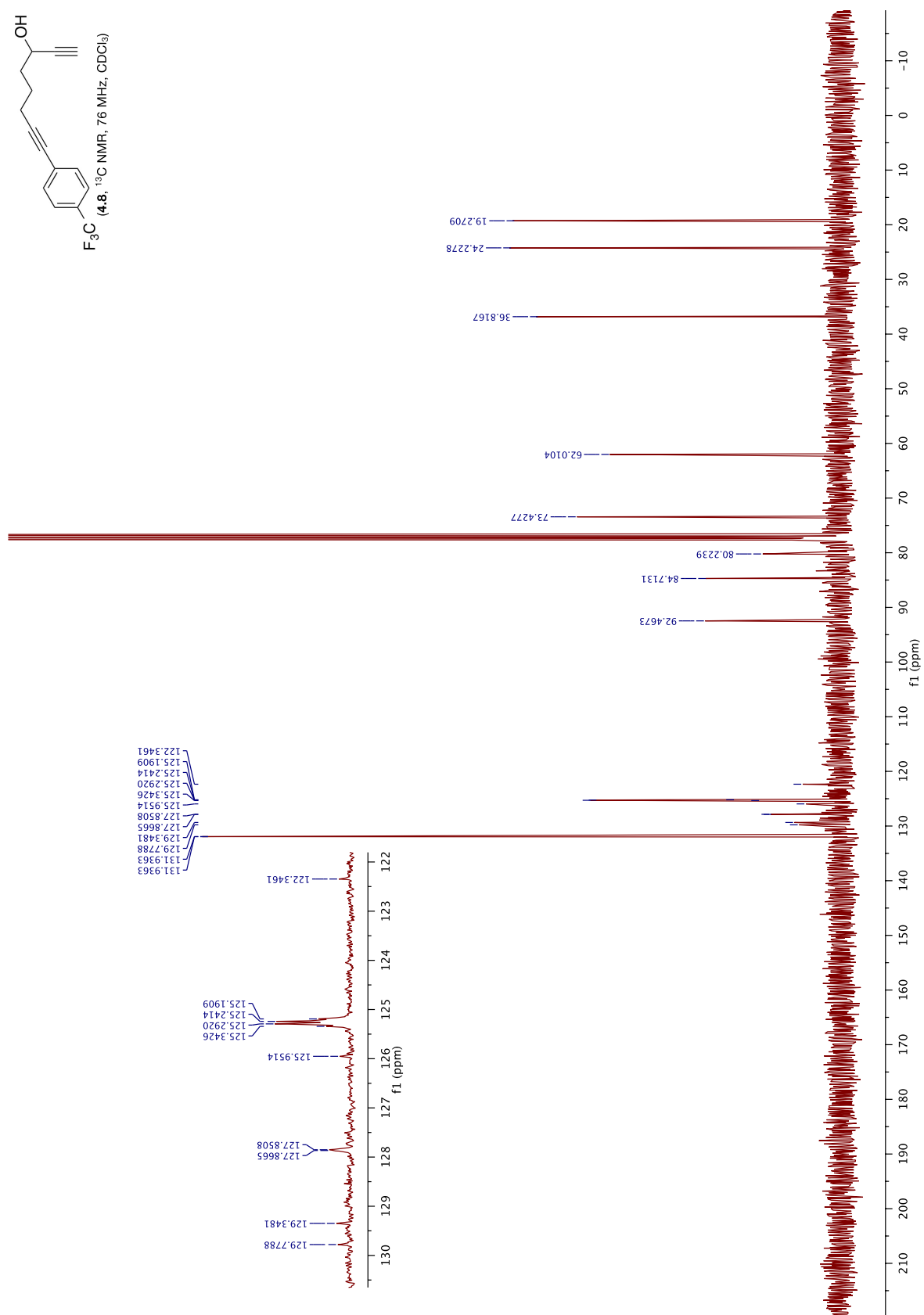
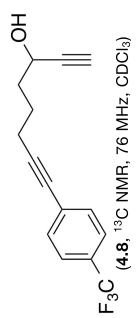


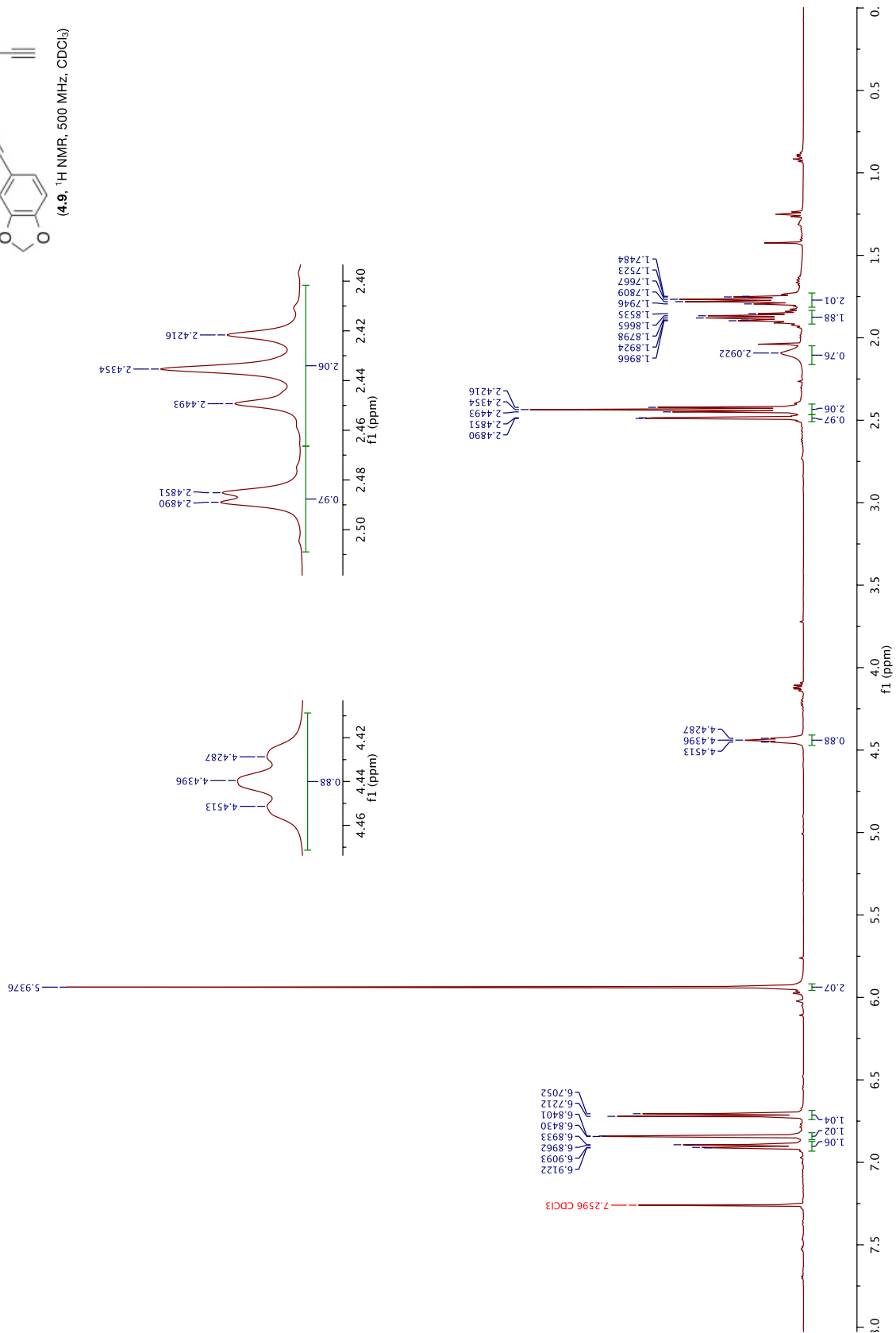
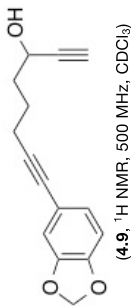


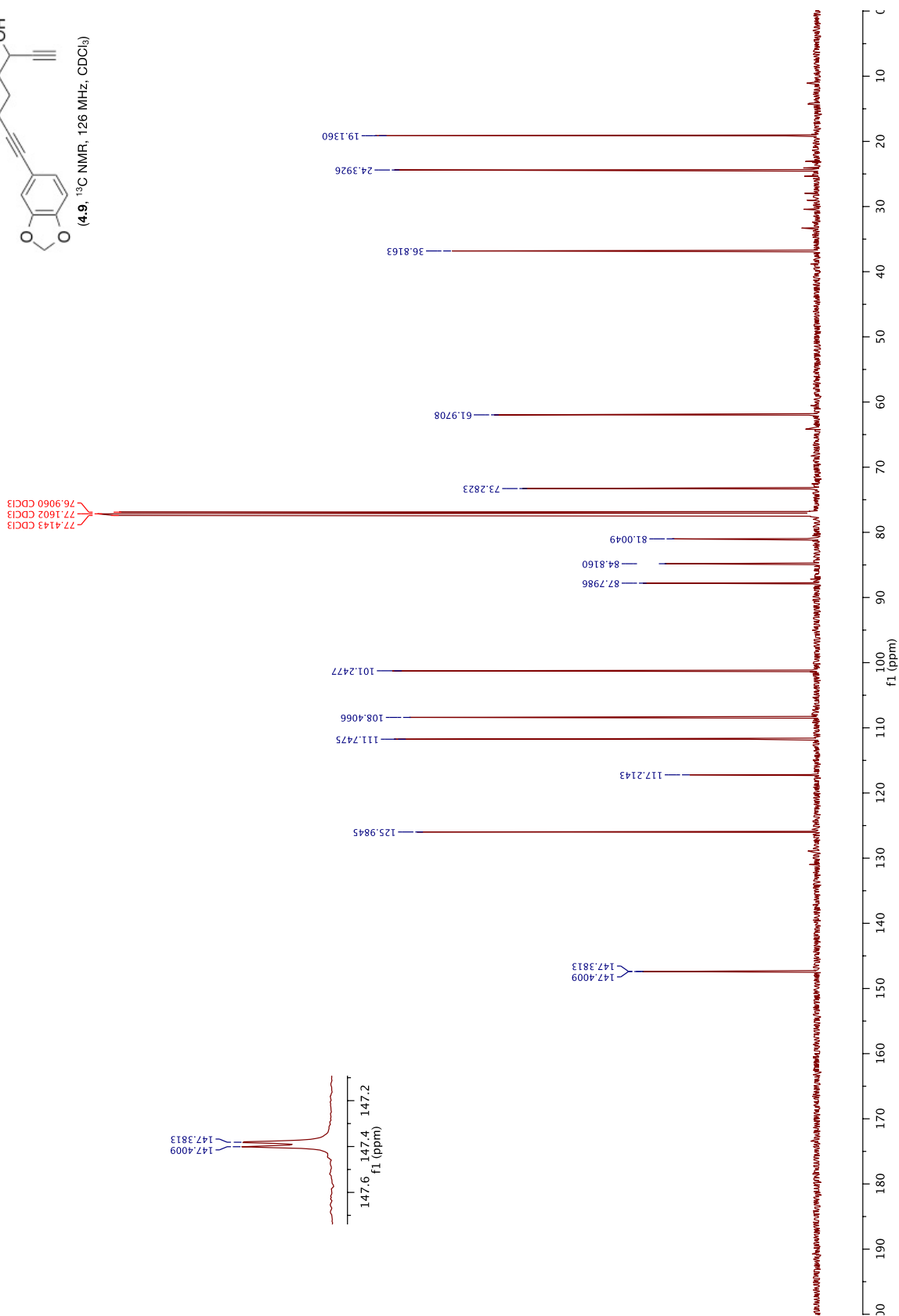
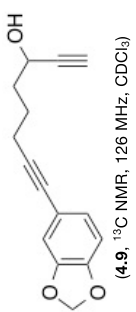
(4.7, ¹³C NMR, 76 MHz, CDCl₃)

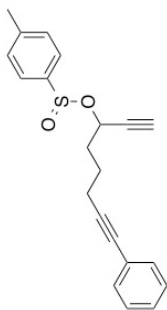




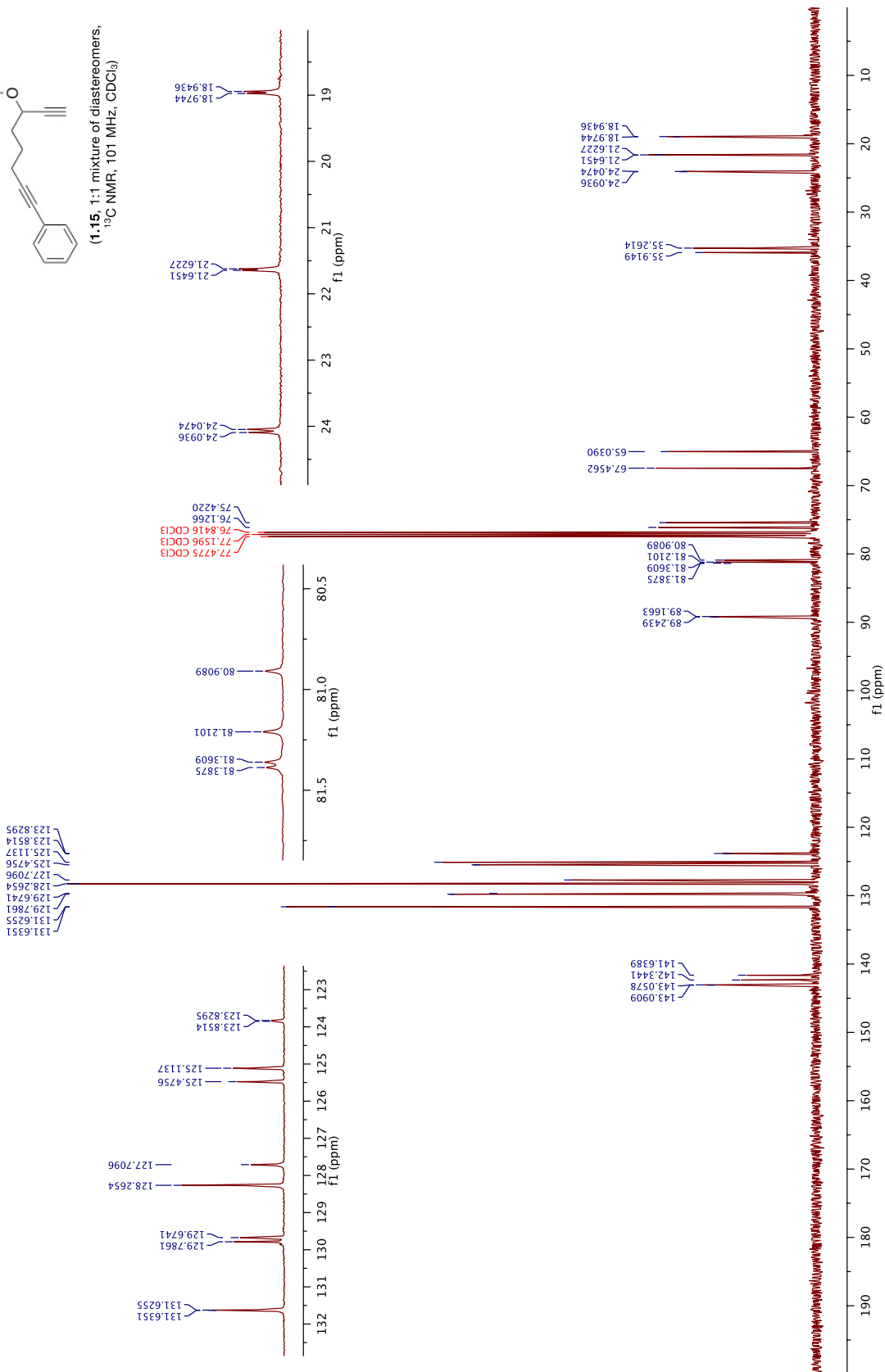


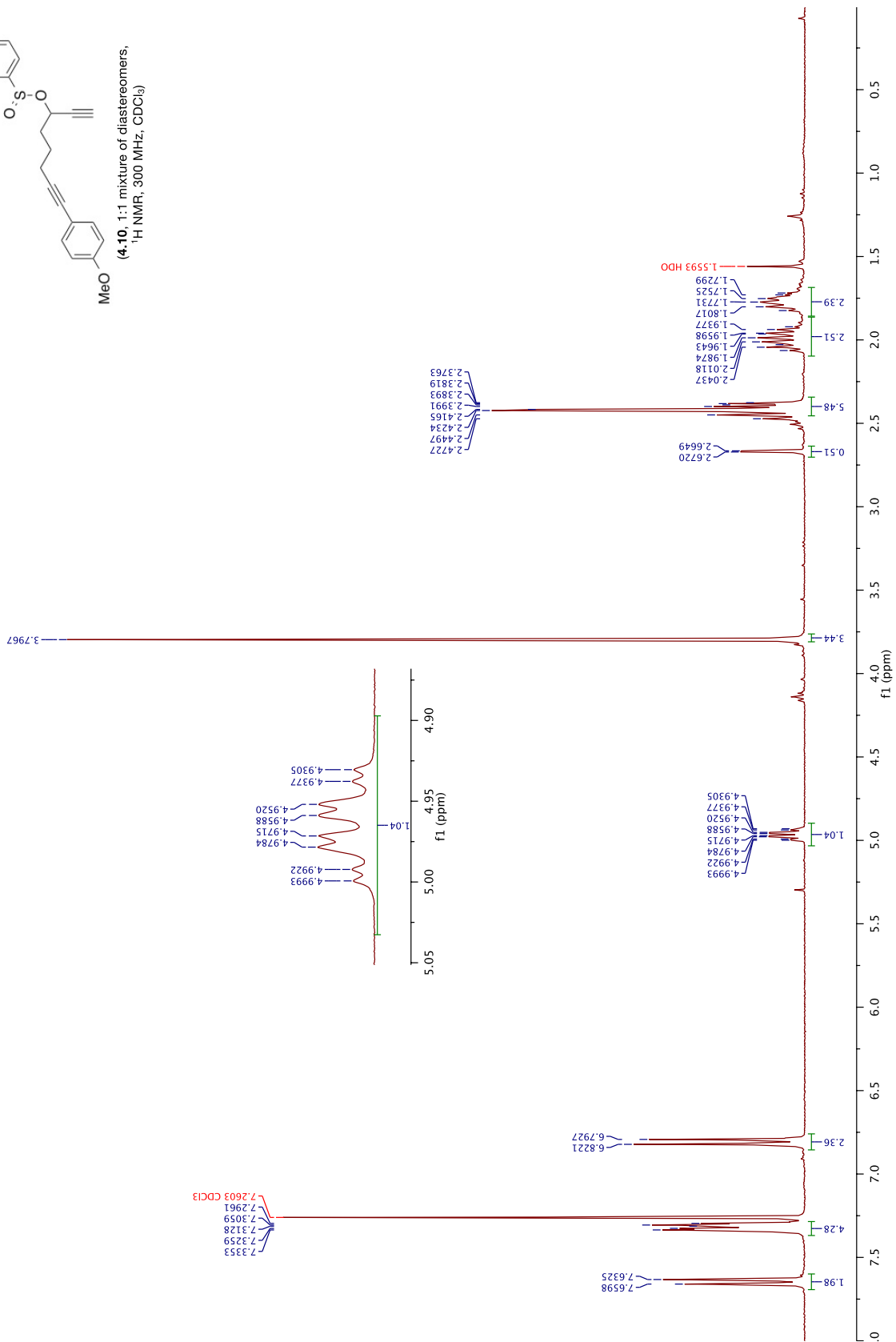
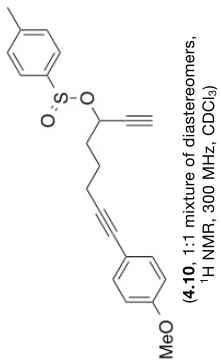


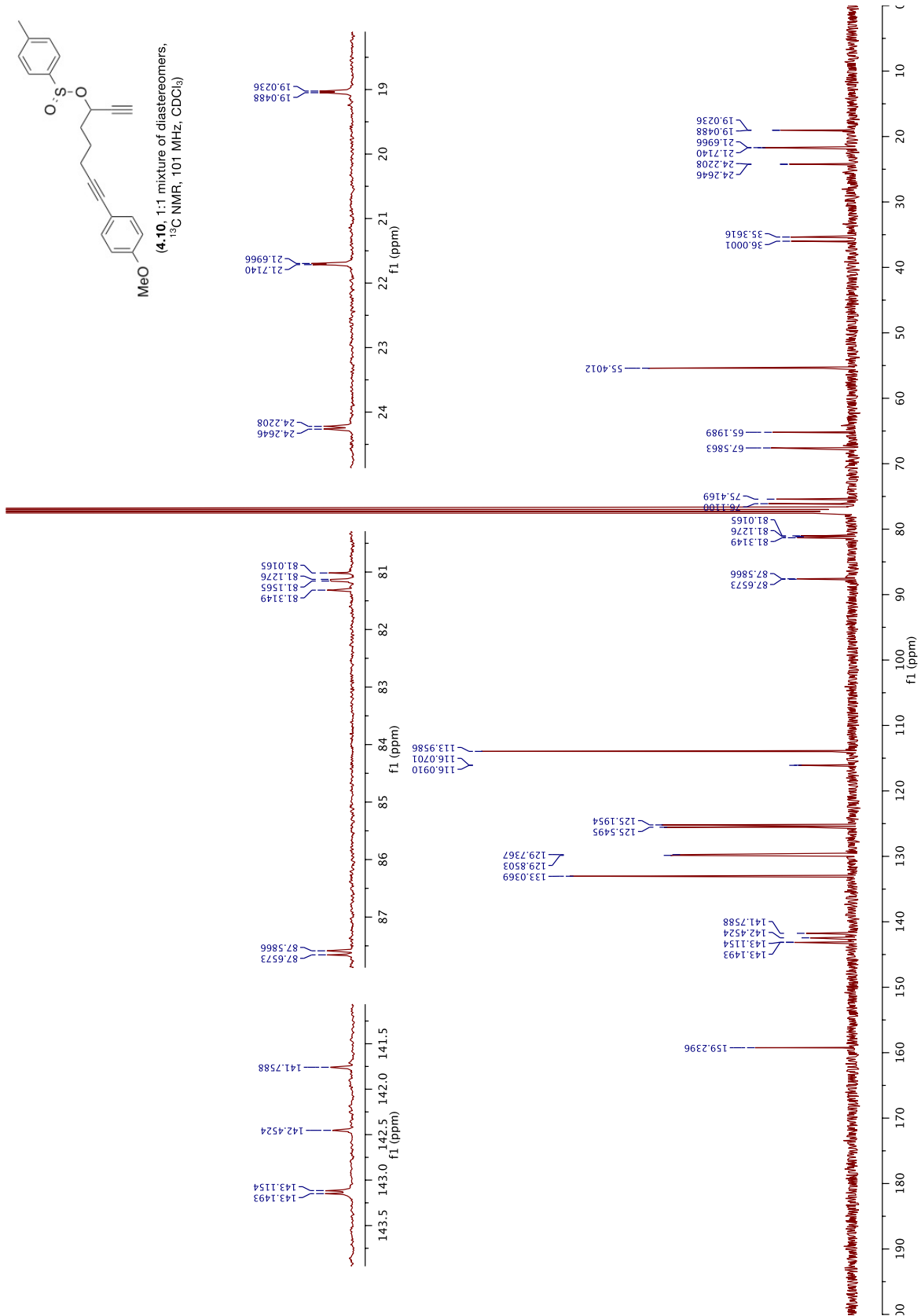


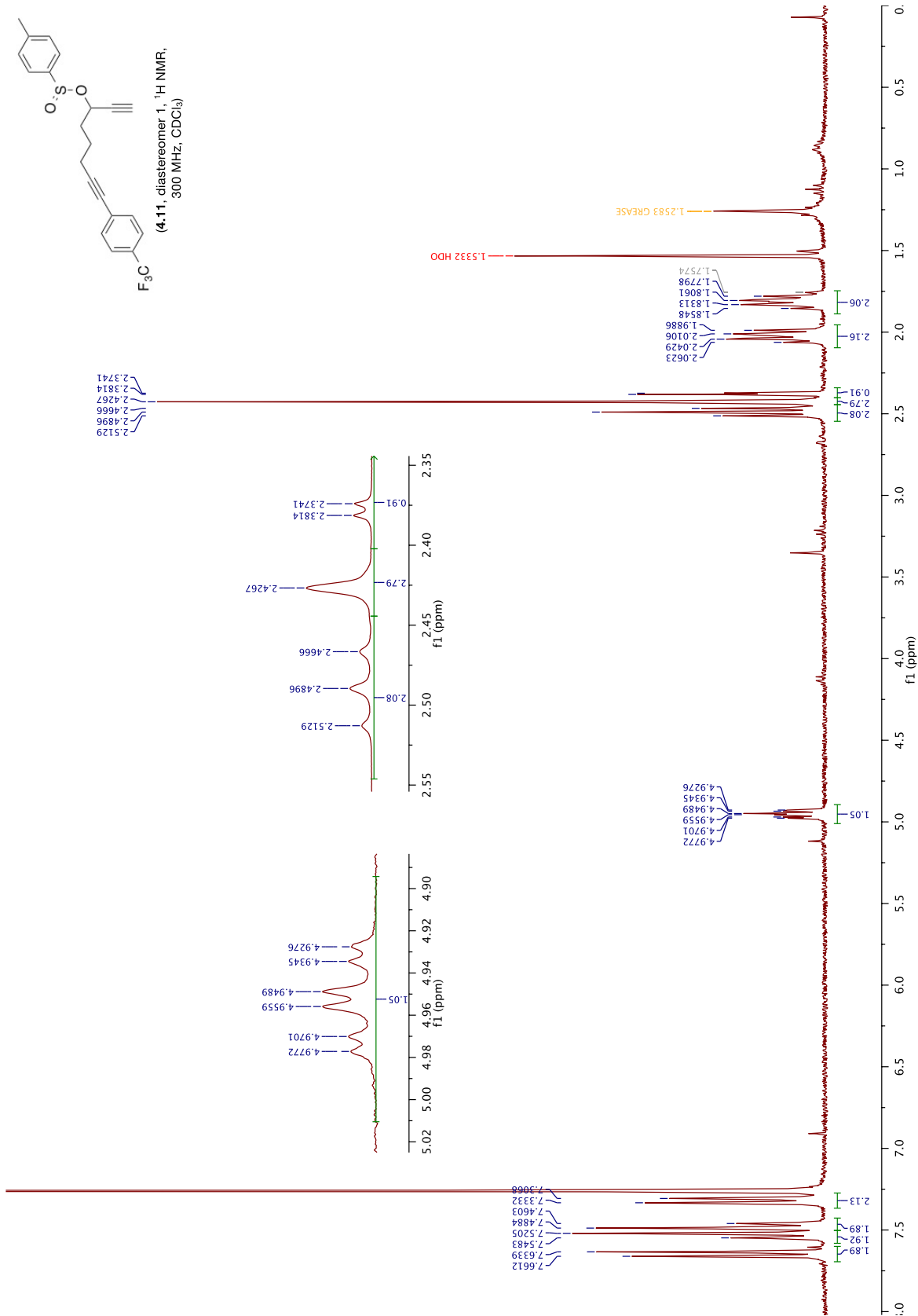


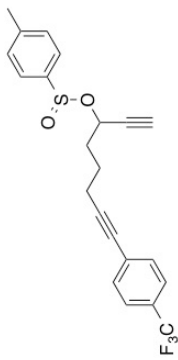
(1-15, 1:1 mixture of diastereomers, ^{13}C NMR, 101 MHz, CDCl_3)



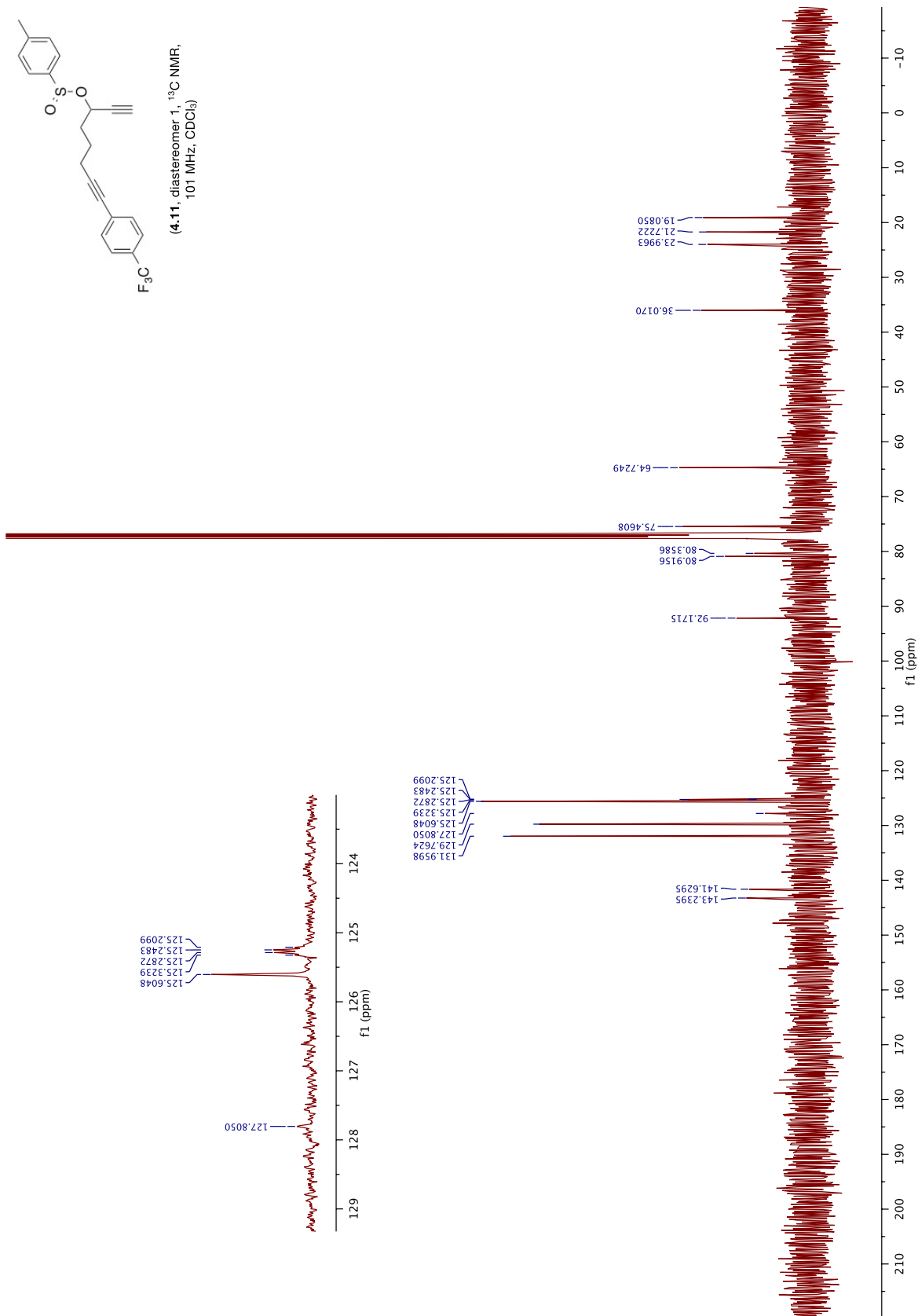


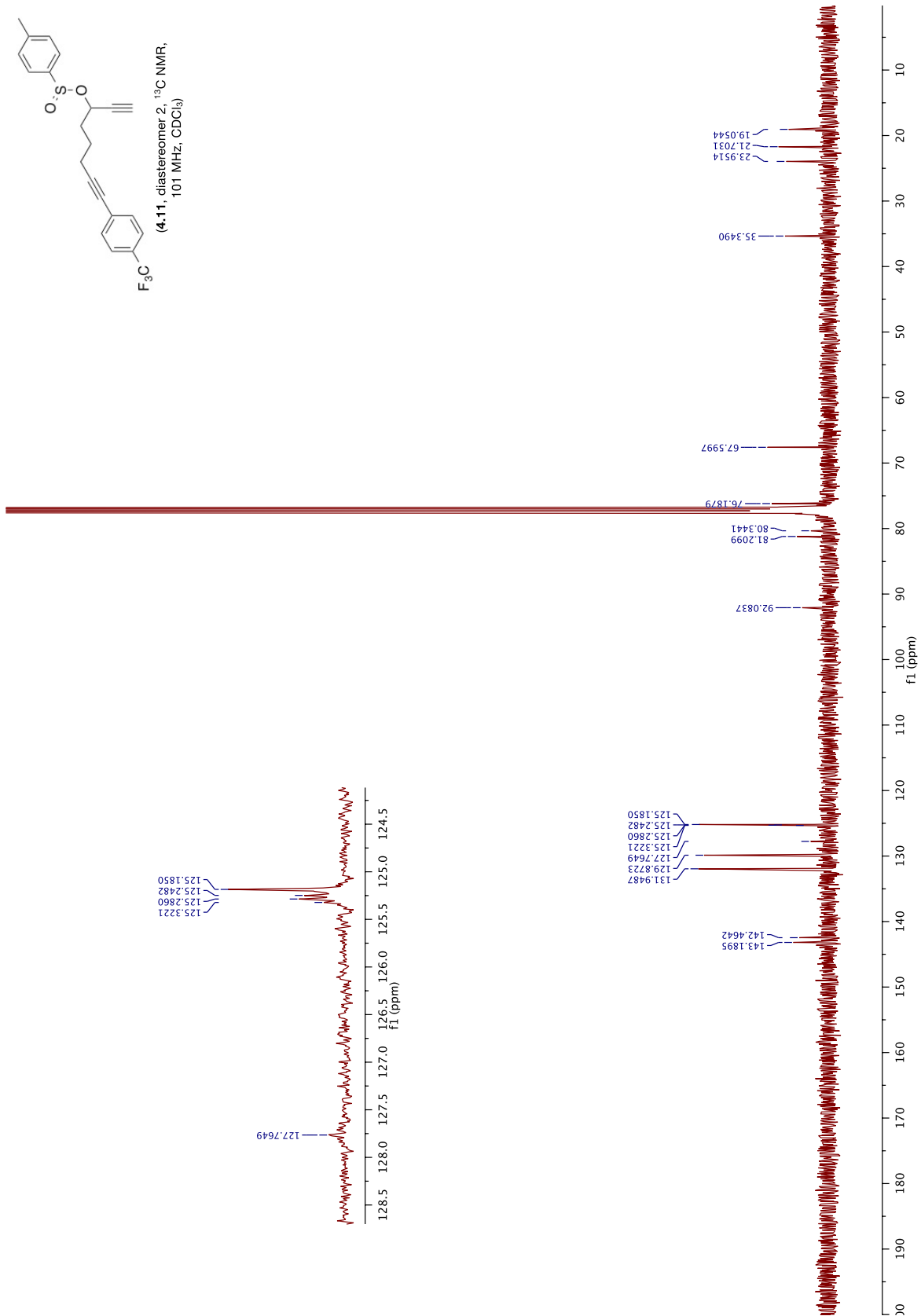


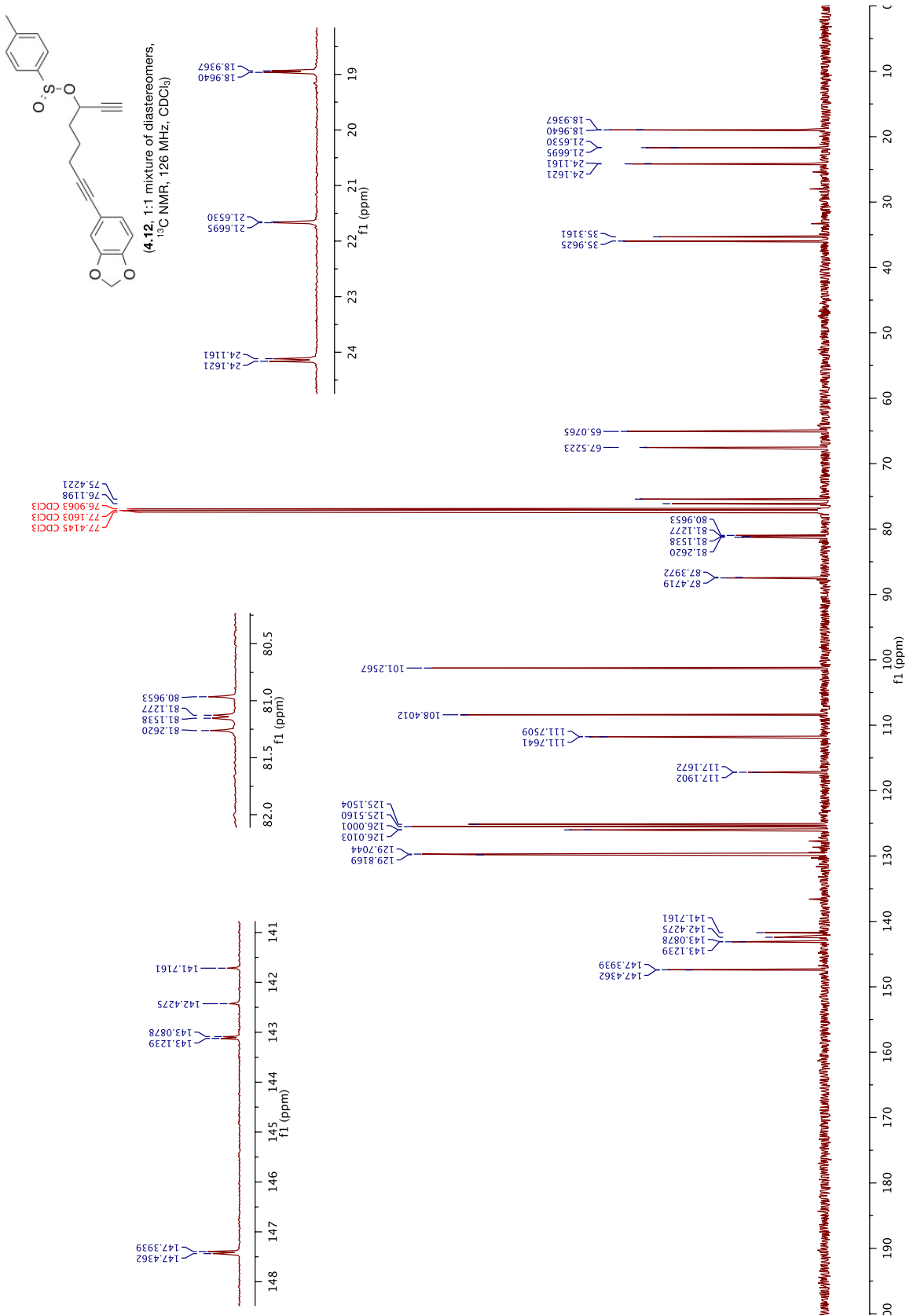


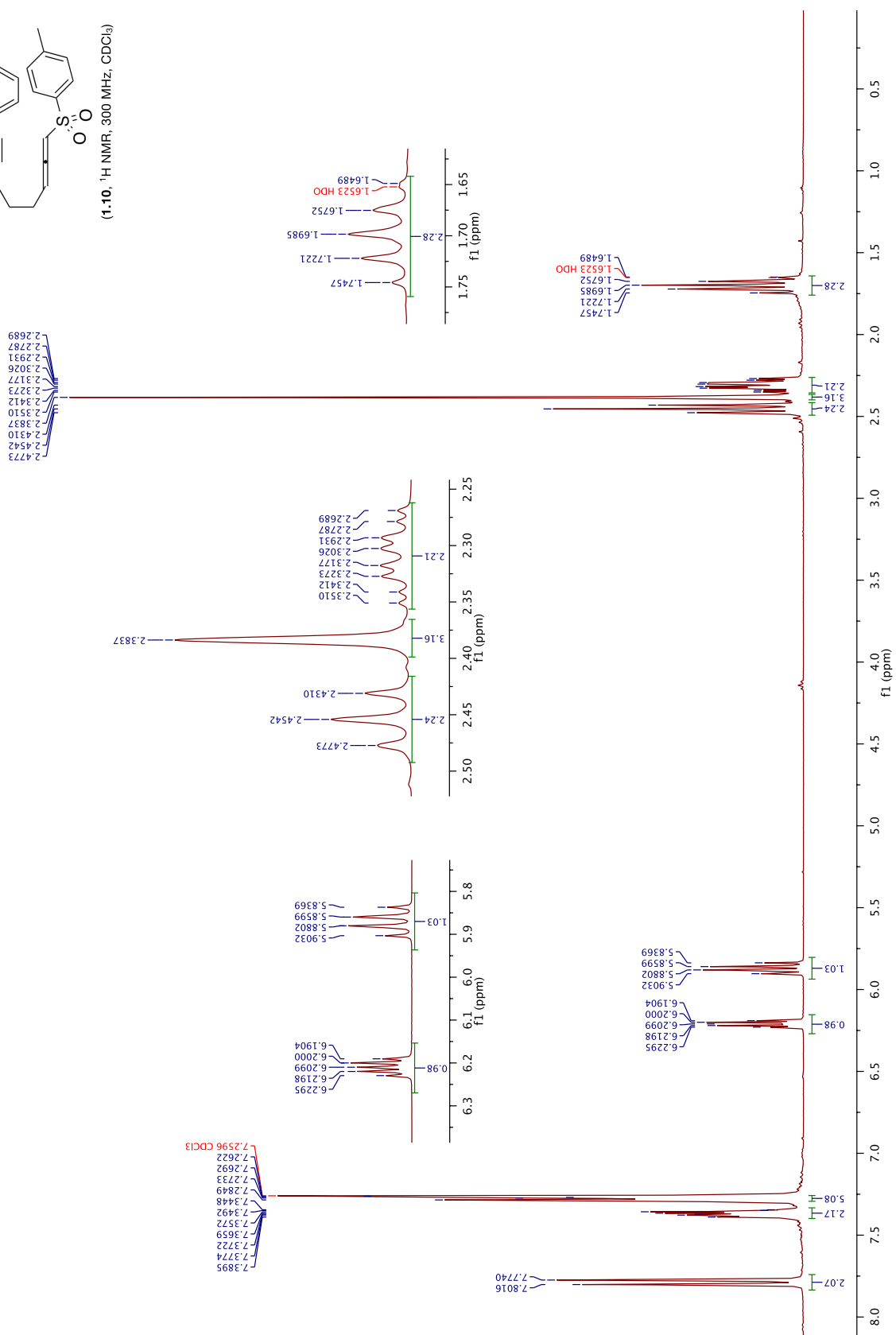
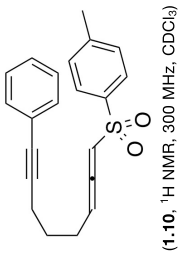


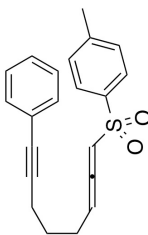
(4.11, diastereomer 1, ^{13}C NMR, 101 MHz, CDCl_3)



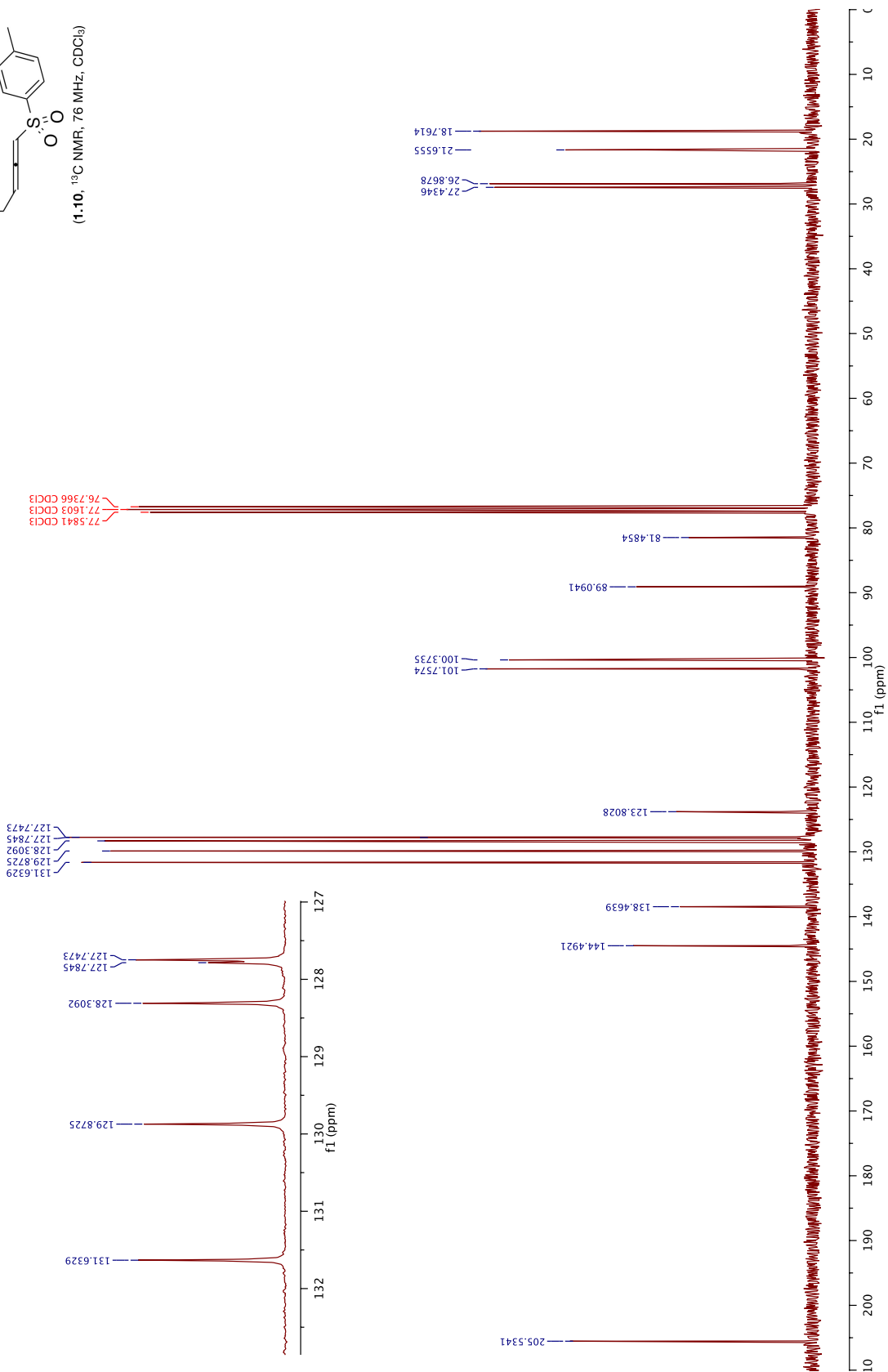


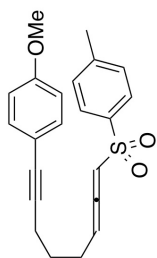




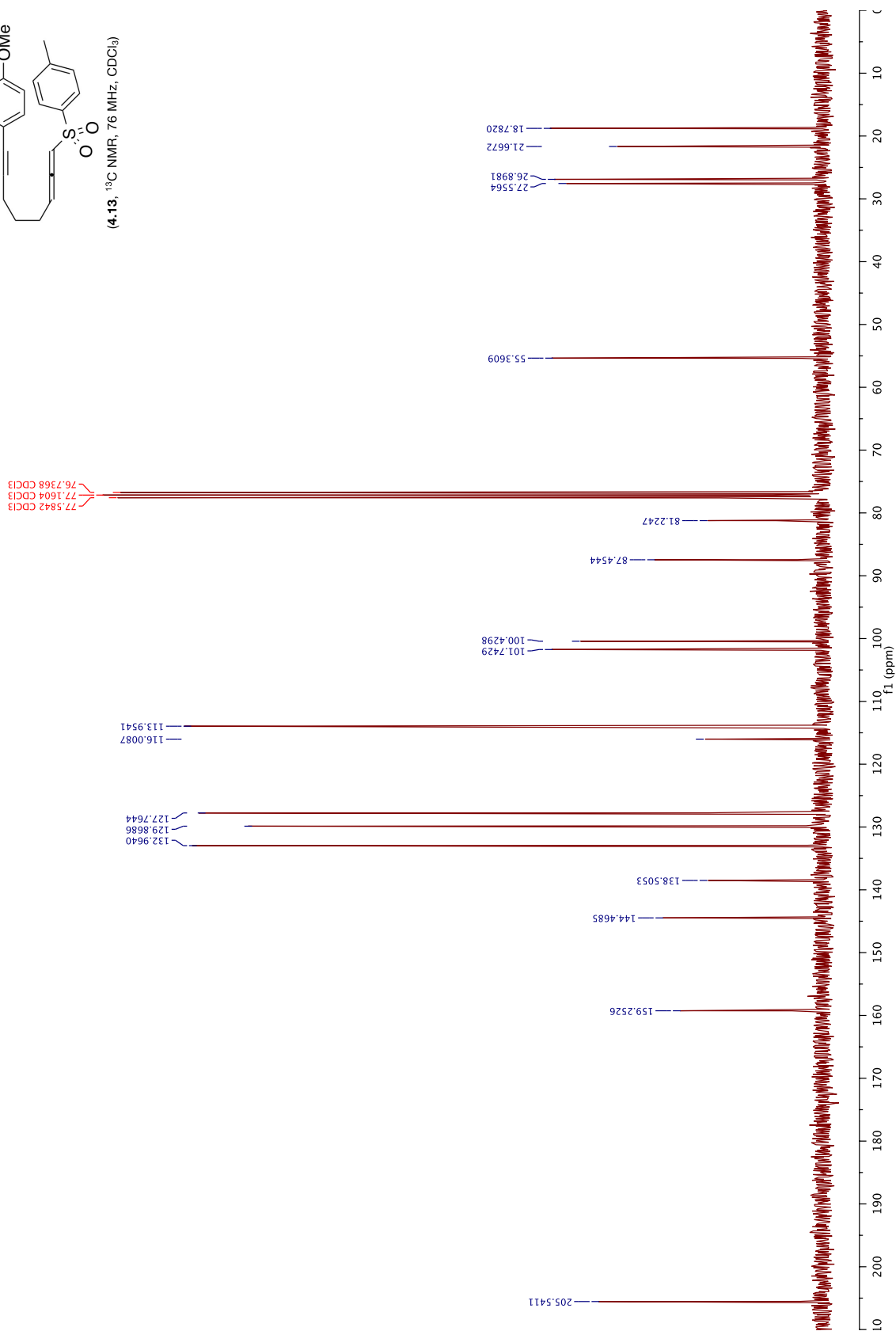


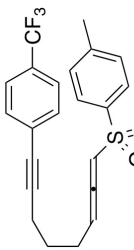
(1.10, ¹³C NMR, 76 MHz, CDCl₃)



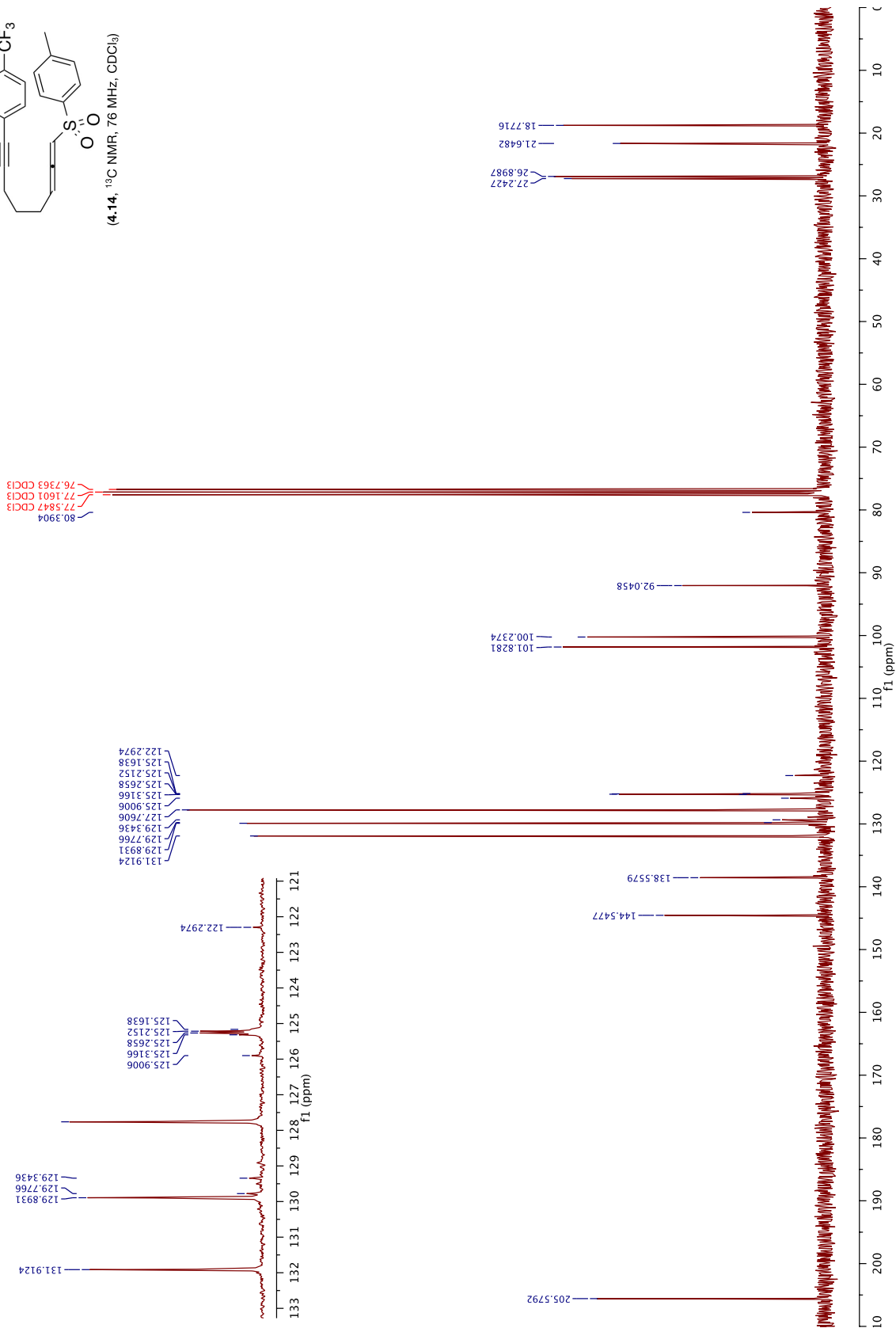


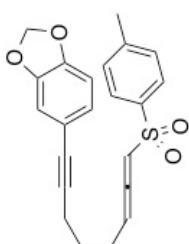
(4-13, ^{13}C NMR, 76 MHz, CDCl_3)



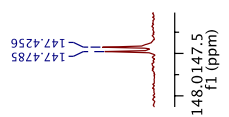
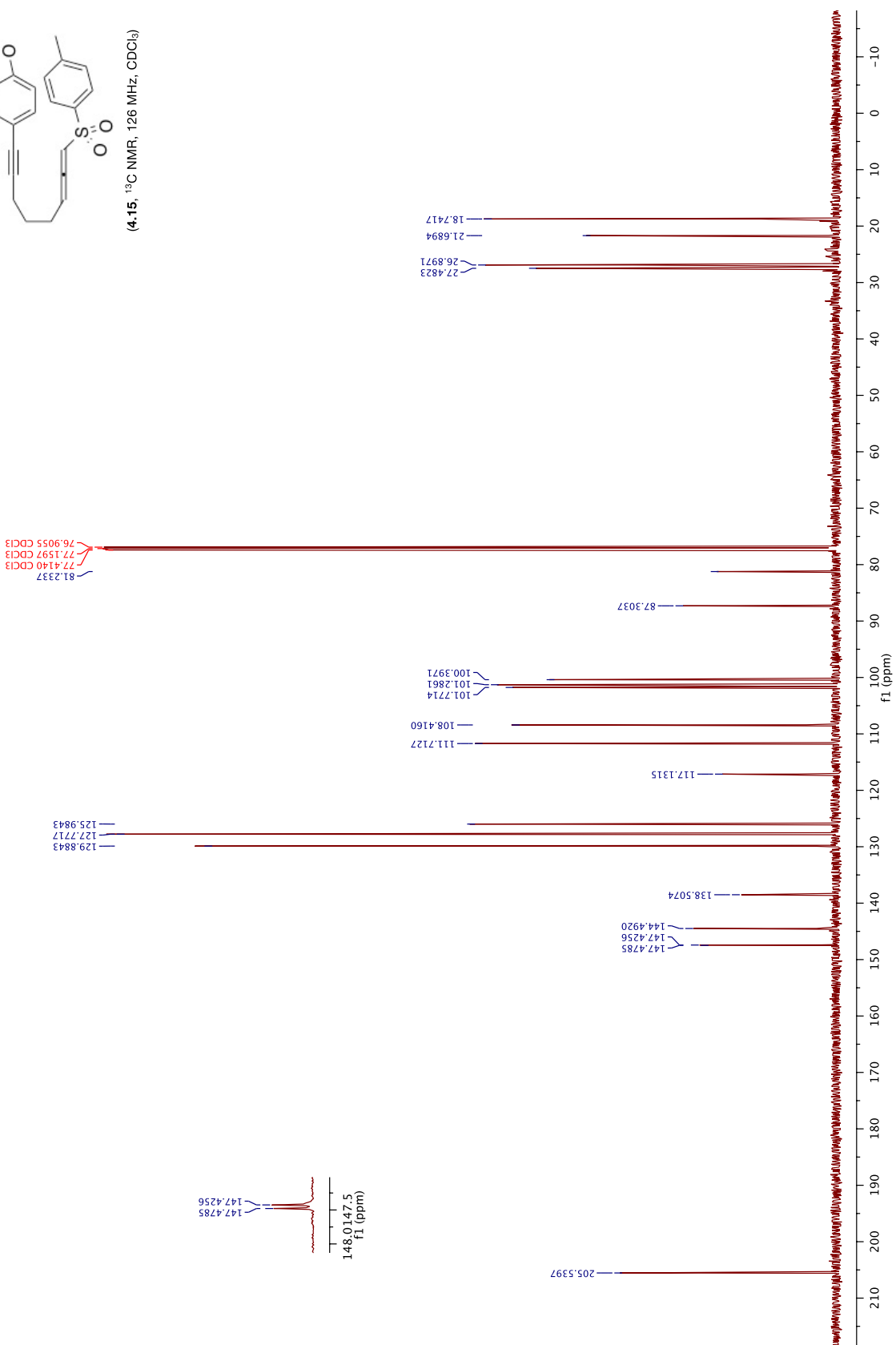


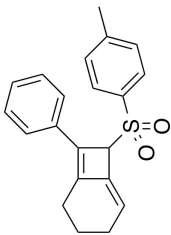
(4-14), ^{13}C NMR, 76 MHz, CDCl_3



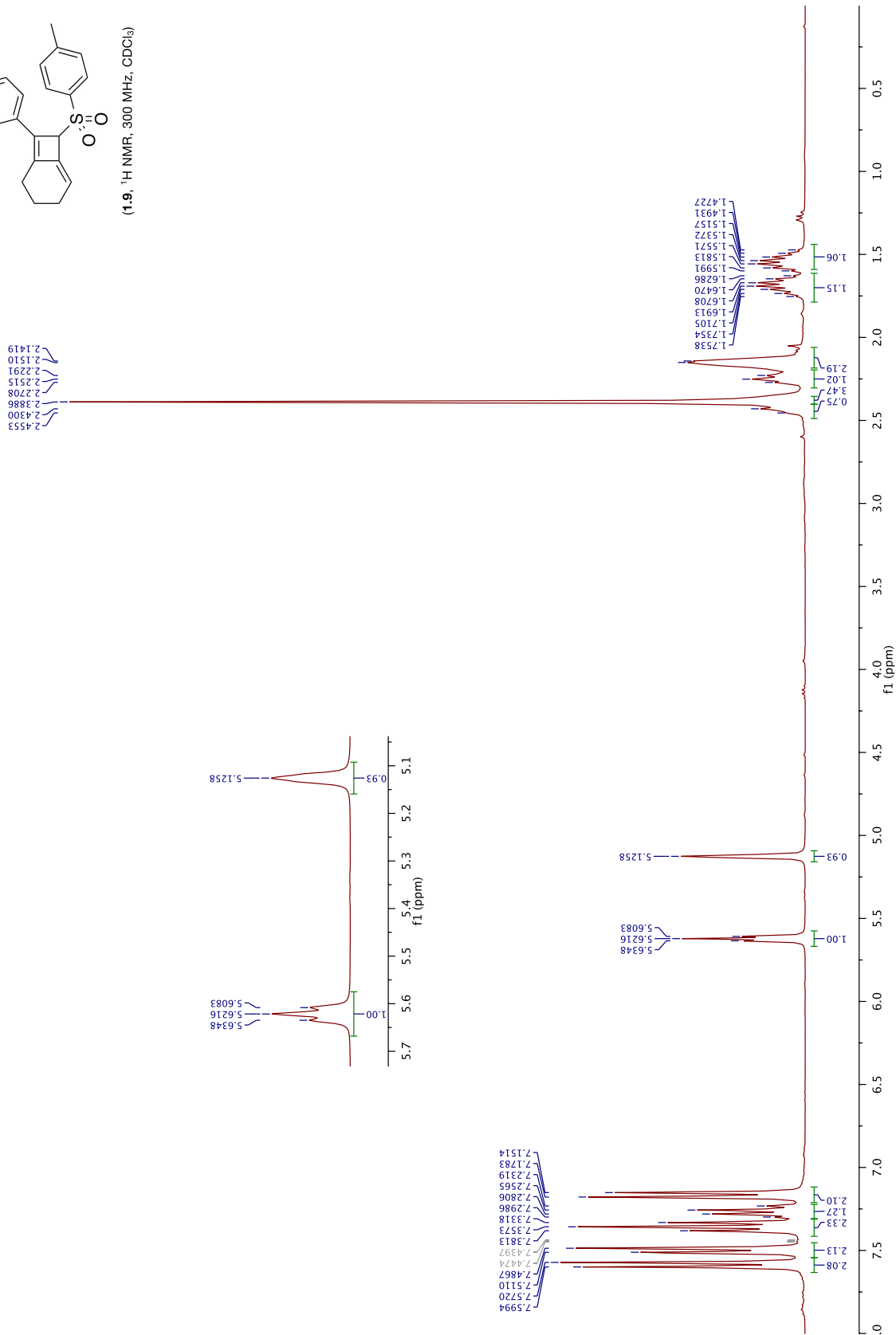


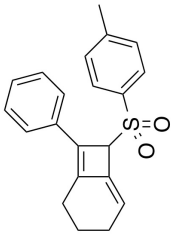
4.15, ¹³C NMR, 126 MHz, CDCl₃



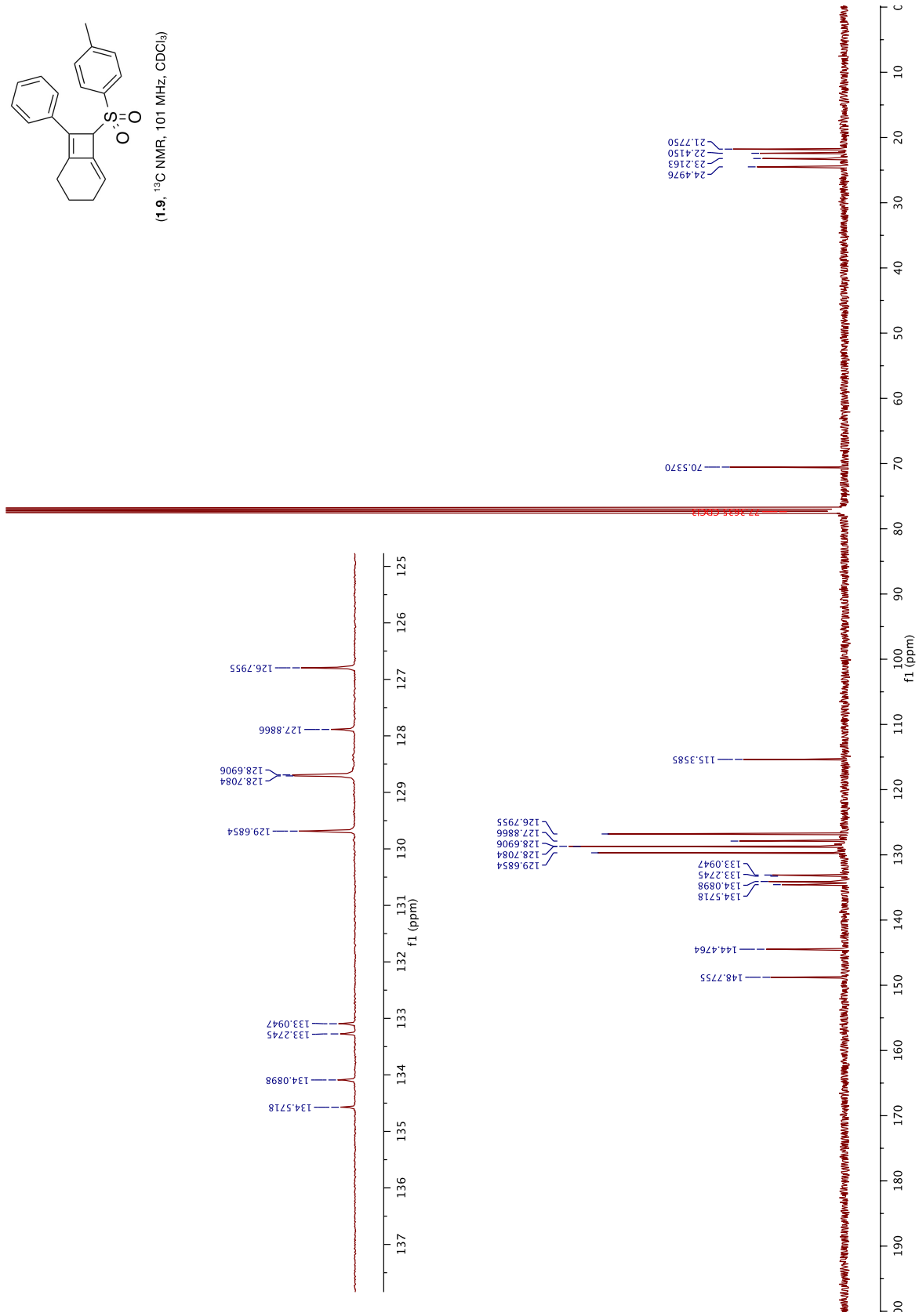


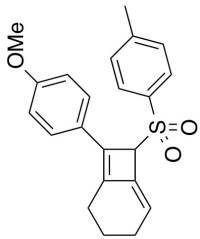
(1.9) ^1H NMR, 300 MHz, CDCl_3



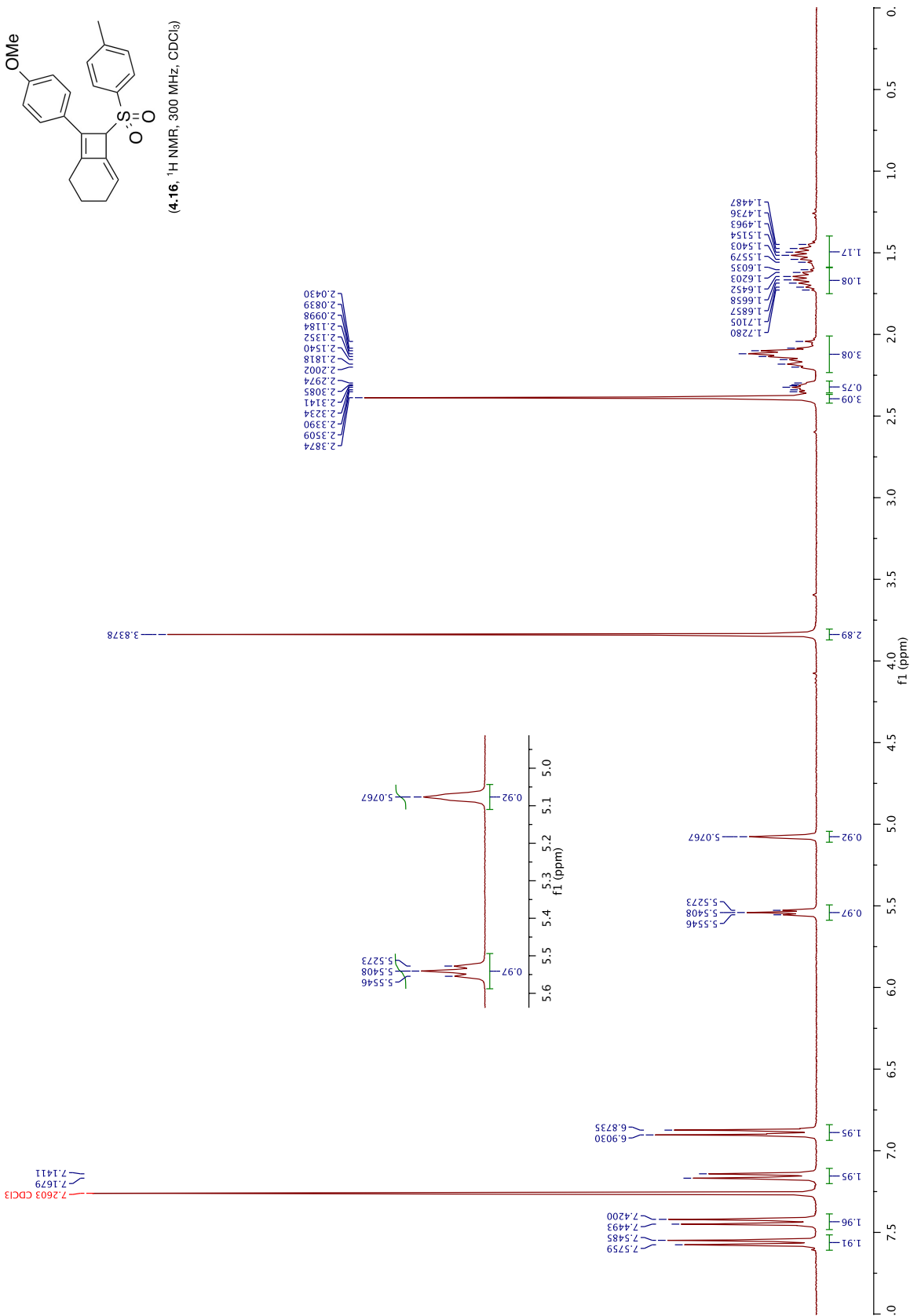


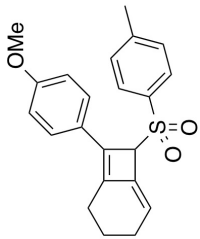
(1.9, ^{13}C NMR, 101 MHz, CDCl_3)



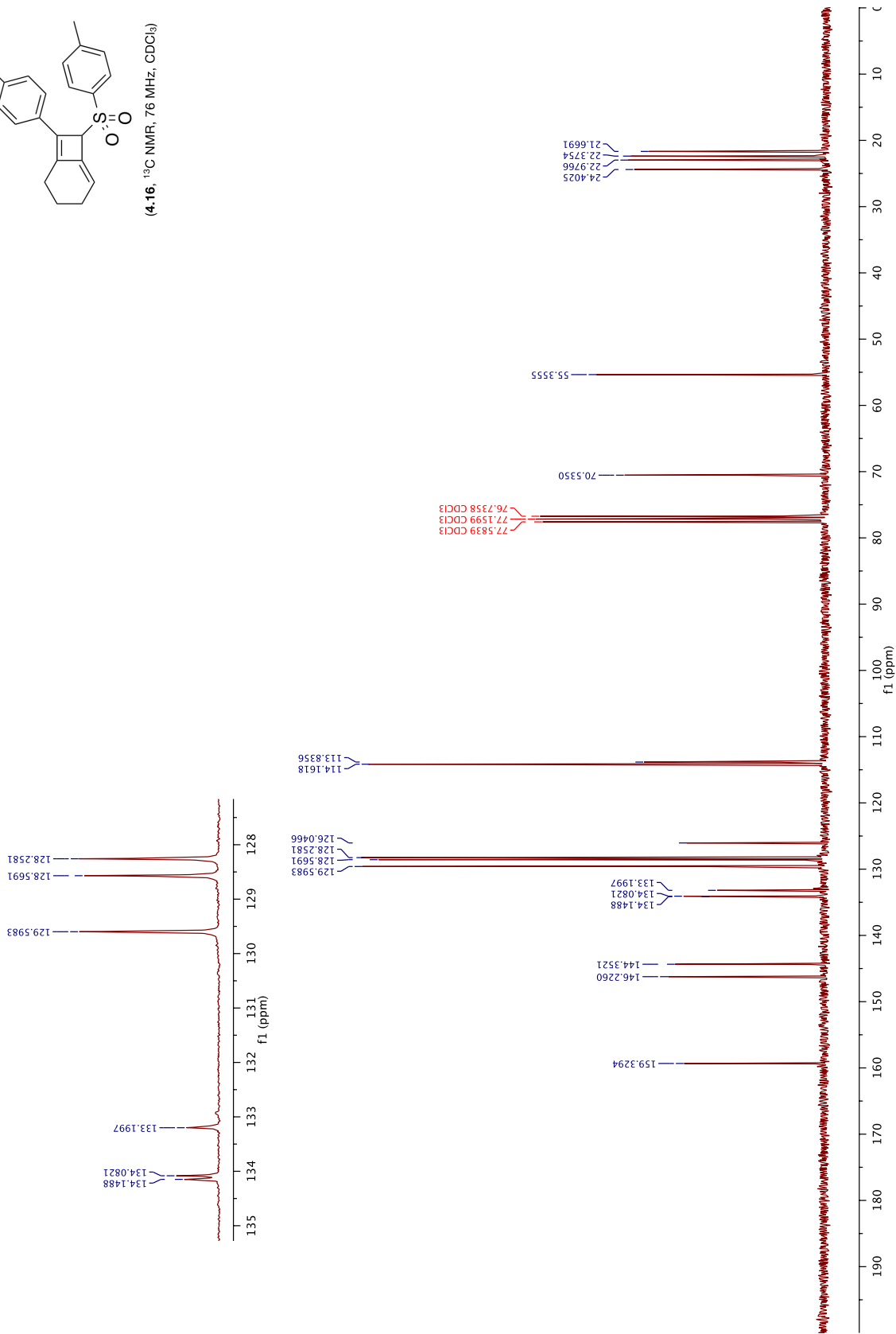


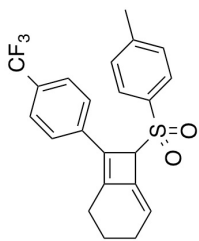
(4.16, ¹H NMR, 300 MHz, CDCl₃)



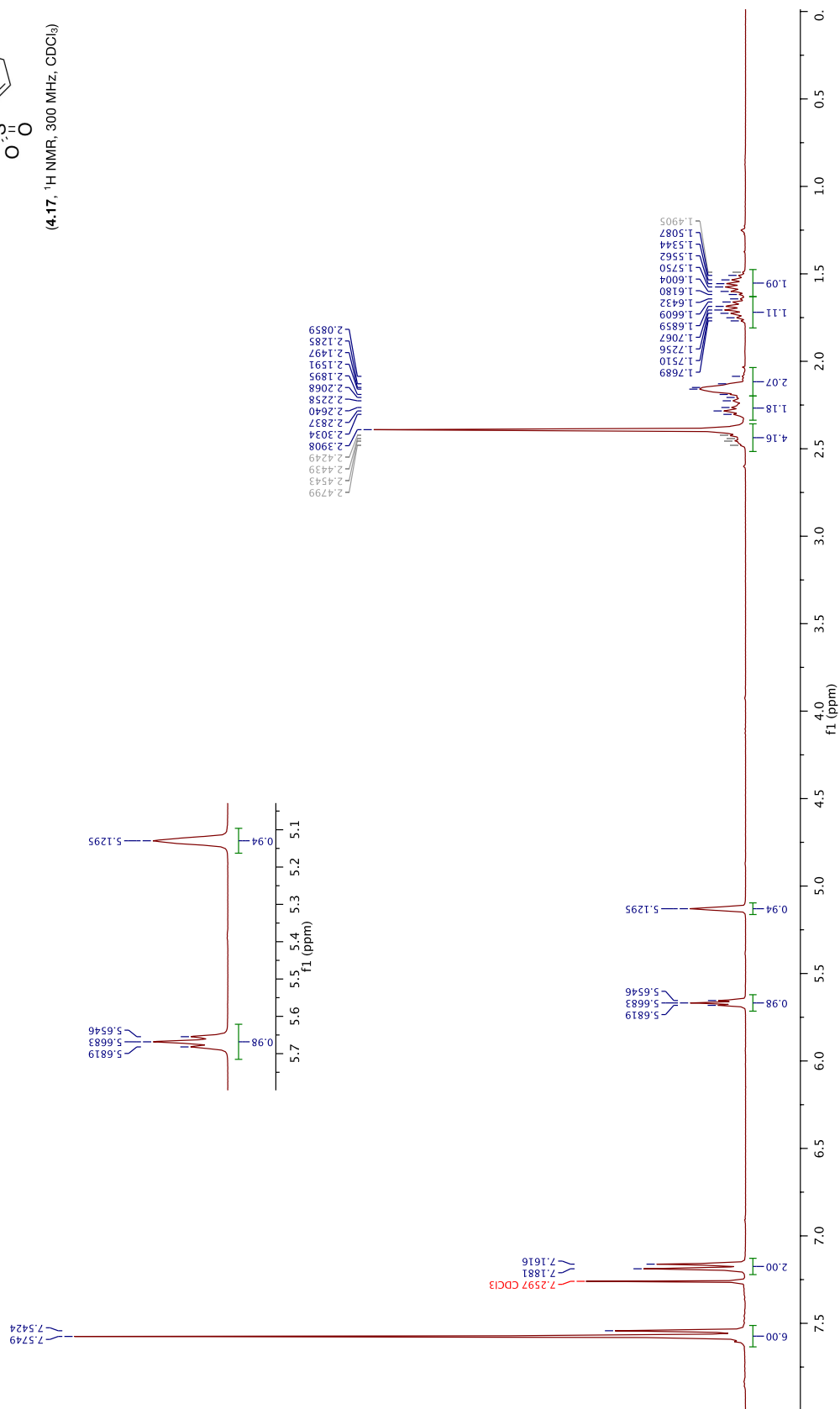


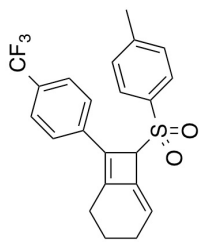
(4.16, ^{13}C NMR, 76 MHz, CDCl_3)



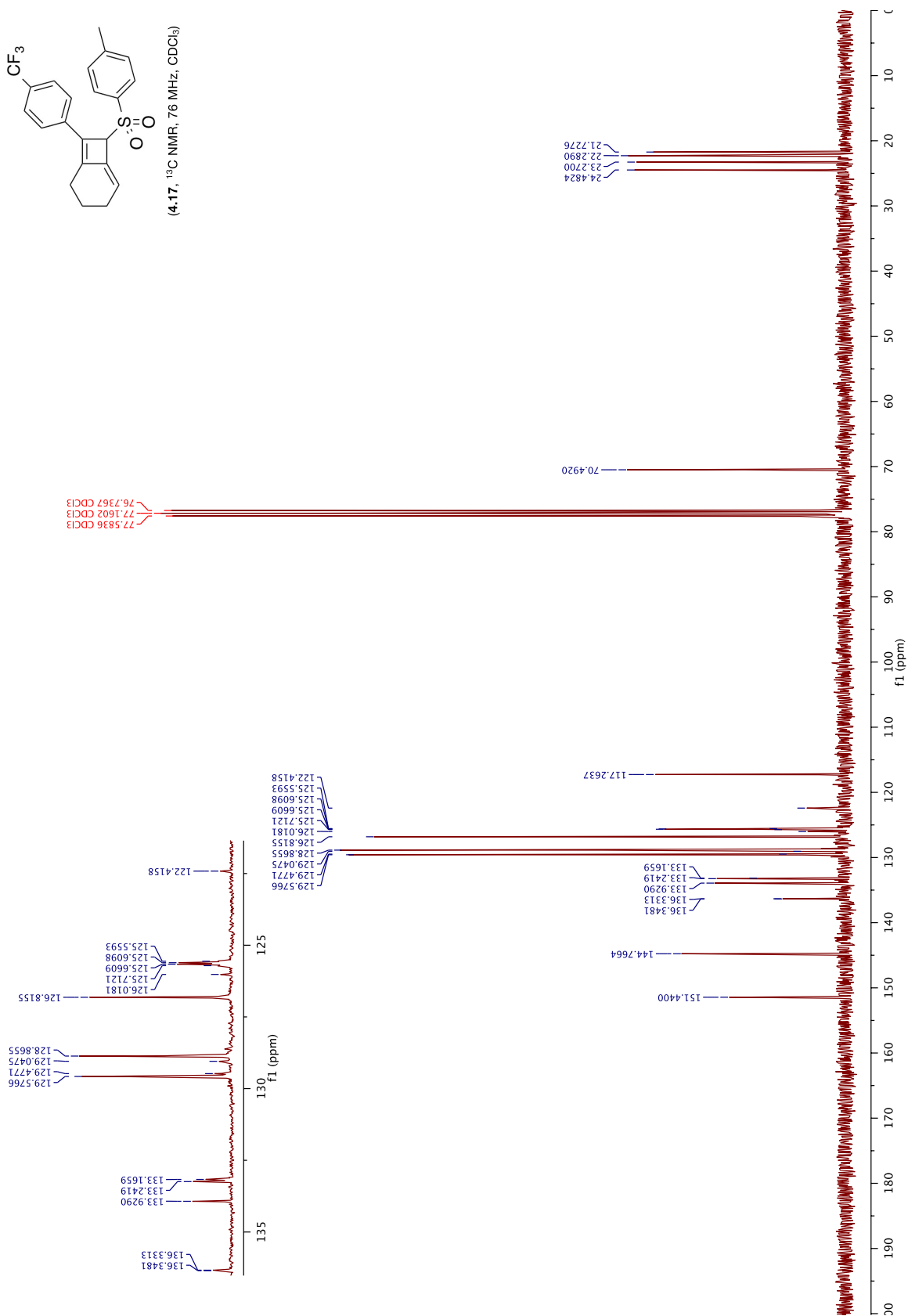


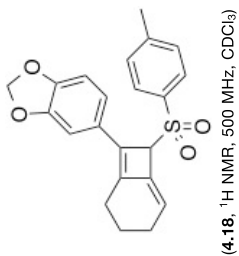
(4.17, ^1H NMR, 300 MHz, CDCl_3)



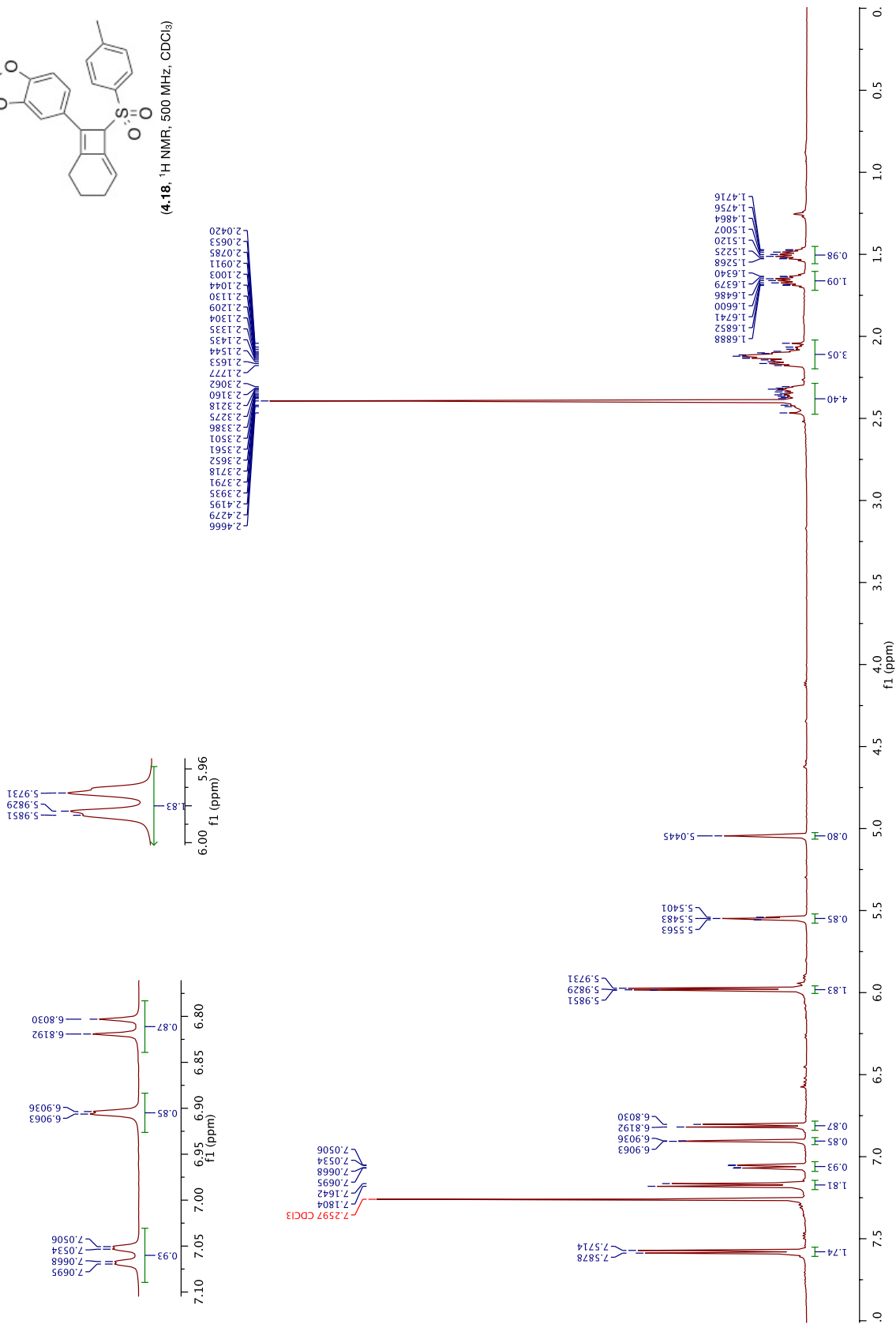


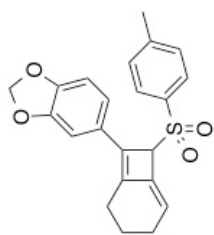
(4.17, ^{13}C NMR, 76 MHz, CDCl_3)



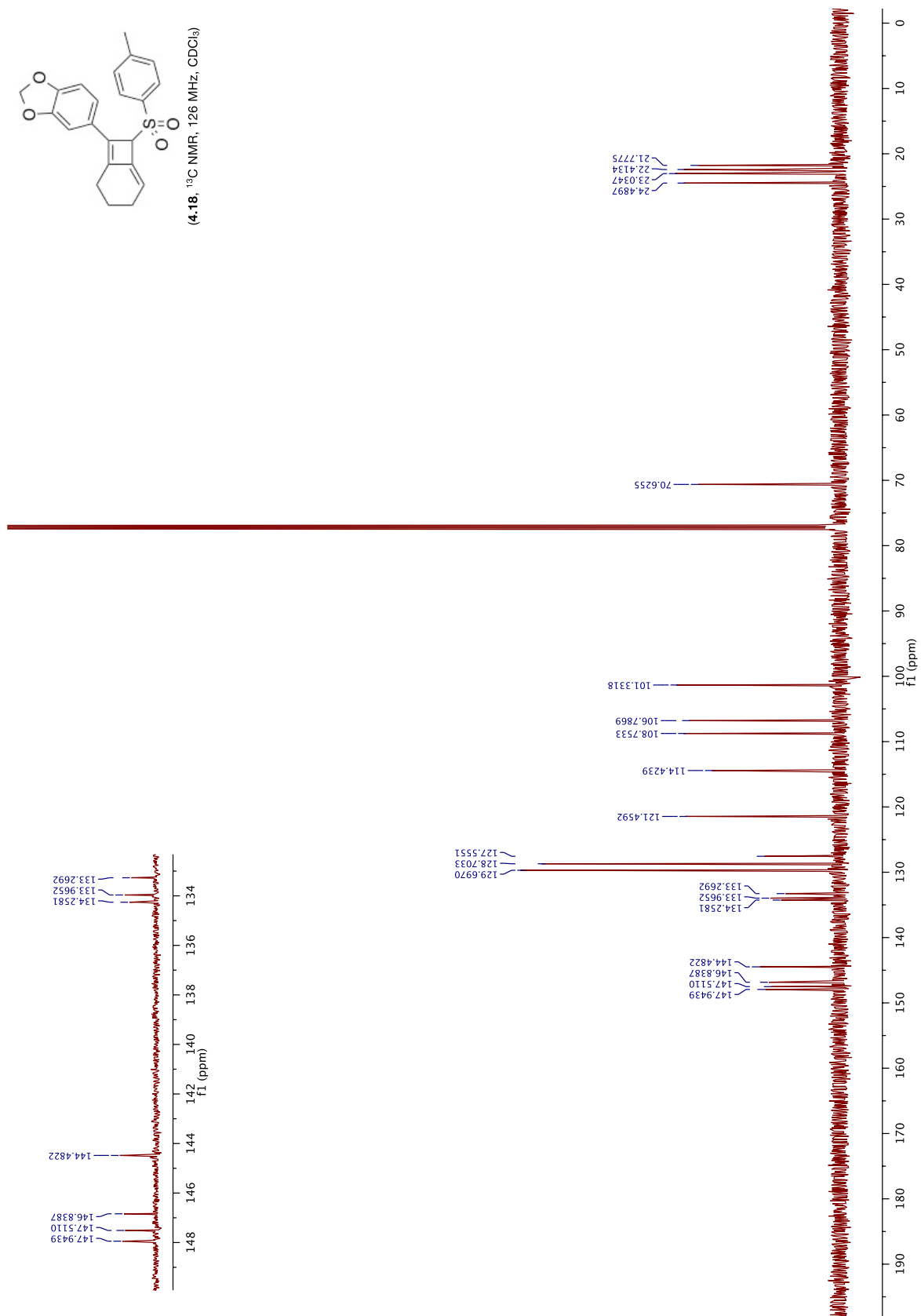


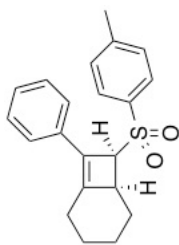
(4-18), ¹H NMR, 500 MHz, CDCl₃



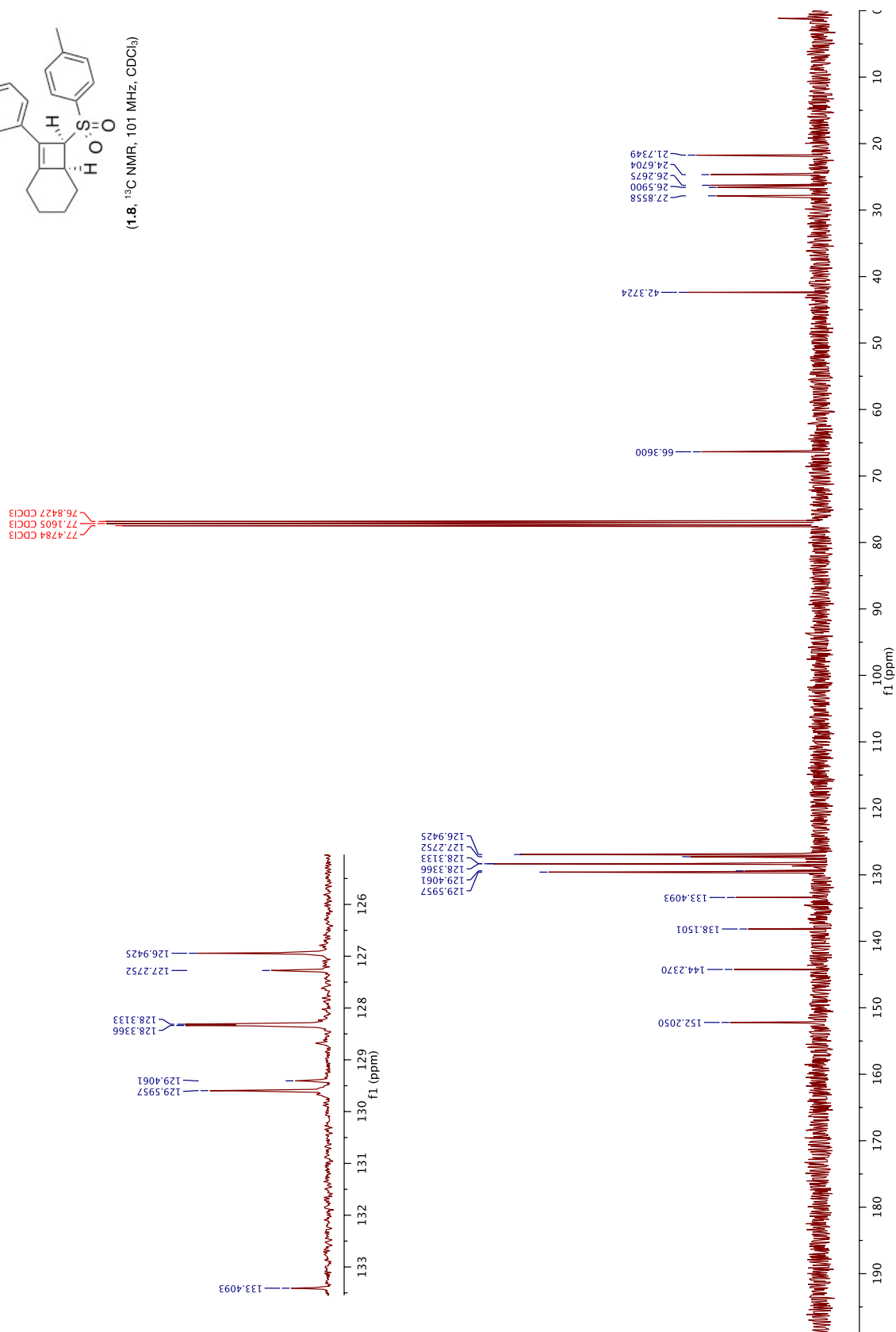


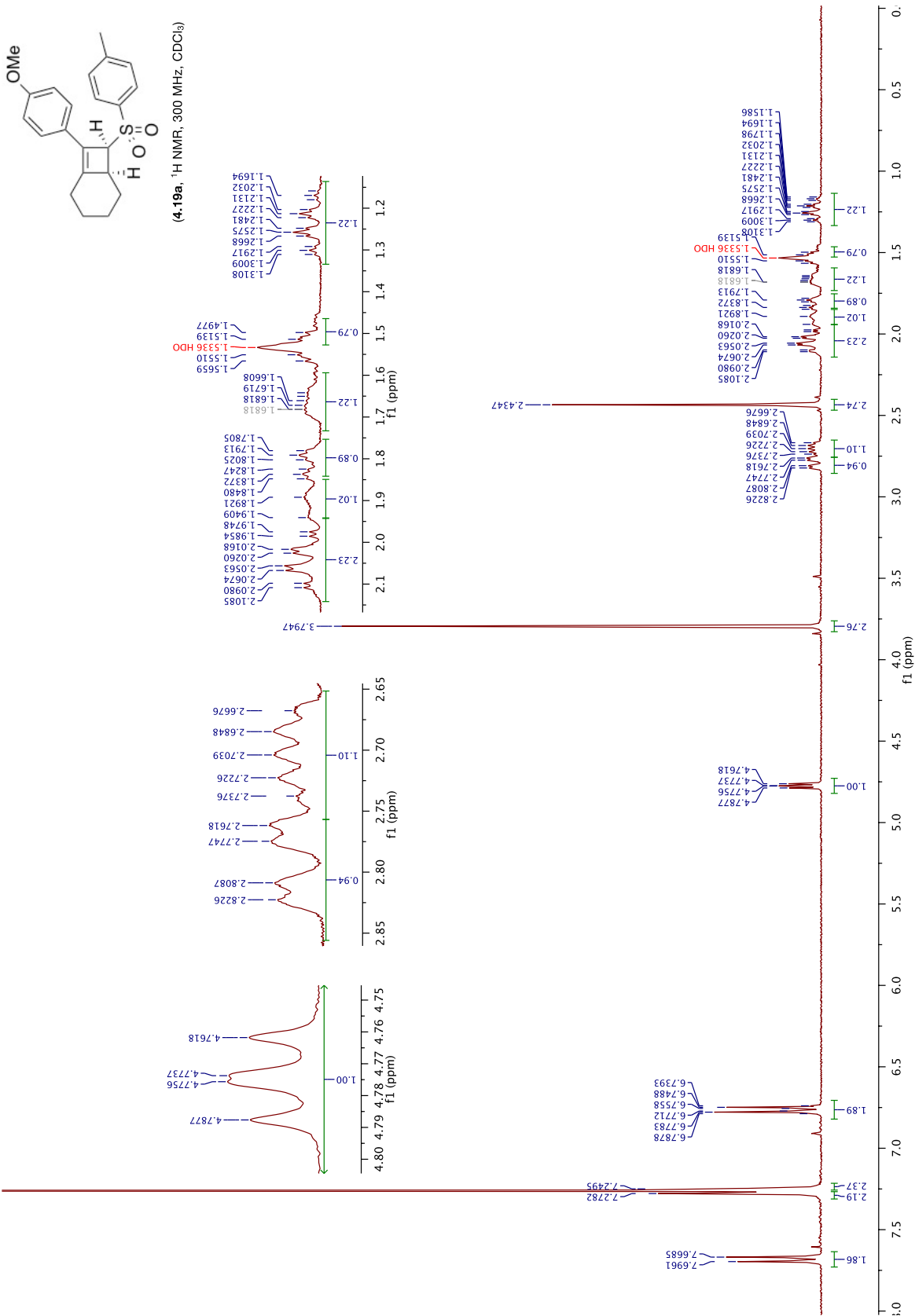
(4-18), ^{13}C NMR, 126 MHz, CDCl_3

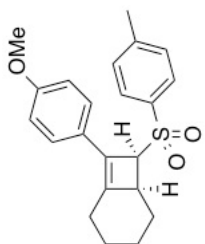




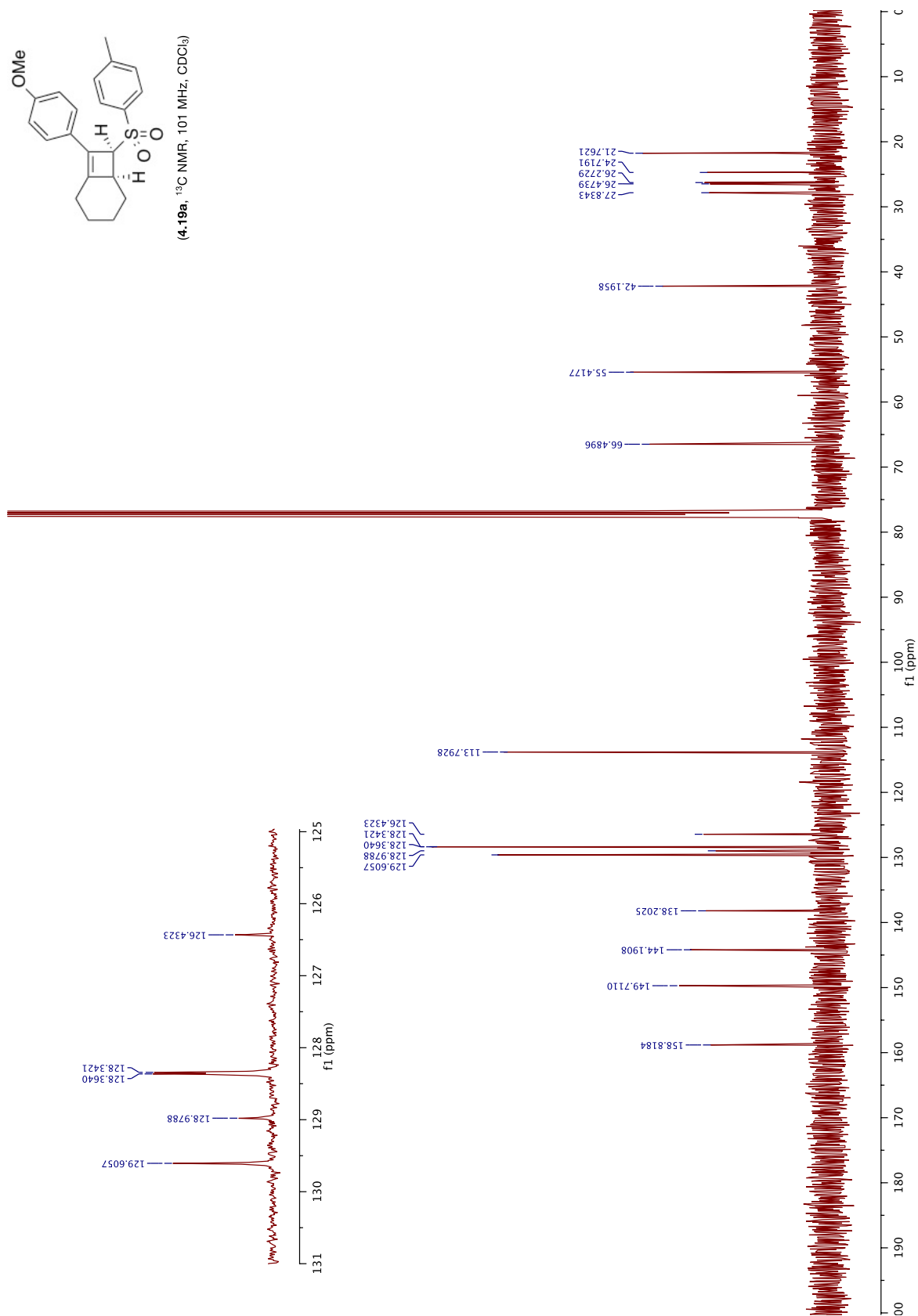
(1.8) ^{13}C NMR, 101 MHz, CDCl_3

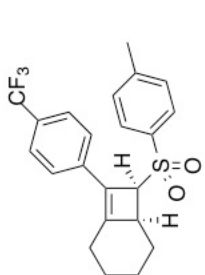




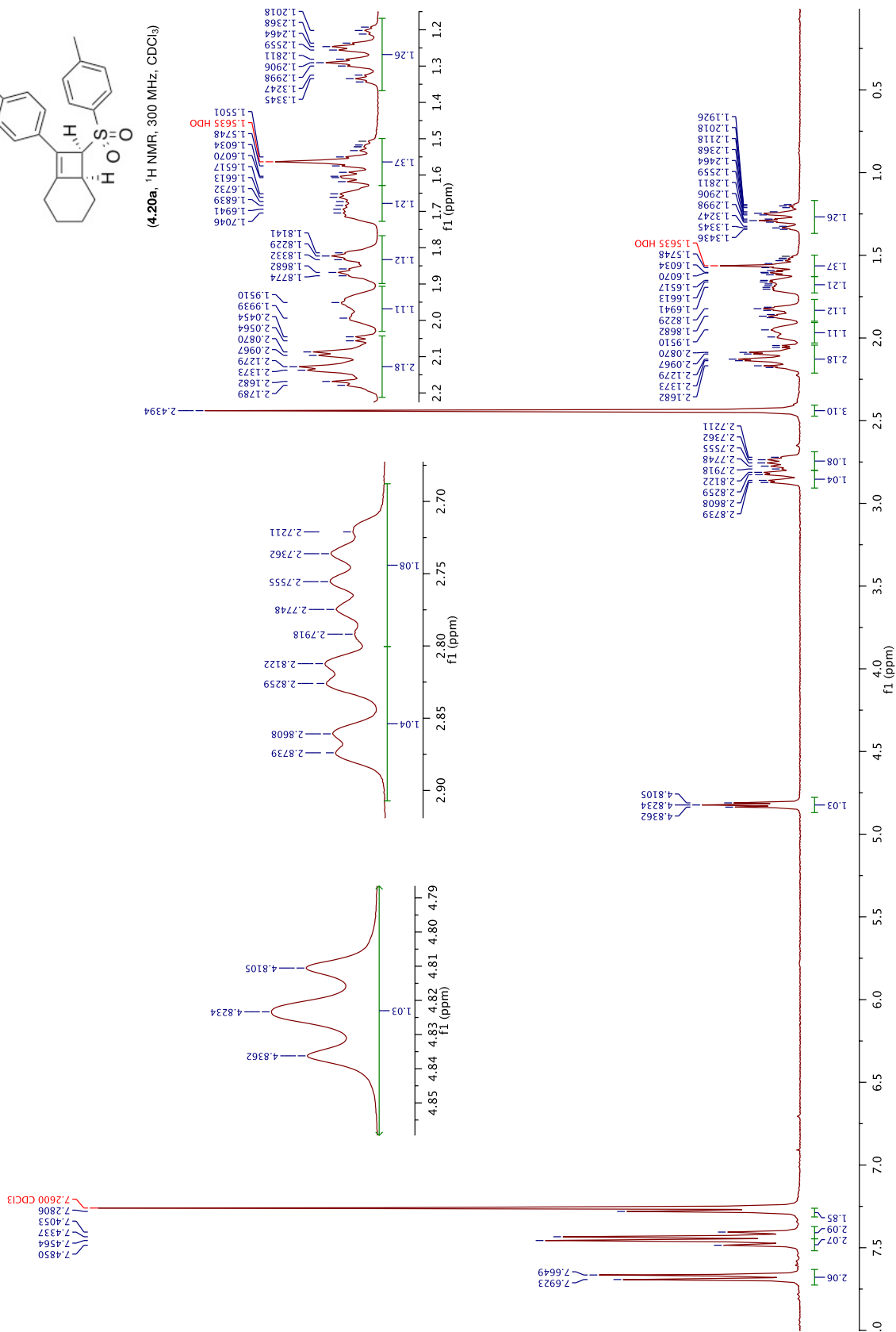


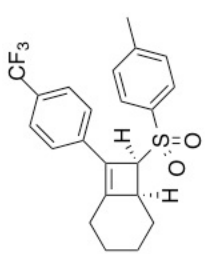
(4.19a, ^{13}C NMR, 101 MHz, CDCl_3)



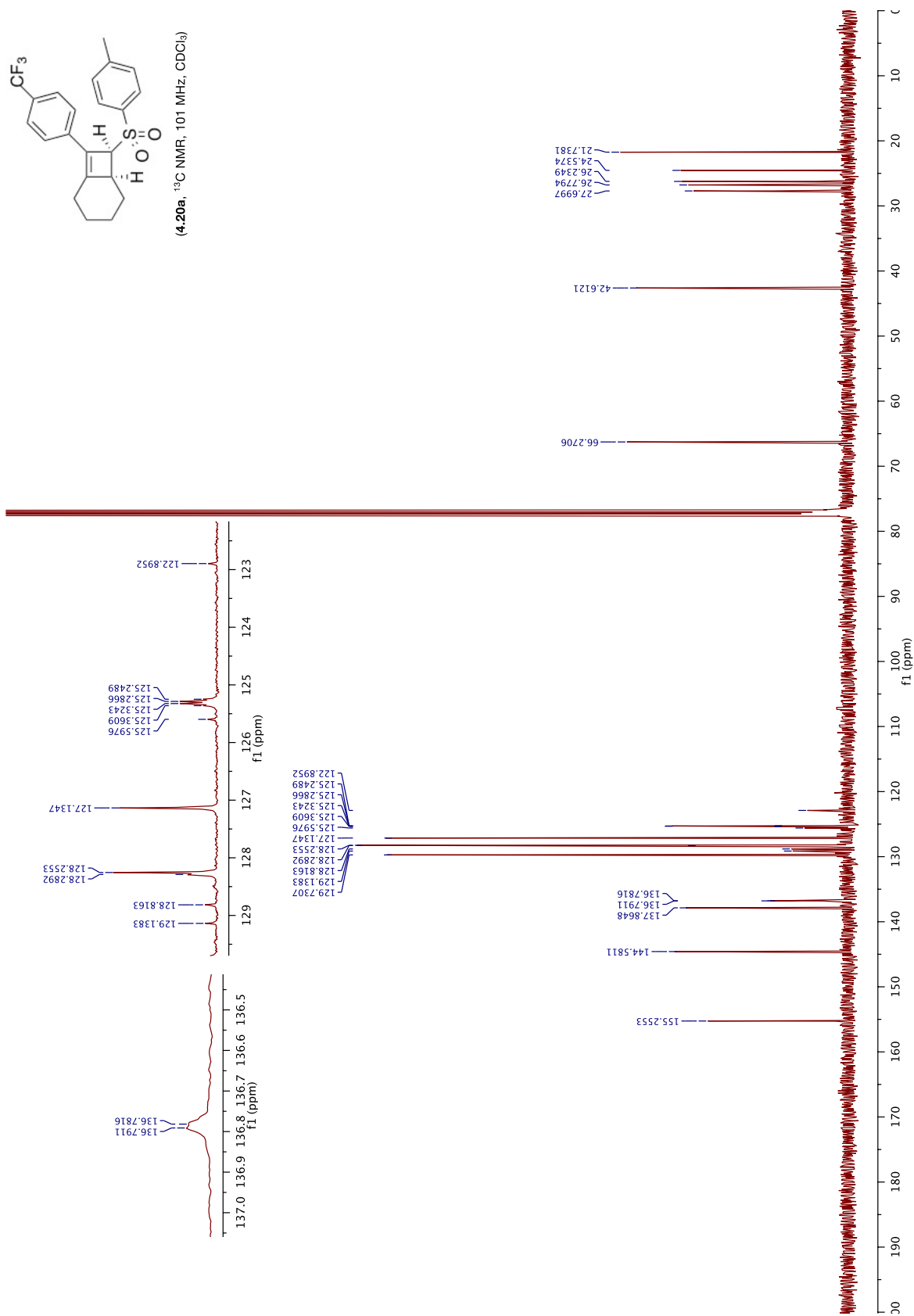


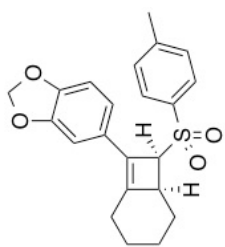
(4.20a, ¹H NMR, 300 MHz, CDCl₃)



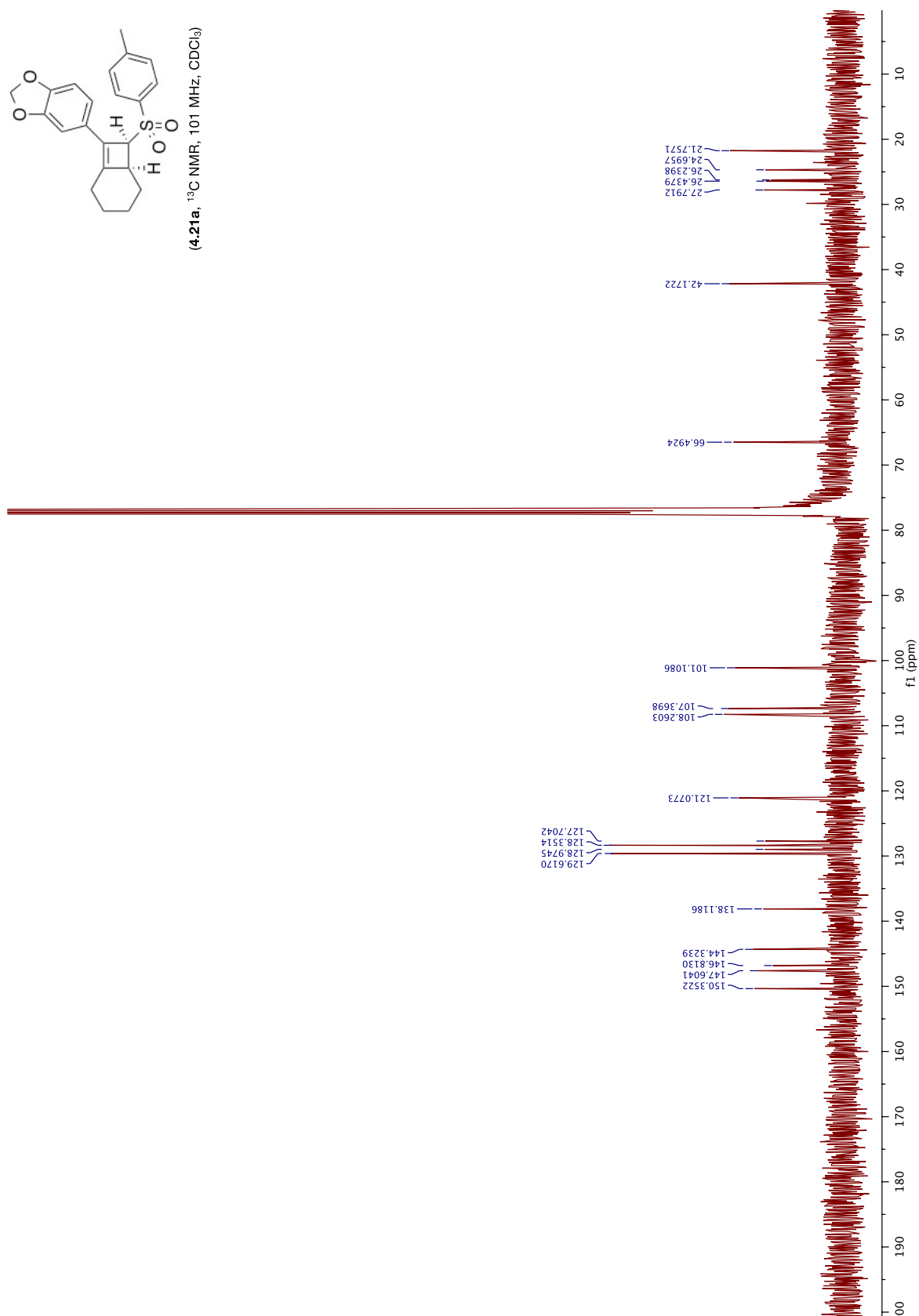


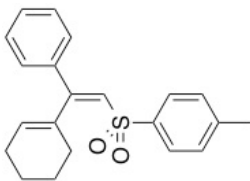
(4-20a, ^{13}C NMR, 101 MHz, CDCl_3)



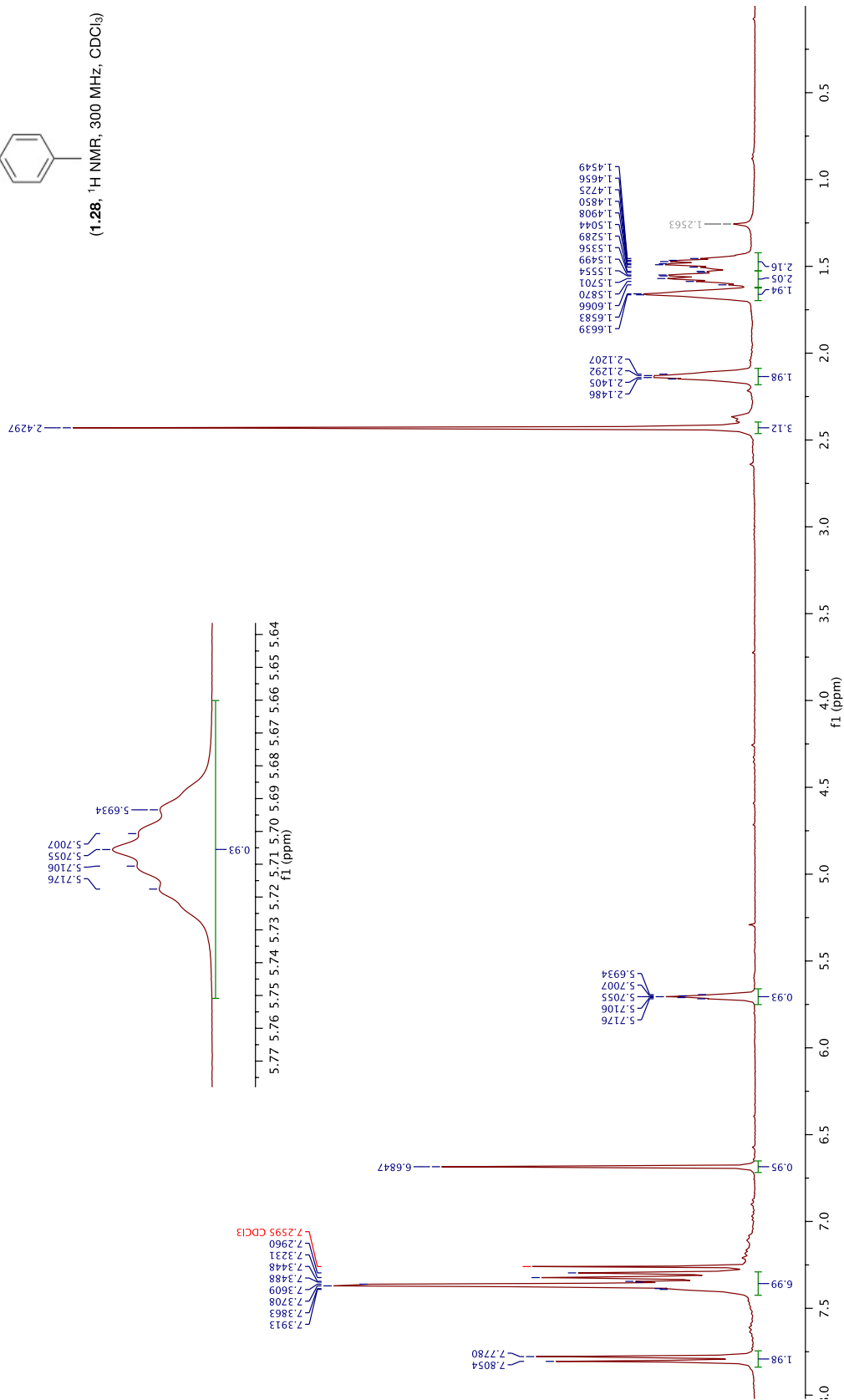


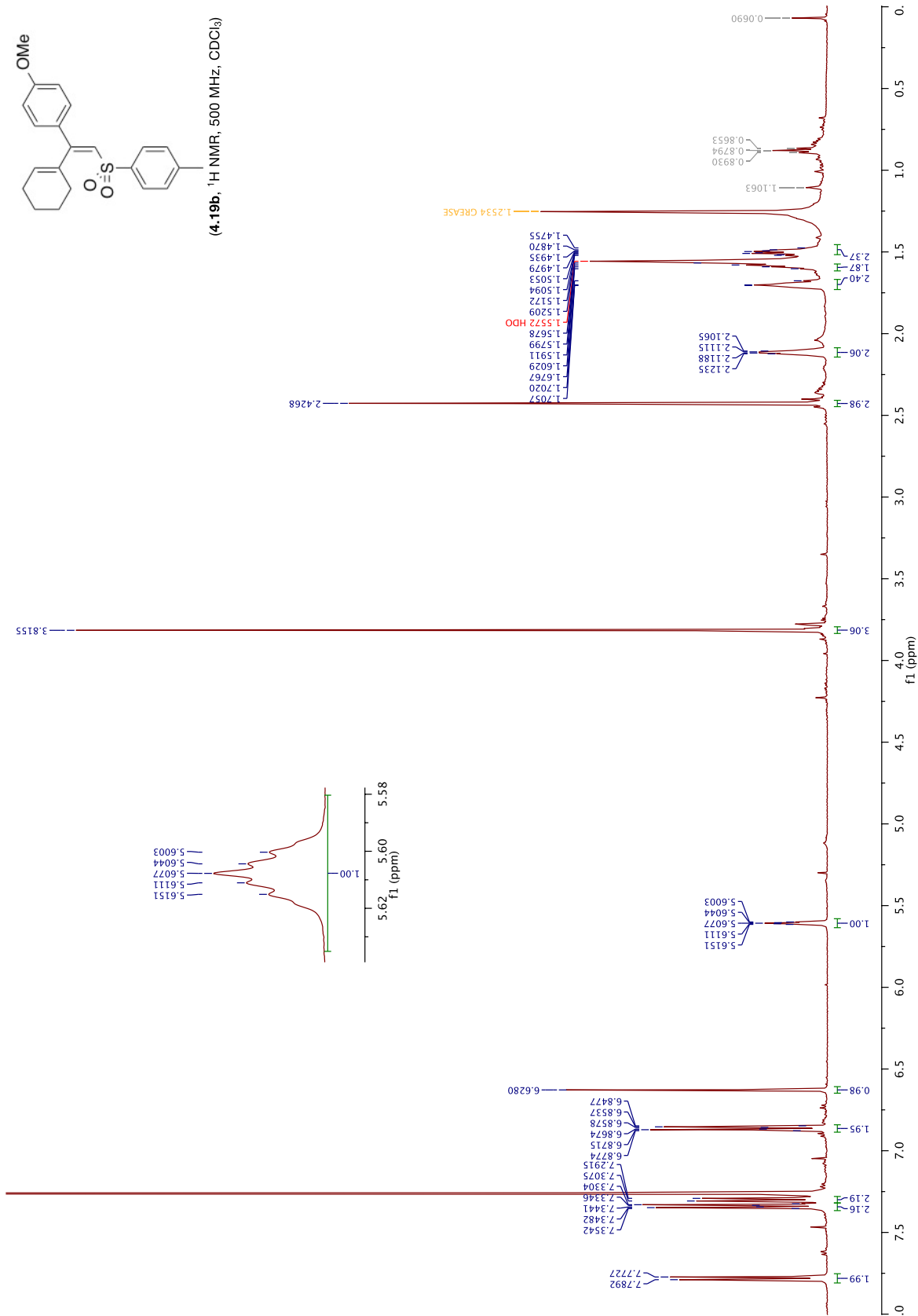
(4.21a, ^{13}C NMR, 101 MHz, CDCl_3)

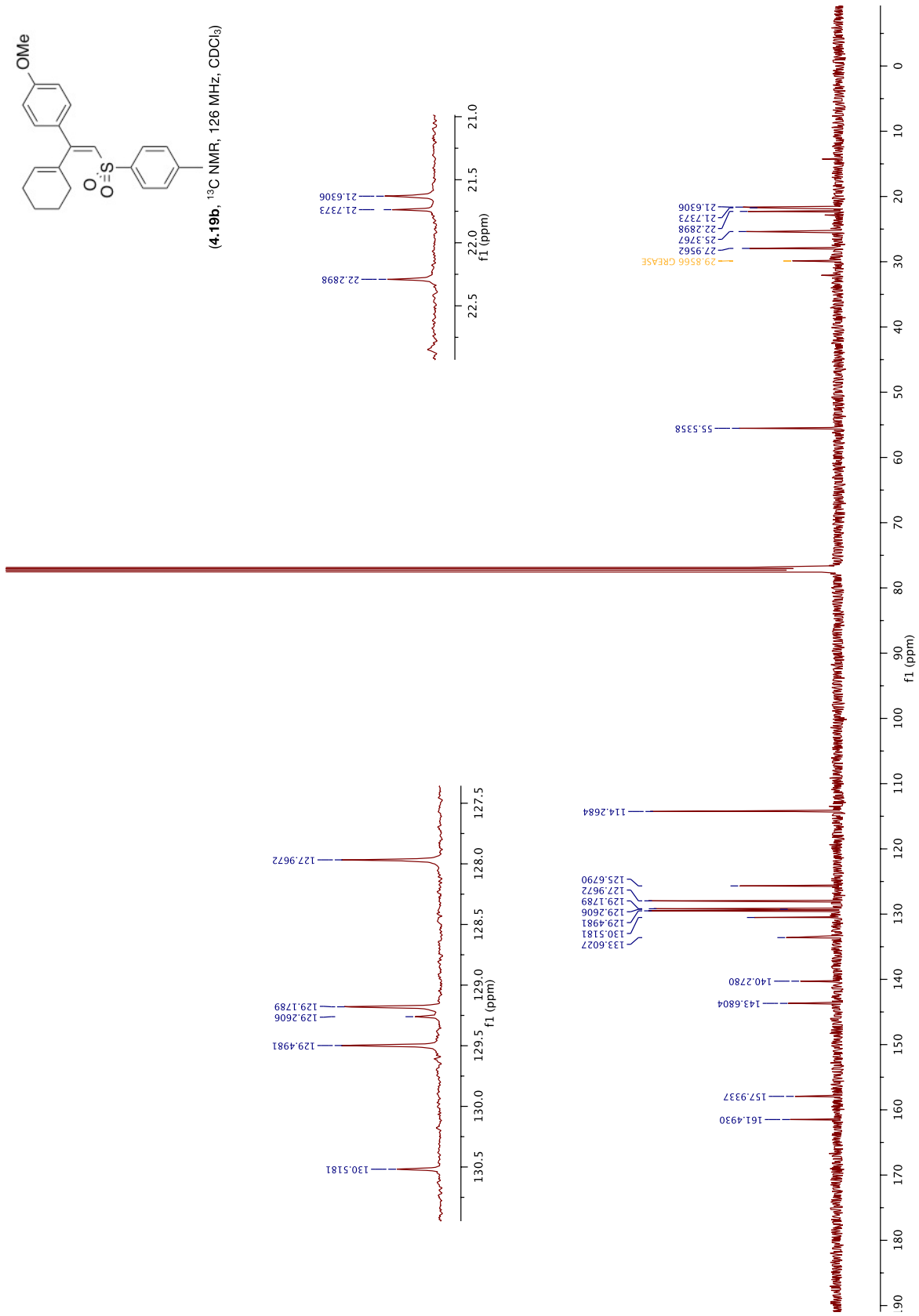


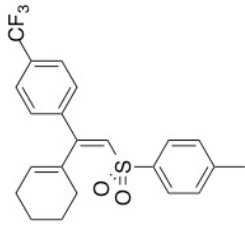


(1.28, ^1H NMR, 300 MHz, CDCl_3)

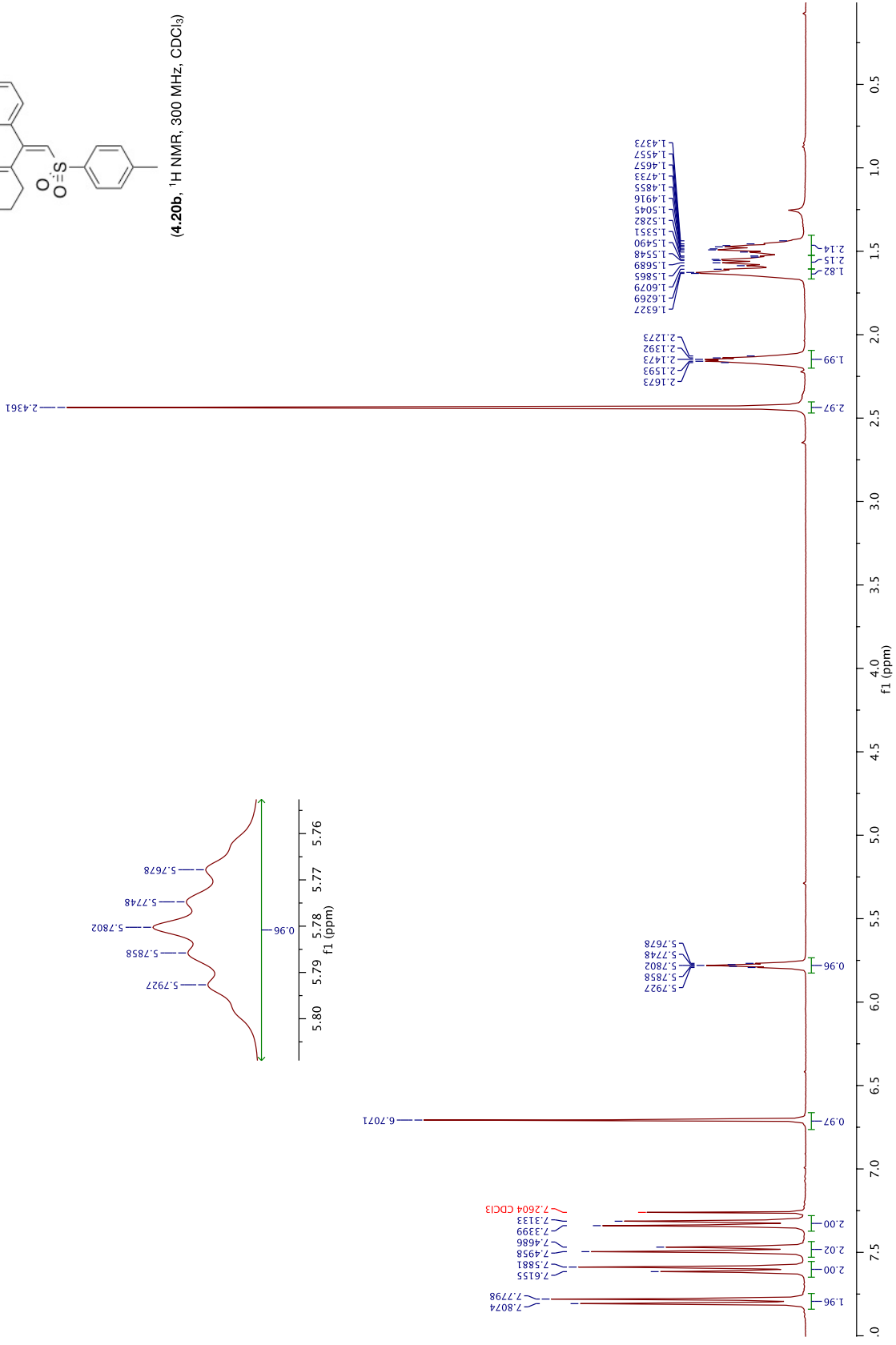


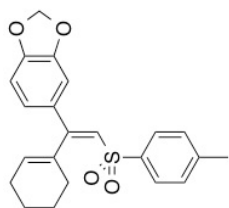




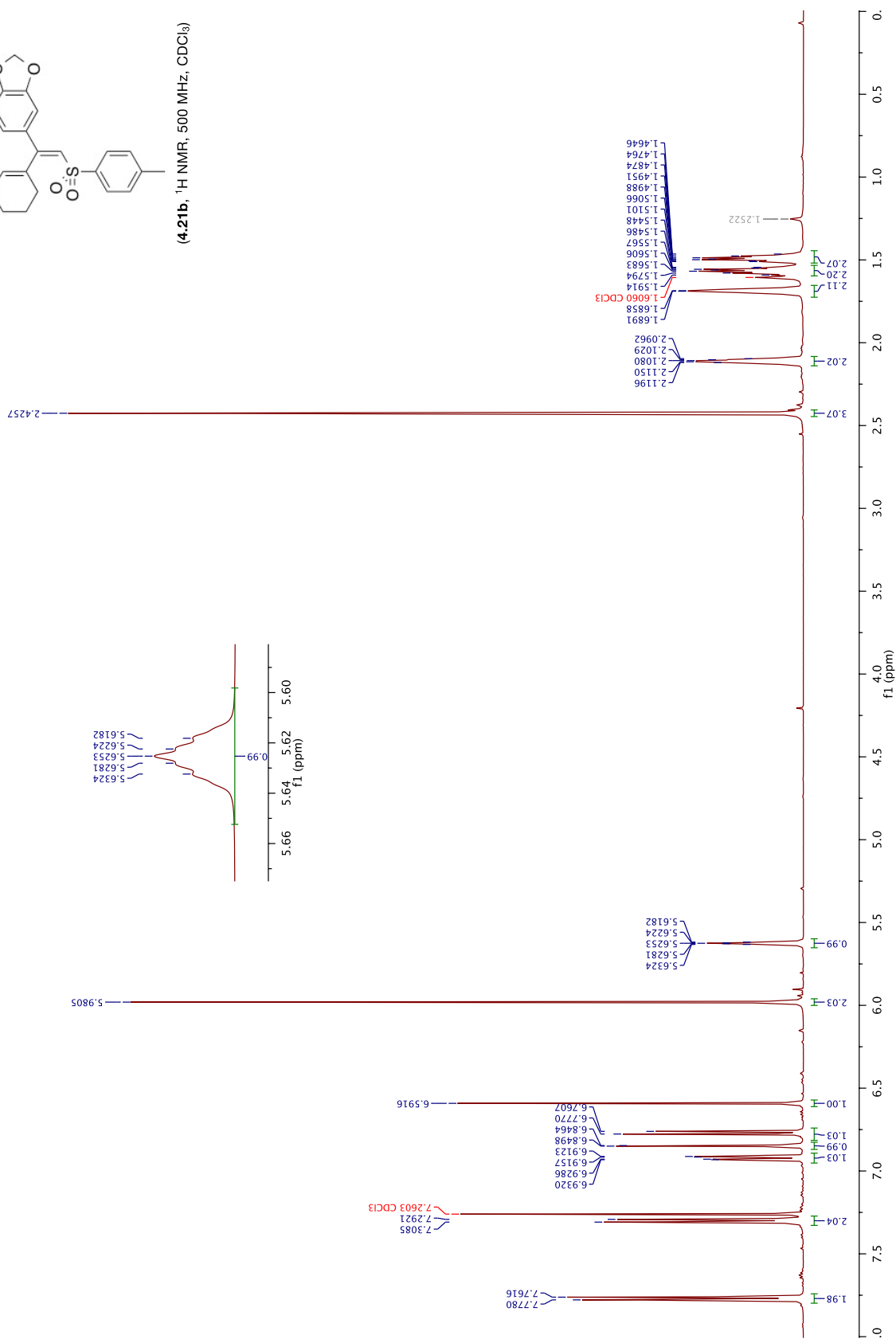


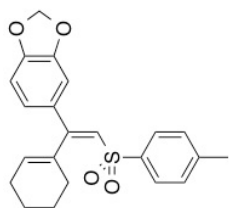
(4.20b), ¹H NMR, 300 MHz, CDCl₃



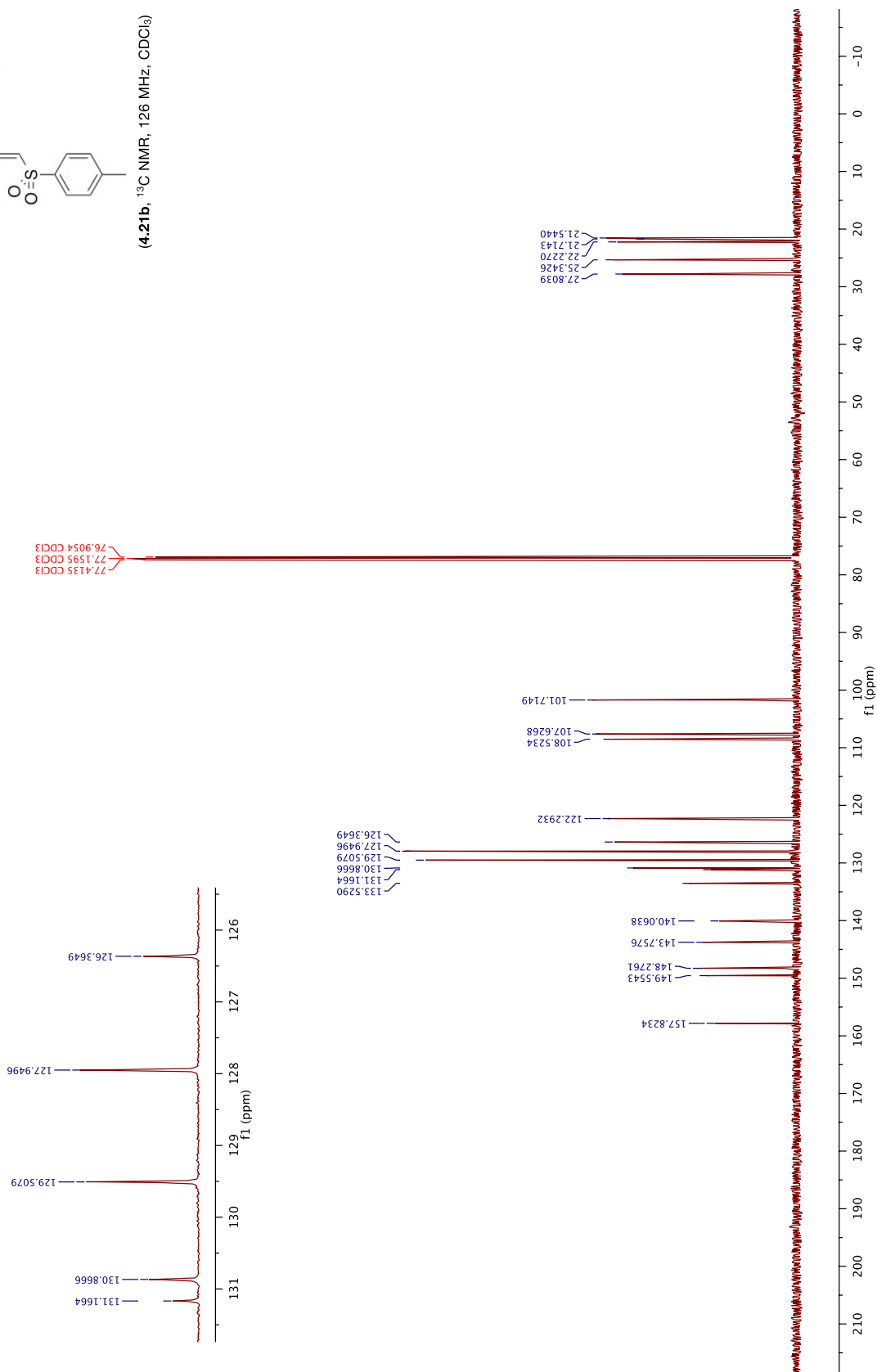


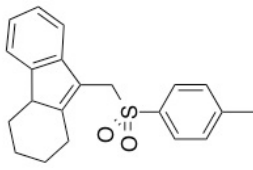
(4.21b), ¹H NMR, 500 MHz, CDCl₃



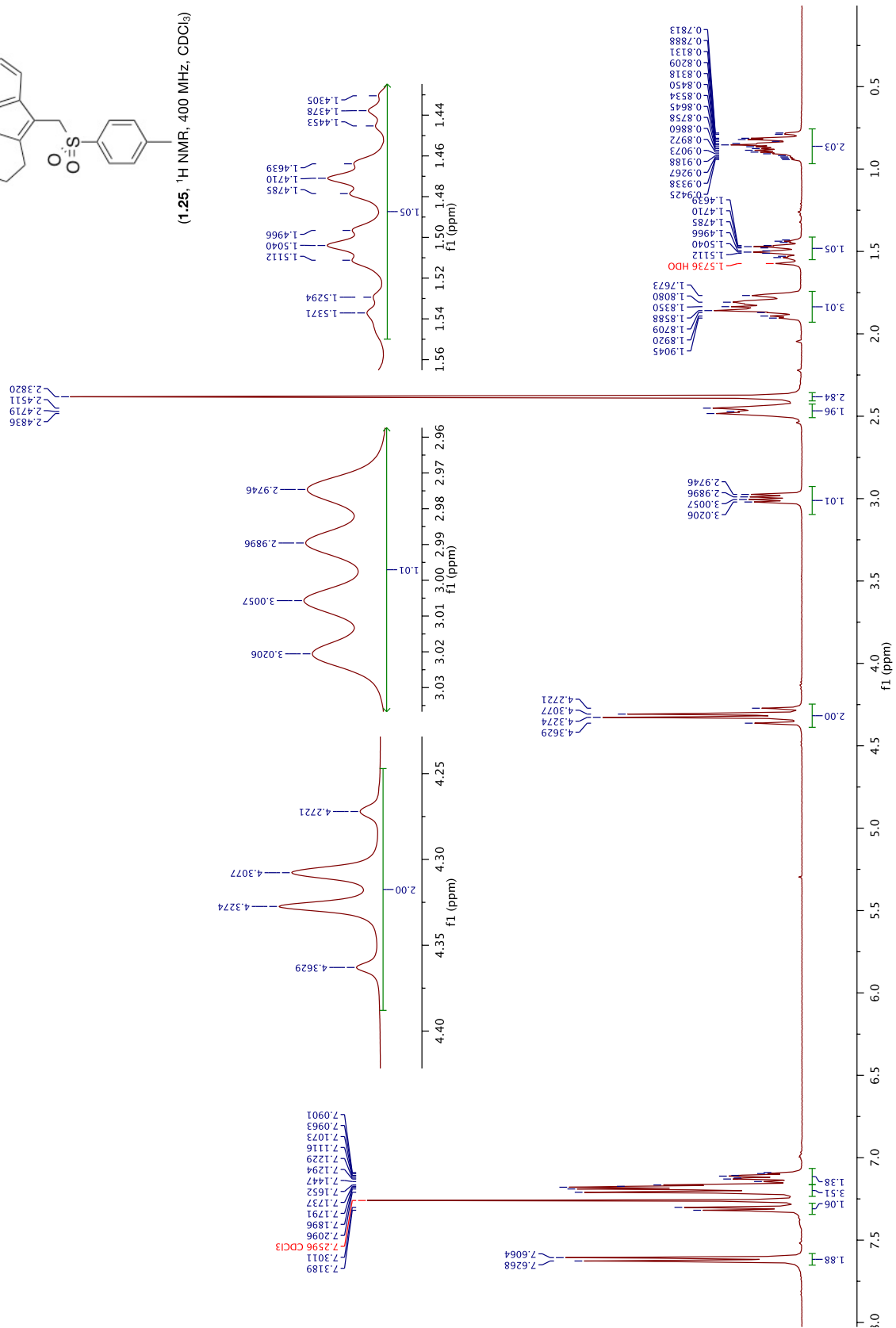


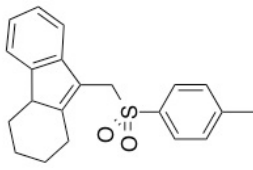
(4.21b), ^{13}C NMR, 126 MHz, CDCl_3



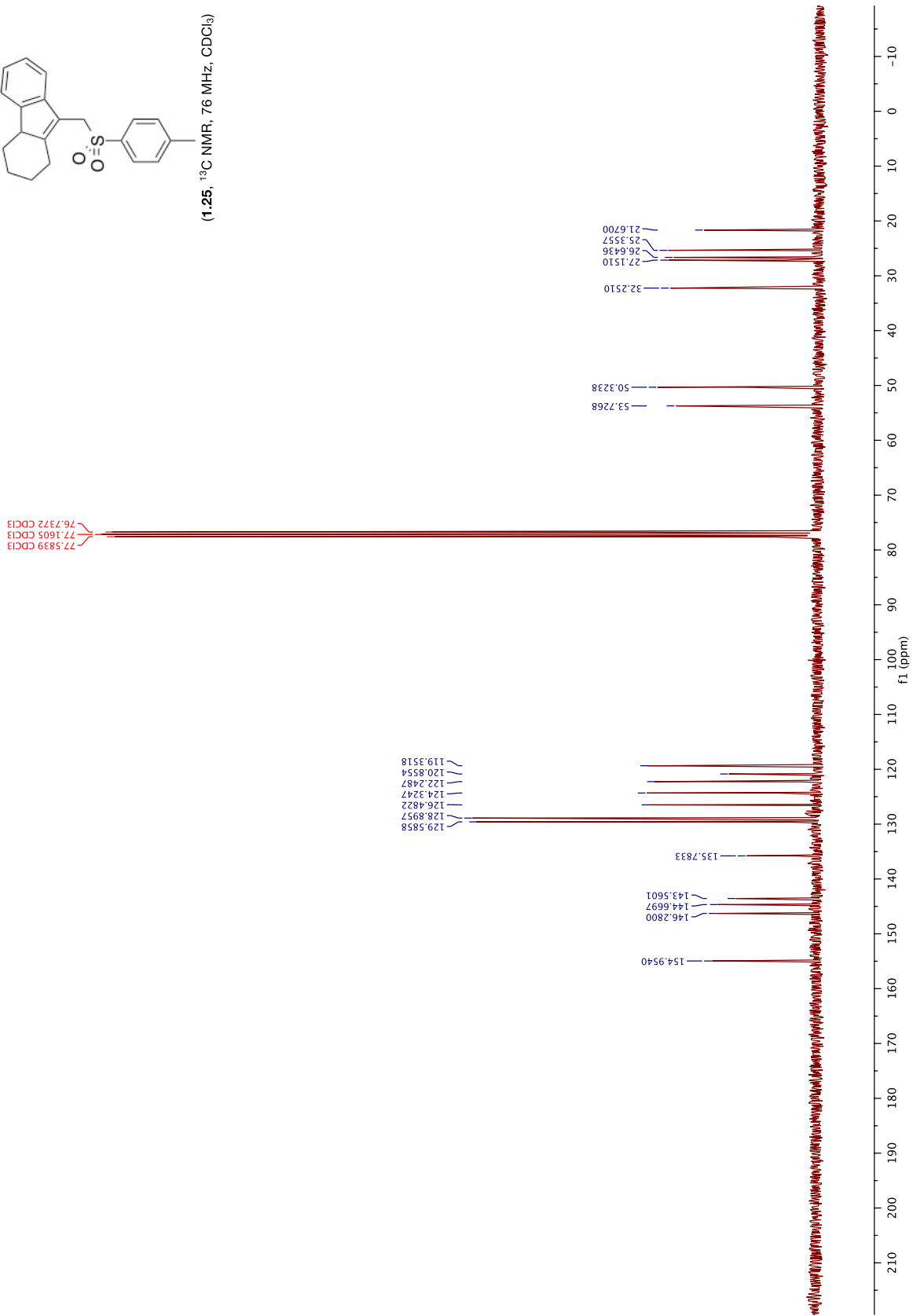


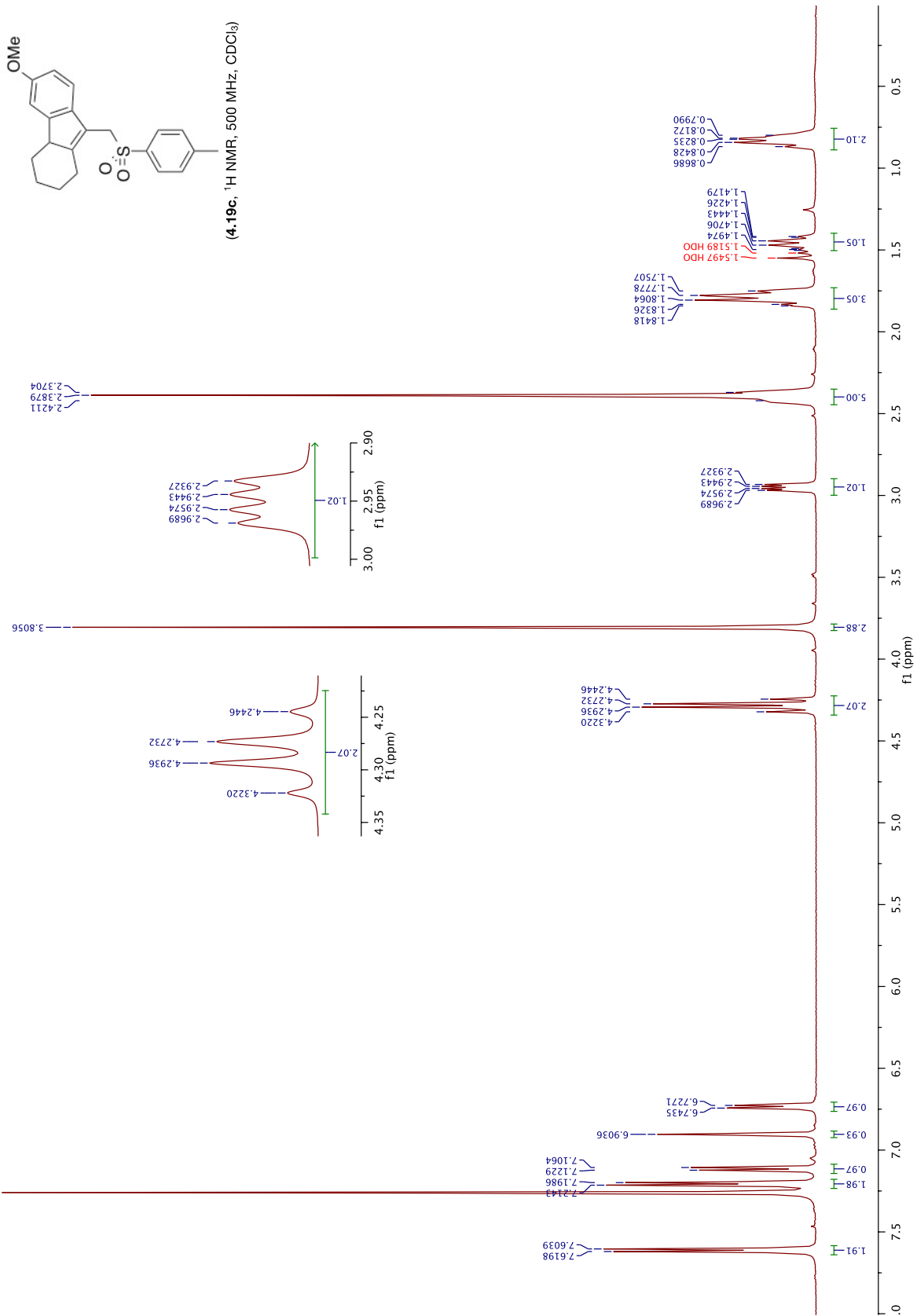
(1.25, ¹H NMR, 400 MHz, CDCl₃)

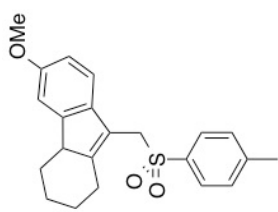




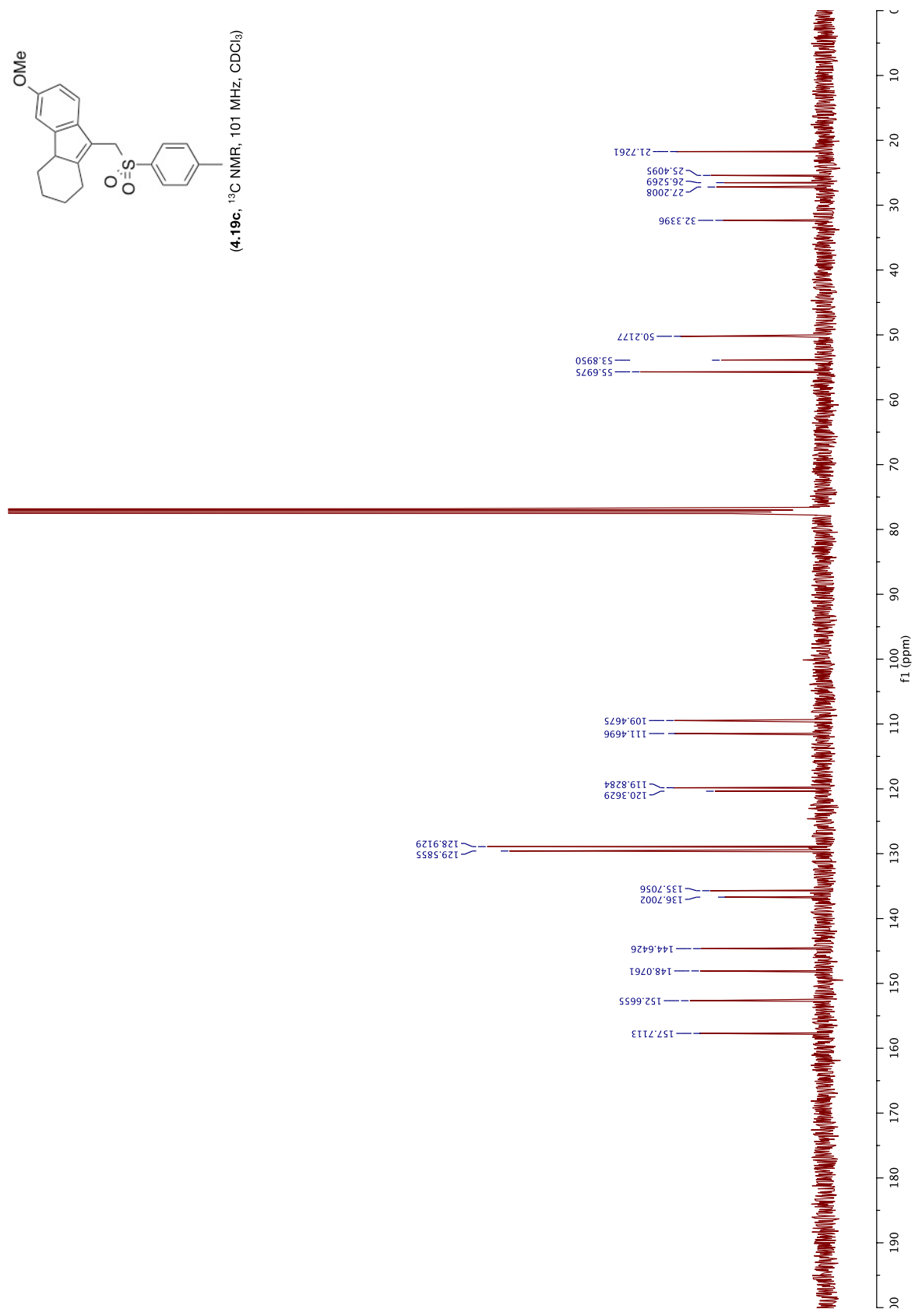
(1.25, ¹³C NMR, 76 MHz, CDCl₃)

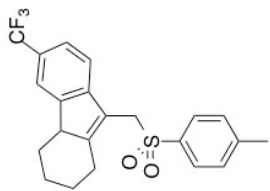




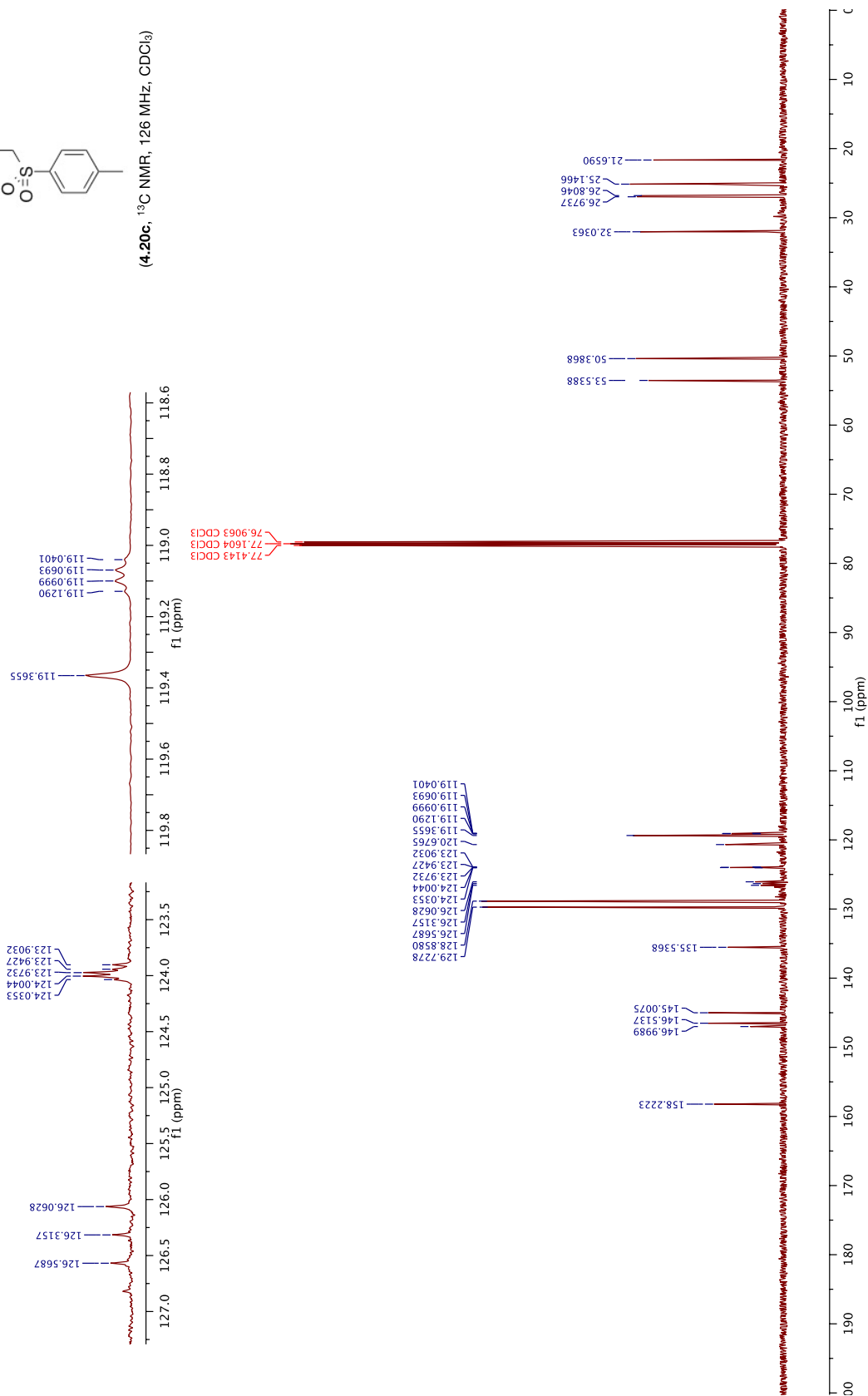


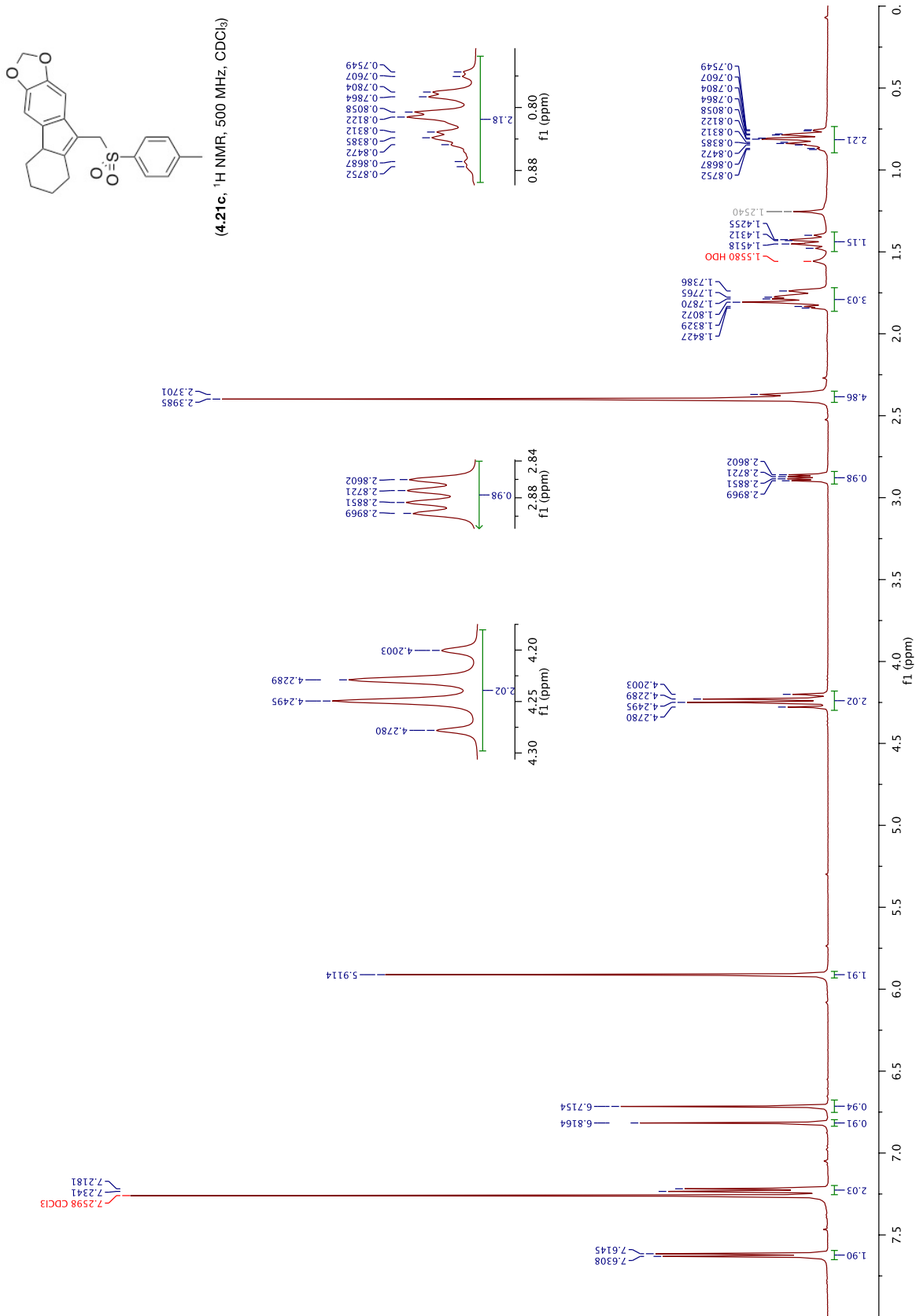
(4-19c, ^{13}C NMR, 101 MHz, CDCl_3)

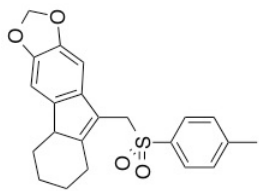




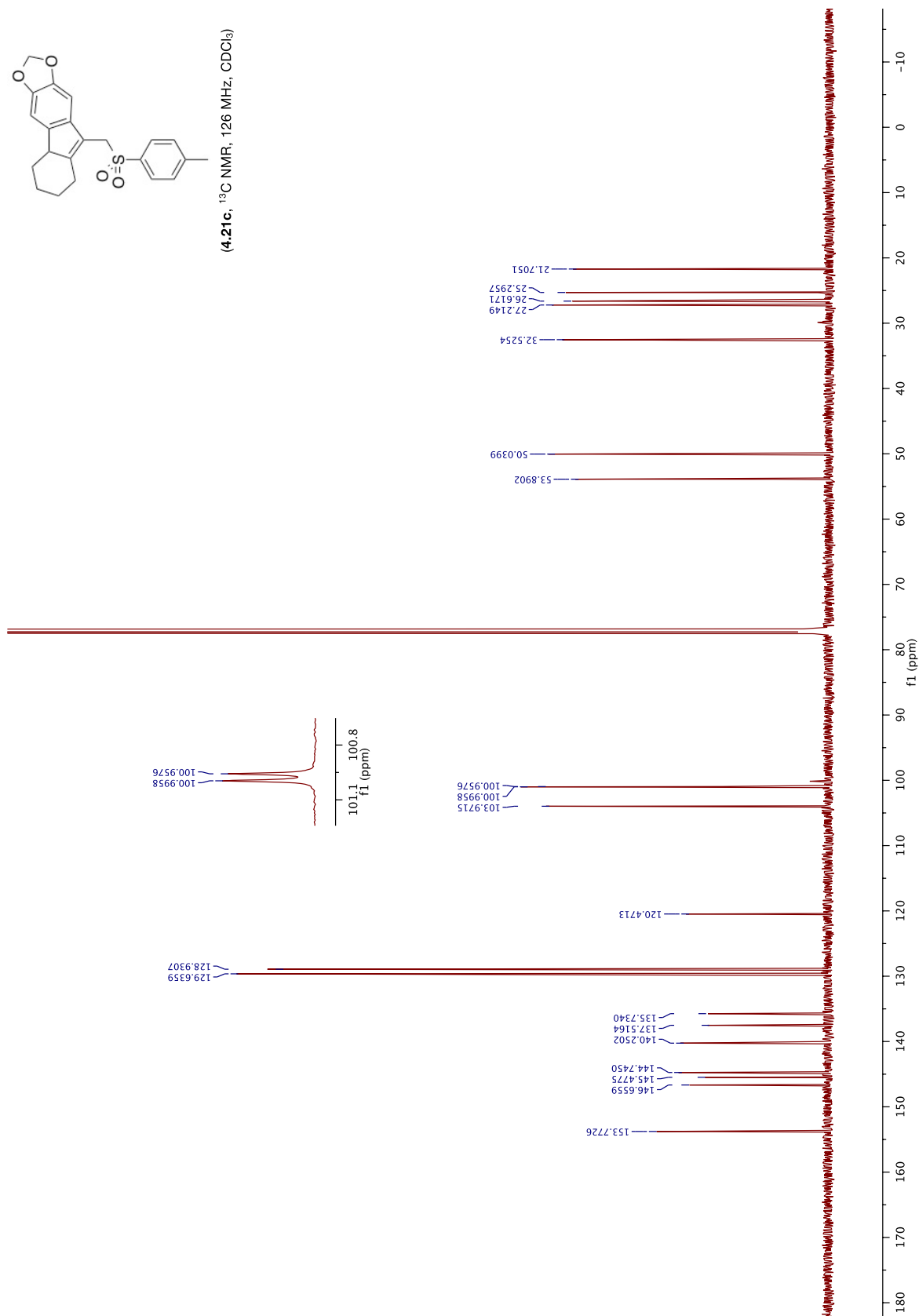
(4.20c), ^{13}C NMR, 126 MHz, CDCl_3

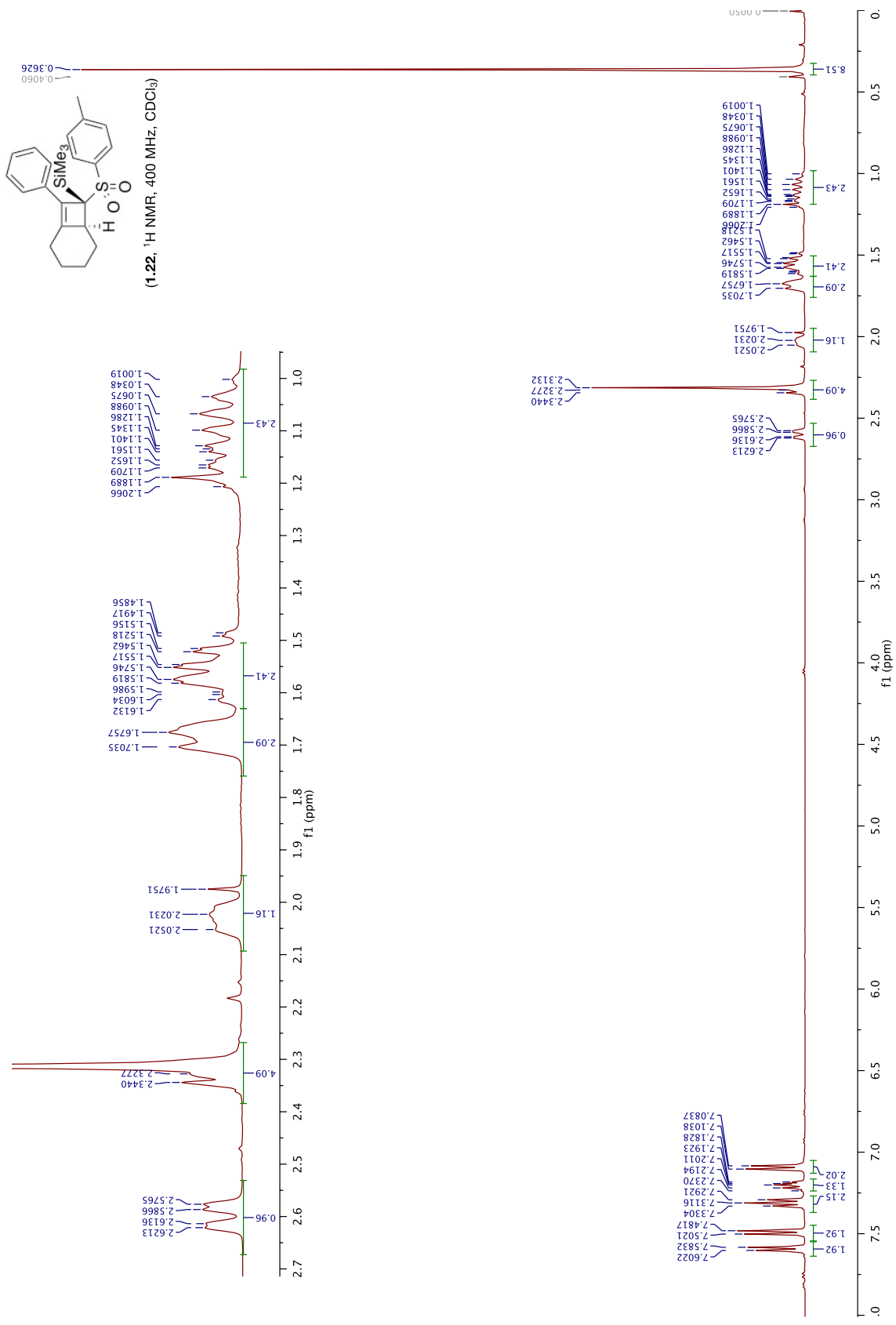


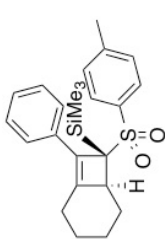




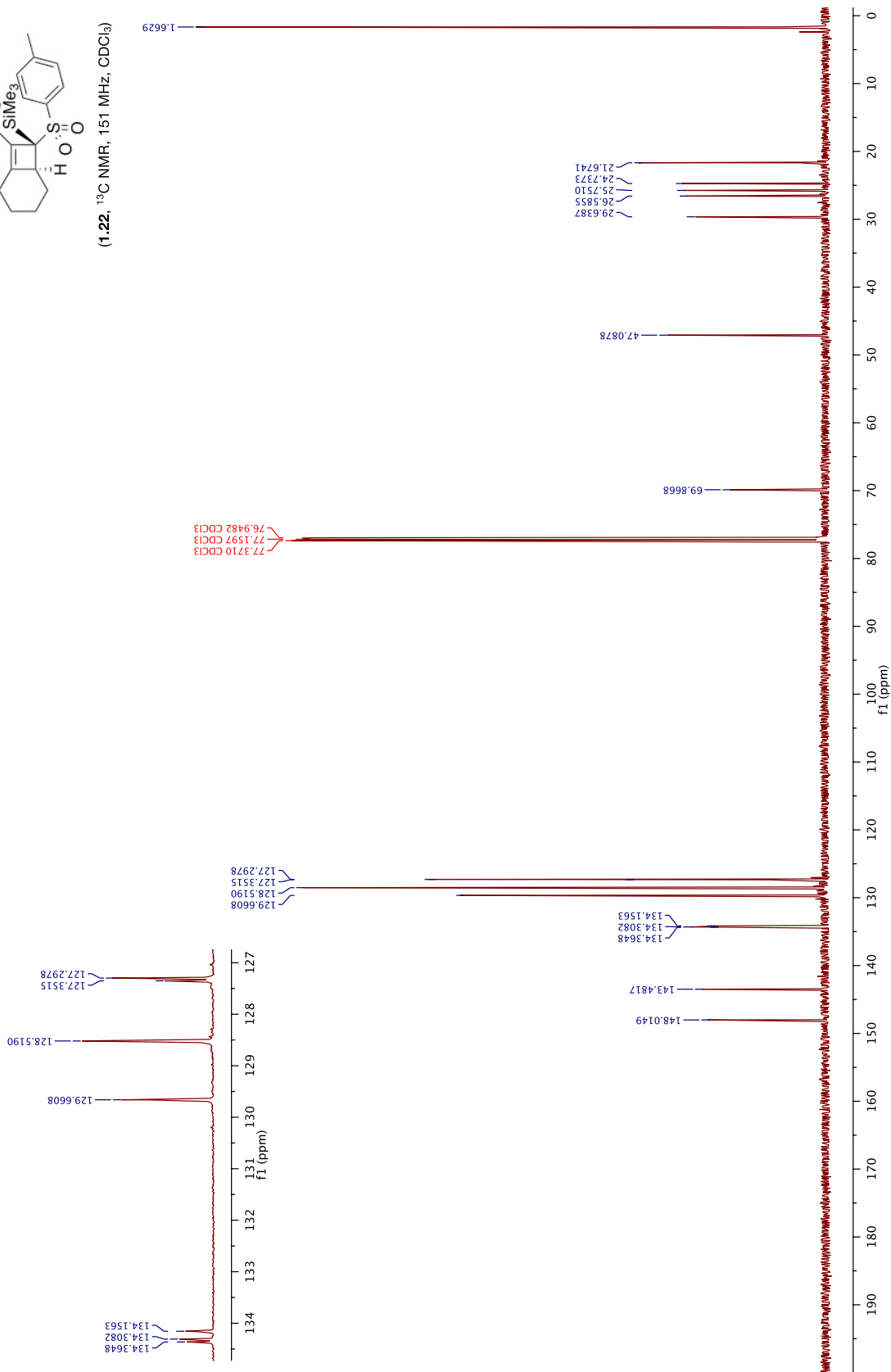
(4.21c), ^{13}C NMR, 126 MHz, CDCl_3

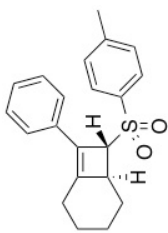




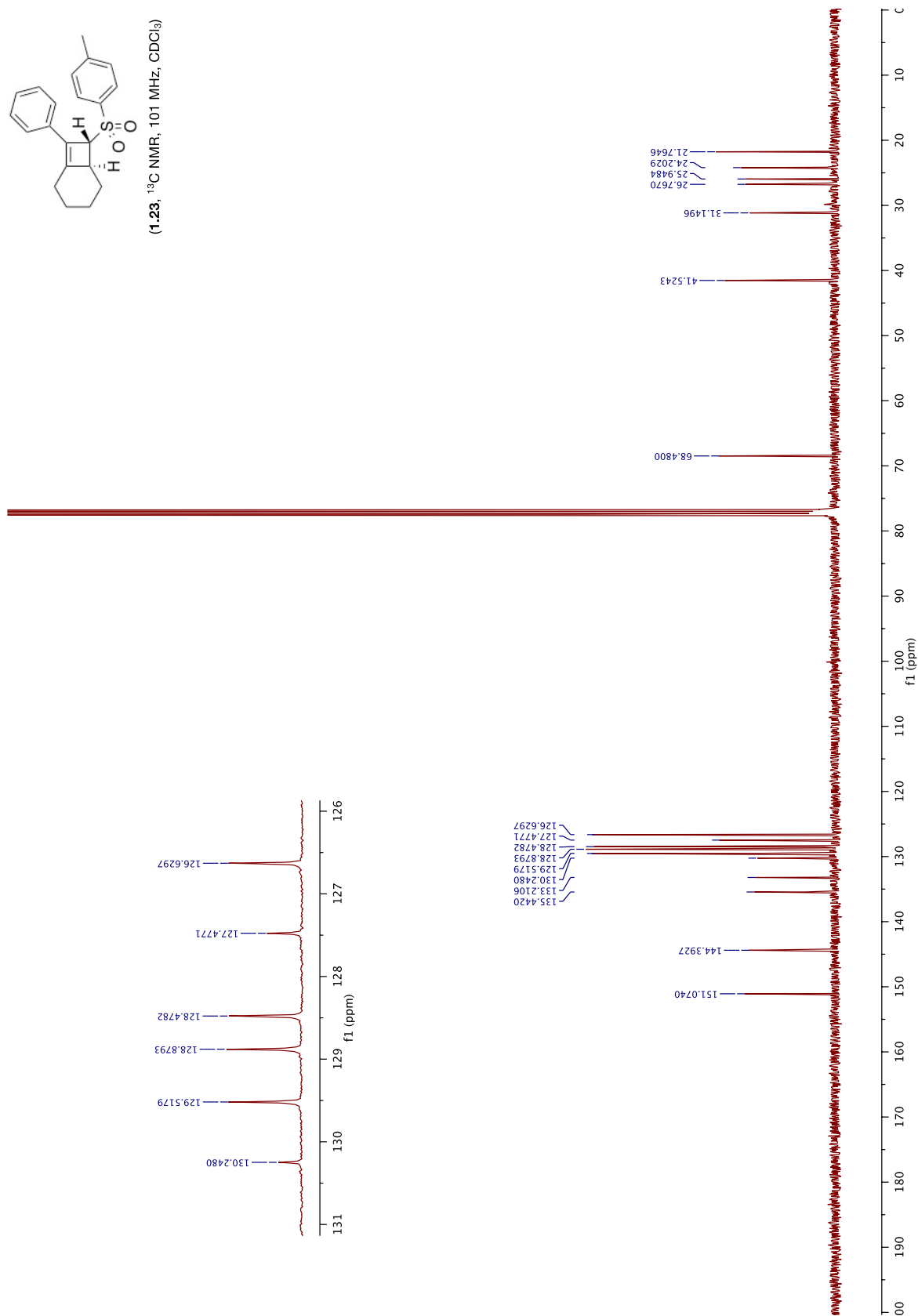


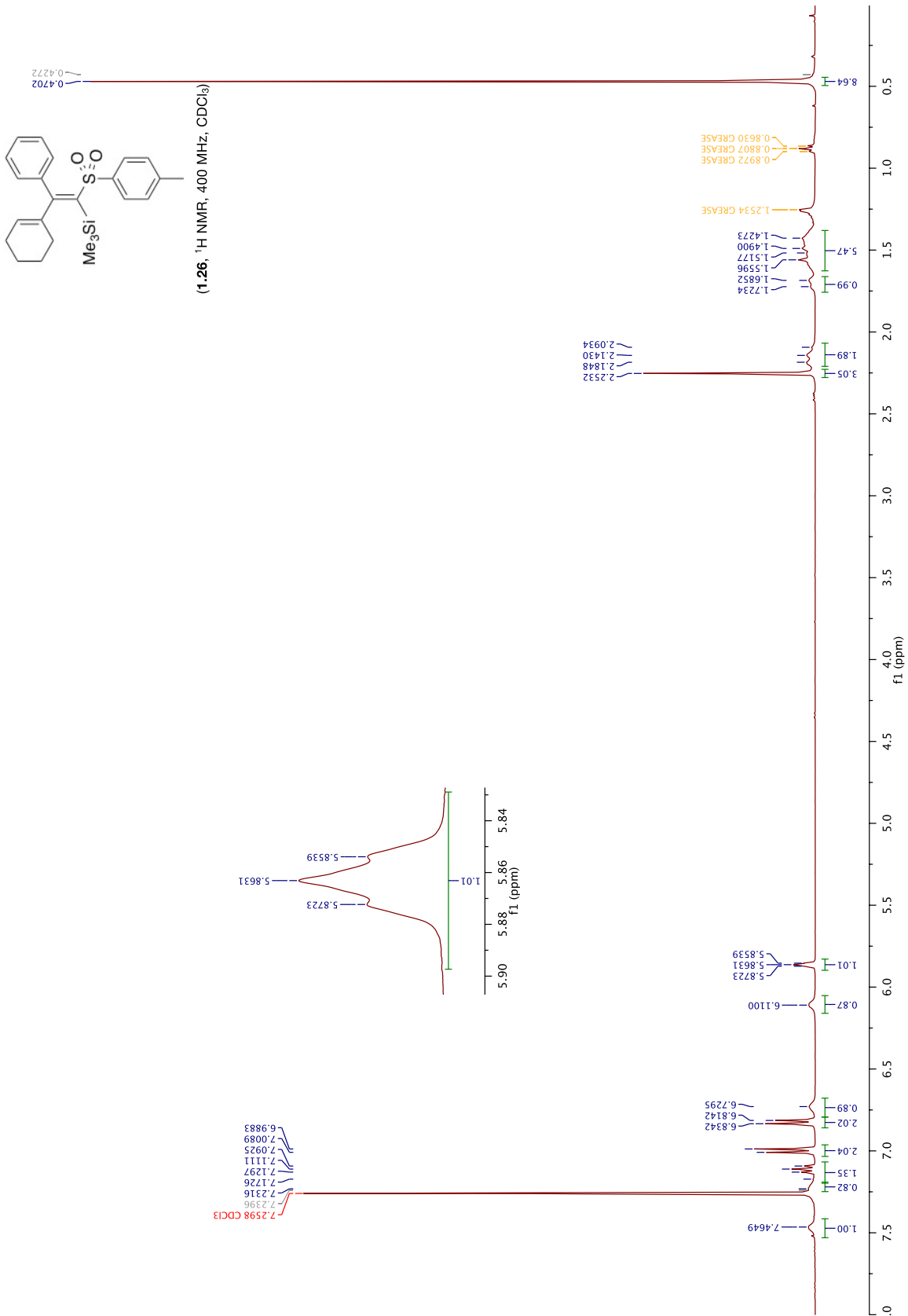
(1.22, ^{13}C NMR, 151 MHz, CDCl_3)

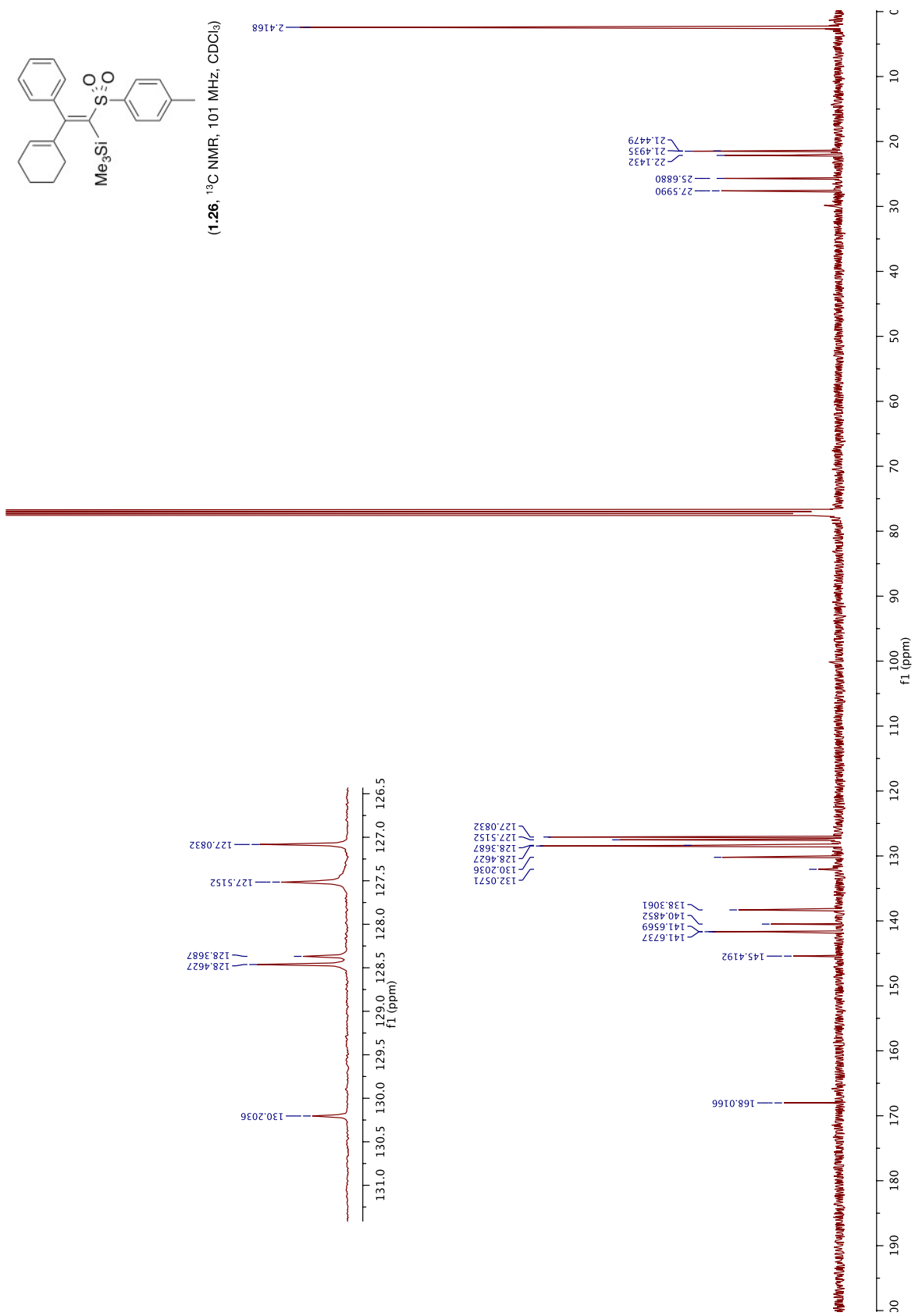


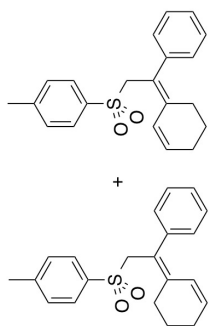


(1.23, ^{13}C NMR, 101 MHz, CDCl_3)

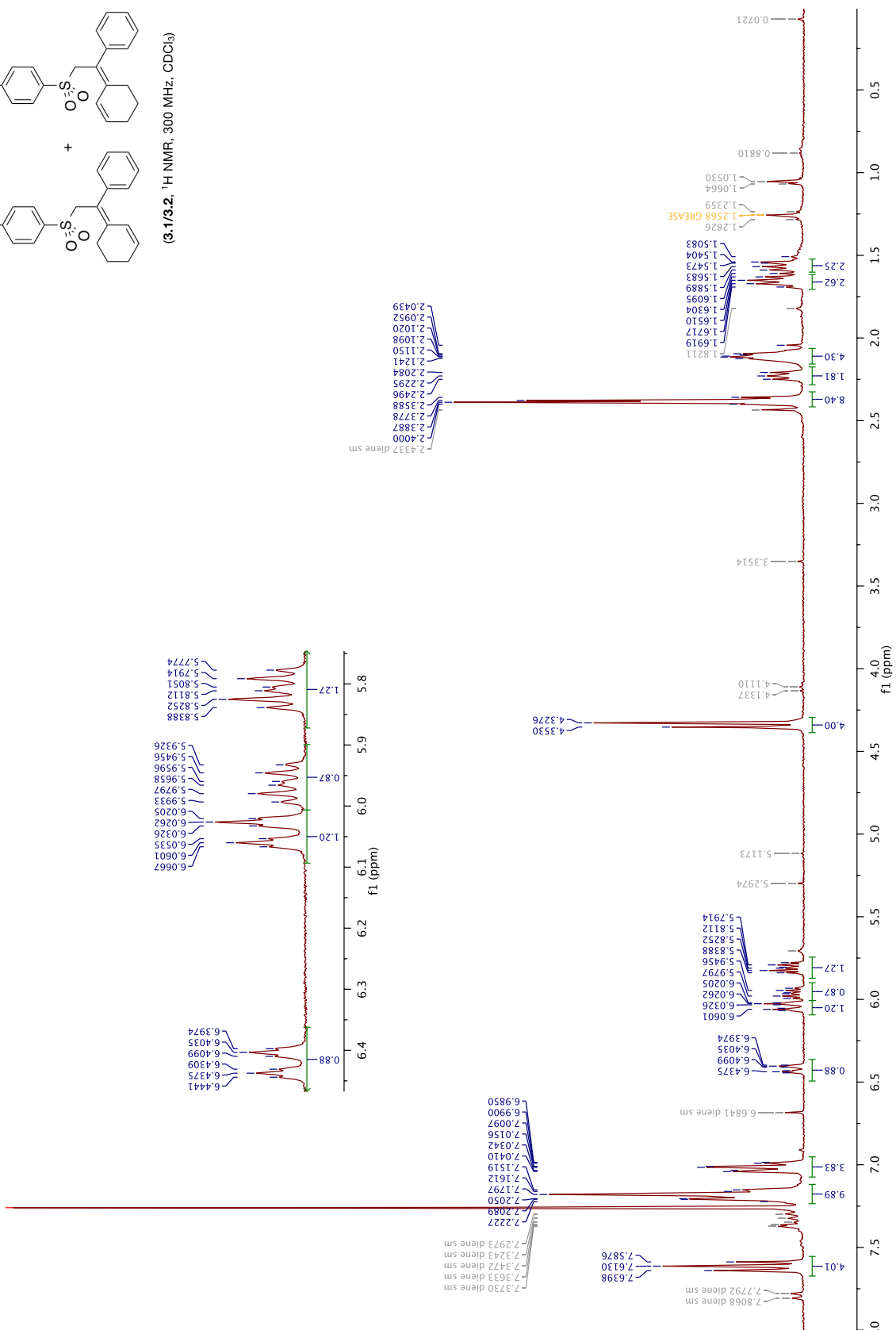


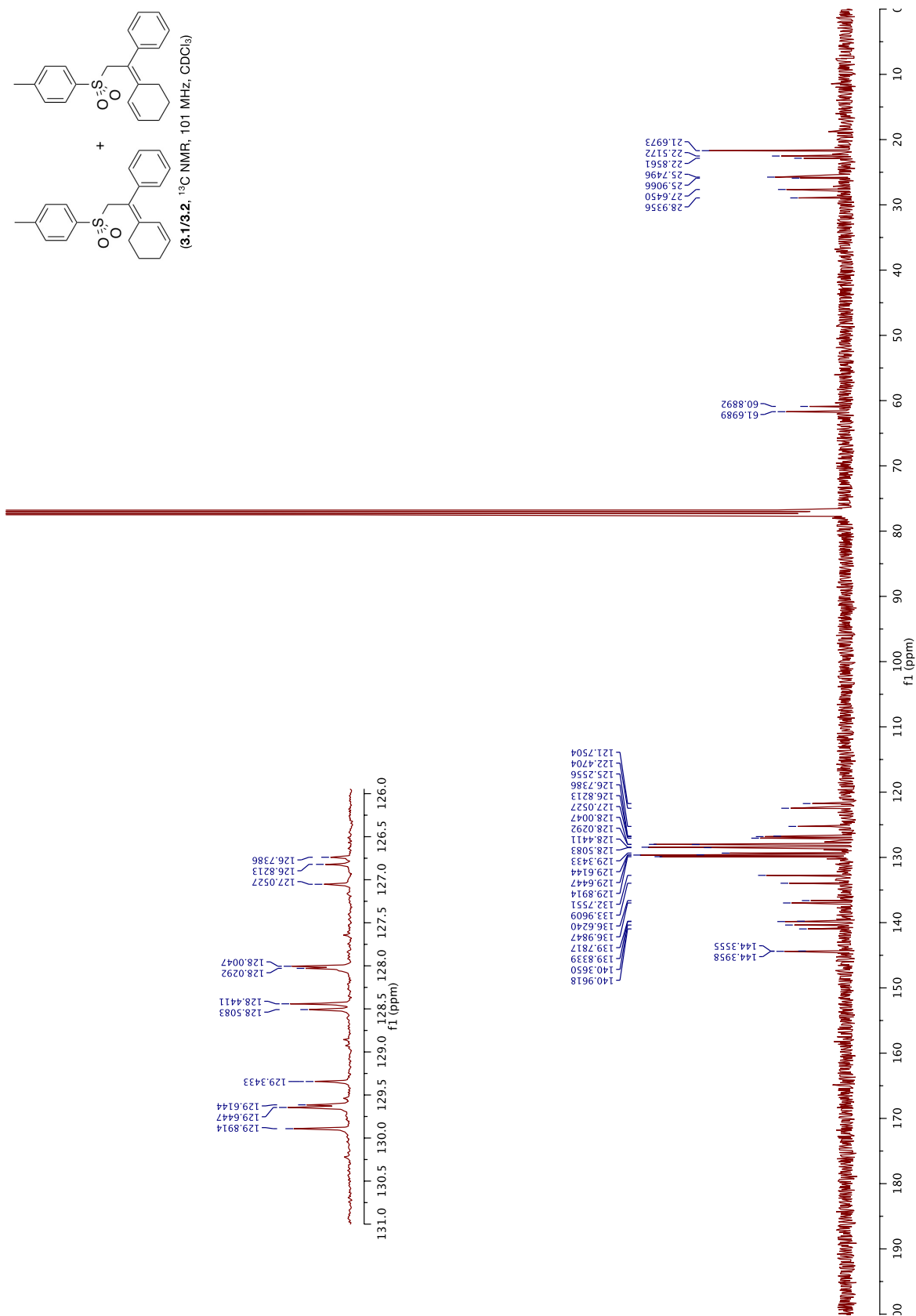
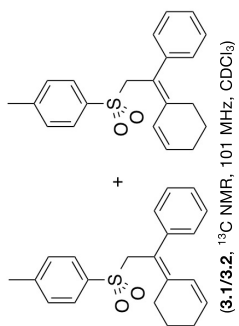






(3:1/3:2, ¹H NMR, 300 MHz, CDCl₃)





BIBLIOGRAPHY

1. Brummond, K. M.; Chen, D. Microwave-Assisted Intramolecular [2 + 2] Allenic Cycloaddition Reaction for the Rapid Assembly of Bicyclo[4.2.0]octa-1,6-dienes and Bicyclo[5.2.0]nona-1,7-dienes. *Org. Lett.* **2005**, *7*, 3473-3475.
2. Strous, M.; Fuerst, J. A.; Kramer, E. H. M.; Logemann, S.; Muyzer, G.; van de Pas Schoonen, K. T.; Webb, R.; Kuenen, J. G.; Jetten, M. S. M. Missing lithotroph identified as new planctomycete. *Nature* **1999**, *400*, 446.
3. Damsté, J. S. S.; Strous, M.; Rijpstra, W. I. C.; Hopmans, E. C.; Geenevasen, J. A. J.; van Duin, A. C. T.; van Niftrik, L. A.; Jetten, M. S. M. Linearly concatenated cyclobutane lipids form a dense bacterial membrane *Nature* **2002**, *419*, 708-712.
4. Masciutti, V.; Corey, E. J. Enantioselective Synthesis of Pentacycloanammoxic Acid. *J. Am. Chem. Soc.* **2006**, *128*, 3118.
5. Funk, R. L.; Umstead-Daggett, J.; Brummond, K. M. Stereoselective preparation of vinyl sulfones by protodesilylation of allyl silanes. *Tetrahedron Lett.* **1993**, *34*, 2867-2870.
6. Delaunay, J.; Orliac, A.; Simonet, J. A Cathodic mode of access to 1-arylsulfonylcyclobutenes. *Tetrahedron Lett.* **1995**, *12*, 2083-2084.
7. Nájera, C.; Yus, M. Desulfonylation Reactions: Recent Developments. *Tetrahedron* **1999**, *55*, 10547-10658.
8. Sonogashira, K; Tohda, Y.; Hagihara, N. A Convenient Synthesis of Acetylenes: Catalytic Substitutions of Acetylenic Hydrogen with Bromoalkenes, Iodoarenes and Bromopyridines. *Tetrahedron Lett.* **1975**, *16*, 4467-4470.
9. Harmata, M.; Cai, Z.; Huang, C.; Brummond, K. M.; Wen, B. Silver-catalyzed Rearrangement of Propargylic Sulfinates: Synthesis of Allenic Sulfones. *Org. Synth.* **2011**, *88*, 309-316.
10. Mukai, C.; Hara, Y.; Miyashita, Y.; Inagaki, F. Thermal [2+2] Cycloaddition of Allenynes: Easy Construction of Bicyclo[6.2.0]deca-1,8-dienes, Bicyclo[5.2.0]nona-1,7-dienes, and Bicyclo[4.2.0]octa-1,6-dienes. *J. Org. Chem.*, **2007**, *72*, 4454-4461.
11. de Vries, J G.; Elsevier, C. J. *Handbook of Homogenous Hydrogenation*; Wiley-VCH: Weinheim, Germany, 2007; Vol. 1, pp 8.

12. Thompson, H. W.; McPherson, E. Stereochemical Control of Reductions. IV. Control of Hydrogenation Stereochemistry by Intramolecular Anionic Coordination to Homogenous Catalysts. *J. Am. Chem. Soc.* **1974**, *96*, 6232-6233.
13. (a) Snider, B. B.; Kirk, T. C.; Roush, D. M.; Gonzalez, D. Lewis Acid Catalyzed Ene Reactions of Ethynyl *p*-Tolyl Sulfone. *J. Org. Chem.* **1980**, *45*, 5015-5017. (b) Trost, B. M.; Adams, B. R. A Cyclocontraction–Spiroannulation: A Stereoselective Approach to Spirocycles. *J. Am. Chem. Soc.* **1983**, *105*, 4849-4850. (c) Trost, B. M.; Ghadiri, M. R. Sulfones as Chemical Chameleons. Cyclization via 1,1-Dipole Synthons. *J. Am. Chem. Soc.* **1984**, *106*, 7260-7261. (d) Harmata, M.; Gamlath, C. B. Intramolecular 4 + 3 Cycloadditions of 2-Alkoxyallylic Cations Derived from 2-Alkoxyallylic Sulfones. *J. Org. Chem.* **1988**, *53*, 6156-6158.
14. Frontier, A. J.; Collison, C. The Nazarov cyclization in organic synthesis. Recent advances. *Tetrahedron* **2005**, *61*, 7577-7606.
15. El-Awa, A.; Noshi, M. N.; Jourdin, X. M.; Fuchs, P. L. Evolving Organic Synthesis Fostered by the Pluripotent Phenylsulfone Moiety. *Chem. Rev.* **2009**, *109*, 2315–2349.
16. Nielson, M.; Jacobsen, C. B.; Holub, N.; Paixão, M. W.; Jørgensen, K. A. Asymmetric Organocatalysis with Sulfones. *Angew. Chem. Int. Ed.* **2010**, *49*, 2668 – 2679.
17. Xu, K.; Khakyzadeh, V.; Bury, T.; Breit, B. Direct Transformation of Terminal Alkynes to Branched Allylic Sulfones. *J. Am. Chem. Soc.* **2014**, *136*, 16124-16127.
18. Pandya, V. G.; Mhaske, S. B. Transition-Metal-Free C-S Bond Formation: A Facile Access to Aryl Sulfones from Sodium Sulfinates via Arynes. *Org. Lett.* **2014**, *16*, 3836-3839.
19. Mander, L. N. The Chemistry of Gibberellins: An Overview. *Chem. Rev.* **1992**, *92*, 573-612.
20. (a) Chang, C. I.; Chang, J. Y.; Kuo, C. C.; Pan, W. Y.; Kuo, Y. H. Four New 6-Nor-5(6→7)*abeo*-abietane Type Diterpenes and Antitumoral Cytotoxic Diterpene Constituents from the Bark of *Taiwania cryptomerioides*. *Planta Med.* **2005**, *71*, 72–76. (b) Lee, S. M.; Kuo, Y. H. Three Novel 5(6→7)*Abeo*abietane-Type Diterpenes from the Bark of *Taiwania cryptomerioides*. *Chem. Pharm. Bull.* **2003**, *51*, 1420–1422.
21. Liang, G.; Xu, Y.; Seiple, I. B.; Trauner, D. Synthesis of *Taiwania*quinoids via Nazarov Triflation. *J. Am. Chem. Soc.* **2006**, *128*, 11022–11023.
22. Majetich, G.; Shimkus, J. M. Concise syntheses of (±)-dichroanone, (±)-dichroanal B, (±)-*taiwania*quinol B, and (±)-*taiwania*quinone D *Tetrahedron Lett.* **2009**, *50*, 3311–3313.
23. Deng, J.; Li, R.; Luo, Y.; Li, J.; Zhou, S.; Li, Y.; Hu, J.; Li, A. Divergent Total Synthesis of *Taiwania*quinones A and F and *Taiwania*quinols B and D. *Org. Lett.* **2013**, *15*, 2022-2025.
24. Alvarez-Manzaneda, E.; Chahboun, R.; Cabrera, E.; Alvarez, E.; Haidour, A.; Ramos, J. M.; Alvarez-Manzaneda, R.; Hmamouchi, M.; Es-Samti, H. A thermal 6 π electrocyclization strategy

towards taiwaniaquinoids. First enantiospecific synthesis of (-)-taiwaniaquinone G. *Chem. Commun.* **2009**, 592-594.

25. (a) Tius, M. A.; Chu, C. C.; Nieves-Colberg, R. An imino Nazarov cyclization. *Tetrahedron Lett.* **2001**, *42*, 2419-2422. (b) Bow, W. F.; Basak, A. K.; Jolit, A.; Vicic, D. A.; Tius, M. A. Enamine-Iminium Ion Nazarov Cyclization of α -Ketoenones. *Org. Lett.* **2010**, *12*, 440-443. (c) Shimada, N.; Ashburn, B. O.; Basak, A. K.; Bow, W. F.; Vicic, D. A.; Tius, M. A. Organocatalytic asymmetric aza-Nazarov cyclization of an azirine. *Chem. Commun.* **2010**, *46*, 3774-3775. (d) Ma, Z.-X.; He, S.; Song, W.; Hsung, R. P. α -Aryl-Substituted Allenamides in an Imino-Nazarov Cyclization Cascade Catalyzed by Au(I). *Org. Lett.* **2012**, *14*, 5736-5739. (e) Bonderoff, S. A.; Grant, T. N.; West, F. G.; Tremblay, M. Nazarov Reactions of Vinyl Cyclopropylamines: An Approach to the Imino-Nazarov Problem. *Org. Lett.* **2013**, *15*, 2888-2891.

26. Smith, D. A.; Ulmer II, C. W. Effects of Substituents in the 3-Position on the [2 + 2] Pentadienyl Cation Electrocyclization. *J. Org. Chem.* **1997**, *62*, 5110.

27. Rieder, C. J.; Winberg, K. J.; West, F. G. Cyclization of Cross-Conjugated Trienes: The Vinylogous Nazarov Reaction. *J. Am. Chem. Soc.* **2009**, *131*, 7504.

28. (a) Halterman, R. L.; Tretyakov, A.; Combs, D.; Chang, J.; Khan, M. A. Synthesis and Structure of C_2 -Symmetric, Doubly Bridged Bis(indenyl)titanium and -zirconium Dichlorides. *Organometallics* **1997**, *16*, 3333-3339. (b) Ogura, K.; Arai, T.; Kayano, A.; Akazome, M. Novel photochemical addition of aromatic aldehydes to ketene dithioacetal *S,S*-dioxides and its application to organic synthesis. *Tetrahedron Lett.* **1998**, *39*, 9051-9054.

29. (a) He, W.; Sun, X.; Frontier, A. J. Polarizing the Nazarov Cyclization: Efficient Catalysis under Mild Conditions. *J. Am. Chem. Soc.* **2003**, *125*, 14278-14279. (b) Malona, J. A.; Colbourne, J. M.; Frontier, A. J. A General Method for the Catalytic Nazarov Cyclization of Heteroaromatic Compounds. *Org. Lett.* **2006**, *8*, 5661-5664.

30. Singh, R.; Panda, G. Application of Nazarov type electrocyclicization to access [6,5,6] and [6,5,5] core embedded new polycycles: an easy entry to tetrahydrofluorene scaffolds related to Taiwaniaquinoids and *C-nor-D* homosteroids. *Org. Biomol. Chem.*, **2011**, *9*, 4782-4790.

31. Alvarez-Manzaneda, R. *et al.* A Very Efficient Route toward the 4a Methyltetrahydrofluorene Skeleton: Short Synthesis of (\pm)-Dichroanone and (\pm) Taiwaniaquinone H. *J. Org. Chem.*, **2009**, *74*, 3384-3388.

32. Eom, D.; Park, S.; Park, Y.; Ryu, T.; Lee, P. H. Synthesis of Indenes via Brønsted Acid Catalyzed Cyclization of Diaryl- and Alkyl Aryl-1,3-dienes. *Org. Lett.* **2012**, *14*, 5392-5395.

33. Smith, C. D.; Rosocha, G.; Mui, L.; Batey, R. A. Investigation of Substituent Effects on the Selectivity of 4π -Electrocyclization of 1,3-Diaryllallylic Cations for the Formation of Highly Substituted Indenes. *J. Org. Chem.* **2010**, *75*, 4716-4727.

34. Naredla, R. R.; Klumpp, D. A. Contemporary Carbocation Chemistry: Applications in Organic Synthesis. *Chem. Rev.* **2013**, *113*, 6905-6948.
35. Lamb, A. B.; Jacques, A. G. The Slow Hydrolysis of Ferric Chloride in Dilute Solution. I. The Change in Conductance, Color and Chloride Ion Concentration. *J. Am. Chem. Soc.* **1938**, *60*, 967.
36. Snider, B. B. Jackson, A. C. Use of Ethylaluminum Dichloride as a Catalyst for the Friedel Crafts Acylation of Alkenes. *J. Org. Chem.* **1982**, *47*, 5393 – 5395.
37. Bäckvall, J-E.; Juntunen, S. K. 2-(Phenylsulfonyl)-1,3-dienes as Versatile Synthons in Organic Transformations. Multicoupling Reagents and Diels-Alder Dienes with a Dual Electron Demand. *J. Am Chem. Soc.* **1987**, *21*, 6396-6403.
38. Crumbie, R. L.; Ridley, D. D. Reactions of 2,5-Dihydrothiophen and S-Substituted Derivatives with Bases. Preparations of 1-(Alkylthio)buta-1,3-dienes and the Corresponding Sulfoxides and Sulfones. *Aust. J. Chem.* **1981**, *34*, 1017-1026.
39. Chumachenko, N.; Sampson, P.; Hunter, A. D.; Zeller, M. β -Acyloxysulfonyl Tethers for Intramolecular Diels–Alder Cycloaddition Reactions. *Org. Lett.*, **2005**, *7*, 3203-3206.
40. Bors, D. A.; Streitwieser, A., Jr., Theoretical Study of Carbanions and Lithium Salts Derived from Dimethyl Sulfone. *J. Am. Chem. Soc.* **1986**, *108*, 1397-1404.
41. Patil, N.T.; Lutete, L. M.; Wu, H.; Pahadi, N. K.; Gridnev, I. D.; Yamamoto, Y. Palladium Catalyzed Intramolecular Asymmetric Hydroamination, Hydroalkoxylation, and Hydrocarbonation of Alkynes. *J. Org. Chem.* **2006**, *71*, 4270-4279.